CLINICAL APPLICATION AND EVALUATION OF ADVANCED DIAGNOSTIC TOOLS IN WOMEN WITH ENDOMETRIAL CANCER

Miss Diana Marcus, MBBS, BSc (Hons) MRCOG MRCS MRCP

Imperial College London

Department of Cancer and Surgery

2020

This thesis is submitted in partial fulfilment of the requirements for the degree of Doctor of Philosophy.

SUPERVISORS

Professor Sadaf Ghaem-Maghami, PhD MRCOG
Professor & Honorary Consultant in Gynaecology and Gynaecological Oncology
Imperial College London
Division of Cancer & Reproductive Biology
Hammersmith Hospital, IRDB, Du Cane Road, London, W12 0HS
s.ghaem-maghami@imperial.ac.uk

Professor Zoltan Takats, PhD
Professor of Analytical Chemistry,
Division of Computational and Systems Medicine
Department of Surgery and Cancer, Faculty of Medicine
Imperial College London
South Kensington Campus, Sir Alexander Fleming Building, SW7 2AZ
z.takats@imperial.ac.uk

Mr Joseph Yazbek, MD MRCOG
Consultant in Obstetrics, Gynaecology and Gynaecological Oncology
Imperial College London
Hammersmith Hospital, Du Cane Road, London, W12 0HS
Joseph.Yazbek@imperial.nhs.uk

Professor Andrea Rockall, BA (Hons), MA, MB BChir, MRCP, FRCR
Consultant Radiologist and visiting Professor
Imperial College London
Hammersmith Hospital, Du Cane Road, London, W12 0HS
a.rockall@imperial.ac.uk

DECLARATION OF ORIGINALITY

I declare that all work presented in my thesis is entirely my own. That which is not is referenced accordingly.

DECLARATION OF COPYRIGHT

The copyright of this thesis rests with the author. Unless otherwise indicated, its contents are licensed under a Creative Commons Attribution-Non-Commercial 4.0 International Licence (CC BY-NC).

Under this licence, you may copy and redistribute the material in any medium or format. You may also create and distribute modified versions of the work. This is on the condition that: you credit the author and do not use it, or any derivative works, for a commercial purpose.

When reusing or sharing this work, ensure you make the licence terms clear to others by naming the licence and linking to the licence text. Where a work has been adapted, you should indicate that the work has been changed and describe those changes.

Please seek permission from the copyright holder for uses of this work that are not included in this licence or permitted under UK Copyright Law

“Do not go where the path may lead, go instead where there is no path and leave a trail”

Ralph Waldo Emerson

ABSTRACT

Endometrial cancer (EC) is the most common gynaecological cancer in the developed world, with a demand for developments in diagnostic and treatment strategies. This thesis evaluates the current diagnostic pathway and investigates the potential for novel technologies to improve the speed of diagnosis and minimise cost.

Firstly, a psychological, prognostic and economic evaluation of the current pathway was performed. A retrospective audit of all EC cases in the west London cancer network demonstrated that delays to surgical treatment negatively impact survival. Furthermore, a psychological survey of 250 women attending the rapid access clinic with suspected EC revealed, unsurprisingly, a desire for a rapid point of care (POC) diagnosis and high levels of anxiety and stress. The economic evaluation found POC testing minimised cost too. These findings provided justification for further research in novel technologies in POC testing.

In the second part of this thesis, these novel technologies were evaluated against current gold standards. Rapid evaporative ionisation mass spectrometry (REIMS) analyses aerosols generated by surgical diathermy, to provide a real time tissue diagnosis. In a pilot study, 150 endometrial biopsy samples were analysed, yielding 453 spectra. REIMS distinguished benign from malignant EC samples with an accuracy of almost 90% on cross validation.

Ultrasound guided biopsy was also found to be an effective alternative to hysteroscopy guided biopsy in a study of 10 consecutive patients. It was successful with sufficient tissue in 90% of cases. Though painful, it had high acceptability.

Three-dimensional ultrasound was found to have moderate diagnostic performance compared to MRI, in detecting deep myometrial infiltration in women with EC; in both the current study and in a meta-analysis of 627 women. Finally, radiomics using MR images helped predict survival.

In conclusion, POC testing has psychological, survival and financial benefits. REIMS, ultrasound guided biopsy, and 3D ultrasound can provide POC testing with promising results, but further work is necessary to evaluate effectiveness on a wider scale.

ACKNOWLEDGEMENTS

Theodore Roosevelt once said, “nothing in the world is worth having or worth doing unless it means effort”. This PhD represents one of the most challenging and satisfying projects I have done and am I grateful for the opportunity to have brought my vision to completion.

I am indebted to my supervisors, Professor Sadaf Ghaem Maghami, Mr Joseph Yazbek, Professor Takats and Professor Andrea Rockall who have guided and supported me during this PhD journey. I am grateful for their trust and patience. This PhD would not have been possible without their input.

I have had the honour, privilege, and pleasure, of working with some incredible individuals throughout my PhD who have provided comradery, friendship and support. To name but a few of the iKnife group – Jayce Ip, David Phelps, Julia Balog, Eftychios Manoli, Julia Abda, Julia Balog, Adele Savage, Emma White, Petra Paizs, Pamela Pruski, Stefania Maneta, Stavrakaki Luisa Doria, Renata Soares, Holly Lewis, Olivia Raglan and Menelaos Tzafetas - who have helped me with all thing’s mass spectrometry. Particular thanks to Zsolt Bodai, James McKenzie and Alvaro Perdones-Montero in the bioinformatics team for help with post processing analysis. I would also like to thank Waters Corporation for offering their instrumentation and support. Their collaboration enabled the world’s first use of iKnife in endometrial cancer patients.

In am also grateful for my fellow colleagues for the tireless support, namely Ala Amgheib, John Wahba, Marina Natoli, Kirsty Flowers, Ben Jones and Ben Carter, to name just a few.

The first pilot study of endometrial cancer used tissue samples from Imperials Experimental Cancer Medicine Centre (ECME) tissue bank. Many thanks to both Nona Rama and Naina Patel who were instrumental in sourcing these first samples.

The pipelle tissue samples were obtained from both rapid access clinics and theatres in St Marys hospital and Queen Charlotte hospital. It has been a pleasure working with the lovely staff in both sites. Special mention to Lulu, Connie, Marcella, Erica, Val and Linda – some of the lovely nurses in Gynae oncology and clinic. In addition to the

consultants Miss Stalder and Chiara Landolfo, and all the helpful registrars; Patricia Cox, Tanya Maric, Claudia, Nick, Mia, Saso, Lin and Holly Lewis who helped me collect samples. But, most of all, I am enormously grateful for the hundreds of patients who selflessly donated their time and tissue for my research in the hope that it might help other women in the future.

Histopathological quality control was an essential part of the iKnife project and I grateful to Dr Francesca Rossi, Dr Roberto Dina and Hiromi Kudos for their help with this.

The psychological and economic project would not have been possible without Dr Alex King, Dr Mark Pennington and Dr. Elena Pizzo who provided insightful comments and honest feedback of my work. Two incredibly helpful SHOs also assisted with the mammoth task of data collection for the survival data– Gabriella Yongue and Yu Shen, thank you. Amrita, Dr James Russell and Dr Nishat Bharwani also helped with data collection and segmentation of radiomics cases. Ioannis and Xingfeng performed the mathematical modelling for the radiomics project. I thank them all for their invaluable contribution.

Imperial College London is a world class university, with research at the frontiers of science. Thank you for providing me the academic freedom to pursue my own interests, and the resources to carry it out. Special thanks to the statistics department and graduate school for their guidance throughout my research.

To my mentors, Mr Tim Duncan, Mr Jo Nieto and Mr Nikos Burbos, thank you inspiring me towards my chosen career path, and for acting as such exceptional role models.

Lastly, and most importantly, I am grateful to my husband, friends and family for their continued help and support. You have been nothing short of my rock. To my siblings, Mr Hani Marcus and Dr Adam Marcus you will never know how much you have inspired me and impacted my work. Adam, your IT wizardry skills and stats knowledge are second to none. I am indebted and wish you good luck as you begin your own PhD journey. Hani, you have been one of the biggest mentors and influences throughout my life, thank you for your honest and critical feedback. Aidan, thank you for providing me with perspective, encouragement and humour throughout my studies. To my

parents, Mr Samuel Marcus and Mrs Nisrin Marcus, thank you for all the sacrifices you made to give me a better life. Love you.

CONTENTS

ABSTRACT **5**

ACKNOWLEDGEMENTS **6**

CONTENTS **9**

LIST OF FIGURES **14**

LIST OF TABLES **18**

LIST OF ABBREVIATIONS **20**

CHAPTER 1: HYPOTHESES AND AIMS **24**

1.1 Hypotheses: **25**

1.2. Aims and Objectives: **25**

CHAPTER 2: INTRODUCTION **27**

2.1 Diagnosis of endometrial cancer **30**
2.1.1 Techniques to evaluate the endometrium 31
2.1.2 Analysis of the histology 40

2.2. Additional Considerations **41**
2.2.1 Recurrent symptoms 41
2.2.2 Risk of dissemination of cancer 42

2.3 Following a diagnosis of cancer **43**
2.3.1 Pre-op planning and Staging 43
2.3.2 Surgery 46
2.3.3 Further treatment 48

2.4 New technologies **49**
2.4.1 USS guided biopsy 49
2.4.2 Three-dimensional (3D) ultrasound 49
2.4.3 Rapid evaporative ionization mass spectrometry 49
2.4.4 Radiomics 54

CHAPTER 3: EVALUATION OF THE CURRENT PATHWAY, A NEED FOR CHANGE? **58**

3.1 Health effect of delayed treatment **60**
Acknowledgements: 60
3.1.1 Summary 60
3.1.2 Introduction 60
3.1.3 Methods 63
3.1.4 Results 66
3.1.5 Discussion 72

3.2 Psychological effect **78**
Collaborators: 78
3.2.1 Summary 78
3.2.2 Introduction 79
3.2.3 Methods 80
3.2.4 Results 84
3.2.5 Discussion 95

3.3 Overall need for change ... **102**
3.3.1 Clinical trial ... 102
3.3.2 Cost-effectiveness analysis ... 104

CHAPTER 4: THE IKNIFE ... **105**
Collaborators: ... 106

4.1 Summary ... **106**

4.2 Introduction ... **106**

4.3 Pilot study – Can iKnife distinguish between normal and cancer endometrial tissue bank samples? ... **110**
4.3.1 Materials and methods ... 110
4.3.2 Results ... 122
4.3.3 Discussion ... 140

4.4 The pipelle ... **146**
4.4.1 Methods ... 146
4.4.2 Results ... 149
4.4.3 Discussion ... 154

4.5 A new pipelle model ... **156**
4.5.1 Methods ... 156
4.5.2 Results of conventional diathermy iKnife ... 164
4.5.3 Results CO2 laser ... 171
4.5.4 Results - Learning curve of best model ... 176
4.5.5 Results - Choosing the best model ... 177
4.5.6 Results – which m/z values are important? Loading plots, univariate analysis and volcano plot ... 179
4.5.7 Discussion ... 183

4.6 Lipid identification – tandem mass spectrometry ... **188**
4.6.1 Methods ... 188
4.6.2 Results ... 189
4.6.3 Discussion ... 192

CHAPTER 5: ULTRASOUND GUIDED BIOPSY ... **196**

5.1 Summary ... **197**

5.2 Introduction ... **197**

5.3 Methods ... **200**
5.3.1 The technique ... 201
5.3.2 Statistical analysis ... 202

5.4 Results ... **202**

5.5 Discussion ... **204**
5.5.1 Main findings ... 204
5.5.2 Strengths and Limitations ... 205
5.5.3 Conclusion ... 206

CHAPTER 6: 3D ULTRASOUND ... **210**

6.1 Summary ... **211**

6.2 Introduction ... **211**

6.3 Methods **212**
6.3.1 Ultrasound assessment 213
6.3.2 Image analysis 214
6.3.3 Statistical analysis 215

6.4 Results **215**

6.5 Discussion **218**
6.5.1 Main Findings 218
6.5.2 Strengths and Limitations 219
6.5.3 Conclusions 221

CHAPTER 7: 3D ULTRASOUND SYSTEMATIC REVIEW AND META-ANALYSIS **222**

7.1 Summary **223**

7.2 Introduction **223**

7.3 Methods **225**
7.3.1 Search Strategy 225
7.3.2 Study selection and Data extraction 226
7.3.3 Quality assessment and risk of bias assessment 226
7.3.4 Statistical analysis 227

7.4 Results **228**
7.4.1 Literature search and study selection 228
7.4.2 Trial Characteristics 229
7.4.3 Overall Diagnostic performance of 3D Ultrasound for myometrial invasion 236
7.4.4 Diagnostic performance of 3D Ultrasound using subjective assessment for the detection of deep myometrial invasion 236
7.4.5 Diagnostic performance of 3D Ultrasound using objective assessment for the detection of deep myometrial invasion 239
7.4.6 Diagnostic performance of 3D Ultrasound using subjective assessment for the detection of cervical invasion 240

7.5 Discussion **240**
7.5.1 Main findings 240
7.5.2 Strengths and Limitations 243
7.5.3 Conclusions 246

CHAPTER 8: RADIOMICS **247**
Collaborators: 248

8.1 Summary **248**

8.2 Introduction **248**

8.3 Methods **250**
8.3.1 Patient characteristics and study centre 250
8.3.2 Histological analysis 251
8.3.3 MRI acquisition 251
8.3.4 Image segmentation and analysis 251
8.3.5 Radiomic features, selection and statistical analysis 252

8.4 Results: Pilot study – 60 cases analysed by Mr Ioannis Lavdas **256**

8.5 Discussion of pilot study results **260**

8.6 Results: Larger study – 464 cases analysed by Mr Xingfeng Li **260**

8.6.1 Patient characteristics 260
8.6.2 Prediction of risk classification 261
8.6.3 Prediction of high-risk histology: type, grade and lymphovascular space involvement 262
8.6.4 Prediction of stage including deep myometrial and stromal invasion. 265
8.6.5 Prediction of survival and recurrence 267

8.7 Discussion 269
8.7.1 Main findings 269
8.7.2 Strengths and Limitations 271
8.7.3 Conclusions 272

CHAPTER 9: COST – EFFECTIVESNESS ANALYSIS 273

9. Economic effect: cost-effectiveness analysis 274
Collaborators: 274

9.1 Summary 274

9.2 Introduction 274

9.3 Methods 275

9.4 Results 284

9.5 Discussion 287
9.5.1 Strengths and Limitations 287
9.5.2 Strengths and Limitations 289
9.5.3 Conclusion 290

CHAPTER 10: CONCLUSION AND FUTURE WORK 291

10.1 Achievements 292

10.2 Future work 293
10.2.1 Extension of psychological and survival impact of delayed diagnosis and treatment 293
10.2.2 Development of the iKnife as diagnostic tool 294
10.2.3 Development of 3D Ultrasound for pre-operative assessment 295
10.2.4 Development of radiomics model 295
10.2.5 Future integrated pathway 295

10.3 Final Conclusion 295

CHAPTER 11: REFERENCES 297

CHAPTER 12: APPENDIX 331

12.1 Publications, presentations, prizes and grants 332
12.1.1. Publications 332
12.1.2 Conference presentations 332
12.1.3 Prizes and grants 332

12.2 Summary Clinical Trial Protocol 334

12.3 Patient Information Sheet and questionnaire 339

12.4 Tissue bank classification of uterine samples 343

12.5 Other tissue bank models evaluated 347

12.6 Other pipelle models evaluated 350

..... 351

12.7 Combining pipelle and tissue bank model 355

12.8 Combining pipelle CO2 laser samples and iKnife diathermy tissue bank 357

LIST OF FIGURES

FIGURE 1. HISTOLOGICAL IMAGE OF AN ENDOMETRIAL BIOPSY TAKEN FROM A PATIENT WITH GRADE 1 ENDOMETRIOID ENDOMETRIAL CANCER. 36
FIGURE 2. HISTOLOGICAL IMAGE OF AN ENDOMETRIAL BIOPSY TAKEN FROM A PATIENT WITH CARCINOSARCOMA OF THE UTERUS (A FORM OF TYPE 2 ENDOMETRIAL CANCER).....37
FIGURE 3. OUTPATIENT ENDOMETRIAL BIOPSY DEVICES.....38
FIGURE 4. PICTORIAL DIAGRAM OF REIMS, IMAGE TAKEN FROM THE WATERS CORPORATION WEBSITE [190].....52
FIGURE 5. PHOTOGRAPHS OF THE IKNIFE APPARATUS. ON THE LEFT THE MASS SPECTROMETER AND HANDHELD DIATHERMY DEVICE ON RIGHT, AS USED IN THIS PHD. 52
FIGURE 6. NUMBER OF NEW ARTICLES IN RADIOMICS 2010-2019 USING A PUBMED SEARCH RADIOMICS.....55
FIGURE 7. ILLUSTRATION OF RADIOMICS PROCESS.....56
FIGURE 8. KAPLAN-MEIER CURVE ILLUSTRATING THE SURVIVAL OF WOMEN WITH ENDOMETRIAL CANCER, ACCORDING TO THEIR STAGE. 67
FIGURE 9. KAPLAN MEIER CURVE ILLUSTRATING THE SURVIVAL OF WOMEN WITH ENDOMETRIAL CANCER, ACCORDING TO THEIR TIME FROM DIAGNOSIS TO SURGERY: 14 OR LESS DAYS, 15-42 DAYS, 43-84 DAYS AND 85 DAYS OR MORE. TYPE 1 AND TYPE 2 ENDOMETRIAL CANCER DATA SHOWN SEPARATELY; GRAPH A AND B RESPECTIVELY. ..68
FIGURE 10. TIMING OF ENDOMETRIAL CANCER RECURRENCE FROM THE DATE OF SURGERY.71
FIGURE 11. LIKERT SCALE FOR QUANTIFICATION OF STRESS SCORES. 81
FIGURE 12. GAD7 ANXIETY QUESTIONNAIRE USED TO QUANTIFY ANXIETY LEVELS.....82
FIGURE 13. BREAKDOWN OF AGES OF WOMEN PARTICIPATING IN THE STUDY. 85
FIGURE 14. BREAKDOWN OF RELIGIOUS IDENTITY FOR WOMEN PARTICIPATING IN THE STUDY.....86
FIGURE 15. BREAKDOWN OF HIGHEST EDUCATION COMPLETED, IN WOMEN PARTICIPATING IN THE STUDY.....86
FIGURE 16. SOURCES OF INFORMATION WOMEN ATTENDING THE CLINIC USED. 87
FIGURE 17. BREAKDOWN OF STRESS SCORES.....87
FIGURE 18. ANXIETY SCORES USING GAD 7 QUESTIONNAIRE. 88
FIGURE 19. IMPORTANCE OF A QUICK DIAGNOSIS AS REPORTED BY WOMEN FILLING THE QUESTIONNAIRE. 89
FIGURE 20. SELF-PERCEPTION OF A CANCER DIAGNOSIS BEFORE SEEING A CLINICIAN.....90
FIGURE 21. BOX AND WHISKERS PLOT FOR GAD7 ANXIETY SCORES IN WOMEN WHO IDENTIFIED THEMSELVES AS DISABLED. 91
FIGURE 22. GAD7 ANXIETY SCORES RELATED TO HIGHEST LEVEL OF EDUCATION COMPLETED. 92
FIGURE 23. BOX AND WHISKERS PLOT, FOR ASSOCIATION BETWEEN PERCEPTION OF A CANCER DIAGNOSIS AND ENGLISH AS 1ST LANGUAGE. 94
FIGURE 24. NEW PATIENT PATHWAY WITH NOVEL TECHNOLOGY.....102
FIGURE 25. THE PHOSPHOLIPID BILAYER AND LIPID SYNTHESIS. 108
FIGURE 26. LEFT IMAGE - CALIBRATION SIGNAL SEEN WITH SODIUM FORMATE. CHROMATOGRAM FOLLOWING 2 MINUTES OF CALIBRATION 113
FIGURE 27. PHOTOGRAPH OF CUT OPEN UTERUS FOLLOWING HYSTERECTOMY FOR OVARIAN CYST.....116
FIGURE 28. PICTORIAL DIAGRAM OF THE IKNIFE SET-UP. 117
FIGURE 29. TISSUE SAMPLE PLACED ON BLUE CASSETTE SPONGE PRIOR TO FORMALIN. 118
FIGURE 30. CHROMATOGRAM WITH PEAKS SELECTED. 119
FIGURE 31. TISSUE SAMPLES ON BLUE CASSETTES PRE-FORMALIN.....123
FIGURE 32. FOUR SPECTRAL PATTERNS.....125
FIGURE 33. MULTIVARIATE ANALYSIS OF NORMAL VS CANCER VS HYPERPLASIA TISSUE BANK SAMPLES PRE-HISTOPATHOLOGICAL QUALITY CONTROL. 126
FIGURE 34. INVESTIGATION OF OUTLIERS FROM THE NORMAL VS CANCER VS HYPERPLASIA LDA TISSUE BANK MODEL.....127

FIGURE 35. MULTIVARIATE ANALYSIS OF NORMAL VS CANCER TISSUE BANK SAMPLES POST-HISTOPATHOLOGICAL QUALITY CONTROL.....129
FIGURE 36. MULTIVARIATE ANALYSIS OF NORMAL VS TYPE 1 CANCER VS TYPE 2 CANCER TISSUE BANK SAMPLES. 130
FIGURE 37. MULTIVARIATE ANALYSIS OF NORMAL VS TYPE 1 (ENDOMETRIOID) CANCER TISSUE BANK SAMPLES POST-HISTOPATHOLOGICAL QUALITY CONTROL.....132
FIGURE 38. MULTIVARIATE ANALYSIS OF NORMAL VS HIGH VOLUME TYPE 1 (ENDOMETRIOID) CANCER TISSUE BANK SAMPLES.....133
FIGURE 39. MULTIVARIATE ANALYSIS OF CANCER SUBDIVIDED INTO % TUMOUR BURDEN VS NORMAL TISSUE BANK SAMPLES. 135
FIGURE 40. RECOGNITION SOFTWARE ANALYSING A TISSUE SAMPLE.....137
FIGURE 41. LOADING PLOT OF TISSUE BANK MODEL. 138
FIGURE 42. BOX PLOT SHOWING AN EXAMPLE M/Z VALUE RESPONSIBLE FOR SEPARATION IN THE MODEL. 139
FIGURE 43. PHOTOGRAPHS OF ENDOMETRIAL TISSUE OBTAINED FROM PIPELLE BIOPSIES. 146
FIGURE 44. THE HANDPIECE ATTACHMENTS FOR REIMS. 147
FIGURE 45. EXAMPLE OF A VOLCANO PLOT. 158
FIGURE 46. CHROMATOGRAMS OF DIFFERENT SAMPLES.....159
FIGURE 47. ENDOMETRIAL CANCER SAMPLES, HEAVILY DIATHERMISED. 161
FIGURE 48. ENDOMETRIAL CANCER SAMPLES. LOSS OF CELL POLARISATION. 162
FIGURE 49. BENIGN ENDOMETRIAL PIPELLE SAMPLES. 163
FIGURE 50. MULTIVARIATE ANALYSIS OF NORMAL VS CANCER VS HYPERPLASIA PIPELLE SAMPLES, PRE-HISTOLOGICAL VALIDATION, PROCESSED WITH THE DIATHERMY IKNIFE. 164
FIGURE 51. MULTIVARIATE ANALYSIS OF NORMAL VS CANCER VS HYPERPLASIA PIPELLE SAMPLES, POST-HISTOLOGICAL VALIDATION, PROCESSED WITH THE IKNIFE.....166
FIGURE 52. MULTIVARIATE ANALYSIS OF NORMAL VS CANCER PIPELLE SAMPLES POST-HISTOLOGICAL VALIDATION, PROCESSED WITH THE IKNIFE.....167
FIGURE 53. MULTIVARIATE ANALYSIS OF NORMAL VS TYPE 1 VS TYPE 2 CANCER PIPELLE SAMPLES POST-HISTOLOGICAL VALIDATION, PROCESSED WITH THE DIATHERMY IKNIFE. 168
FIGURE 54. MULTIVARIATE ANALYSIS OF NORMAL VS TYPE 1 CANCER PIPELLE SAMPLES, POST-HISTOLOGICAL VALIDATION, PROCESSED WITH THE DIATHERMY IKNIFE. 169
FIGURE 55. MULTIVARIATE ANALYSIS OF NORMAL VS CANCER SAMPLES PROCESSED WITH THE DIATHERMY IKNIFE, SEPARATED ACCORDING TO WHETHER PROCESSED FRESH OR SNAP-FROZEN INITIALLY AND THAWED. 170
FIGURE 56. CHROMATOGRAM AND CORRESPONDING SPECTRA OF THE SAME SAMPLE PROCESSED WITH THE CONVENTIONAL DIATHERMY IKNIFE (ABOVE) AND CO2 LASER IKNIFE (BELOW).....172
FIGURE 57. MULTIVARIATE ANALYSIS OF NORMAL VS CANCER VS HYPERPLASIA PIPELLE SAMPLES, PRE-HISTOLOGICAL VALIDATION, PROCESSED WITH THE CO2 LASER.....173
FIGURE 58. MULTIVARIATE ANALYSIS OF NORMAL VS CANCER VS HYPERPLASIA PIPELLE SAMPLES, POST-HISTOLOGICAL VALIDATION, PROCESSED WITH THE CO2 LASER. 174
FIGURE 59. MULTIVARIATE ANALYSIS OF NORMAL VS CANCER PIPELLE SAMPLES, POST-HISTOLOGICAL VALIDATION, PROCESSED WITH THE CO2 LASER. 175
FIGURE 60. LEARNING CURVE OF *TYPE 1 CANCER VERSUS NORMAL (NO HYPERPLASIA) IKNIFE MODEL* BASED ON 35 NORMAL AND 35 CANCER SAMPLES. 177
FIGURE 61. LOADING PLOT OF 2 BEST PIPELLE MODELS.....180
FIGURE 62. VOLCANO PLOT OF IKNIFE (TOP) AND CO2 LASER MODELS (BOTTOM). BOX PLOT TO THE RIGHT OF EACH VOLCANO PLOT DEPICTS THE SINGLE M/Z VALUE WHICH IS STARRED ON THE VOLCANO PLOT.....181
FIGURE 63. TANDEM MS SPECTRA OF TWO M/Z VALUES: 722.54 AND 700.55. 191
FIGURE 64. INADEQUATE MS/MS SPECTRA OF M/Z 679.55.....192
FIGURE 65. VISUAL ANALOGUE SCALE USED FOR THE ASSESSMENT OF PAIN.....201
FIGURE 66. IMAGE OF ULTRASOUND GUIDED BIOPSY. 202
FIGURE 67. BOX AND WHISKERS PLOT OF PATIENT'S PERCEPTION OF PAIN USING VAS.....203
FIGURE 68. THREE-DIMENSIONAL ULTRASOUND IMAGE. 214
FIGURE 69. 3D SCAN IMAGES. 217

FIGURE 70. SUMMARY ROC CURVE SHOWING DIAGNOSTIC PERFORMANCE OF 3D ULTRASOUND USING DIFFERENT THRESHOLD FOR DEEP MYOMETRIAL INVASION (9MM, 7MM AND 5MM) ALONG WITH MRI SCANS. 218
FIGURE 71. FLOWCHART OF STUDIES INCLUDED IN 3D ULTRASOUND META-ANALYSIS. 229
FIGURE 72. GRAPHS DEPICTING QUALITY EVALUATION OF INCLUDED STUDIES. TOP LOOKING AT RISK OF BIAS AND BOTTOM LOOKING AT CONCERNS OVER APPLICABILITY. 230
FIGURE 73. FOREST PLOT OF INCLUDED STUDIES IN META-ANALYSIS LOOKING AT ACCURACY OF SUBJECTIVE ASSESSMENT OF DEEP MYOMETRIAL INVASION USING 3D ULTRASOUND. 237
FIGURE 74. SUMMARY ROC CURVE OF POOLED STUDIES IN META-ANALYSIS LOOKING AT ACCURACY OF SUBJECTIVE ASSESSMENT OF DEEP MYOMETRIAL INVASION USING 3D ULTRASOUND. 238
FIGURE 75. FAGAN NOMOGRAMS, SHOWING LIKELIHOOD RATIOS BASED UPON POOLED RESULTS FROM META-ANALYSIS 238
FIGURE 76. DEEKS FUNNEL PLOT FOR PUBLICATION BIAS. 239
FIGURE 77. FOREST PLOT OF INCLUDED STUDIES IN META-ANALYSIS LOOKING AT ACCURACY OF OBJECTIVE ASSESSMENT OF DEEP MYOMETRIAL INVASION USING 3D ULTRASOUND 239
FIGURE 78. FOREST PLOT OF INCLUDED STUDIES IN META-ANALYSIS LOOKING AT ACCURACY OF SUBJECTIVE ASSESSMENT OF CERVICAL INVASION USING 3D ULTRASOUND 240
FIGURE 79. SEGMENTATION PROCESS ILLUSTRATED. LEFT IS A T2 SAGITTAL IMAGE OF THE PELVIS. THE AREA OF THE THE TUMOUR (VOI) IS OUTLINED AS IN THE RIGHT IMAGE, AND THIS CREATES A MASK (MIDDLE PICTURE) 252
FIGURE 80. RADIOMICS WORKFLOW, SHOWING TEST AND VALIDATION DATA. 254
FIGURE 81. ALL MACHINE LEARNING CLASSIFICATION ALGORITHMS USED. CALIBRATED CLASSIFIER IS ALSO KNOWN AS THE ABBREVIATION CCC. 255
FIGURE 82. 5-FOLD CROSS VALIDATION. 256
FIGURE 83. EXAMPLE CONFUSION TABLE FOR TEST DATA USING 64GL AND SEEING IF THE MODEL CAN PREDICT TYPE 1 VS TYPE 2 CANCER, SEE * IN TABLE 28. 258
FIGURE 84. SUMMARY ROC CURVE SHOWING THE PERFORMANCE OF THE RADIOMICS PILOT MODEL. NOTE, TRUE POSITIVE RATE REFERS TO SENSITIVITY AND FALSE POSITIVE RATE EQUATES TO 1-SPECIFICITY. 259
FIGURE 85. UNSUPERVISED FEATURE CORRELATION MATRIX PRESENTED AS A HEAT MAP. 261
FIGURE 86. ACCURACY OF PREDICTION OF RISK SCORE USING VARIOUS CLASSIFICATION METHODS 262
FIGURE 87. ACCURACY OF PREDICTION OF BINARY RISK SCORE USING VARIOUS CLASSIFICATION METHODS 262
FIGURE 88. ACCURACY OF PREDICTION OF TYPE OF ENDOMETRIAL CANCER USING VARIOUS CLASSIFICATION METHODS 263
FIGURE 89. ACCURACY OF PREDICTION OF GRADE OF ENDOMETRIAL CANCER (3 GROUPS) USING VARIOUS CLASSIFICATION METHODS. 264
FIGURE 90. ACCURACY OF PREDICTION OF GRADE OF ENDOMETRIAL CANCER (2 GROUPS, HIGH GRADE AND LOW GRADE) USING VARIOUS CLASSIFICATION METHODS 264
FIGURE 91. ACCURACY OF PREDICTION OF PRESENCE OF LYMPHOVASCULAR SPACE INVOLVEMENT USING VARIOUS CLASSIFICATION METHODS. 265
FIGURE 92. ACCURACY OF PREDICTION OF STAGE OF ENDOMETRIAL CANCER USING VARIOUS CLASSIFICATION METHODS 266
FIGURE 93. ACCURACY OF PREDICTION OF DEEP MYOMETRIAL INVASION USING VARIOUS CLASSIFICATION METHODS 266
FIGURE 94. ACCURACY OF PREDICTION OF CERVICAL STROMAL INVASION USING VARIOUS CLASSIFICATION METHODS 267
FIGURE 95. ACCURACY OF PREDICTION OF OVERALL SURVIVAL USING VARIOUS CLASSIFICATION METHODS 268
FIGURE 96. ACCURACY OF PREDICTION OF RECURRENCE OF ENDOMETRIAL CANCER USING VARIOUS CLASSIFICATION METHODS. 268
FIGURE 97. DECISION TREE FOR 5MM USS PATHWAY. THE SCENARIO STARTS WITH THE PROBABILITY OF A CANCER DIAGNOSIS AND THEN GOES THROUGH THE FOLLOWING STEPS OF INVESTIGATION AND TREATMENT WITH THEIR RESPECTIVE COSTS, RISKS

AND BENEFITS. AT THE END OF THE PATHWAY ALL OUTCOMES; THEIR LIKELIHOOD AND COSTS ARE OUTLINED. 277
FIGURE 98. INCREMENTAL COST-EFFECTIVENESS PLANE. 286
FIGURE 99. SENSITIVITY ANALYSES 287
FIGURE 100. INVESTIGATION OF OUTLIERS FROM THE NORMAL VS CANCER TISSUE BANK PCA. 347
FIGURE 101. INVESTIGATION OF OUTLIERS FROM THE NORMAL VS TYPE 1 VS TYPE 2 CANCER TISSUE BANK MODEL. 348
FIGURE 102. MULTIVARIATE ANALYSIS OF NORMAL VS TYPE 1 CANCER (ENDOMETRIOID) TISSUE BANK SAMPLES, AFTER EXCLUSION OUTLIERS 349
FIGURE 103. MULTIVARIATE ANALYSIS OF NORMAL VS CANCER VS HYPERPLASIA SAMPLES SEPARATED ACCORDING TO WHETHER PROCESSED WITH THE DIATHERMY IKNIFE OR CO2 LASER. 351
FIGURE 104. MULTIVARIATE ANALYSIS OF NORMAL VS CANCER PIPELLE SAMPLES, PROCESSED WITH THE LIQUID PROBE. 353
FIGURE 105. MULTIVARIATE ANALYSIS OF NORMAL VS CANCER VS HYPERPLASIA SAMPLES SEPARATED ACCORDING TO WHETHER PROCESSED WITH THE DIATHERMY IKNIFE, CO2 LASER OR LIQUID PROBE. 354
FIGURE 106. MULTIVARIATE ANALYSIS OF NORMAL VS CANCER SAMPLES PROCESSED WITH THE IKNIFE, SEPARATED ACCORDING TO WHETHER SAMPLES WERE OBTAINED FROM PIPELLE BIOPSIES OR TISSUE BANK. 356
FIGURE 107. MULTIVARIATE ANALYSIS OF PIPELLE SAMPLES PROCESSED WITH THE CO2 LASER AND TISSUE BANK SAMPLES PROCESSED WITH THE IKNIFE, SEPARATED ACCORDING TO WHETHER SAMPLES WERE OBTAINED FROM PIPELLE BIOPSIES OR TISSUE BANK 357

LIST OF TABLES

TABLE 1. 2009 FIGO ENDOMETRIAL CANCER STAGES. 44
TABLE 2. CHARACTERISTICS OF THE PATIENT COHORT ACCORDING TO THEIR TIME TO SURGERY (TTS). ABBREVIATIONS: SD = STANDARD DEVIATION, † LVSI = LYMPHOVASCULAR SPACE INVASION. 67
TABLE 3. FACTORS PROGNOSTIC FOR SURVIVAL IN ALL WOMEN WITH ENDOMETRIAL CANCER. ABBREVIATIONS: † LVSI = LYMPHOVASCULAR SPACE INVASION. HR = HAZARD RATIOS. 69
TABLE 4. FACTORS PROGNOSTIC FOR SURVIVAL IN LOW RISK WOMEN (GRADE 1-2, STAGE 1A ENDOMETRIOID CANCER). ABBREVIATIONS: † LVSI = LYMPHOVASCULAR SPACE INVASION. HR = HAZARD RATIOS. 70
TABLE 5. CORRELATION OF GAD7 ANXIETY SCORES AND STRESS SCORES. 89
TABLE 6. FACTORS AFFECTING GAD 7 ANXIETY SCORES. P VALUES <0.05 CONSIDERED SIGNIFICANT AND SHOWN WITH A*. 93
TABLE 7. TYPES OF ANXIETY SCORING SYSTEM CURRENTLY USED AND THEIR KEY FEATURES. 100
TABLE 8. LIST OF CHEMICALS, SOLVENTS, MATERIALS AND EQUIPMENT 111
TABLE 9. HISTOLOGICAL BREAKDOWN OF TISSUE SAMPLES OBTAINED FROM TISSUE BANK. 115
TABLE 10. BREAKDOWN OF TISSUE SAMPLES ANALYSED BY EACH MODALITY. HYPERPLASIA NOT SHOWN IN TABLE. TISSUE SAMPLE NUMBERS REFLECT NUMBER OF PATIENTS SUPPLYING A SAMPLE. 122
TABLE 11. SUMMARY TABLE DIAGNOSTIC PERFORMANCE OF ALL TISSUE BANK MODELS. 136
TABLE 12. TOP 15 SIGNIFICANT M/Z VALUES AND TENTATIVE LIPID ASSIGNMENTS. 140
TABLE 13. SUMMARY TABLE OF THE PATIENT DEMOGRAPHIC FROM WHICH THE PIPELLE BIOPSIES WERE OBTAINED, ALONG WITH THE SAMPLE QUALITY. 150
TABLE 14. SUMMARY TABLE OF PIPELLE SAMPLES PROCESSED WITH REIMS DIATHERMY IKNIFE. 151
TABLE 15. SUMMARY TABLE OF PIPELLE SAMPLE CLASSIFICATION ACCORDING TO THE TISSUE BANK MODEL. 153
TABLE 16. SUMMARY TABLE OF CYTOLOGICAL AND HISTOLOGICAL FEATURES OF NORMAL AND MALIGNANT ENDOMETRIUM. 160
TABLE 17. SUMMARY TABLE DIAGNOSTIC PERFORMANCE OF ALL PIPELLE MODELS. 179
TABLE 18. TOP 30 SIGNIFICANT M/Z VALUES AND TENTATIVE LIPID ASSIGNMENTS. 183
TABLE 19. TOP 10 MOST ABUNDANT M/Z VALUES SEEN IN NORMAL AND MALIGNANT ENDOMETRIAL PIPELLE BIOPSIES, ALONG WITH THE CONFIRMED LIPID ASSIGNMENTS FOLLOWING MSMS. 190
TABLE 20. BREAKDOWN OF FINAL HISTOLOGY FOR WOMEN UNDERGOING ULTRASOUND GUIDED BIOPSY. 203
TABLE 21. SUMMARY TABLE OF PATIENTS WHO UNDERWENT ULTRASOUND GUIDED BIOPSY. ACRONYMS: ET = ENDOMETRIAL THICKNESS, ND = NOT DOCUMENTED, PMB = POST-MENOPAUSAL BLEED. 209
TABLE 22. HISTOLOGICAL SUMMARY OF PATIENTS WHO UNDERWENT A 3D ULTRASOUND. 216
TABLE 23. RESULTS OF SUBJECTIVE ASSESSMENT IN THE DIAGNOSIS OF DEEP MYOMETRIAL INVASION (MI). 217
TABLE 24. SUMMARY TABLE OF DIAGNOSTIC PERFORMANCE OF 3D ULTRASOUND USING DIFFERENT THRESHOLD FOR DEEP MYOMETRIAL INVASION (9MM, 7MM AND 5MM) ALONG WITH MRI SCANS. 217
TABLE 25. SUMMARY TABLE OF KEY FEATURES OF INCLUDED STUDIES. 234
TABLE 26. SUMMARY TABLE OF DIAGNOSTIC ACCURACY USING 3D ULTRASOUND TO ASSESS MYOMETRIAL INVASION. LR = LIKELIHOOD RATIOS 236
TABLE 27. TABLE 27. RISK OF LYMPH NODE METASTASIS FROM GOG STUDY. 241
TABLE 28. RISK CLASSIFICATION USED FOR RADIOMICS PATIENTS 251

TABLE 29. ACCURACY OF RADIOMICS MODEL TO DETECT TYPE AND GRADE OF ENDOMETRIAL CANCER AND PRESENCE OF LYMPHOVASCULAR SPACE INVOLVEMENT (LVSI). 258
TABLE 30. ESTIMATED PROBABILITIES FOR EACH PARAMETER. 280
TABLE 31. COST FOR EACH STEP DURING THE PATIENT PATHWAY. 283
TABLE 32. SUMMARY RESULTS OF COSTS (DIAGNOSIS AND TREATMENT, IN £ PER PATIENT) AND EFFECTIVENESS (% OF WOMEN SURVIVING 5 YEARS), BASED UPON MOST LIKELY ASSUMPTIONS. 285
TABLE 33. CONFUSION TABLE OF A MODEL COMBINING SAMPLES PROCESSED WITH THE CO2 LASER AND STANDARD DIATHERMY IKNIFE RECLASSIFIED ACCORDING TO WHETHER SAMPLES WERE NORMAL OR CANCER, NOT ENERGY MODALITY. 352
TABLE 34. CONFUSION TABLE OF TISSUE BANK (TB) AND PIPELLE SAMPLES PROCESSED WITH THE IKNIFE, CLASSIFIED ACCORDING TO TISSUE CLASS STATUS (NORMAL VS CANCER) AND NOT THE SAMPLING MODALITY. 356
TABLE 35. CONFUSION TABLE OF TISSUE BANK PROCESSED WITH THE DIATHERMY IKNIFE AND PIPELLE SAMPLES PROCESSED WITH THE CO2 LASER, CLASSIFIED ACCORDING TO TISSUE CLASS STATUS (NORMAL VS CANCER) AND NOT THE SAMPLING MODALITY. 358

LIST OF ABBREVIATIONS

£/LYG	The cost per additional life year gained
3D	Three dimensional
abdo	Abdominal
AH	Endometrial hyperplasia
AMX	Abstract model builder (a version of Offline Model Builder)
ANOVA	Analysis of variance
ATP	Adenosine Triphosphate
AUC	Area under the curve
Ca-125	Carbohydrate Antigen-125
CCC	Calibrated Classifier
CDP-DAG	Cytidine Diphosphate Diacylglycerol
Cer	Ceramide
CI	Confidence interval
CIN	Cervical intraepithelial neoplasia
CO2	Carbon dioxide
CT	Computed axial tomography
Da	Dalton, unified atomic mass unit
D&C	Dilation and curettage
DCC	Dissemination of cancer cells
DAG	Diacylglycerol
DESI	Desorption Electrospray Ionisation
DNA	Deoxyribonucleic Acid
DWI	Diffusion-weighted imaging
EIN	Endometrial intraepithelial neoplasia
EC	Endometrial Cancer
ER	Oestrogen receptor
ESI (-)/(+)	Electrospray Ionization, negative or positive ion mode
ESGO	European Society of Gynaecological Oncology
ESMO	European society of medical oncology
ESTRO	European Society for Radiotherapy & Oncology
ET	Endometrial thickness

EV	Endometrial volume
FAS	Fatty Acid Synthase
FDA	Food and Drug Administration
FFPE	Formalin fixed paraffin embedded
FIGO	International Federation of Gynaecology and Obstetrics
FO	First order
FS	Frozen section
GA	General anaesthetic
GAD7	Generalised Anxiety Disorder 7 (anxiety score)
g/l	Grams per litre
GPC	Gaussian Process Classifier
HADS	Hospital and Anxiety Depression Scale
H&E	Haematoxylin and eosin Stain
HMB	Heavy menstrual bleeding
HNPCC	Hereditary nonpolyposis colorectal cancer
HO	Higher order
HR	Hazard Ratio
HRT	Hormone replacement therapy
ICER	Incremental cost per unit of effectiveness
ICGC	International Cancer Genome Consortium
ICHNT	Imperial College healthcare NHS trust
ICL	Imperial College London
IETA	International Endometrial Tumour Analysis group
IMB	Intermenstrual bleeding
IPA	Isopropyl alcohol (also known as 2-Propanol and isopropanol)
IQ	Interquartile range
IRDB	Institute of Reproductive and Developmental Biology
LASSO	Least absolute shrinkage and selection operator logistic regression
LC-MS	Liquid chromatography MS
LDA	Linear Discriminant Analysis
LeuEnk	Leucine enkephalin
LMSD	LipidMaps structure bulk database
LPO	Leave one patient out (type of cross validation)

LR+	Positive likelihood ratio
LR-	Negative likelihood ratio
LVSI	Lymphovascular space invasion
LYG	Life year gained
MALDI	Matrix Assisted Laser Desorption Ionisation
MI	Myometrial invasion
MLP	Multi-layer perception classifier
MRI	Magnetic resonance imaging
MAPK	Mitogen activated protein kinase
MMC	Maximum margin criterion
MMT	Malignant mixed mesodermal tumour
MS	Mass Spectrometry
MSI	Mass Spectrometry Imaging
MS/MS	Tandem mass spectrometry
m/z	Mass to charge ratio
NaF	Sodium formate
NCD	National cancer database
ng	Nanograms
NPV	Negative predictive value
OEB	Outpatient endometrial biopsy
OMB	Offline Model Builder
OPH	Outpatient hysteroscopy
OPO	Optical para-metric oscillator (type of laser)
OR	Odds ratio
OS	Overall survival
PA	Phosphatidic Acid
PC	Phosphatidylcholine
PC1	Principal component 1
PC2	Principal component 2
PCA	Principal Component Analysis
PCR	Polymerase chain reaction
PE	Phosphatidylethanolamine
PETCT	Positron emission tomography CT scan
PFS	Progression free survival

PG	Phosphatidylglycerol
PI	Phosphatidylinositol
PL	Phospholipid
PLD	Phospholipase D
PLS	Partial least square regression
PMB	Post-menopausal bleeding
POC	Point of care
POLE	Polymerase epsilon
PPV	Positive predictive value
PS	Phosphatidylserine
QC	Quality Control
q-ToF	Quadrupole time of flight
QALY	Quality-adjusted life years
RAC	Rapid access clinic
REIMS	Rapid evaporative ionisation MS
ROC	Receiver operating characteristic
SD	Standard deviation
SIS	Saline infusion sonography
SLN	Sentinel lymph nodes
SO	Second order
sROC	Summary receiver operating characteristics
TCGA	The cancer genome atlas
TIC	Total ion chromatogram
TDS	Shortest tumour distance to serosa
TOF	Time-of-Flight
TTS	Time to surgery
TVUSS	Transvaginal ultrasound
USS	Ultrasound
VEGF	Vascular endothelial growth factor
VAS	Visual analog scale
VOI	Volumes of interest
WHO	World health organisation

CHAPTER 1: HYPOTHESES AND AIMS

1.1 Hypotheses:

The endometrial cancer pathway from referral to treatment is complex and dynamic. Innovations, particularly frugal innovations may enable the introduction of new technology that improves effectiveness but minimises cost. A baseline evaluation of the current pathway and the need for change, particularly a reduction in treatment time will be performed. This will be subdivided into survival, psychological and economic benefits to a quicker diagnosis. Followed by an evaluation of the new technologies used in the diagnosis and subsequent staging of women with suspected endometrial cancer. Finally, radiomics will be assessed to see if it can help prognosticate patients with endometrial cancer.

The hypothesis can be divided into 5 specific statements:

- There is a psychological, economic and prognostic benefit to earlier surgical treatment in endometrial cancer.
- Rapid Evaporative Ionisation Mass Spectrometry (REIMS) i.e. the iKnife can correctly identify endometrial cancer from pipelle biopsy samples.
- Ultrasound guided biopsy is a safe effective alternative to hysteroscopic guided biopsy.
- 3D ultrasound can be used as an effective alternative to Magnetic resonance imaging (MRI) in pre-operative staging for endometrial cancer.
- Radiomics (and potentially radiogenomics) have prognostic power and could be used as predictive biomarkers.

1.2. Aims and Objectives:

To investigate these hypotheses, the main aims of this research are to:

1. Investigate whether a shorter time from referral to treatment is beneficial, from a psychological, economical and prognostic perspective.

2. Assess if REIMS can accurately diagnose cancer and pre-cancer from endometrial biopsy samples. If successful, this will lead to a true ‘one-stop clinic’ where patients can be diagnosed on the same day.

3. Determine if a directed biopsy can be performed under ultrasound without the need for hysteroscopy. This procedure is likely to be quicker, cheaper and better tolerated than hysteroscopy and can be performed on the same day in clinic.

4. Determine if three-dimensional ultrasound can be used as a safe, effective and cheap alternative to MRI for pre-operative imaging of endometrial cancer in the assessment of myometrial invasion.

5. Assess if ultrasound and MRI models (radiomics) can predict tumour grade, type and prognosis thereby improving counselling to women post-operatively.

Each chapter will now address each of the above aims, starting with a background to provide context for this work (Chapter 2), then an assessment of the current pathway and need for change (Chapter 3), followed by an evaluation of REIMS (Chapter 4), USS guided biopsy (Chapter 5), 3D Ultrasound (Chapter 6 and 7), radiomics (Chapter 8) and a cost-effectiveness analysis (Chapter 9). Finally, the conclusion (Chapter 10) will summarise whether there is a benefit for a faster time to treatment and whether the new technologies can facilitate it effectively and help prognosticate patients.

CHAPTER 2: INTRODUCTION

CHAPTER 2: INTRODUCTION

Endometrial cancer is the most common gynaecological cancer in the UK. In 2018, there were almost 400,000 new cases diagnosed worldwide [1]. Advanced age is one of the most significant risk factors for the development of endometrial cancer with a median age at diagnosis of 63 years. However, up to 15% of cases occur in pre-menopausal women and 4% of cases arise in women under the age of 40 [2, 3]. The lifetime risk of developing endometrial cancer is 1.7%-3.1% [1, 4-6]. Reassuringly, most endometrial cancers are diagnosed early (70-80% in stage 1) and offer good prognosis with 5-year survival of over 95%. In cases where there is regional or distant spread the 5-year survival falls significantly (69% and 17% respectively) [3, 5].

The exact cause of endometrial cancer remains unknown; however, a number of endogenous and exogenous risk factors have been identified. One of the best established is chronic exposure to oestrogen as occurs in obesity, nulliparity and oestrogen only hormone replacement therapy (HRT) [7-14]. Indeed, one of the explanations for the rising incidence of endometrial cancer is its association with obesity [15]. In a meta-analysis by Bergstrom they estimated that the proportion of endometrial cancers due to obesity in European women was 39% [16, 17]. Diabetes and metabolic syndrome are also well recognised risk factors [18, 19].

Endometrial cancer is typically classified into two main histological groups: type 1, the more common endometrioid adenocarcinoma (accounting for 80-90% of cases) and type 2 comprising a heterogenous group of non-endometrioid cancers including: serous, clear cell, and undifferentiated carcinoma (10-20% cases). Type 1 tumours are linked to oestrogen excess, obesity and hormone-receptor positivity and are associated with a good prognosis. Type 2 tumours are more aggressive tumours more common in older non-obese women and have a worse prognosis.

Molecular data also supports division of these cancers into distinct groups [20]. Type 1 cancers are typically associated with alterations in *PTEN*, *KRAS*, *FGFR2*, *CTNNB1* and *MLH1* promoter hypermethylation [3, 21]. Microsatellite instability is more common in type I tumours [22]. Conversely, *p53*, *PIK3CA*, *PPP2R1A* mutations and *Her2/neu* overexpression are more common in type 2 cancers [23]. All these alterations are known as driver mutations, namely genetic alterations that give cancer cells a

fundamental growth advantage accelerating malignant transformation Interestingly, a recent study by Moore et al., looked at the mutational landscape of normal endometrium and found high rates of driver mutations in normal endometrial glands [24]. However, the burden of driver cell mutations increased with age and parity [24].

The Cancer Genome Atlas (TCGA) performed integrated genomic, transcriptomic and proteomic characterisation of 373 women with endometrial cancer, they identified not 2, but 4 distinct groups: (i) POLE (polymerase epsilon), (ii) microsatellite instability hypermutated, (iii) copy-number low (iv) copy-number high [21]. Together in combination with risk factors these molecular classifiers are effective at predicting prognosis [25].

Immunohistochemical markers and molecular alterations are also used to help distinguish benign endothelial lesions from pre-cancerous lesions. Precancerous lesions are classified using either the WHO schema based upon glandular complexity and nuclear atypia, or the endometrial intraepithelial neoplasia (EIN) diagnostic schema developed by the International Endometrial Collaborative Group [26]. The WHO classification system has 4 categories: (i) simple hyperplasia, (ii) complex hyperplasia, (iii) simple hyperplasia with atypia, and (iv) complex hyperplasia with atypia / atypical endometrial hyperplasia (AH). Loss of *PAX-2* by down regulation and loss of *PTEN* expression typically by mutation, occur in 70% and 40-50% of AH/EIN cases respectively [3, 27, 28]. The treatment for AH is often the same of endometrial cancer as up to 40% of patients with a diagnosis of AH are found to have concurrent endometrial cancer on histology following hysterectomy [29]. Typical endometrial hyperplasia; simple or complex, is associated with lower rates of cancer progression, 1% and 3% correspondingly [30].

Most endometrial cancers are still thought to be sporadic with only approximately 10% due to hereditary causes [31-33]. In those genetically predisposed women, Hereditary nonpolyposis colorectal cancer (HNPCC syndrome), also known as Lynch syndrome, is the most frequently encountered syndrome and accounts for 2-3% of all endometrial cancers [34]. Traditionally colon cancer is the most studied malignancy in this syndrome, although interestingly, endometrial cancer is the sentinel cancer to develop in more than 50% of women with this syndrome [35-37]. The lifetime risk of endometrial cancer is estimated as 40-60% in women with this syndrome [35]. Overall, these cancers present more commonly as type 1 though there is a higher proportion of type

2 cancers compared to the background population [36]. High levels of microsatellite instability are seen frequently due to germline mutations of the DNA mismatch repair genes *MSH2*, *MLH1*, *MSH6* or, methylation of *MLH1* in the sporadic setting [36].

2.1 Diagnosis of endometrial cancer

Endometrial cancer classically presents with postmenopausal bleeding (PMB), or intermenstrual bleeding. Postmenopausal bleeding is defined as bleeding that occurs at least one year after the last menstrual period. In the UK, this prompts urgent referral to a rapid access gynaecology clinic (RAC), to be seen within 2 weeks [38]. Reassuringly over 90% of these women will not have endometrial cancer and can be discharged home following assessment.

The recommendations for diagnosis and referral in the UK are a combination of guidelines derived from: the National Institute of clinical excellence, the European Society of Medical Oncology (ESMO), European Society for Radiotherapy & Oncology (ESTRO), European Society of Gynaecological Oncology (ESGO) and the Uterus commission of the German gynecological working group (AGO-S2K) [3, 30, 38-40].

A complete focused history is needed, including: an account of the presenting symptoms, establishment of any risk factors for malignancy, a full drug history, gynaecological history, relevant medical, surgical and family history. An abdominal and pelvic examination is then performed, the latter to rule out any other sources of bleeding such as lesions on the cervix, vagina or vulva.

Although routine management for these women does vary, in general a screening test is performed, typically a pelvic ultrasound to assess the endometrium followed by an endometrial biopsy when indicated. The biopsy can be taken blindly or under scan or hysteroscopic guidance. The pre-test probability of endometrial cancer in women presenting with postmenopausal bleeding is approximately 10%, but this increases with age and other risk factors [41]. There is also geographical variation; in a meta-analysis of over 40000 women with endometrial cancer, the pre-test probability was lowest in North America (5%) and Northern Europe (7%) and highest in Western Europe (13%) [42].

2.1.1 Techniques to evaluate the endometrium

2.1.1.1 Ultrasound

Postmenopausal women have a much thinner mean endometrial thickness than premenopausal women. Consequently, thickening of the endometrium may indicate the presence of endometrial pathology [43]. A normal endometrium in postmenopausal women is defined as a thin symmetrical endometrial line of less than 4–5 mm (average 2.3mm) double endometrial thickness in the sagittal plane [44, 45].

Ultrasound is routinely used as a screening test to identify women with thin regular endometrium, (whose endometrium is clearly visualised throughout) which are unlikely to have malignancy and can be reassured and discharged. Above this endometrial thickness threshold, an endometrial biopsy is recommended.

Ultrasound can be performed vaginally or abdominally. Doppler or colour flow can also be used to assess velocity and resistance in vessels, providing additional information. The administration of saline to distend the cavity; saline infusion sonography, can be used to enhance the view of the endometrial cavity. Each technique will now be evaluated.

Transvaginal ultrasound

Transvaginal ultrasound (TVUSS) also known as endovaginal ultrasound can be reliably used to assess endometrial thickness and morphology [46]. There are different endometrial thickness thresholds that may be used for recommending further investigation. However, there is a trade-off between sensitivity and specificity. A large and commonly cited met-analysis by Smith-Bindman et al in 1998 included 5892 women and found that the sensitivity of picking up women with endometrial cancer using TVUSS was 96% [47]. If an endometrial cut off value of ≤4mm is used, the risk of endometrial cancer is <1%, even in longitudinal studies with 10-year follow up [46].

However, a more recent individual patient data meta-analysis by Timmermans et al in 2010 with 2896 women had a significantly lower overall diagnostic accuracy than Smith-Bindman's study [48]. They reported that cut-off values of 3mm (i.e. endometrial thickness more than 3 mm warrants endometrial sampling), 4 mm and 5 mm had

sensitivities of 98%, 95% and 90% respectively [48]. To this end, the authors recommended the use of a 3mm cut off.

TVUSS is generally well tolerated, minimally invasive with minimal complications [43]. In premenopausal women normal endometrial thickness varies significantly during the menstrual cycle and so the value of TVUSS is more limited [44].

Similarly, women on tamoxifen have thicker endometrial linings compared to controls [32, 49] and this alters the diagnostic abilities TVUSS. Tamoxifen triples the risk of endometrial cancer and also increases the development of benign endometrial lesions [44, 50-54]. Interestingly, in a study by Lahti over 80% of women on tamoxifen had endometrial linings more than 5mm but on further investigation no cancer cases were observed [32, 55].

Additionally, in women on HRT, the findings of TVUSS should be interpreted with caution, as ultrasound cannot effectively discriminate between endometrial proliferation and cancer. The specificity for TVUSS in this group falls significantly: from 92% to 77% [47].

Abdominal Ultrasound

Transabdominal ultrasonography has been superseded by transvaginal ultrasonography in the majority of cases. It can be used as a complementary investigation in those women with a significantly enlarged uterus or in cases where a wider view of the pelvis or abdomen is required. It is also helpful in those women whom it is technically impossible to perform a TVUSS.

2.1.1.2 Saline-infusion sonography (SIS)

SIS is also known as sonohysterography, saline contrast hysterosonography, transvaginal sonography and fluid contrast augmentation. It is another technique that can be employed to evaluate the endometrium. It involves the insertion of a fine catheter into the endometrial cavity and insertion of sterile saline to separate the walls of the endometrium [56]. It has been used in the assessment of fertility patients, those with congenital uterine abnormalities or recurrent pregnancy loss and, in the last 15 years, in those with postmenopausal bleeding. SIS is easy to perform; safe and well

tolerated and has a high diagnostic accuracy; with a sensitivity of 95% and specificity of 88%, but with reduced feasibility in postmenopausal women [57].

Several small studies have found SIS superior to TVUSS in the assessment of women with postmenopausal bleeding [58-60]. During SIS, endometrial cancer can present as a diffuse thickening of the endometrium or a focal inhomogeneous mass. It is a helpful tool to discern if the abnormality is focal or global, aiding decision-making. One of the most consistent findings of SIS in endometrial cancer is the lack of distensibility of the cavity [61, 62].

2.1.1.3 3D, Power and Colour Doppler TVUSS

Angiogenesis is known to play a pivotal role in tumour growth. Studies have suggested that assessment of tissue vascularization by colour flow or power Doppler may be used to discern benign from malignant endometrial changes; with malignancy associated with increased blood flow [63]. At present, the value of colour flow and power Doppler in the diagnosis of endometrial cancer remains controversial.

A variety of measurements have been used to assess the neovascularization of endometrial lesions. Some studies have evaluated the blood flow in uterine arteries, using a number of parameters such as: the vascularity index, pulsatility index, resistance index, maximum end-diastolic velocity, time-averaged maximum velocity and peak systolic velocity [64-69]. Of these, a reduction in the resistance and pulsatilitiy indices of uterine arteries, particularly in those women with postmenopausal bleeding and a thickened endometrium appears to be the most promising finding [65, 67, 68]. Other studies have looked at the blood flow characteristics of the intratumoural arteries [70, 71].

Studies are generally small however, and differences in definitions, methodology and metrics being recorded limits comparison between studies. In an effort to minimise this shortfall, the International Endometrial Tumour Analysis group (IETA) provided a consensus opinion in 2010 and 2018; defining terms to aid comparison [72, 73].

The visualization of a feeding blood vessel to a polyp can also be seen on colour Doppler; aptly named the pedicle artery sign and has a high positive predictive value

for intracavity pathology [74]. Furthermore, atypical endometrial polyps are associated with low blood flow resistance [75].

There has been conflicting data as to whether 3D is helpful in the investigation of women with postmenopausal bleeding [64, 76-80]. In Gruboeck et al. study of 103 symptomatic women, an endometrial volume of 13ml diagnosed endometrial cancer with 100% sensitivity and 98% specific [76]. However, prospective studies failed to achieve such good results (sensitivity 70%) [81]. These studies suggest a limited role for 3D ultrasound and volume measurements in the diagnosis of endometrial cancer [81].

A number of mathematical models have also been developed to calculate the risk of malignancy in women with postmenopausal bleeding based on sonographic features [82, 83]. Dueholm created a risk of endometrial cancer score (REC) using a mathematical model derived from TVUSS and SIS features including Doppler. It has good diagnostic accuracy but needs to be prospectively tested [84].

2.1.1.4 Hysteroscopy

This procedure allows direct visualization of the endometrial cavity and endocervical canal. In addition, it enables directed biopsy of any visualized abnormality. During hysteroscopy either fluid or carbon dioxide (CO2) can be used as a distension medium [85]. As CO2 does not allow for clearing of fluid and endometrial debris, the image quality is not as good; subsequently CO2 is not commonly used in practice; there is also a risk of gas embolism. Normal saline, Ringers lactate and Hartmanns solution are the most commonly used distension mediums. In cases where monopolar electrosurgery is performed glycine or glucose solution are frequently used as they are non-conductive; though are associated with higher rates of hyponatraemia.

In the UK, a vaginoscopic 'non-touch' approach is now considered the standard technique for outpatient hysteroscopy, especially where successful insertion of a vaginal speculum is anticipated to be difficult [86]. It is associated with lower procedural pain compared to diagnostic rigid outpatient hysteroscopy [87].

The advent of small diameter hysteroscopes (3-4mm), flexible hysteroscopes, smaller

operative instruments and a vaginoscopic approach, has meant that office, also known as ambulatory or outpatient hysteroscopy, has rapidly expanded. Inpatient or day case hysteroscopy under general anaesthesia remains an option in those who can tolerate the outpatient procedure due to cervical stenosis or discomfort; and in those who have had an inadequate outpatient biopsy.

Two large systematic reviews have shown that hysteroscopy has a high diagnostic accuracy in diagnosing endometrial cancer in women with abnormal uterine bleeding [88, 89]. A positive hysteroscopy increased the probability of cancer to 71.8% (pooled likelihood ratio 60.9), whereas a negative hysteroscopy result reduced the probability of cancer to 0.6% (pooled likelihood ratio of 0.15) [88].

Hysteroscopy is also a more sensitive tool for the detection of polyps and other benign endometrial lesions, which may contain cancer, compared to other methods of endometrial sampling [32]. The sensitivity for diagnosing AH at hysteroscopy is significantly lower than for endometrial cancer, 75% versus 83% respectively [90, 91]. It should also be noted that a normal hysteroscopic image does not always exclude malignancy, supporting the need for histology in those women with thickened endometrium [44, 88, 92].

Hysteroscopy has also been shown to be safe, with a low failure rate (4%) and a low incidence of serious complications (0.1- 1%) [88, 89, 93]. In practice it is often coupled with an endometrial biopsy, usually a pipelle or directed biopsy in the outpatient setting and curettage when performed under general anaesthesia.

2.1.1.5 Endometrial Biopsy

A definitive diagnosis of endometrial cancer remains histological (Figure 1 and 2). Over the last 3 decades there has been a rapid expansion in endometrial biopsy techniques that can be performed as an outpatient, colloquially these are referred to as office or outpatient endometrial biopsy (OEB) methods. Historically, dilation and curettage (D&C) used to be the norm, however, OEBs have now largely replaced conventional D&C, for convenience and cost. Hysteroscopic and ultrasound guided biopsies can also be used to provide targeted biopsies.

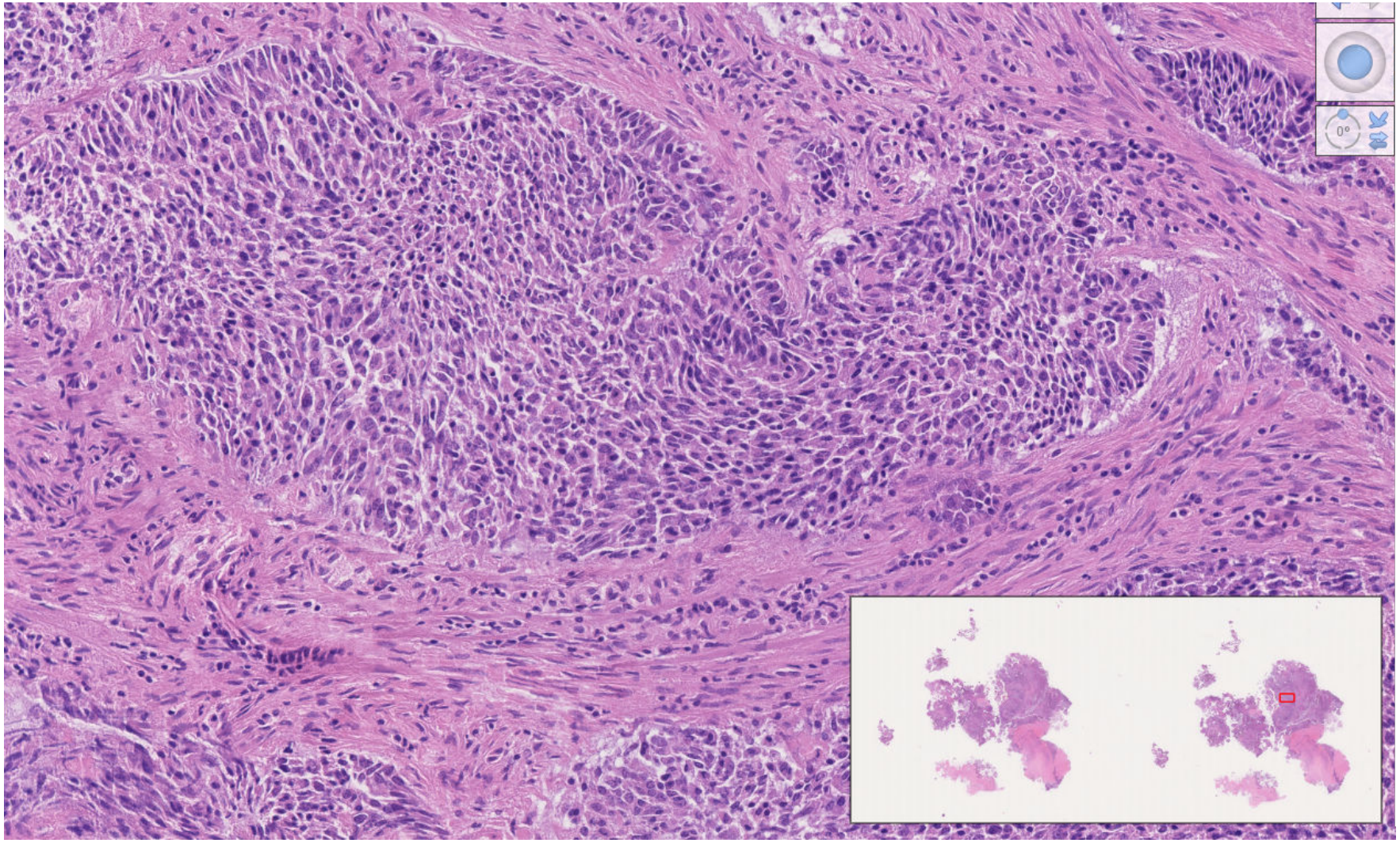


Figure 1. Histological image of an endometrial biopsy taken from a patient with grade 1 endometrioid endometrial cancer.

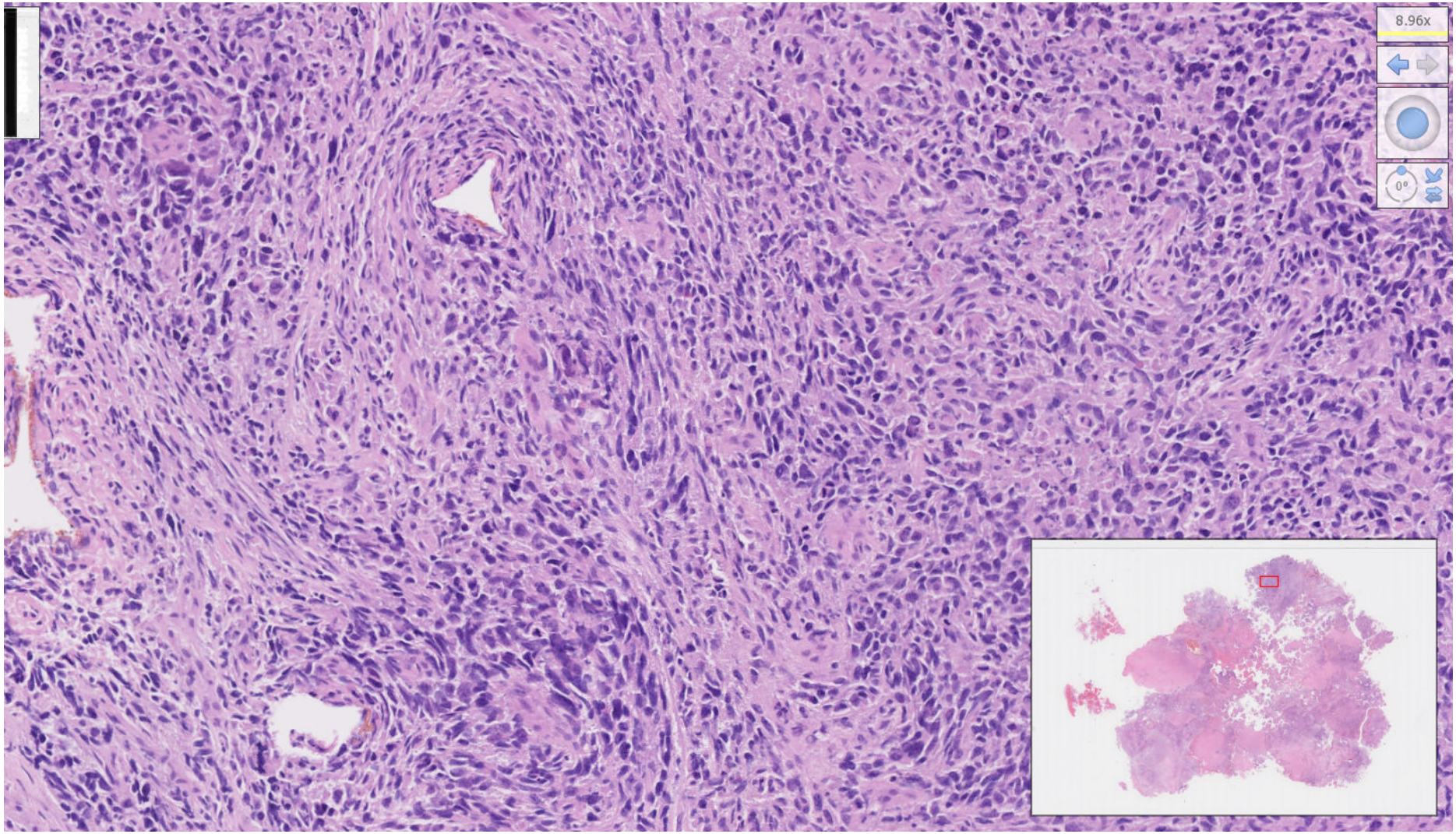


Figure 2. Histological image of an endometrial biopsy taken from a patient with carcinosarcoma of the uterus (a form of type 2 endometrial cancer).

Office endometrial biopsy.

A number of different OEB instruments are currently available in the outpatient setting; most are based on the plastic disposable pipelle de cornier prototype (see Figure 3). The pipelle device is the most extensively used; it is a small catheter (2.9mm inner and 3.1 outer diameter) that is introduced into the endometrial cavity and suctions cells. Other devices available include: accurette, gynoscann, pipelle mark 2, novak curette, uterobrush, Tao brush, H pipelle, cornier pipelle, explora, mi-mark spiral sampler, graclee jet washer, vabra aspirator, endopap, z sampler and endosampler.

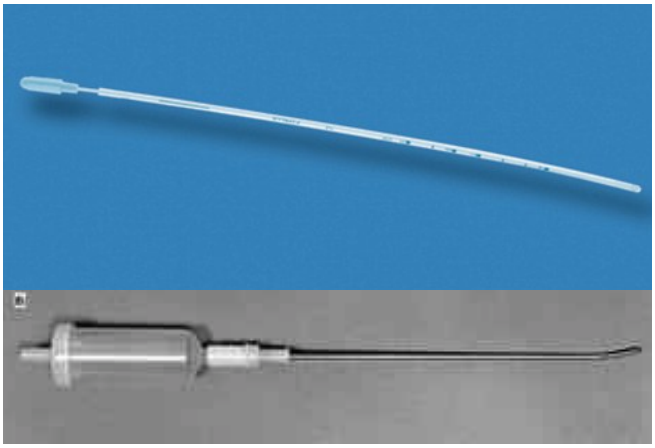


Figure 3. Outpatient endometrial biopsy devices.
Top Pipelle, bottom Vabra aspirator

Outpatient endometrial biopsy procedures have been shown to have high diagnostic accuracies in diagnosing cancer [94, 95]. In a systematic review including 11 primary studies and 1013 subjects, the pre-test probability of cancer increased from 6. 3% to 81.7% (likelihood ratio of 66.48) with a positive result; and decreased to 0.9% (pooled likelihood ratio 0.14) with a negative result [94]. A meta-analysis has shown that the pipelle device was the best sampling device with a sensitivity of 91 and 99% for premenopausal and postmenopausal women respectively [95].

Office endometrial biopsy requires little of no dilatation of the cervix, and can therefore be performed easily in outpatient clinics, with little or no anaesthesia. It is fast and cost effective compared to inpatient procedures.

An inherent limitation of these office endometrial biopsy techniques is that it is a blind technique and may miss focal lesions. In a study by Guido et al, 65 women undergoing a hysterectomy with known endometrial cancer had a pipelle sample prior to surgery; the biopsy missed 11 cases of endometrial cancer, of which 5 had tumours only present in an endometrial polyp [96]. In all 11 cases the pathology involved <50% of the endometrium [96]. A further larger meta-analysis by Clark et al., reassuringly, had better success, and only missed 3 cases of endometrial cancers amongst 807 women with adequate samples [94]. In their meta-analysis the overall failure rate was 7% and inadequate sample rate was 15% [94].

Dilation and Curettage (D&C)

This still remains the gold standard in some countries. Typically, it is performed under general anaesthesia and following hysteroscopy. Though largely replaced by office endometrial biopsy it is helpful in cases where the office biopsy is non-diagnostic or insufficient, and in high-risk cases (persistent symptoms, thickened endometrium on TVUSS or multiple risk factors). One of the biggest limitations of D&C is the lack of complete sampling – only 60% of the cavity is sampled on average [32, 95]. It has a false negative rate of 2-6% for endometrial cancer and hyperplasia, and a 1-2% complication rate [97]. Curettage of the cervical component has particularly high false positive (25-50%) and negative rate (10%) [32].

Studies have shown that D&C is a more accurate depiction of tumour grade than office endometrial biopsy techniques such as the pipelle. To this end, those women with grade 1 endometrioid carcinoma or AH who are being managed conservatively as part of fertility sparing management in young women - D&C is the preferable method of tissue sampling [98, 99].

Hysteroscopic guided biopsy

Hysteroscopic biopsy enables the clinician to directly visualise the cavity and biopsy under vision; thus, reducing sampling errors. In a study by Gimpelson and Rappold 276 women underwent hysteroscopy and directed biopsies and dilatation and curettage. In 223 cases, the results of hysteroscopy and curettage were congruent [100]. In 44 cases, hysteroscopy revealed more information than curettage. This

supports hysteroscopic biopsy being more accurate than other methods; such as D&C [100]. Hysteroscopic directed biopsy has also been shown to be more accurate than office endometrial biopsy at distinguishing AH from endometrial cancer [101].

Furthermore, a more recent study by Tinelli et al., investigated 752 women with postmenopausal bleeding who underwent a TVUSS, outpatient hysteroscopy and directed biopsy [102]. Hysteroscopy had a high sensitivity (98%) and negative predictive value (98%). In three cases hysteroscopy revealed an atrophic endometrium but biopsy showed endometrial carcinoma [102]. This confirms the need to perform endometrial biopsy on all women who undergo hysteroscopy for postmenopausal bleeding.

Ultrasound guided biopsy

In theory an ultrasound-guided biopsy using bettocchi forceps or equivalent can be used instead of hysteroscopy-guided biopsies for targeting sampling of the endometrium. In the literature, predominately case reports exist; showing its use in the context of investigations for postmenopausal bleeding in women with cervical stenosis [103]. This was followed by more recently by one larger retrospective study using abdominal ultrasound to guide OEB [104]. However, the technique of ultrasound-guided biopsy is ubiquitous when used elsewhere in the body. It is frequently used to provide histological diagnosis of pelvic masses, (presumed ovarian origin), both abdominally and transvaginally. Potentially ultrasound guided biopsies could be used as a cheaper and less painful alternative to a hysteroscopy directed biopsies – its feasibility and diagnostic ability have yet to be fully evaluated.

2.1.2 Analysis of the histology

Once the endometrial biopsy is performed, it is sent to the histologist for further examination. Histological analysis may take several days, and patients are either brought back to clinic for discussion of the results or are given a telephone appointment. In cases where the endometrial biopsy is non-diagnostic, the patient is usually brought back for a hysteroscopy (if not already performed).

Units that able to perform an ultrasound, outpatient hysteroscopy and biopsy during the initial consultation are referred to as one-stop clinics and are based on the same

model as rapid access breast clinics. They help reduce hospital admissions, waiting lists and hospital visits per patient [105, 106].

Frozen sections are a well-recognised method of providing rapid microscopic analysis of histological specimens. It is currently used in oncological surgery, in the assessment of suspicious adnexal masses to provide intra-operative diagnosis [107]. It has also been used to look for the presence of chorionic villi in women with suspected ectopic pregnancies; albeit with poor results [108]. Thus far, it has not been used in rapid access gynaecological clinics to provide point of care diagnosis.

Point of care (POC) diagnosis whereby an endometrial biopsy taken in clinic can be analysed in the same session would help streamline patient management further and prevent patients being brought back into clinic on another day. Novel diagnostic tests, such as rapid evaporative ionization mass spectrometry may also enable point of care diagnosis in clinic, however, these have yet to be evaluated.

2.2. Additional Considerations

2.2.1 Recurrent symptoms

Recurrent postmenopausal bleeding is common, and if recurrent bleeding persists the same diagnostic investigations should be repeated as normal findings on both imaging and histology does not exclude endometrial cancer with 100% certainty [44].

In women with an endometrial thickness greater than 4 mm at initial presentation, who were discharged following confirmation of benign endometrial sampling, on average, 20% of women will represent back to clinic with recurrent symptoms, most within a year [109].

In women who were discharged following a reassuring scan with an endometrial thickness ≤ 4mm with postmenopausal bleeding, 10% of women re-presented with bleeding within 5 years [110]. Of these, 8% were diagnosed with cancer on repeat investigations [110].

Overall, however, women presenting with recurrent bleeding, are less likely to have premalignant or malignant disease compared to first attenders, with endometrial

polyps being more common [111]. Hence, tests with a high accuracy of diagnosing focal disease are recommended. In practice this usually involves a hysteroscopy as part of the diagnostic work up.

2.2.2 Risk of dissemination of cancer

Historically, it was thought that hysteroscopy might disseminate malignant endometrial cells into the peritoneum, because of the increase in intrauterine pressure during distention media inflation, thereby potentially upstaging cancer and decreasing survival. It is known that hysteroscopy flushes endometrial cells into the abdomen. In a randomised study investigating infertile women with concomitant laparoscopy and hysteroscopy; endometrial cells were found in 7% of women before and 25% of women after hysteroscopy [112, 113].

Two large meta-analyses, the most recent of which included 2944 women, have shown that hysteroscopy does in fact result in higher rates of positive peritoneal cytology compared to no hysteroscopy, particularly with a liquid distension medium [114, 115]. However, hysteroscopy did not appear to increase the risk of adnexal, abdominal or retroperitoneal lymph node metastases [116].

Similarly, there is also a potential risk of dissemination of malignant cells with saline infusion sonography. Subsequently, if an endometrial biopsy confirms malignancy SIS and hysteroscopy should be avoided.

The prognostic significance of isolated malignant cells in the peritoneal cavity remains uncertain. The pathophysiology of metastasis is complex. Even tiny tumours release vast numbers of cancer cells, but most women will never relapse or will do so after a prolonged period of remission. Cancer cells by nature are invasive and motile and can therefore end the circulation, or peritoneum in the case of endometrial cancer long before a cancer diagnosis is made [117]. While most of these cells die, a handful of cells will survive and colonise distant organs and spread. This relies on several factors according to the ‘seed and soil’ theory including: organ infiltration, escape of the immune system, growth of tumour cells and survival in supportive niches and microenvironment [117-120].

Current thinking suggests that dissemination of cancer cells (DCC) from primary to distant sites happens fairly early on in the course of disease [121-123]. Studies looking at genomic similarities between primary tumours and late metastasis have variable results – some showing highly similar genetic profile between the two which suggests that the metastasis was caused by late DCC, others studies have shown very different genomic profiles suggesting very early DCC [121, 124].

Tumour dormancy is well recognised phenomena [118], with the observation of relapse many years after the removal of the primary tumour, with rates of late metastasis (>5 years) reaching almost 10% in endometrial cancer [125]. Tumour dormancy, also known as metastatic latency, can be a at a single cell level or tumour mass level. At tumour mass level inadequate recruitment of blood vessels and attack by the immune cells are thought to be key players [118].

In endometrial cancer, Changs's review found no association between preoperative hysteroscopic examination and worse prognosis [114]. However, only 6 studies were included in Chang's meta-analysis evaluating prognosis and they all had small sample sizes with short follow up-durations. The lack of follow-up in these studies will not be able to address any potential concerns about tumour dormancy and late recurrence due to DCC into the peritoneum. Furthermore, as normal saline hysteroscopy is so widely used as part of the investigative work up, until recently, there was no way to establish this with certainty.

2.3 Following a diagnosis of cancer

2.3.1 Pre-op planning and Staging

Once women have a confirmed histological diagnosis of endometrial cancer, they require immediate referral to a specialised oncological centre. Patients are then assessed for fitness for surgery and further imaging is performed to stage the cancer and assess for extrauterine spread.

The International Federation of Gynaecology and Obstetrics (FIGO) is the most commonly used staging system (see Table 1). The classification system was first

developed in 1958, but then altered from clinical to surgical-pathologic system in 1988 [126-128]. This was mainly due to the results of the GOG 33 study which demonstrated that clinical staging was incorrect in over 20% of cases [44, 129]. The staging system was revised again, in 2009, for the first time in over a decade to reflect the significance of histopathological prognostic indicators [32, 128, 130]. Of note, positive peritoneal cytology has been excluded from the surgical staging and involvement of the endocervical glands of the cervix is now considered as stage 1 cancer [130].

Stage 1 – confined to the Uterus
1A Tumour confined to Uterus no or <50% myometrial invasion
1B Tumour confined to Uterus, >50% myometrial invasion
Stage 2 – Extension to the cervical stroma, but not beyond uterus
Stage 3 –Local and/or regional spread
3A Tumour invades serosa and/or adnexa
3B Vaginal and/or parametrial involvement
3C1 Pelvic node involvement
3C2 Para-aortic node involvement
Stage 4 – Invasion to distant organs or distant metastases
4A Tumour invasion to bladder and/ or bowel mucosa
4B Distant metastases including abdominal metastases and/or inguinal lymph nodes

Table 1. 2009 FIGO endometrial cancer stages.

Pre-operative investigations include a number of blood tests (full blood count, serum electrolytes and kidney function, liver function tests, group and save), urinalysis and a chest X-ray. A CT scan of the chest, abdomen and pelvis may be helpful in selected cases (such as sarcomas). Positron emission tomography with fluorine-18- labelled 2-fluoro-2-deoxy-D-glucose (PET- CT) is costly and only moderately sensitive for extra-uterine disease and is not routinely used for staging [44, 131, 132].

Accurate staging of the cancer is needed to identify women most at risk of metastatic disease who would require more radical surgery, lymph node evaluation and subsequent tailoring of adjuvant treatments. In particular, imaging should assess the depth of myometrial invasion, presence of cervical invasion, pelvic and lymph node

enlargement. A contrast-enhanced dynamic MRI remains the current gold standard for assessing for uterine and locoregional pelvic extension of the disease [3, 39]. A large meta-analysis comparing CT, USS and MRI imaging in staging endometrial cancer, found that contrast MRI had highest efficacy, with an accuracy of approximately 91% [133, 134].

The MRI process is complex, time-consuming, and costly. A significant proportion of women are unable to undergo or complete an MRI scan due to their morbid obesity or claustrophobia. Whilst open MRI exists to minimise this problem, they are more expensive and not readily available. To this end, many have assessed the role of ultrasound in the pre-operative assessment of endometrial cancer, as a cheaper and easier alternative to an MRI. It has been shown to have moderate diagnostic performance in the detection of deep myometrial infiltration [135]. During ultrasound either subjective or objective methods can be used to assess depth of invasion [136].

There is a paucity of data on the role of 3D ultrasound in the assessment of myometrial invasion [137-142]. Of the studies performed, most are promising [137, 139, 140]. Three dimensional ultrasound has several advantages in assessing invasion; in particular the coronal view may add valuable information about myometrial invasion in the uterine corners and 3D rendering techniques may enhance tissue demarcation [138, 139]. Furthermore, it has low observer variation [138] and images can also be stored and rendered to provide volume measurements.

Other methods used for the assessment of deep myometrial invasion include: intra-operative gross visual estimation and frozen sections. Intra-operative gross visual estimation can be used to assess depth of myometrial invasion and help select patients who might benefit from pelvic lymphadenectomy [143, 144]. In a pooled meta-analysis the pooled sensitivity was 75% [144].

Frozen section analysis involves flash-freezing the specimen, followed by sectioning and staining the sample without a proper embedding process, and only takes 20-30 minutes. By contrast, standard histological examination involves fixation, embedding, staining and sectioning which takes several hours, and is also dependent on the subjective assessment of morphological features in the specimen. Studies have reported that frozen tissue analysis can determine tumour grade and myometrial

invasion with a reasonable accuracy [145-150]. In a large meta-analysis by Alcazar including 35 studies, intraoperative frozen section was found to have better diagnostic performance than intraoperative gross evaluation in the detection of deep myometrial invasion [151]. A limitation with both these approaches is the inability to preoperatively plan the surgical procedure.

Ca-125 is a tumour blood test commonly used in the assessment of women with suspected ovarian cancer. Studies have also assessed its use in the evaluation of endometrial cancer [152-156]. It is raised more commonly in women with type 2 cancers or advanced cancers; however, a normal result does not exclude malignancy [152]. Currently there is not enough evidence to support its routine use in clinical practice.

2.3.2 Surgery

Approximately 70-80% of patients diagnosed with endometrial cancer present early in FIGO stage 1. In these cases, surgical treatment is routinely recommended. This involves a hysterectomy and bilateral salpingo-oophorectomy. Previously this was performed as an open operation, namely a laparotomy. More recently, the procedure is commonly performed laparoscopically as several large meta-analyses (which include data from the commonly cited LACE trial) reassuringly showed no significant difference in survival and recurrence between the open and keyhole procedure [157-160]. Keyhole operations also improve recovery and reduce length of stay in hospital [158].

The role of lymphadenectomy (pelvic and para-aortic) in the surgical management of women with stage 1 endometrial cancer has not been fully elucidated. This has led to significant variations in practice worldwide. In the UK, pelvic lymphadenectomy is not routinely performed for Stage 1 disease unless high risk features. This is supported by the Cochrane collaboration review and findings from the ASTEC trial; which did not find any evidence of survival benefit or reduction in disease when lymphadenectomy was performed [161, 162]. Conversely, in the USA, pelvic lymphadenectomy is routinely performed. The outcome of these women suggests an improved survival in women with stage 1 grade 3 who undergo a lymphadenectomy [163]. One of the pitfalls of previous trials investigating lymphadenectomy was the lack of clear protocol

regarding adjuvant treatment post-surgery. The newest STATEC trial, looking at the role of lymphadenectomy to direct adjuvant therapy for high risk endometrial cancer, hopes to clarify the uncertainty in this field [164].

Pelvic and especially para-aortic lymphadenectomy are complex procedures and add significant morbidity. To this end, many have advocating only performing the procedure in those with affected lymph nodes. Pre-operative diagnosis of involved lymph node metastasis with MRI or CT has a reported accuracy of up to 90% [165], but cannot replace surgical staging. Intra-operative palpation has been proposed by some as a useful technique to assess for metastasis. However, this is impossible for patients undergoing robotic or laparoscopic surgery. Furthermore, it has been shown that even amongst experienced gynaecological oncologists a high proportion of positive lymph nodes are missed (36%) [166]. Frozen sections have not been found to be beneficial either, as it tends to upstage cancer.

An alternative technique is the utilisation of sentinel lymph nodes (SLN). The aim of using this tool is to target the lymph nodes that are the most likely to be involved with metastatic cancer cells (sentinel lymph nodes) and thereby limit the extent of surgery. The main benefits of adopting sentinel nodes regards pathological ultrastaging with the potential to detect low volume disease not detectable by conventional histological examination and avoiding the morbidity associated with full lymphadenectomy [164, 167-169].

One of the earlier studies by Favero et al; 42 women with endometrial cancer were injected with Tc-99 hysteroscopically underneath the tumour minutes before definitive surgery [170]. In their study the specificity of sentinel lymph nodes was 100% but the sensitivity was only 58% [170]. The larger multicentre FIRES study with almost 400 patients reported high rates of SLN detection [171]. This has been followed up by 3 consecutive meta-analyses [167, 172, 173], which reported an overall sentinel lymph node detection rate of 87%, bilateral pelvic node dissection rate of 61% and 6% for para-aortic detection [173]. Use of indocyanine and cervical injection increased the bilateral sentinel lymph node dissection rate [164].

Rapid intraoperative cytological assessment using peritoneal washing cytology and imprint cytology of pelvic lymph nodes has recently been evaluated in a study by

Anastasiadis [174]. They achieved good correlations with standard histological diagnosis (23% versus 26.2%) [174]. Additionally, novel techniques such as Rapid Evaporative Ionization Mass Spectrometry (REIMS) rapid may help determine if lymph nodes are involved and aid intra-operative decision-making. The histological diagnosis and mass spectrometry spectra of the metastasis can be compared to the primary tumour, to provide clues in the pathophysiology of cancer.

In women with more advanced disease (stage 2+) a modified radical hysterectomy is performed including a hysterectomy, bilateral salpingo-oopherectomy, lymph node dissection and omentectomy. Maximal debulking surgery should be offered if patients are good surgical candidates as it confers a survival benefit [175]. If macroscopic extrauterine disease is found unexpectedly at the time of operation a conversion to a midline laparotomy is advocated [44].

Some gynaecological oncologists believe that there is a risk of upstaging cancer and disseminating cancer cells outside the uterine cavity and into the surrounding vaginal tissue during instrumentation of the uterus at hysterectomy (thereby increasing the chance of vaginal vault recurrence). These concerns have arisen as studies have shown a high frequency of positive peritoneal cytology when using a uterine manipulator at hysterectomy [176]. Therefore a minority of surgeons have avoided using an intrauterine manipulator [44].

2.3.3 Further treatment

Following surgical treatment women will be seen back at clinic to discuss further follow up and management. This may involve radiotherapy and/or chemotherapy. This decision will be influenced by both patient factors and disease factors (grade, stage and type of cancer). Recent innovations may enable greater use of individualised medicine. Various immunohistochemical and DNA sequencing techniques have been developed so that they can be performed on formalin-fixed, paraffin embedded tissues; these include: L1 cell adhesion molecule (L1CAM), markers of the *p53* pathway, hormone receptor expression and microsatellite instability [22, 25, 164, 177-183].

Furthermore, radiomics and the extraction of large amounts of quantitative features from medical images of a given modality can provide a comprehensive quantification

of tumour phenotype. A combination of genomics, biomarkers, imaging and mass spectrometry data of the individual tumour may also help classify disease, prognosticate patients and enable individualised treatment and monitoring.

2.4 New technologies

2.4.1 USS guided biopsy

As discussed previously, whilst ultrasound guided biopsies are ubiquitous in interventional radiology, its role in the diagnosis of endometrial cancer has not been established or evaluated. A handful of case reports and papers discuss its use. As part of this PhD, the acceptability and feasibility of USS guided biopsy in women with suspected endometrial cancer will be performed. Please see Chapter 5 for a comprehensive evaluation of the studies to date.

2.4.2 Three-dimensional (3D) ultrasound

In the last 20 years there has been a rise in the use of 3D ultrasound as it has become commercially available. A critical review by Jurkovic discussed the current evidence regarding 3D ultrasound in endometrial cancer [81]. Evidence is lacking in the role of 3D ultrasound in the assessment of myometrial invasion. To this end, Chapter 6 and 7, will attempt to establish the diagnostic ability of 3D ultrasound in the assessment of myometrial invasion, first by performing a clinical trial (Chapter 6) followed by systematic review and meta-analysis of studies to-date (Chapter 7).

2.4.3 Rapid evaporative ionization mass spectrometry

Mass spectrometry in general

Mass spectrometry (MS) is an analytical technique that has been around over a century. It involves ionising and fragmenting solid, liquid or gas states and measuring the resultant mass-to-charge ratios (m/z) of gas phase charged ions [184]. The ions are separated by their mass-to-charge ratio by accelerating and deflecting them by electric or magnetic fields. The m/z values and their relative intensities are typically presented as a mass spectrum. Ionic species can then be identified by their m/z values using libraries of previously characterised compounds.

There are 3 key components of a mass spectrometer: an ion source, mass analyser and detector. The ioniser converts the sample to ions. A number of ionisation techniques exist depending on the phase of the sample and the amount of energy needed. Ionisation techniques are typically classified into hard and soft. Hard ionisation imparts high quantities of residual energy into the molecule causing large degrees of fragmentation. The most common example is electron ionisation, which is frequently used for the interrogation of gas phase states.

Conversely, soft ionisation processes impart little residual energy and therefore results in less fragmentation [184]. Common examples include chemical ionisation, electrospray ionisation (ESI), desorptive electrospray ionisation (DESI) and matrix assisted laser desorption ionisation (MALDI). MALDI and ESI techniques sample source material directly, ideal for biological samples, however, the sample needs to be in a vacuum [184]. Ambient ionisation techniques such as: DESI and rapid evaporative ionisation MS (REIMS) overcomes this limitation. Ions form outside the vacuum of the mass spectrometer. This has revolutionised MS of biological samples, as ambient ionisation techniques require little or no sample preparation, no chromatography and it facilitates the manipulation of samples during data acquisition [184].

MALDI, secondary ion mass spectrometry (SIMS) and DESI are emerging MS imaging tools. In the latter, samples of histological slides are taken and imaged pixel-by-pixel; producing mass spectra for each pixel [185]. It can therefore provide topographically localized biochemical information to supplement standard histopathological classification systems [186]. It has several advantages: it requires very little pre-processing (only requirement is fine 10nm slides and cryo-freezing), it can be performed in ambient atmospheric conditions and provides very high-resolution images [185]. The biggest disadvantage is processing time.

The second key component of a mass spectrometer is the mass analyser, which separates ions, usually electrically based on their m/z values [184] . The four most widely used analysers are: quadrupole, quadrupole ion trap, time of flight (ToF) analyser and the Fourier transform ion cyclotron resonance [184]. Each analyser will vary with respect to size, resolution, mass range and cost. ToF uses an electric field to accelerate the ions through the same potential, and then measures the time they take to reach the detector; ions with lower mass will reach the detector first [184]. A

quadrupole analyser uses oscillating electrical fields to stabilize or destabilize the paths of ions passing a quadrupole (a radio frequency created between 4 parallel rods). This enables selective ions in a certain range of mass/charge ratio to pass through the system at any time, thus acting as mass filter [184]. Hybrid Quadrupole ToF (Q-Tof) are now increasingly common analysers and combine benefits of both processes.

The last key component is the detector, which records the charge induced when an ion hits its surface. In a scanning instrument this signal is usually generated every second, producing a mass spectrum, a plot of intensity as a function of the mass-to-charge ratio.

Rapid evaporative ionization mass spectrometry (REIMS)

Rapid evaporative ionization mass spectrometry is an emerging ambient MS technique described by Takats in 2009. It uses standard electrosurgical methods to convert tissue constituents into gas-phase ionic species amenable to mass spectrometry [187-189]. REIMS is the coupling of electrosurgical dissection (handheld diathermy, laser surgery or ultrasonic aspiration), which provides the ion source with a Q-Tof mass spectrometer, see Figure 4 [187]. The employment of standard electrosurgical tools, such as diathermy and CO2 laser, with smoke extraction to generate surgical aerosol makes this an ideal tool for intraoperative and clinical use. The combination of REIMS technology with paired histological spectral libraries has been coined the iKnife or ‘intelligent surgical device’; and it enables near-real-time characterisation of human tissues in vivo and ex-vivo (Figure 5).

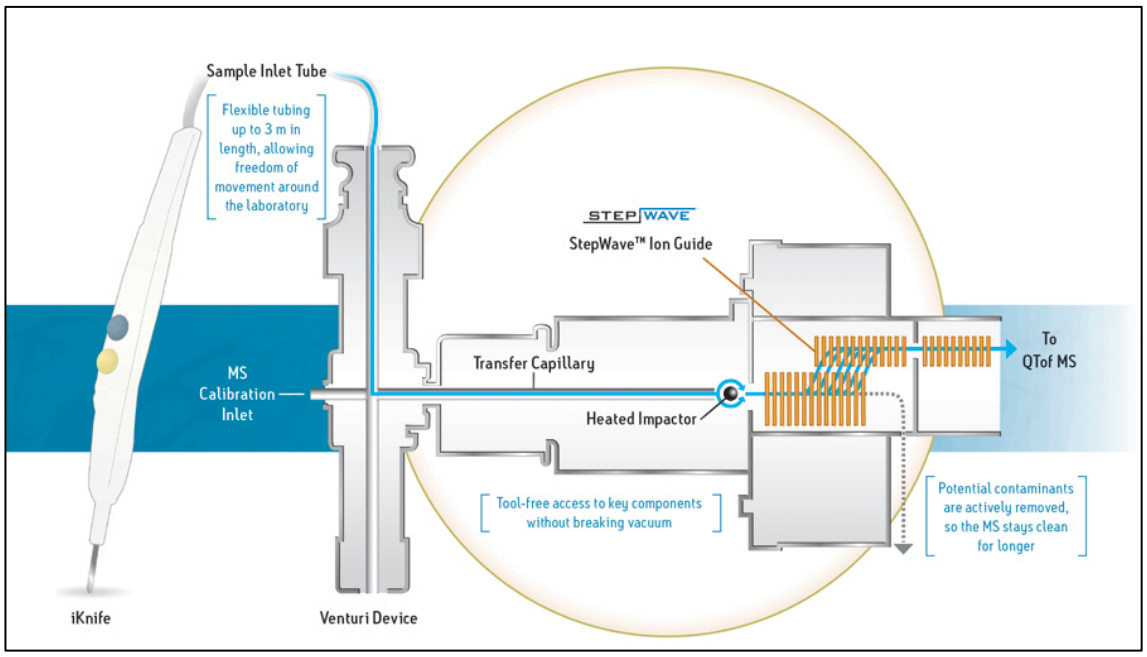


Figure 4. Pictorial diagram of REIMS, image taken from the Waters Corporation website [190].



Figure 5. Photographs of the iKnife apparatus. On the left the mass spectrometer and handheld diathermy device on right, as used in this PhD.

Studies have shown that all human tissues have distinctive phospholipid characteristics; and it is these that are interrogated by mass MS to provide a tissue signature [187]. The compounds identified by REIMS vary, but include: phosphatidylethanolamines (PE), phosphatidylcholines (PC), phosphatidylinositols (PI), sphingomyelins and cardiolipins, which are all in the 600-900 m/z range [187]. Whilst, these compounds are abundant in human tissue, the pattern and distribution of these lipids are diagnostic. The iKnife then uses a combination of principal

component analysis (PCA) and linear discriminant analysis (LDA) to translate these spectral data into more relevant clinical information.

Currently, large spectral reference libraries exist for liver, lung, breast, colorectal and brain both in-vivo and ex-vivo. Ex-vivo studies have demonstrated clear identification of major tissue types; lung, colon and liver [187] based on the distinct pattern of lipids present. Studies have also shown that the iKnife can identify microbiological species such as Candida on growth plates [191], detect fish fraud [192] and identify doping in cattle [193] .

Clinical use of REIMS

The surgical aerosol produced by tissue ablation harbours a plethora of information that can help intra-operative decision-making and diagnoses. It has been used in vivo to identify intestinal cancer, polyps and the origin of metastatic lesions [194]. In Alexander et al., study of 28 patients undergoing endoscopy the iKnife had overall accuracy of 94.4 % for the detection of cancer versus adenoma [195]. They also found that colonic cancer over-expressed long-chain phosphatidylserines (PS) and phosphatidylglycerols whilst adenomas overexpressed ceramides [195]

The iKnife has also been used in cancers where margin status is exceedingly important: brain and breast cancer [196, 197]. In breast cancer almost 25% of patients require a re-operation for positive resection margins, following breast-conserving surgery. In a pilot study of 113 patients, a classification model using histologically validated spectral data provided a 93.4% sensitivity and 94.9% specificity for the detection of tumour [196]. Cancer specimens had higher rates of glycerophospholipids, particularly, with PEs, PCs, phosphatidic acids (PAs), phosphatidylserines (PSs) and phosphatidylglycerols (PGs) [196].

In the field of gynaecology, Takats and Ghaem-Maghamis' group and Takats and Kyrgiou group have evaluated the used of the iKnife in ovarian and cervical disease respectively. In a pilot study of 87 women with suspected cervical disease, the iKnife discriminated with 100% accuracy normal vs. HPV ± CIN vs. cancer [198]. Furthermore, data by Takats and Ghaem-Maghamis' group have shown that REIMS

technology can distinguish between normal, benign, borderline and malignant ovarian masses with over 90% diagnostic accuracy [199].

This PhD is the first to investigate the application of REIMS in women with suspected endometrial cancer. If successful, this technology can be used in the rapid access gynaecology clinic to provide point of care diagnosis of endometrial cancer from an endometrial biopsy. It may also enable accurate assessment of lymph node involvement to help intra-operative decision-making.

2.4.4 Radiomics

Over the last decade there has been an evolution in medical imaging. Significant advances in medical hardware, imaging agents, standardised protocol imaging and imaging analysis have paved the way for individualised medicine [200]. Treatment is then tailored to the specific features of the disease and the patient. Genomic and proteomic technologies have provided molecular characterisation of human tissue and now imaging can also be used to capture tumour phenotypic heterogeneity enabling personalised medical treatment accordingly [201].

Radiomics has been defined as the extraction and analysis of vast amounts of quantitative imaging features from images attained using magnetic resonance imaging (MRI), computed tomography (CT) and positron emission tomography (PET) [202]. It has only existed as an entity for less than 10 years, and since then the research interest in it has developed rapidly (Figure 6).

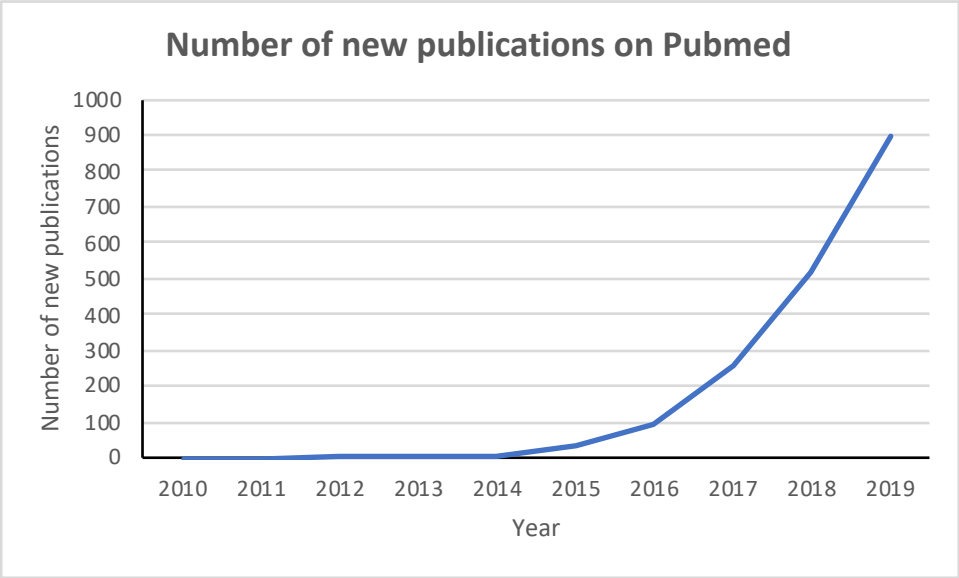


Figure 6. Number of new articles in radiomics 2010-2019 using a Pubmed search Radiomics
As can be seen since 2014 there is almost an exponential rise in citations in radiomics.

It has been suggested that the imaging features seen can have prognostic power and could be used as predictive biomarkers. Indeed, in a large study looking at 1019 lung and head-and-neck cancer patients, radiomic data contained strong prognostic information [203]. Furthermore, in their study, a subset of 89 patients also had 'radiogenomics' whereby gene expression studies were also performed. Interestingly, the radiomic data was associated with underlying gene-expression patterns [203].

Conventional radiology involves the perception and recognition of patterns that are consistent with a diagnosis. As a result, it is unsurprising that there is a degree of interobserver variability [204, 205]. Training, clinical experience and judgement will all impact the radiology report. It is well recognised that reviews of imaging by an experienced radiologist will have a significant impact on patient outcome. In a study by Lakhman et al, 486 gynaecological oncology MRI's were reviewed by a second radiologist. The second opinion review by an expert would have affected outcome in 12.8 to 21.5% cases [206]. Subsequently, tools, such as radiomics, that support automatic pattern recognition and image analysis may enable reduction in this variability.

The process of radiomics is roughly divided into 5 key steps (1) Image acquisition (2) Image segmentation (3) Feature extraction (4) Database (5) Adhoc analysis [202, 207]. This process is summarised in Figure 7. Each step will now be discussed in more detail:

(1) Image acquisition plus reconstruction. This step ensures that the best image is obtained and includes everything from correct positioning of the patient, correct resolution of the image, correct field of view, field strength and slice thickness. An

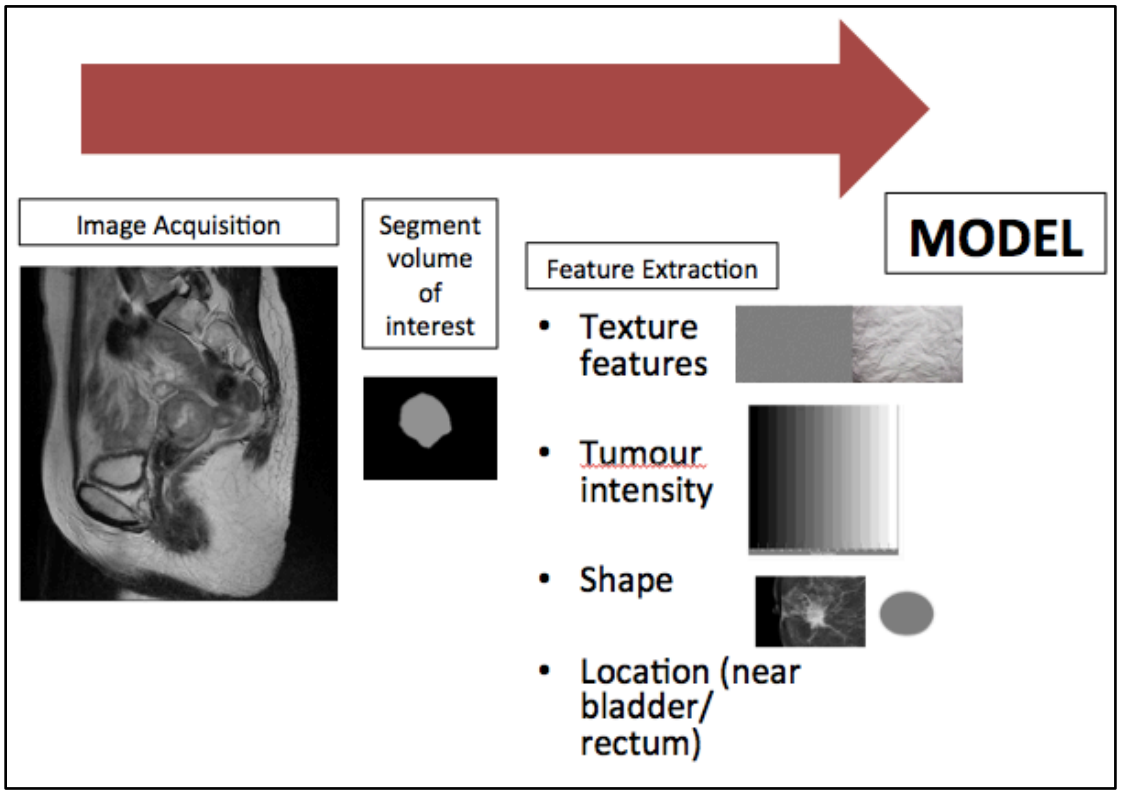


Figure 7. Illustration of radiomics process.
As can be seen the radiomics process starts with image acquisition, followed by segmentation and then textural analysis and model building.

optimized scanning protocol is essential, particularly in MRI, as signal intensities will depend on dynamic tissue properties e.g. relaxation times.

(2) Image segmentation into volumes of interest (VOI) e.g. tumour region and normal tissue. This can be performed manually, by an expert (regarded as 'ground truth'), or automatic / semi-automatic. Manual segmentation is time consuming and suffers from inter-reader variability. Of the automatic segmentation methods, 'region growing' is a popular technique that involves selecting a seed point within the VOI and allowing it to grow. This method is most suitable for homogenous regions. Currently there is no consensus as to the agreed best segmentation algorithm, with each having several advantages and disadvantages.

(3) Feature extraction once the region of cancer is defined. Various characteristics of the tumour can be compared to the surrounding area, looking for patterns. These

features include: the texture pattern (e.g. homogeneous or heterogeneous), tumour intensity histogram (e.g. high or low contrast), the shape (e.g. speculated or square), surface to volume ratio and the location of the tumour in relation to surrounding tissues (e.g. the bladder). A large number of imaging features will be obtained in this step, but all will not be useful, and will reduce the power of the study. An important step is therefore to select a handful of the most useful, non-redundant features to develop the model.

(4) Integrated database. In this step, de-identifying information is essential to ensure confidentiality. But an integrated database is needed to link image phenotype features to molecular and clinical data.

(5) Statistical and radio-informatics analysis. In this step, the model built using the test data set will be validated with another data set. Supervised and unsupervised data analysis exists. Supervised analysis creates models that try to predict an outcome or phenotype based on the data. Conversely, unsupervised analysis does not use any outcome variable; instead it offers only summary information of the data, which may be in a graphical form.

Whilst radiomics as a field has evolved rapidly, there is a paucity of studies using radiomics in endometrial cancer. Three studies have used PETCT or MRI to predict lymph node metastases [208-210], three studies have used MRI to predict deep myometrial invasion [211-213] and two studies to predict lymphovascular space invasion involvement [214, 215]. Whilst some have shown promise, all studies are limited by small sample sizes (range 54-200 patients).

This PhD is the first study to investigate the efficacy of MRI based radiomics for pre-operative prediction of grade, deep myometrial invasion, tumour type, survival and recurrence in endometrial cancer patients.

CHAPTER 3: EVALUATION OF THE CURRENT PATHWAY, A NEED FOR CHANGE?

CHAPTER 3: EVALUATION OF THE CURRENT PATHWAY, A NEED FOR CHANGE?

In order to establish whether the novel technologies discussed already can improve and shorten the patient pathway, it was important at the outset to establish whether a shorter treatment pathway is indeed beneficial. This question was answered by performing 3 separate sub-studies.

The first, a large retrospective audit of all endometrial cancer cases of in the West London Gynaecological Cancer Centre, looking at whether time from diagnosis to surgery had any impact on overall survival.

The second was a prospective survey and paired observational study looking at whether patients were anxious and stressed and were keen for a rapid tissue diagnosis.

The final sub-study was an economic evaluation of the current pathway, and a cost-effectiveness analysis of the new technologies compared to the current reference standard. This sub-study was performed after the introduction of the new technologies (Chapter 9). The is because the cost-effectiveness model required multiple assumptions about the effectiveness of each innovations.

The first two sub-studies will now be discussed in detail, starting with a short summary of the findings.

3.1 Health effect of delayed treatment

Acknowledgements:

Gabriella Young and Yu Shen who helped with data collection. Adam Marcus helped with statistical analysis using R software.

3.1.1 Summary

Objective: To determine the effect of surgical waiting times on the survival of women with endometrial cancer.

Methods: Retrospective cohort study of women diagnosed with endometrial cancer between February 2012 to September 2017 in the West London Gynaecological Cancer Centre. Patients were stratified according to their histology and the number of days from biopsy diagnosis to surgery (TTS): 14 days or less, 15-42 days, 43-84 days, and 85 days or more days. Kaplan-Meier curves were created for survival and log rank test was used to compare these differences. Multivariate cox proportional hazard regression models were used to evaluate factors affecting survival.

Results: 611 patients were diagnosed with endometrial cancer during this period, with a recurrence rate of 14.5%. Recurrences were most common within the first 3 years of diagnosis (81%). TTS data was available for 403 patients. Overall, patients with TTS of ≥85 days had a worse survival. Hazard ratios: 14 days or less (reference standard), 15-42 days (HR 1.03, 95% CI 0.53-2.00), 43-84 days (HR 0.64, 95% CI 0.28-1.48), and 85 days or more days (HR 4.28, 95% CI 1.59-11.50). Older age, grade 3 cancer, advanced stage and the presence of lymphovascular space invasion (LVSI) also influenced survival. TTS curves was significant for type 2 cancer ($p < 0.0001$).

Conclusions: Longer wait times from tissue diagnosis to definitive surgery negatively impact survival, particularly in type 2 cancer.

3.1.2 Introduction

Uncontrolled cellular proliferation is a hallmark of cancer. Invariably the longer it takes for definitive treatment the more the cancer will have grown. Although the exact rate of growth will vary with the tumour size and type. The additional wait time will facilitate local and distant tumour invasion and adverse prognostic features such as

lymphovascular space involvement. It is unsurprising therefore, that studies have shown that long waiting times for cancer surgery can negatively impact patient satisfaction, quality of life and survival [216-218].

In uterine cancer, the 5-year survival for stage 1 disease is over 90% but falls to less than 20% once the cancer has spread to distant sites. Given that the primary treatment of uterine cancer is a hysterectomy, a timely hysterectomy may be considered to improve survival. Initial studies that focussed predominately on relationship between time from onset of bleeding to disease stage and overall survival, did not show any associations [219-221]. These studies were hampered by small sample sizes and mixed tumour histology.

More recent large observational studies however, have shown that, in general, the time to surgery is negatively associated with overall survival [222-224]. A large Canadian study of 9417 women found after adjusting for multiple factors using a multivariable model (accounting for age, co-morbidities and type of cancer), wait time from biopsy to hysterectomy remained a highly significant prognostic factor for survival (P 0.001) [222]. The 5-year overall survival for women with wait times of 2.1-6 weeks, 6.1-12 weeks and >12 weeks were 81.8%, 79.5% 71.9% respectively [222]. Excluding patient with wait times ≤2weeks, hazard Ratios for women with wait times of 2.1 to 6 weeks was 0.79 (95% CI, 0.70 to 0.91), and women with wait times of 6.1 to 12.0, 0.80 (95% CI, 0.71 to 0.91) compared to women waiting >12 weeks [222].

Critics argued that in the Canadian study, almost 23% of patients had high risk histologies (type 2) and were included in the analysis. It is known that these high risk histologies (e.g. clear cell, serous tumours) behave differently than endometrioid carcinoma and are associated with unfavourable prognosis. As such, many of these patients received adjuvant treatment, and this would have biased the results. In a subsequent reanalysis, 3381 low risk women with endometrioid cancers undergoing a simple hysterectomy with no adjuvant treatment revealed the same findings – prolonged surgical waiting times adversely impacted survival [225]. This finding was supported by three large population studies in America using the data from the National Cancer Database (NCD) [223, 224, 226], albeit contrary to a smaller American study [227].

In Alhili study using the NCD, the impact of delay in time to surgery on survival was examined with respect to both histology and stage. Interestingly, they found a positive association between prolonged time to surgery and worse survival in women with early stage (I-II) type 1 cancer, but not in type 2 stage I-III [226]. Paradoxically, a time to surgery of more than 6 weeks and improved overall survival was observed for stage IV type 2 cancer [226].

Also paradoxically, in both the Canadian study, and Shalowitz et al., study though the overall trend was that longer waiting times led to worse overall survival, both studies observed that those having surgery less than 2 weeks from biopsy had a worse overall survival rate, 71.1% [222, 223]. The authors felt this was a reflection of sicker patients with more severe disease such as sarcoma being more likely to be operated within the first 2 weeks of diagnosis.

Overall, these studies suggest that the delay between diagnosis and surgery should not exceed 6 weeks [164, 224]. All these studies have been performed internationally, but UK data on time to surgery and survival are lacking, limiting generalisability. In the UK the government targets recommend that patients should not wait more than 28 days from referral to finding out a diagnosis of cancer (as part of NHS England faster Diagnosis standard). In addition, patients should wait no more than 2 months (62 days) the date the hospital receives an urgent referral for suspected cancer and the start of treatment [228].

In a survey of practice in South West England there were delays in all stages of the endometrial cancer pathway, particularly waiting for a GP appointment, were over 50% of women waited more than a month [229]. In an audit of 700 endometrial cancer cases in Scotland, the median interval from referral to definitive operation was 62 days [230]. They also found that patients who experience the longest delay in treatment were more likely to survive [230].

The primary aim of this study is to assess whether time to surgery adversely affects the prognosis of patients with endometrial cancer using data from London, England. The secondary outcomes were to assess recurrence trends in endometrial cancer and whether time to surgery adversely affects histological grade and type.

3.1.3 Methods

Data source and study population

This study followed the STROBE guideline for retrospective cohort studies. Cancer cases were identified using Somerset, the cancer database for West London Gynaecological Cancer Centre, Imperial College NHS Trust, London, UK. Ethics approval was not required for this study because no patient or hospital identifiers were examined.

For the primary study aim, all endometrial cancer (type 1 and type 2) patients who underwent primary surgical treatment between Feb 2012 to Sept 2017 were included in the analysis. Patients who had a primary tumour was outside the uterine corpus or who were diagnosed with primary cervical cancer were excluded. Patients were also excluded if they underwent neoadjuvant chemotherapy or hormonal therapy prior to surgery. All patients were treated by gynaecological oncologists. The outcome of women who did not undergo primary surgery were reviewed a separately.

For recurrence trends all patients with endometrial cancer between Feb 2012 to Sept 2017 were included in the analysis.

Patient characteristics, time periods and definitions

Data was extracted using CERNER, the electronic patient record system used by Imperial NHS trust. Data collected included 1) clinical demographics, such as: age at time of diagnosis, date and method of initial diagnosis (pipelle or hysteroscopy), type of initial treatment (surgical, radiotherapy or chemotherapy), date of surgical treatment, adjuvant treatment. 2) Tumour characteristics including type and grade of endometrial cancer, presence of lymphovascular space invasion (LVSI) and stage of cancer. 3) Survival data, date and location of recurrence, disease free survival and overall survival at time of data collection.

The date of diagnosis was determined by the date that the endometrial tissue biopsy was reported (day 0), usually using a pipelle biopsy or curetting's. In the few cases where the date of biopsy was documented incorrectly (biopsy date was after date of definitive surgery) the date of the MRI scan was used. Date of treatment was

determined by the date of the surgical staging procedure (commonly hysterectomy). The interval between date of diagnosis to date of surgical treatment, in days, was the Time to Surgery (TTS). TTS was stratified into 4 groups: 14 days or less, 15-42 days, 43-84 days, and 85 days or more. The groupings were based on work from other studies [222, 227]. If the date of the biopsy or definitive surgery was not available, the patient was excluded from the analysis. Similarly, if follow up data was not available patients were excluded.

Recurrence was defined as new disease after a disease-free interval of 3 or more months. Recurrence was classified as vaginal (vault) recurrence, pelvic recurrence (including pelvic and para-aortic lymphadenopathy) and distant recurrence (abdominal and chest). Disease free survival was defined as the interval between hysterectomy and the first recurrence or last follow up date. Overall survival was defined as the interval between date of endometrial biopsy and the date of death, or last follow up date.

All surgical specimens were reviewed by a dedicated gynaecological histopathologist. Tumour histology was defined as per International classification of disease for oncology as Type 1 or Type 2. Carcinosarcoma (also known as malignant mesodermal tumour, or malignant mixed mullerian tumours) were classified as a type 2 tumour. Tumour grades were classified according to the FIGO system, whereby grade 1 has ≤5% solid components, grade 2 6-50% solid components and grade 3 ≥50% solid components.

If the tissue biopsy grade was different to the final grade at hysterectomy this was defined as a grade change. If pre-operative histology revealed hyperplasia with atypia and final histology reported endometrioid cancer this was classified as tumour upgrade. If grade 1 endometrioid tumours became 2 or 3 on final histology, or, if grade 2 endometrioid samples became grade 3 on final histology this was classified as upgrade. Similarly, if tumours were classified as type 1 endometrioid on tissue sampling but were then classified as type 2 on the final hysterectomy sample this was also defined as a tumour upgrade. Conversely, if a tumour was grade 3 or 2 on biopsy and later became 2/1 or 1 or final histopathology this was termed a downgrade. If a tumour was type 2 on tissue biopsy but then was classified as type 1 on the final hysterectomy sample this was defined as a tumour downgrade.

Statistical analysis

Kaplan-Meier curves were created to show the overall survival of women according to the stage of cancer. Kaplan-Meier curves were also created to show the relationship between TTS (in days) and survival; with separate graphs for type 1 and type 2 endometrial cancer. Log rank test was used to compare the differences in survival distribution curves.

Multivariate cox proportional hazard regression models were used to evaluate whether each variable was associated with survival for all endometrial cancer patients. A separate sub-analysis was also performed for low risk (grade 1-2 stage 1a endometrioid cancer) cases only. Analysis was right-censored to account for patients who didn't die prior to the end of the follow-up period. Hazard ratios (HR) were used to calculate effect size for all co-variates. For cox models, P values were calculated using the likelihood ratio test.

To account for missing values, complete case analysis was performed. All survival and hazard regression analyses were performed in R version 4.0.2 (R Foundation for Statistical Computing, Vienna, Austria).

Recurrence rates were also calculated. Chi-squared test and Kruskal-Wallis test were used to assess for any difference in recurrence between type and stage of cancer respectively. To assess whether time to surgery adversely affected tumour histology and grade i.e. tumour upgrade or downgrade status, Kruskal-Wallis test was used. Statistical Package for Social Sciences, version 26.0 (SPSS Inc., Chicago, IL, USA) was used to perform these analyses.

Statistical significance was defined as $P<0.05$, with 95% confidence intervals where appropriate, and all tests were two-sided.

3.1.4 Results

Six hundred and eleven patients were diagnosed with endometrial cancer between February 2012 and August 2017. 184 lacked a date of initial diagnosis, and 24 patients did not undergo definitive treatment - these patients were excluded, leaving 403 patients for the TTS and survival analysis. Characteristics of the patient cohort are shown in Table 2.

	Time to surgery				
Characteristic	**14 or less days (n = 50)**	**15 to 42 days (n = 231)**	**43 to 84 days (n = 82)**	**85 or more days (n = 32)**	**P value**
Age in years, mean (SD)	65.86 (11.01)	65.78 (11.60)	65.82 (12.15)	58.66 (17.15)	0.018*
Type 2 (%)	16 (32.0)	61 (26.4)	17 (20.7)	5 (15.6)	0.279
Stage (%)					0.044*
1	34 (68.0)	174 (75.3)	63 (76.8)	23 (71.9)	
2	4 (8.0)	16 (6.9)	4 (4.9)	2 (6.2)	
3	8 (16.0)	33 (14.3)	12 (14.6)	1 (3.1)	
4	4 (8.0)	8 (3.5)	3 (3.7)	6 (18.8)	
Grade (%)					0.069
1	12 (24.0)	75 (32.5)	38 (46.3)	14 (43.8)	
2	20 (40.0)	70 (30.3)	24 (29.3)	11 (34.4)	
3	18 (36.0)	86 (37.2)	20 (24.4)	7 (21.9)	
Chemotherapy (%)	11 (22.0)	56 (24.2)	16 (19.5)	7 (21.9)	0.847
Radiotherapy (%)	21 (42.0)	113 (48.9)	31 (37.8)	8 (25.0)	0.040*
Lymph node removal (%)	23 (46.0)	73 (31.6)	22 (26.8)	10 (31.2)	0.140
LVSI† (%)	21 (42.0)	72 (31.2)	28 (34.1)	7 (21.9)	0.262
Year of surgery (%)					0.001*
2014 or earlier	3 (6.0)	37 (16.0)	15 (18.3)	8 (25.0)	
2015	24 (48.0)	59 (25.5)	12 (14.6)	5 (15.6)	
2016	12 (24.0)	80 (34.6)	41 (50.0)	11 (34.4)	

2017 or later	11 (22.0)	55 (23.8)	14 (17.1)	8 (25.0)	
Survival in weeks, mean (SD)	119.06 (89.75)	125.48 (87.96)	118.63 (88.77)	82.36 (90.77)	0.084

Table 2. Characteristics of the patient cohort according to their time to surgery (TTS). Abbreviations: SD = standard deviation, † LVSI = lymphovascular space invasion.

For each variable such as age and use of adjuvant chemotherapy, statistical analysis was performed to determine if the variable was related to time to surgery. The p-value is reported and * represents significance. Note as data is right censored and there was some missing data (8 cases) within this, subsequently this table only shows 395 cases.

The average age of women diagnosed with endometrial cancer was 65 years old. In terms of stage of disease at diagnosis, 299 women (74%) were stage 1, 26 women (6%) stage 2, 56 women (14%) stage 3 disease and 22 women (5%) stage 4 disease. The overall survival of women with endometrial cancer according to stage is illustrated in Figure 8. Overall 302 women (75%) had type 1 endometrial cancer and 101 (25%) had type 2 endometrial cancer.

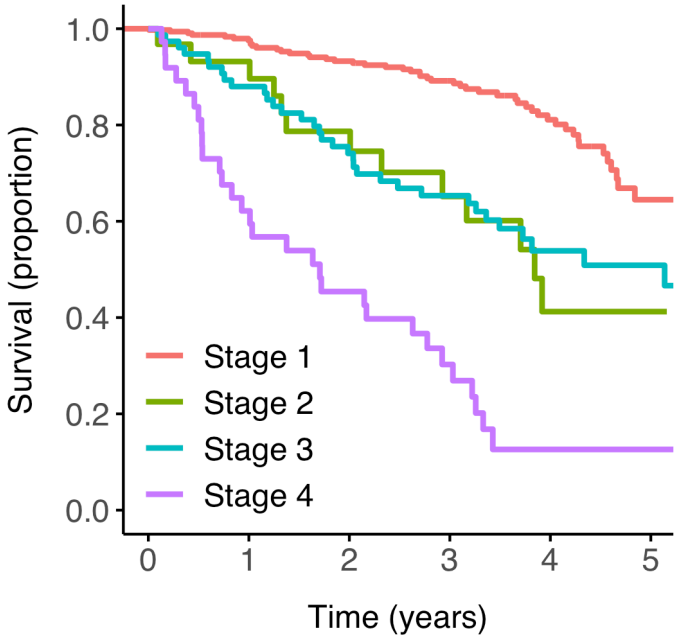


Figure 8. Kaplan-Meier curve illustrating the survival of women with endometrial cancer, according to their stage.

The Kaplan-Meier curves have not adjusted for any of the co-variables e.g. age. As can be seen the proportion of patients alive at 5 years with stage 4 is much less than those with stage 1 disease.

Effect of surgical wait time (TTS) and survival

At time of data collection 323 were alive and 80 patients had died. It is important to recognise that the cause of death was unknown for patients in this study, and that

deaths include all causes for mortality. The overall median interval from diagnosis to surgery was 30 days (interquartile range: 20-45). Figure 9 illustrates the overall survival of women, stratified by type of endometrial cancer and the time to surgery. The log rank test to compare the differences in survival distribution TTS curves was significant for type 2 cancer only (p values: type 2 p <0.0001; type 1 p = 0.63)

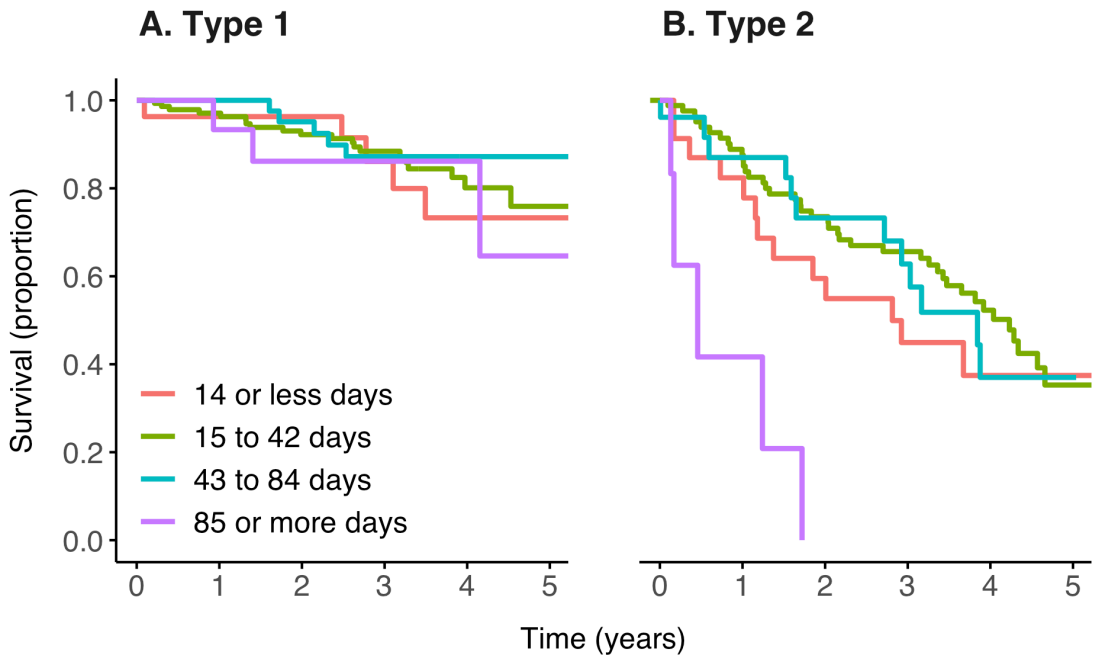


Figure 9. Kaplan Meier curve illustrating the survival of women with endometrial cancer, according to their time from diagnosis to surgery: 14 or less days, 15-42 days, 43-84 days and 85 days or more. Type 1 and Type 2 endometrial cancer data shown separately; Graph A and B respectively.

On further inspection of the 32 women with long delays from tissue biopsy to surgery (>84 days): 8 women (25%) were young and delayed surgery for fertility, 7 women (22%) had delays in palliative surgery for stage 4 disease and 5 women (16%) had complex medical co-morbidities causing delays. Furthermore, 9 women (28%) had delays due to transfer of care from peripheral district general hospitals and 4 women (13%) had no clear reason for the delay.

Factors affecting survival

In the analysis, amongst all women with endometrial cancer, the following factors were statistically significant for poorer survival: time to surgery greater than 84 days, older age, grade 3 cancer, advanced stage, presence of lymphovascular space invasion (LVSI) and the absence of radiotherapy. Women who underwent surgery between 15-

84 days had the best survival. This is demonstrated in Table 3. The year that the surgery was performed, whether a lymphadenectomy was performed, type of cancer and use of adjuvant chemotherapy was not associated with survival.

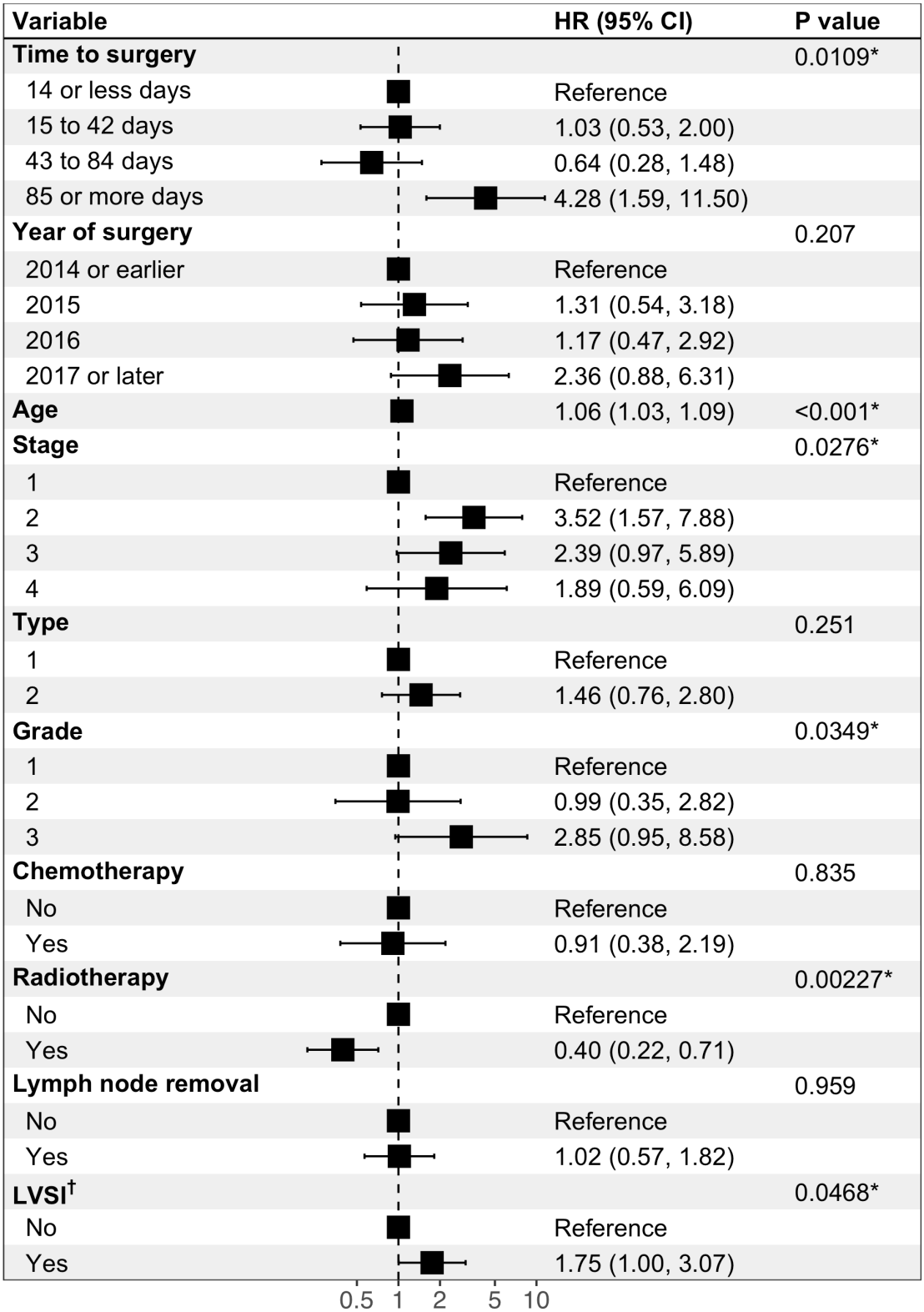


Table 3. Factors prognostic for survival in all women with endometrial cancer. Abbreviations: † LVSI = lymphovascular space invasion. HR = Hazard ratios.
The p-value is reported and * represents significance <0.05.

Factors affecting survival in low risk women

A sub-analysis was performed to assess factors affecting survival in only low risk women (grade 1-2, stage 1A endometrioid cancer). Similar to the analyses of all women with endometrial cancer, advanced age was associated with poor prognosis (Table 4). The presence of LVSI was not associated with survival, neither the timing if surgery. As these were low risk cases, no women underwent chemotherapy or radiotherapy and the vast majority (>90%) did not have lymphadenectomy. Whilst a similar tendency of worse survival with long delays to surgery was observed, this did not reach statistical significance.

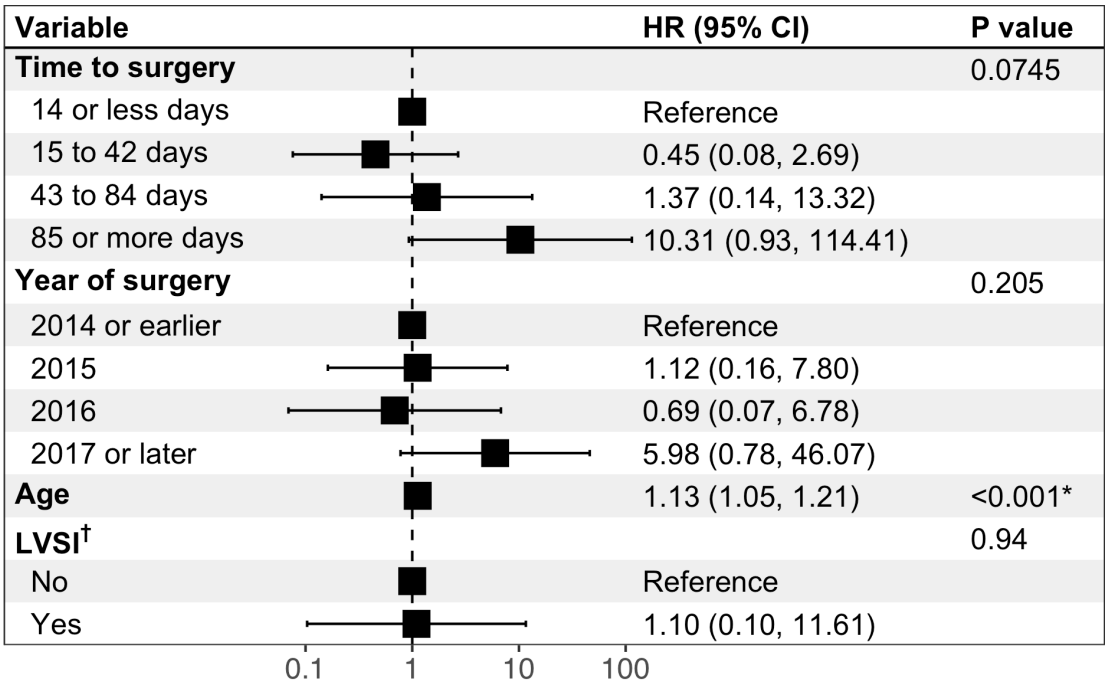


Table 4. Factors prognostic for survival in low risk women (grade 1-2, stage 1A endometrioid cancer). Abbreviations: † LVSI = lymphovascular space invasion. HR = Hazard ratios.
The p-value is reported and * represents significance <0.05.

Time to surgery and Tumour grade or type change

Of the 611 women with endometrial cancer during the period of study, 104 had their tumour status upgraded (worse grade/tumour type), and 34 had their tumour downgraded (better grade/tumour type). Of those who had their tumour upgraded almost half of these cases were hyperplasia with atypia pre-operatively but endometrioid cancer on final histology (44/104). Time to surgery did not affect tumour characteristics, namely grade or type change (P = 0.330).

Recurrence

Overall, 14% of all patients with endometrial cancer underwent lymph node sampling or full lymphadenectomy as part of their treatment; 19% received adjuvant chemotherapy and 40% adjuvant radiotherapy. Of the original 611 patients with endometrial cancer during the period of study, 25% died, 86 had disease recurrence within 5 years of initiating treatment (14%) and 89 had disease recurrence during the period of follow up (14.5%). Most patients (72/89, 81%) had recurrence within the first 3 years following treatment, see Figure 10.

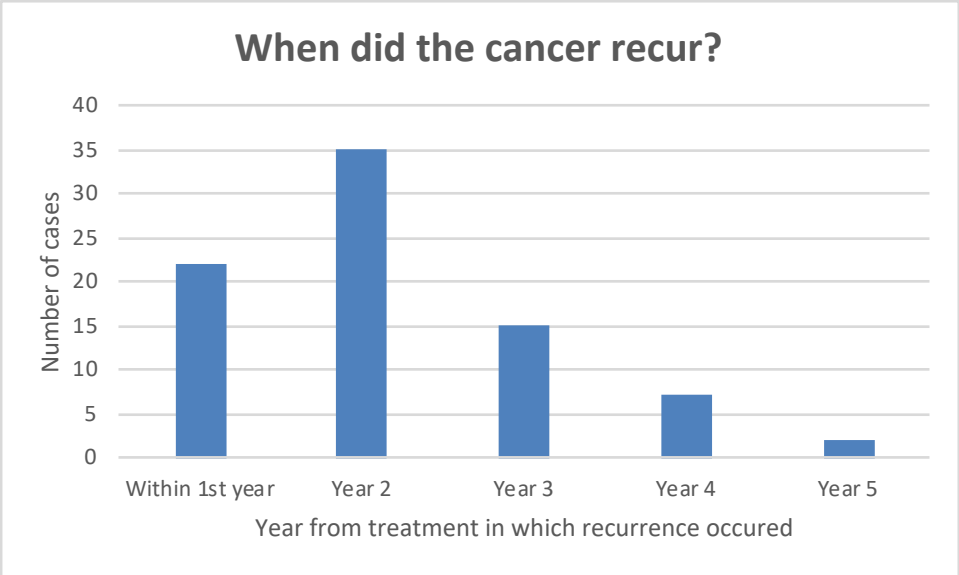


Figure 10. Timing of endometrial cancer recurrence from the date of surgery.
Number of new recurrence cases with each consecutive year following surgical treatment.

Of patients who recurred, the median recurrence (and interquartile range in the months, IQ) for all patients, type 1, type 2 were: 18 (IQ 12-30), 18 (IQ 13-34) and 17.5 (IQ 12-28). Only 12 low risk cases (stage 1A, type 1, grade 1-2) recurred, with a median of 17 and IQ range 10.5-31months. The remaining 74 recurrence cases which did not satisfy the criteria for low risk had similar recurrence pattern with median 18 and IQ range 12.5-30.5months.

Overall, recurrence was fairly evenly split between local (vault and pelvic) and distant recurrence (49% vs 51% respectively). Over half of the distant recurrences were lung metastases. Approximately half of recurrences were symptomatic (49%), with abdominal pain and vaginal bleeding being the most common two symptoms. Other symptoms included: back pain, cough, an umbilical lump, groin swelling, and seizures

Asymptomatic recurrences were detected on routine imaging surveillance. Imaging did not selectively improve the detection of either local or distant recurrence, with a detection rate similar to the observed overall recurrence rates (51% local vs 49% distant recurrence). Recurrence was more common depending on the type of cancer ($P = 4.92 \times 10^{-20}$) and stage of cancer (P = 1.8965 x 10-15).

Outcome of those not having surgery

Within the 5-year period of data collection, 611 patients were diagnosed with endometrial cancer. Twenty-four patients did not undergo definitive surgery, 11 were deemed medically unfit (46%), 4 wanted to preserve fertility (17%), 8 had advanced cancer (33%) and one was due to patient choice (4%).

Of the 4 women wishing to preserve fertility, the age ranged between 31 and 38 years old. All had stage 1A endometrioid tumours either grade 1 or 2. One had a Mirena IUS and 3 had Provera tablets. One moved overseas and was lost to follow up, 3 continued local follow up (3-6 years thus far), which included either CT or MR imaging and endometrial biopsies. Two showed regression of the tumour and one progressed after 3 years despite hormonal treatment to ovarian metastases.

Of the 8 women with advanced disease (stage 3b or 4), all women died within the follow up period, median 12.5 months (range 2-40 months). Of the 11 women who were not fit for surgery, all women also died within the follow up period, median 17.5 months (range 1-49 months).

3.1.5 Discussion

Key findings

This study demonstrates that women who wait more than 85 days for surgery, or who receive surgery within 2 weeks from a biopsy diagnosis of endometrial cancer in England are more likely to have a worse survival, particularly in type 2 cancers. This is in keeping with the findings of several other large cohort studies in other countries demonstrating worse survival with delays to definitive surgery [222-224, 226, 231]. Surgical delays understandably can increase the risk of disease progression and

dissemination, and therefore influence survival. But, more curiously, the observation of a worse prognosis in women receiving surgery within 2 weeks of a biopsy diagnosis is more difficult to explain. This finding was also observed by Shalowitz et al. and Elit et al. [222, 223] and is thought to be attributed an acute deterioration necessitating emergency surgery, or factors associated with delivery of care such as more advanced disease and ethnicity [223].

As expected, in this study, the majority of patients had stage 1 cancer (74%) and type 1 endometrioid tumours (75%). In previous studies, critics argued that any effect seen on time to surgery (TTS) and survival would be heavily influenced by stage 1 and type 2 tumours, and therefore it is advantageous to analyse type 1 and type 2 tumours separately [226]. Thus, a separate Kaplan-Meier survival analysis was performed (Figure 9) in this study for type 1 and type 2 tumours; survival was significantly associated with TTS in type 2 tumours; likely a reflection of the more aggressive pattern of disease.

In the present study, a separate sub-analyses of low risk women were also performed, this confirmed the same findings; women who wait more than 85 days for surgery, or who receive surgery within 2 weeks from a biopsy diagnosis of endometrial cancer have a tendency for worse survival, though this did not reach statistical significance. Unlike Shalowitz et al. study, grade 3 endometrioid tumours were excluded from the low risk sub-analyses as they tend to be more aggressive and often require lymphadenectomy and adjuvant treatment. Low risk women in this study were therefore defined as stage 1A grade 1-2 endometrioid cancers and the vast majority of these women did not undergo any underwent adjuvant treatment in the first instance.

In addition to finding changes in survival related to TTS, this study identified a number of variables associated with survival in type 2 cancer, including: age, stage, grade of tumour, presence of lymphovascular space involvement and use of radiotherapy. Interestingly, type of tumour and performance of lymphadenectomy was not associated with overall survival. There has been contention as to whether lymphadenectomy has any inherent survival benefit itself, or merely selects patients requiring adjuvant treatment [161, 162, 164]. In the UK setting, most low risk women do not undergo lymph node sampling. For those with risk factors (e.g. deep myometrial invasion), they are offered lymphadenectomy, and those with positive lymph nodes are

offered adjuvant treatment. Differentiating between any inherent benefit of lymphadenectomy versus benefits associated with the subsequent package of care treatment the patient receives is best evaluated as part of a randomised prospective trial, not an observational study such as this.

The year of surgery was not significant for survival in women, though more recent surgery had a tendency for worse survival on examination of the hazard ratios. This may represent type 1 errors. It may also be due to changes in practice, with more advanced cancers and patients with more complex co-morbidities being operated on. It may also be due to variations in referral volumes to Queen Charlottes Hospital. The centralisation of gynaecological cancer services to selected specialist centres with gynaecological oncologists in an effort to improve clinical care [232-235] has led to an increasing volume patients being referred to a smaller number of units. Studies have shown that this can result in hospital crowding and longer waiting times [216, 236, 237]. In the current study, it was important to have at least 3-year survival data, thus data were collected from Feb 2012 to Sept 2017. Wait times of 85 days and more increased from 5% to 9% from 2015 to 2017. Online records only became integrated into clinical practice from 2012-2013, and as online clinical records were the sole source of information, a greater proportion of missing data was from the earlier 2012-2015 dataset. Thus, any firm conclusions about delays in surgical wait times due to year of diagnosis should be taken with caution.

In the current study, time to surgery did not adversely affect tumour characteristics, namely grade or type change. This is in keeping with findings from Matsuo study [227]. For accurate histological diagnosis, large amounts of tissue are required. Endometrial tissue biopsies are frequently blind, as with most office endometrial biopsy sampling devices, and can be inadequate [238]. Changes in tissue classification from the pre-operative biopsy to final hysterectomy sample are therefore more likely to represent failures in pre-operative tissue sampling rather than a true change in tumour biology. Interestingly in Pirog et al. study they found that the length of time from symptoms to surgery did not correlate with stage or tumour characteristics [220]. Their study was small however, with less than 200 patients and was more concerned with time from symptoms to surgery.

Endometrial cancer recurrence in this study was 14%. This is in keeping with other studies, which found an overall recurrence rate of 11-13%, with equivalent relapses in the pelvis and distant metastasis [239-242]. Recurrences in general can be symptomatic or asymptomatic, with most endometrial cancer recurrences being symptomatic. Though, vaginal vault recurrences often have less symptoms than metastasis [239, 241] and are more common in women treated with surgery alone [241].

Most endometrial cancer recurrences occur within 3 years from diagnosis [239, 243-245]. In this study most recurrences were seen at the vault, pelvic nodes and lungs. Studies have shown that survival rate is related to the site of relapse with recurrent disease limited to the vagina associated with much better survival compared to relapses at other sites [241]. The pattern and timing of recurrences, therefore, has dictated, to some extent, the surveillance offered for women post treatment. However, huge variation exists in the timing of follow up and the investigative modalities, if any, used [239, 246, 247]. These variations exist geographical and within the same regions over a period of time. In the States for example, there has been a clear downward trend in the use of chest radiography and vault cytology, and an increase in more costly imaging modalities [248]. The optimal follow up routine remains unknown. This study suggests that a more intense surveillance regimen is used within the first 3 years to reflect the higher incidence of relapse within this time period. In view of the high amount of asymptomatic recurrence (almost 50%) imaging such a CT scans would be recommended.

Additionally, it must be kept in mind, that there will always be variations in the treatment package offered to each patient depending on unit practices and resources. Thus, differences in the proportion of women receiving adjuvant radiotherapy and chemotherapy in different units will inevitably impact on their individual recurrence and survival data.

Strengths and limitations

This is the first study in England to assess whether delays in surgery affect survival in women with endometrial cancer. Prior studies have investigated these associations in the USA, Canada and Israel, but differences in population demographics and health

systems have left debate as to whether their results can be generalised to the English population.

In addition, the other strength of this study is that it analysed the time from definitive diagnosis to surgical treatment, unlike older studies which focussed on the time interval between onset of bleeding and treatment [220]. Furthermore, this study analysed all cases together (high and low risk histologies) to see if TTS was related to survival and performed a sub-analysis of low risk histologies separately. Elit at al., study received much criticism for including all high risk histologies in their analysis, as it was felt that the majority of cancers are low risk, and longer waiting times may not worsen outcome [249]. A subsequent sub analysis by Elit et al., of more than 3000 low risk cases who underwent a hysterectomy without adjuvant therapy also had a survival disadvantage if waiting >12 weeks for surgery [225].

There are several other limitations to this study. Firstly, there is no information as to the cause of delay for surgery. Surgical treatment delays may be due to a number of reasons including the need for greater pre-operative work needed for those with complex co-morbidities. However, it was not possible to collect the data for co-morbidities in this study, so the reasons remain purely speculative. Irrespective of the reasons for delay in treatment, one of the largest cause of delays in a patient journey overall is the step from initial symptom presentation to referral to secondary care. Patients may be reluctant to access their GP for fear of embarrassment or lack of recognition of seriousness of symptom. Patients may also be unable to get a quick appointment or may not get referred into secondary care on the 2 week wait pathway.

The second biggest limitation in this study is the assumption that all the factors investigated were independent. Moreover, this study did not account for some variables which have been found to be associated with delays to surgery and survival including: race, ethnicity, co-morbidities [222] (such as the Charlson-Deyo score) and socio-economic factors [223, 224]. Multiple studies have reported that women with lower socio-economic status and racial and ethnic minorities are regularly diagnosed with more advanced cancers, receive worse care and have higher mortality rates [224, 231, 250-252]. Indeed, it has been suggested that endometrial cancer treatment delays may be a proxy for more complex sociodemographic factors that affect survival

[224]. As no information was available regarding cause of death, these social factors may play a large role.

In the current study, all surgery was performed in a single hospital by a dedicated team of specialised gynaecological oncologists. Thus, minimising any potential bias due to surgical technique or performance of the surgeon. However, as cancer services have become centralised, potential delays associated with delays in biopsy diagnosis at one of 6 other regional referring hospitals was not assessed in this study.

Finally, this study uses retrospective data from a single cancer network in England, so whilst its study size compares favourably to most of the studies investigating delays to surgery and its impact in survival, it is small compared to the 4 studies using large national datasets [222-224]. Retrospective studies also have inherent limitations including selection bias, incomplete datasets (34%) and coding errors.

Conclusion

This is the first study in England to report the impact of surgical waiting times on all-cause survival in endometrial cancer. It demonstrates that prolonged surgical waiting times negatively impact survival; particularly in type 2 cancer. Furthermore, older age, grade 3 cancer, advanced stage and the presence of lymphovascular space invasion (LVSI) also influenced survival. This study provides impetus to shorten the time to definitive treatment. Shortening the time to tissue diagnosis may also help by speeding up the patient pathway, in an effort to improve survival.

3.2 Psychological effect

Collaborators:

Dr Alex King, a clinical psychologist and Mr Joseph Eliahoo, Statistical consultant both provided help on an advisory capacity.

3.2.1 Summary

Objective: To ascertain the anxiety levels, stress levels, and patient's self-perception of an endometrial cancer diagnosis during the diagnostic period. Assess factors that might affect them.

Methods: Prospective questionnaire study of consecutive women attending the rapid access clinic with suspected endometrial cancer in a tertiary cancer centre in London. A structured questionnaire was used and included: a GAD7 anxiety score and a stress thermometer. Patients were also asked to rank their perception of a cancer diagnosis on 0-5 Likert scale (0 not cancer and 5 has cancer). Patients requiring an endometrial tissue biopsy were asked to rank their pain on a visual analogue scale (VAS) and the duration of the procedure was recorded, this was paired with the survey results. Patients were also asked if they would have the procedure again, as an outpatient, if needed.

Results: 250 patients completed the study and 23 women underwent an endometrial tissue biopsy. The median age was 50-59 years old and 59% of women spoke English as their first language. Almost a third of patients had significant levels of anxiety with GAD7 score ≥10. The median stress score was 3 out of 5 on Likert scale. GAD7 anxiety scores were higher in women who perceived that they received insufficient information prior to clinic (sufficient information 5 vs insufficient information 9.5, P = 0.00036) or had a disability (disability 9 vs no disability 5.5, P = 0.00374). Biopsies took 5 minutes (range 3-12 minutes), with a median VAS score of 7 out of 10 (range 1-10). All patients said they would have the procedure again if needed. Most patients felt that they didn't have cancer (Likert score median 2 out of 5). Patients with higher anxiety levels (GAD7 scores) were more likely to believe they had cancer P <0.00001. Religion and education were not related to perception of cancer, anxiety or stress levels. Almost all women wanted a rapid diagnosis.

Conclusions: These findings confirm high levels of anxiety and stress in women with suspected endometrial cancer. It also suggests the need for adequate pre-clinic information and additional psychological support for minority groups.

3.2.2 Introduction

The detrimental psychological effect of a diagnosis of cancer has been well established [253-257]. To a lesser degree the psychological effect of delays in diagnosis and treatment have also been studied [258, 259]. Surprisingly, only a handful of studies, predominately in breast cancer, have addressed the detrimental psychological impact of waiting and uncertainty of a cancer diagnosis in those referred for suspected cancer [260-262]. A systematic review by Woodward and Webb, reported that the levels of anxiety and psychological distress in the period from first awareness of the problem till the time of receiving a diagnosis were similar whether the women had a final diagnosis of benign or malignant breast disease [262]. However, post diagnosis the anxiety levels fell more for those with benign disease, but still remained at a high level [261-263].

It is well recognised that uncertainty about possible future threats, such as a cancer diagnosis can disrupt our ability to avoid it, or to minimise its negative impact, resulting in anxiety [264, 265]. Anxiety itself is defined as an "anticipatory affective, cognitive and behavioural changes in response to uncertainty about a potential future threat" [264]. Anxiety levels are positively correlated with the level of uncertainty and have been shown to be higher in younger single women [261, 263, 266]. Mischel's uncertainty illness theory state that uncertainty is dynamic and is affected by both personal factors such as previous experience and self-perceived probability of a cancer diagnosis, and social factors such as culture and support network [261, 267].

No studies have addressed psychological impact and anxiety in women with suspected endometrial cancer. This unmeasured, but present psychological impact is highly unreported [268]. Anecdotally, I have found that women attending this particular clinic are very anxious, even though over 80% will get discharged with benign pathology [41]. This study therefore aims to quantify the anxiety levels of women attending the Rapid Access Clinic (RAC) for suspected endometrial cancer.

This study was split into 2 parts:

- Patient survey gauging anxiety and stress levels and factors affecting them
- Paired study observing behavioural response in clinic

Various factors have been reported to influence psychological distress in cancer patients, such as religion, spirituality and education levels [269, 270]. In this study a number of demographic factors that were postulated to affect anxiety levels were measured using patient self-reporting i.e. a questionnaire.

It has long been recognised that there is sometimes discordance between self-reported outcomes and behavioural responses, when patients say when one thing, but their actions aren't congruent [271]. To this end a behavioural element to the study was introduced. I quantified behavioural response in clinic by measuring the time taken to perform tissue biopsies, recording the pain score and correlating these metrics with self-reported anxiety levels. The hypothesis was that women who were very anxious and keen to have a diagnosis quickly will tolerate high levels of pain for prolonged periods of time to get that diagnosis.

Knowledge of uncertainty and anxiety changes around the diagnostic period in endometrial cancer can serve as useful reference for future clinical care. The aims of this study were to (i) ascertain the anxiety and stress levels during the diagnostic period and factors that might affect them (ii) ascertain patient's perception of a cancer during the diagnostic period and factors affecting them (iii) ascertain importance of a quick diagnosis.

3.2.3 Methods

This study formed part of a larger multifaceted clinical trial. Ethics was approved by Bloomsbury REC (REC number:17/LO/0173, IRAS number:210195, JRCO number: 16HH3687).

All women attending the RAC for suspected endometrial cancer in Imperial College Healthcare NHS trust, between July 2018 and April 2019 were approached for consent into the study. Women were given a short 5-minute questionnaire to fill during their first clinic attendance, before seeing any clinician or healthcare provider (see appendix for copy of questionnaire).

Women were excluded if, in the absence of a translator, they did not have sufficient comprehension of English to fill the questionnaire. Patients were also excluded from the analysis if they omitted 3 or more answers from the questionnaire.

3.2.3.1 Patient survey

The questionnaire had 19 questions, split into 4 broad groups: questions quantifying anxiety/stress levels, factors that might affect these, patient's perception of cancer diagnosis and the importance of a quick diagnosis.

Quantifying stress

Patients were asked to score how they perceived their stress levels using a Likert scale, based on a modified version of the distress thermometer [272], see Figure 11. A score of 4 or above was defined as high stress in this study and 3 and below as low stress.

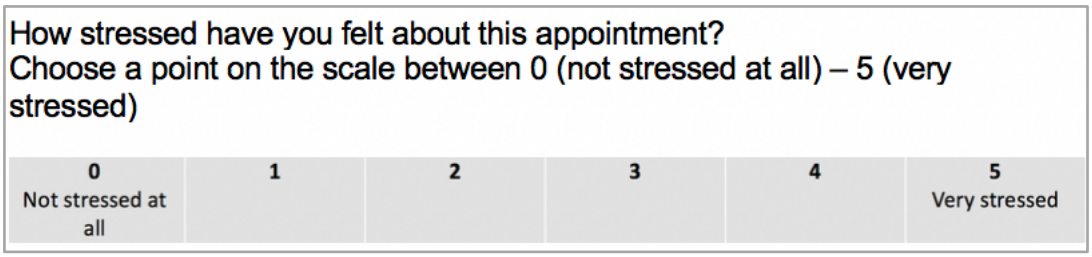


Figure 11. Likert scale for quantification of stress scores.
Patients were asked to select a point on this scale 0-5. This scale was based on the stress thermometer.

Quantifying anxiety

Patients were also asked to fill a Generalised Anxiety Disorder 7 (GAD7) form, see Figure 12. This is a validated 7-point questionnaire; with a total score for the seven items ranging between from 0 to 21- the higher the score the higher the anxiety level. Scores of 0-4, 5-9, 10-14 and 15-21 were assigned normal, mild, moderate and severe anxiety respectively. Scores between 8-11 and above, are commonly cited as high anxiety scores.

Over the last 2 weeks, how often have you been bothered by the following problems? *(Use "✔" to indicate your answer)*		Not at all	Several days	More than half the days	Nearly every day
1.	Feeling nervous, anxious or on edge	0	1	2	3
2.	Not being able to stop or control worrying	0	1	2	3
3.	Worrying too much about different things	0	1	2	3
4.	Trouble relaxing	0	1	2	3
5.	Being so restless that it is hard to sit still	0	1	2	3
6.	Becoming easily annoyed or irritable	0	1	2	3
7.	Feeling afraid as if something awful might happen	0	1	2	3
	GAD-7 Total =				

Figure 12. GAD7 anxiety questionnaire used to quantify anxiety levels.
Patients answered each question in the GAD7 questionnaire, and the total score was then tallied. The overall result was then categorised as mild, moderate or severe anxiety depending on the score.

Median, quartile ranges, box and whiskers plots were created for each variable (as the data was non-Gaussian).

Agreement testing between GAD7 scores and self-reported stress levels were performed.

Factors that might affect anxiety and stress levels

Questions included demographic information, such as: age, ethnicity, educational background and disability. Patients were asked if they received any prior information about the RAC appointment, if so what, and if they felt this information prepared them sufficiently. For each classifier an appropriate test for statistical significance was performed to assess for association between anxiety/stress scores and each independent factor.

Patient's perception of cancer diagnosis and factors affecting perception

Patients were asked to rank whether they believed they had cancer, using a Likert scale (where 0 represents no chance they have cancer and 5 they feel they will have a definite diagnosis of cancer following the appointment). This was based on their first automatic thought and reaction. In this study, a score of 3 and above was considered

strong belief of cancer, and a score of 2 and below was a weak perception of cancer diagnosis.

For each classifier (e.g. religion, disability) an appropriate test for statistical significance was performed to assess for association with perception of cancer.

Importance of a quick diagnosis

Women were asked to rank how important a quick (same day) final diagnosis or final result was, using a Likert scale (where 0, is not important, and 5 very important to have a quick diagnosis). A score of 4 and above was considered significant for a quick cancer diagnosis.

3.2.3.2 A paired observational study assessing behavioural response in clinic

For women needing a pipelle biopsy for clinical indications, the time taken to perform the biopsy, from insertion of the speculum to its removal was recorded in minutes, rounded to the nearest 30 seconds. Women were asked to rank their pain using a visual analogue score (0 to 10, where 0 is no pain and 10 is the worst pain in their life). Women were asked if they would have this procedure again, if they would recommend it to family or friends should they were need it. If women persisted with the procedure, they were asked their motivations for doing so, and what coping mechanisms they used. This paired data was matched to the patient's questionnaire responses.

3.2.3.3 Statistical analysis

Microsoft excel was used to provide the graphs and pie charts for demographics.
SPSS version 25 was used to perform all the sub analyses.

A sub analysis looking at whether religion, education level, presence of disability, English as 1st language, previous clinic attendance and prior information was associated with GAD7 anxiety scores was performed. Median, quartile ranges (IQ), box and whiskers plots were created for each variable (as the data was non-Gaussian). A Mann-Whitney-Wilcox test was used to assess for association between each factor and anxiety as measured with GAD7 score. Mann-Whitney-Wilcox was used to test for significance as each classifier (religion/education level) is nominal and GAD7 is a

continuous variable and the data is unpaired. Mann-Whitney-Wilcox is nonparametric test of the null hypothesis. The questionnaire asked patients to select an age category: <30, 30-39, 40-49, 50-59, 60-69, 70-79 and 80+ years old. In the analysis the young age group were defined as 49years and below inclusive, and older age group as 60 years old and above. Mann-Whitney-Wilcox was used to test for any association between old vs young women and GAD7 anxiety scores.

Stress scores were classified into low stress and high stress by scores of 3 or less and 4 or more respectively. A 2-sided Pearson Chi-square test or Fishers test (if frequency of the cell was 5 or less) was used to compare the stress scores with all variables e.g. religion, education level, with the exception of age. As age constituted multiple categories a Kruskal-Wallis test was used to test for association.

Similarly, perception of cancer was categorised into low belief of cancer diagnosis and high belief of cancer with scores of 2 and below and 3 and above respectively. A Mann-Whitney-Wilcox test was used to assess for association between cancer belief and GAD7 scores. A 2-sided Pearson Chi-square test or Fishers test (if frequency of the cell was 5 or less) was used to compare the perception of cancer with each variable e.g. religion, education level.

Kappa statistic was used to assess for agreement between GAD7 anxiety scores and self-reported stress levels. Values of 0 were used to indicate no agreement, and 0.01–0.20 as slight, 0.21–0.40 as fair, 0.41–0.60 as moderate, 0.61–0.80 as substantial, and more than 0.81 as near perfect agreement.

A 2-sided spearman rank test was used to test for a relationship between Visual analogue pain scores and GAD7 anxiety scores.

3.2.4 Results

3.2.4.1 Overall Results of the Survey

Overall, 295 consecutive patients with suspected endometrial cancer were invited to participate in the survey. 11 patients did not comprehend sufficient English to participate in the survey and were thus were excluded. Twenty-eight patients declined

to fill in the questionnaire (28/295, 9.5%). Six patients were excluded as they did not fill in the questionnaire completely (6/295, 2.0%).

The remaining 250 patients completed the questionnaire. These patients were recruited from St Marys Hospital and Queen Charlotte Hospital, from 30 clinics. The median age range was 50-59 years old (breakdown in Figure 13) and 58.5% of women spoke English as their first language. With respect to ethnicity, the majority defined themselves as White (141/250 56.4%) with the remainder defining themselves as Asian (14.0%), Black (13.6%) and Other (13.2%). Long-term disability was reported by 15% of women. Figure 14 and 15 shows patients self-reported religious identity and highest education achieved, respectively. Well educated was defined in this study as completion of A-levels inclusive and above.

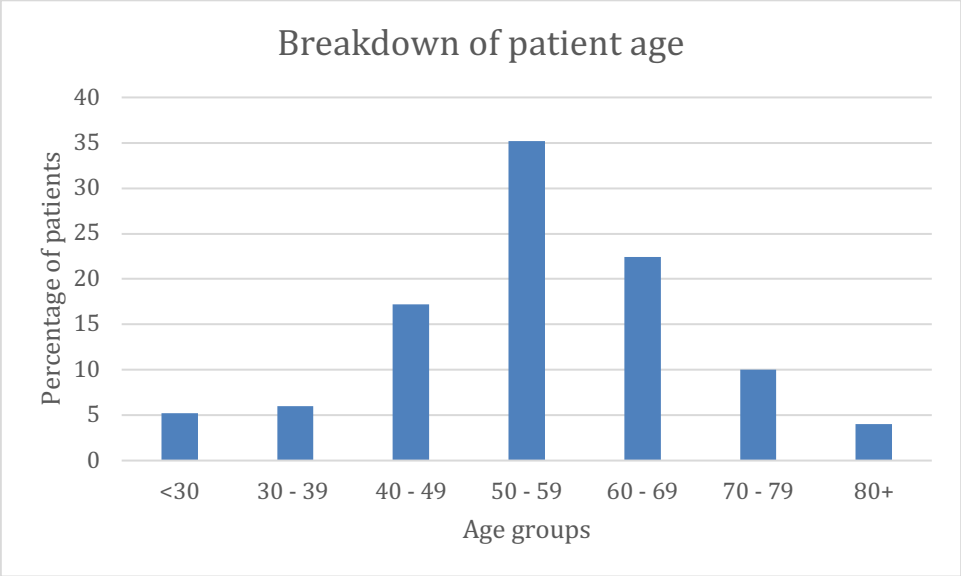


Figure 13. Breakdown of ages of women participating in the study.
The proportion of women participating in the survey within each age group is shown.

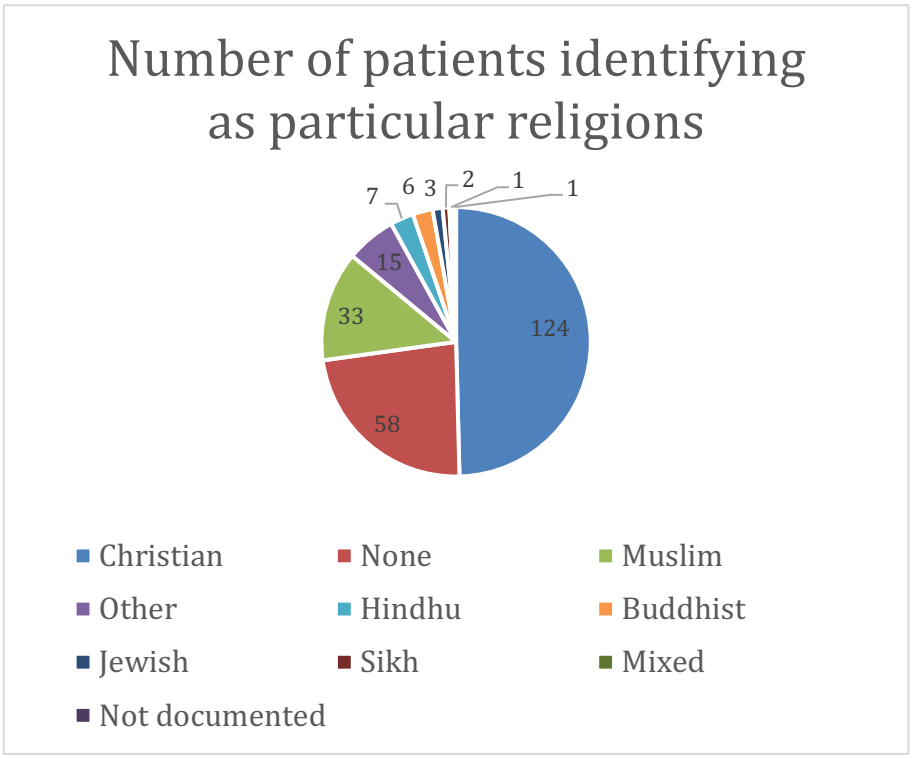


Figure 14. Breakdown of religious identity for women participating in the study.
Numbers represent the number of patients selecting a given religious or spiritual identity.

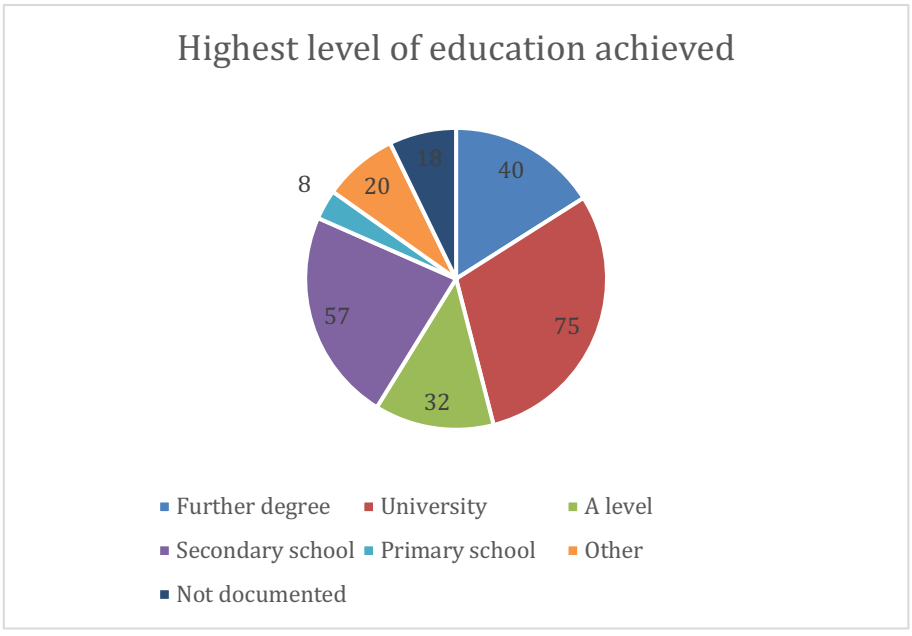


Figure 15. Breakdown of highest education completed, in women participating in the study.
Numbers represent the number of patients selecting a specific education level (maximum level they completed).

Most patients (55%) received prior information regarding the RAC visit. The most common source of information was from the GP (Figure 16). As each patient was able to select multiple sources of information the overall denominator is more than 100%. The number of patients who felt they received sufficient versus too little information

was fairly similar (48% vs 46% respectively). Few patients felt they received too much information prior to the appointment (2%).

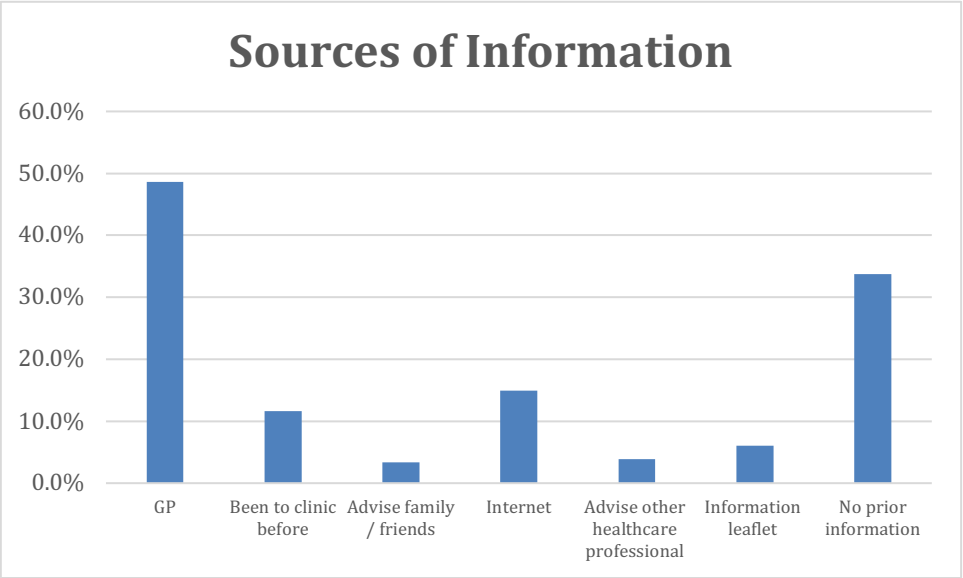


Figure 16. Sources of information women attending the clinic used.
Graph represents the proportion of each source of information selected by all 250 women. Women were able to select more than one source, so total percentage is more than 100%.

Quantifying stress levels

Patients reported a median stress level of 3 out of 5 on Likert scale (IQ 2-4, where 0 represents not stressed at all and 5 very stressed), see Figure 17 for breakdown.

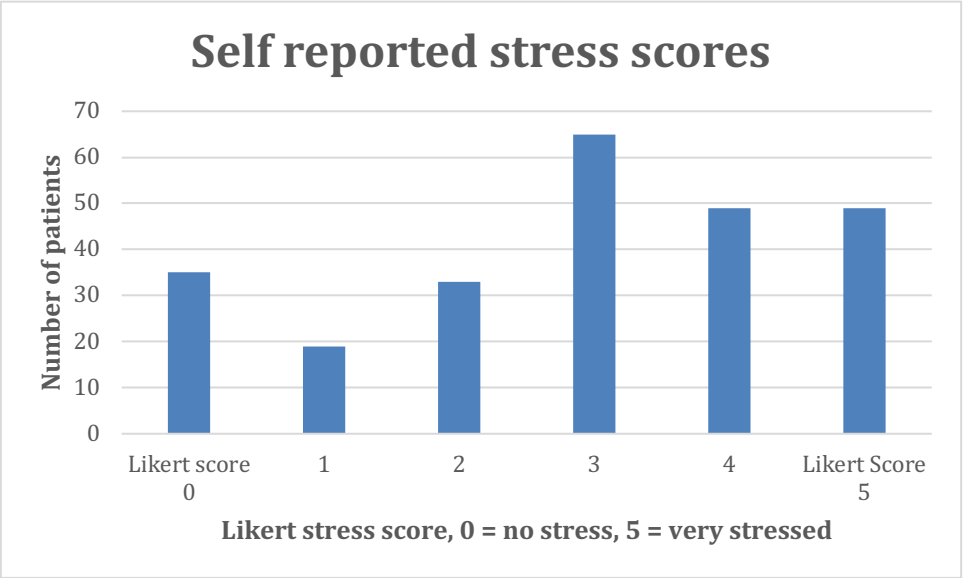


Figure 17. Breakdown of stress scores.
Number of patients who selected each individual stress score

Quantifying anxiety levels

Overall, more than 50% of women had mild to severe anxiety levels, using the GAD7 anxiety score (Figure 18), with a median GAD7 score of 6 (IQ 3-12). Some 32% of patients had a score of 10 or above.

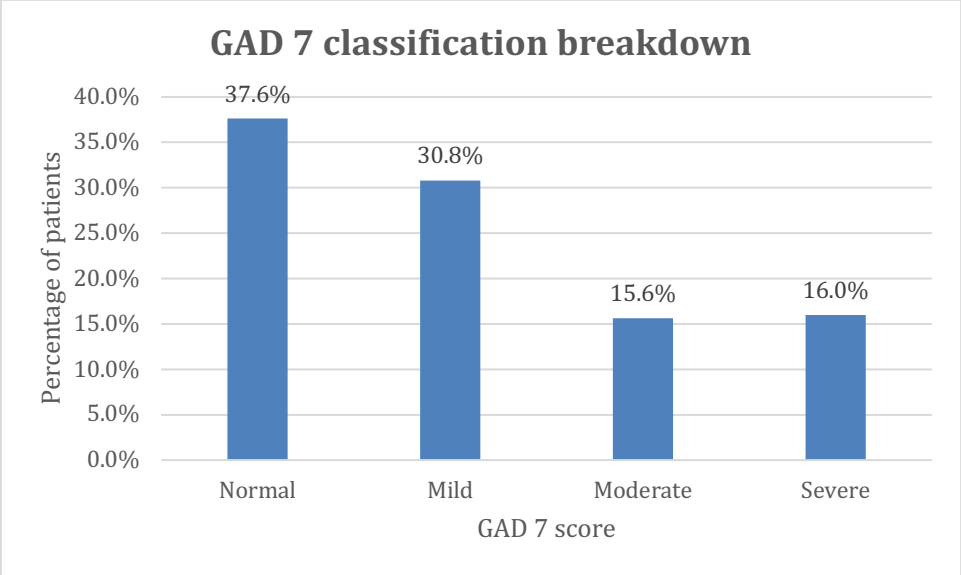


Figure 18. Anxiety scores using GAD 7 questionnaire.
Proportion of patients who have normal, mild, moderate or severe anxiety as assessed using the GAD7 score.

GAD7 anxiety and stress scores were assessed for agreement and had a Kappa value of -0.153. Table 5 below shows breakdown of GAD7 and stress scores.

			Stress score		Total
			Low Stress	High Stress	
GAD 7 score	Normal Anxiety	Count % contribution to group	66 58.9%	46 41.1%	112
	Mild Anxiety	Count % contribution to group	12 17.1%	58 82.9%	70
	Moderate Anxiety	Count % contribution to group	7 20.0%	28 80.0%	35

	Severe Anxiety	Count% contribution to group	2 6.1%	31 93.9%	33
Total			87	163	250

Table 5. Correlation of GAD7 anxiety scores and stress scores.
The table shows the number and proportion of women reporting normal to severe anxiety levels, assessed using the GAD7 score, and low or high stress levels. Agreement for anxiety and stress were evaluated. Based on this table the Kappa value of -0.153.

Importance of a quick diagnosis

Women also felt that a final diagnosis or final result was very important on the same day as first attendance with most women scoring 5 on Likert scale where 0, is not important, and 5 very important to have a quick diagnosis, range 0-5 (Figure 19).

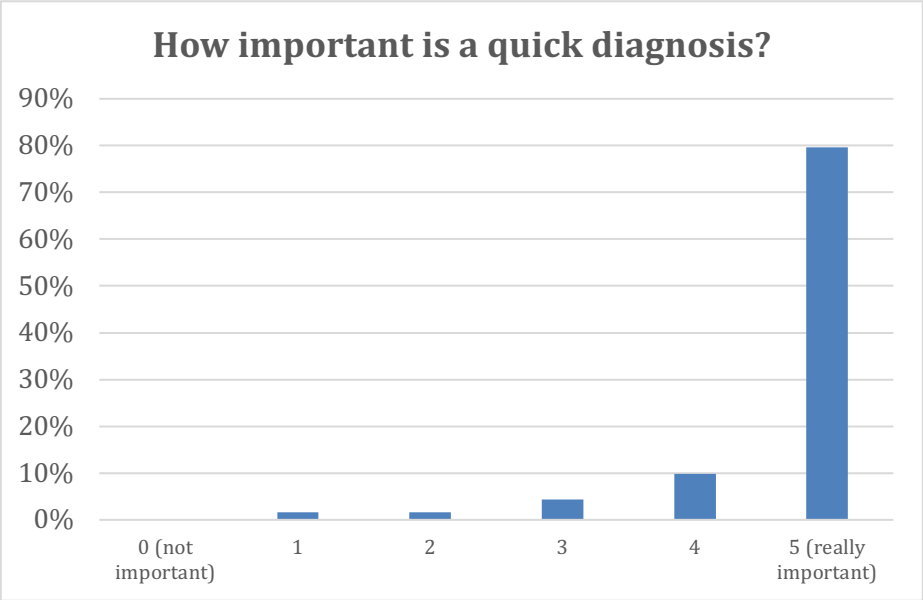


Figure 19. Importance of a quick diagnosis as reported by women filling the questionnaire.
Percentage of women who felt a quick diagnosis was really important.

Patient's perception of cancer diagnosis

Patients were asked to rank whether they believed they had cancer. The median score was 2 out of 5 on Likert scale, IQ 0-3 (where 0 represents no chance they have cancer and 5, where they felt they definitely have a diagnosis of cancer), illustrated in Figure 20. Using 3 and above as cut-off for high perception of cancer, 28% felt strongly that they had a diagnosis of cancer before seeing a clinician in clinic. Whilst using a more

stringent cut off of 4 and above, 9% of women felt strongly they had a diagnosis of cancer before seeing a healthcare provider.

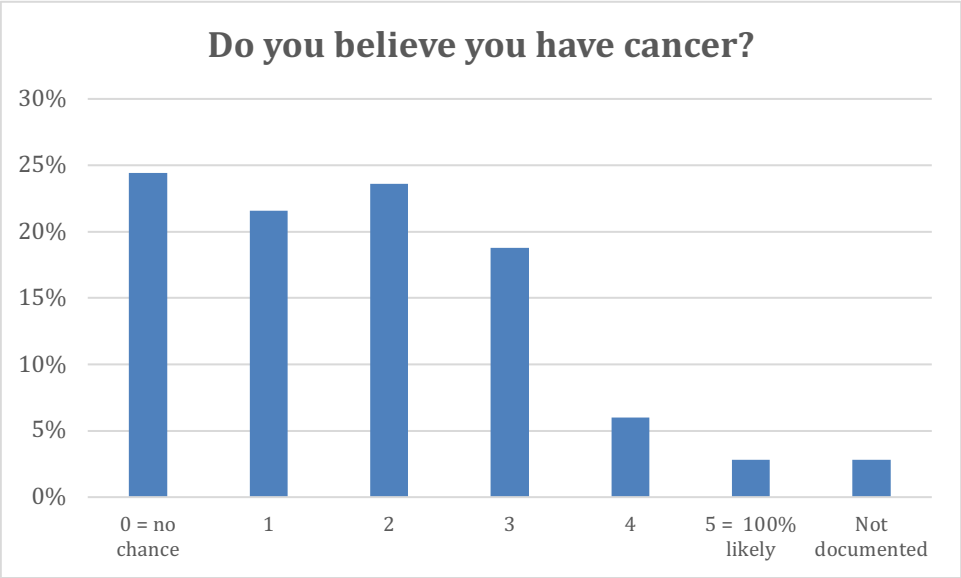


Figure 20. Self-perception of a cancer diagnosis before seeing a clinician.
Proportion of women who felt that they definitely will have a cancer diagnosis (score 5), versus those who felt there is zero chance of a cancer diagnosis (score 0), before seeing any clinician in clinic.

Patients anxiety levels evaluated using the GAD7 score was highly correlated with their belief that they had cancer P <0.00001.

3.2.4.2 Sub-analysis: factors which may affect anxiety and stress levels.

Factors affecting anxiety and stress levels

A sub analysis of factors affecting anxiety levels assessed using the GAD7 questionnaire, is depicted in Table 6. Women who identified themselves as disabled were more likely to have higher GAD7 anxiety scores (disability median GAD7 score 9 vs no disability 5.5, P = 0.00374) (Figure 21). However, no difference was observed in their stress scores P = 0.222.

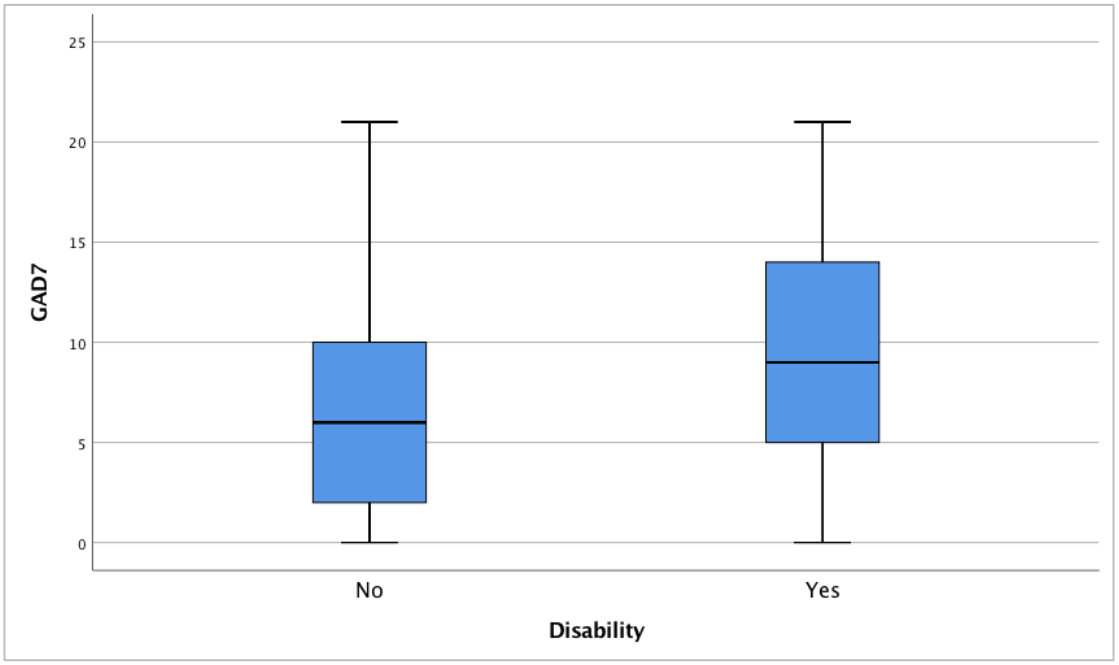


Figure 21. Box and whiskers plot for GAD7 anxiety scores in women who identified themselves as disabled. As seen in the box and whiskers plot, those who defined themselves as disabled had a higher average GAD7 anxiety score compared to those who were not disabled.

Women who felt they received insufficient information prior to clinic also had higher GAD7 anxiety scores (sufficient information median 5 vs insufficient information 9.5, P = 0.00036). Depending on the threshold used for the definition of high stress, impacted the significance of association with sufficient pre-clinic information. If a definition of high stress was 3 or more on a Likert scale p = 0.010, whilst if high stress is defined as 4 and above P=0.142. Stress scores were not influenced by any of remaining factors (P<0.05).

Level of education was not associated with GAD7 scores, as represented in the box and whiskers plot (Figure 22). Similarly, no difference was seen when comparing stress levels between the different education groups P=0.276.

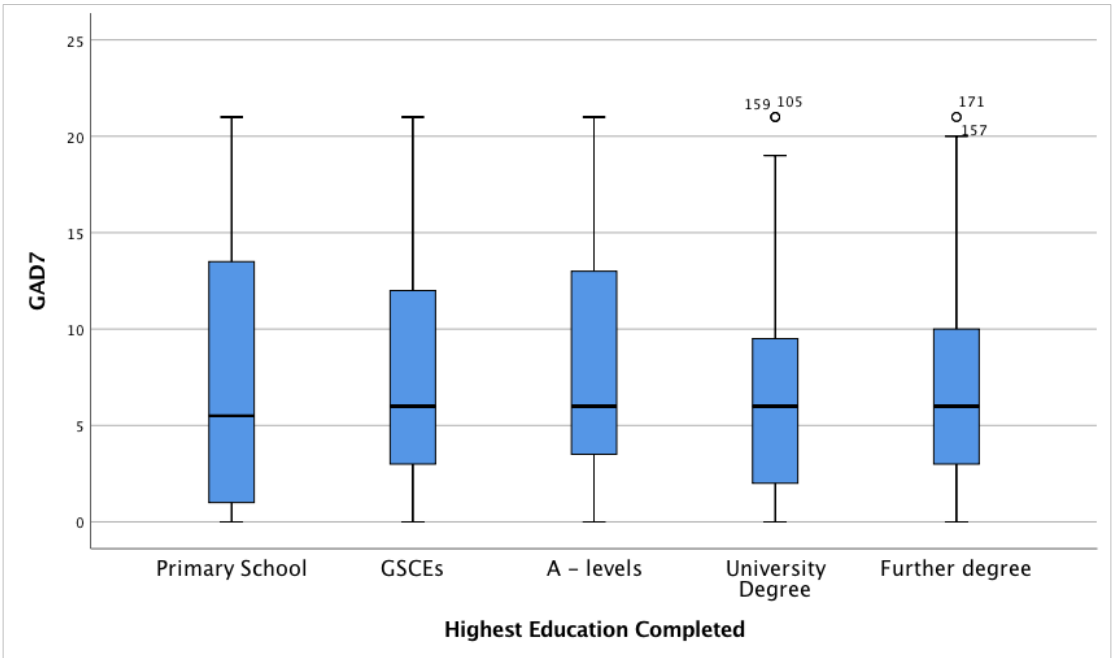


Figure 22. GAD7 anxiety scores related to highest level of education completed.
Box and whiskers plot showing GAD7 anxiety scores with respect to the highest education level completed. Numbers shown above individual box and whiskers plot reflect outlier measurements.

Group Comparisons GAD 7 anxiety scores	**Group 1 Number patients (%) Median GAD 7 score**	**Group 2 Number patients, (%) Median GAD 7 score**	**Mann Whitney test**
Age	Young Number = 71 Median = 7	Old Number = 91 Median = 5	P = 0.078
Religion	Religion Number = 191(77%) Median GAD7 = 6	No Religion Number = 58 (23%) Median GAD7 = 5.5	P = 0.368
Disability	Disabled Number = 35 (14%) Median = 9	Not disabled Number = 211 (86%) Median = 6	P = 0.00374*
English as first language	English 1st language Number = 143 (57%)	English not 1st Number = 107 (43%)	P = 0.238

	Median = 6	Median = 6	
Education level	A-levels and above Number =167 (72%) Median = 6	Up to secondary school Number =65 (28%) Median = 6	P = 0.711
Sufficient information pre-clinic	Patients felt they received sufficient information prior to clinic Number =86 (49%) Median = 5	Patients did not feel they received sufficient information prior to clinic Number =91 (51%) Median = 9.5	P = 0.00036*
Previous clinic attendance vs not	Attended clinic previously Number =21 (19%) Median = 5	Never attended clinic previously N = 156 (81%) Median = 6	P = 0.390

Table 6. Factors affecting GAD 7 anxiety scores. P values <0.05 considered significant and shown with a*. Table showing the median GAD7 score across the variables assessed. Each variable is divided into 2 groups, depending on the individual variable. For example, 'English as first language' vs 'English not first language'. The GAD7 anxiety scores were then assessed for significance between the groups using the Mann-Whitney test.

3.2.4.3 Sub-analysis: factors which may affect perception of cancer diagnosis

Women who felt they didn't receive enough information prior to clinic were more likely to think they have cancer P = 0.0432 (Not enough information Median 2, IQ 1-3, vs sufficient 1 IQ 0-2). The presence of religion, disability, age and education levels were not associated with perception of cancer scores, P=0.269, P=0.141, P=0.103 and P=0.430 respectively. There was also no association between patient's perception of their diagnosis and whether they had attended clinic previously P = 0.616. Patients were more likely to think they had a diagnosis of cancer if they spoke English as a first language P= 0.049 (median perception of cancer score for English not first language 1, IQ 0 - 2 vs English 1st language 2, IQ 1-3), Figure 23.

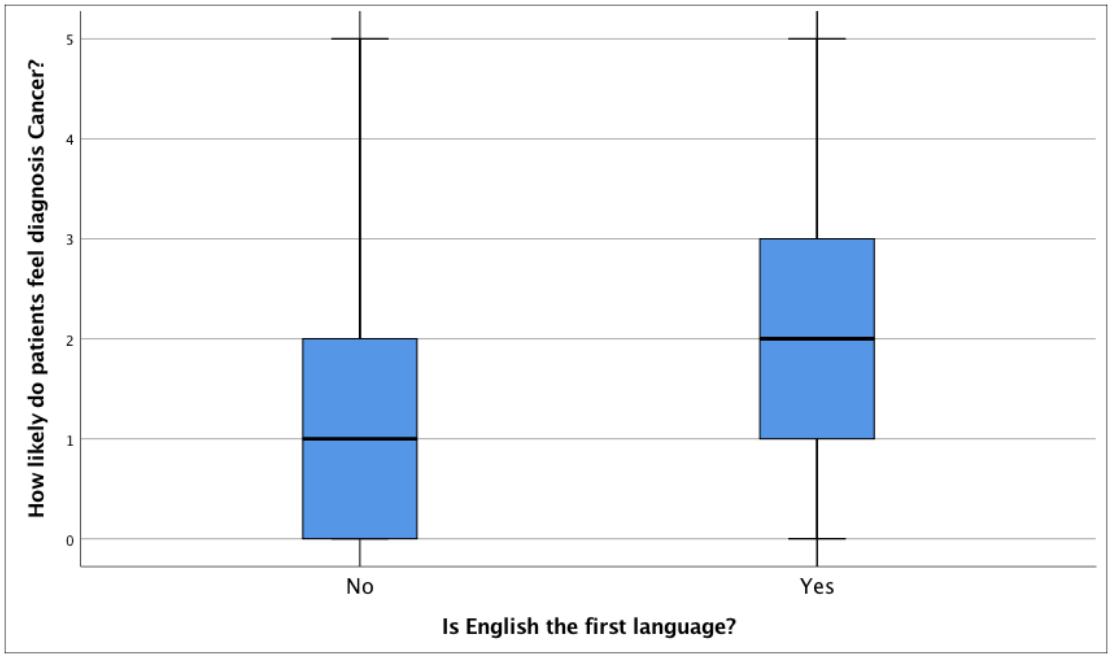


Figure 23. Box and whiskers plot, for association between perception of a cancer diagnosis and English as 1st language.
Box and whiskers plot showing perception of cancer score in those who speak English as a first language and those who don't. In this figure those who speak English as a first language were more likely to think they will have a cancer diagnosis as illustrated by higher score.

3.2.4.4 Observational study looking at behaviour

Of the 250 women who participated in the survey, 23 underwent endometrial biopsy samples. The median visual analogue scale score was 7 out of 10 (range 1-10). The median time taken to perform the endometrial biopsy was 5 minutes (range 3-12 minutes). Out of the 23 biopsies that were performed in clinic, 78% of biopsies were successful. Those which weren't successful were terminated by the doctor due to cervical stenosis, not at patients request. All patients said they would have the outpatient procedure again if they needed it and would recommend the procedure to family/friends if indicated (even those reporting pain scores of 10 out of 10). When asked why the persevered with the procedure the most commonly cited reasons were "I need it" and "need to know what's going on". This is despite clinicians offering to have the procedure performed under general anaesthesia on a different day.

Of those who filled the questionnaire and received a pipelle biopsy, the median GAD7 anxiety score was 7, with self-reported median stress score of 3 out of 5. Spearman's correlation coefficient rs, for association between anxiety (GAD7) and pain perception (VAS) was 0.021 and this was not statistically significant (p = 0.927). Most patients

wanted a diagnosis straight away (median 5 of out 5). The median score for the perception of a cancer diagnosis was 2 out of 5.

3.2.5 Discussion

Main findings

This study shows that almost a third of patients presenting to the Rapid Access Clinic (RAC) had significant levels of anxiety, as evidenced by a GAD7 score of 10 or more, the level at which intervention is routinely offered for cancer patients [273]. It is also in keeping with the self-reported median stress score of 3 out of 5.

Illuminatingly, most patients attending the RAC felt that they didn't have cancer (Likert score median 2), with just under 10% of women feeling fairly sure that they will have a cancer diagnosis (those with Likert score 4 or 5). This figure is actually not much different to actual cancer diagnosis rates within the RAC (10%), which shows that most patients manage to retain perspective, despite the threat. This study also showed a strong association between patients' belief of a cancer diagnosis and GAD7 anxiety scores ($P < 0.00001$) i.e. the more anxious the patient is, the more likely the patient thinks they have cancer. Though one could also consider that if the patient was more likely to think they had cancer they would become more anxious, creating a viscous cycle of anxiety.

Almost half of all patients attending the RAC in this study, felt they did not receive enough information beforehand, and the sub-analysis shows that those patients who perceived that they received insufficient information prior to clinic had higher GAD7 anxiety scores and self-reported stress scores. This is in keeping with the PROFILES study, that found suboptimal information provision was associated higher anxiety and depressive symptoms in cancer survivors [274]. Without sufficient information uncertainty increases and this can increase anxiety levels [261, 266, 275]. Therefore, clinicians should offer timely and sufficient pre-clinic information to improve patients' awareness and decrease their uncertainty.

More worrisomely, in this study patients who felt they didn't receive enough information before the appointment were also more likely to think they had cancer. Despite, reassuring national figures which show that 80% of women on average will receive a benign diagnosis [41]. This finding provides scope to help women in the future, by

offering more information to women, prior to their clinic attendance clinic.

In this study, the internet was the second largest source of information for patients after their GP. This is in concordance with other studies which have shown 33-85% of patients use the internet to gain information about upcoming treatment and, or diagnosis [276, 277]. Given the diversity of health information on the worldwide web, quality information is often lacking [278, 279]. In the context of gynaecological cancers the amount of information is often overwhelming, however a lack of validated quality websites hampers accurate patient knowledge [280]. Thus, it is possible that the use of the internet may either alleviate or create anxiety depending on which websites patients use. This study didn't ask patients to specify which websites were used for information.

Interestingly, though prior information was associated with anxiety levels, previous clinic attendance was not. One might postulate that prior clinic attendance would have provided enough knowledge to reassure patients about future clinic attendances, however this was not demonstrated. Lack of an association may be a reflection of underpowering of this group, as only 21 (<10%) patients had been to the RAC before.

This study also analysed other factors that might be associated with anxiety levels, such as English as first language, age, religion and education levels. This study failed to show any association between any of these factors and GAD7 anxiety scores. Spirituality and religion have often been cited as [269, 281] factors that reduce anxiety. The present study failed to show any association between those who define themselves as religious and those that do not. Whilst spirituality was not directly stated as option on the questionnaire, 15 patients selected other and commented spiritual. It may be that religion and spirituality play a greater role post diagnosis of cancer.

English as a first language was associated with perception of a cancer diagnosis. Patients were more likely to think they had a diagnosis of cancer if they spoke English as a first language P= 0.049. This may reflect a type 1 error, as the P value was only just under 0.05. It may also relate to cultural perceptions of cancer. In this study I did not look at the effect of ethnicity on GAD7 anxiety scores or perception of cancer. English as a first language can be used as a surrogate marker for ethnicity to some extent, with those not speaking English as first language more likely to represent other ethnic groups. It is also possible that not speaking English as first language may prevent patients from easily seeking information about their symptoms, effectively

shielding potentially scary information from the patient, creating effectively 'ignorant bliss'.

Significantly, in this study patients with disability had higher GAD7 anxiety scores and were more likely to think they had a cancer, though this was not reflected in their self-reported stress score. These findings provide evidence for additional psychological support for this minority group.

Previous studies in breast and prostate cancer have reported significantly lower levels of psychological distress in patients with high partner support [282-285]. In Bradley et al study of 152 cervical and breast cancer patients, survivors were especially at risk of mood and mental health difficulties if unemployed or living alone [286]. This study unfortunately did not address partner support; but would be an interesting avenue to explore in future studies.

It is known that lengthy delays to diagnosis for women with abnormal screening mammography causes anxiety and distress [258, 259]. Waiting in itself is thought to cause unintended harm, 'the nocebo effect' [287]. In endometrial cancer, a survey of over 200 patients found longer diagnostic delays were associated with reduced overall quality of life [218]. Furthermore, a meta-analysis of the prevalence of distress surrounding the diagnostic process of suspected cancer showed a rapid decrease of anxiety, in patients eventually not diagnosed with cancer [260]. It was, unsurprising therefore patients were very keen to get a diagnosis as soon as possible (median 5/5 on Likert scale). This is evidenced by their behavioural response - tolerating endometrial biopsy procedures for sometimes over 10minutes with moderate to severe pain scores. Despite this, patients would undergo the procedure again as they 'want to know what is going on'.

To help alleviate pain associated with an endometrial tissue biopsy, a number of options have been suggested. A 'vocal local', namely a healthcare assistant to talk to the patient through the procedure [288]; anecdotally this is thought to be helpful and is recommended by the Royal College of Obstetrics and Gynaecology. Entonox(®) (50% nitrous oxide and 50% oxygen; BOC Healthcare, Manchester, UK) has been shown to be very effective in reducing pain in outpatient urological procedures and could be used effectively in outpatient gynaecology procedures too [289].

Interestingly, in several studies in breast cancer, whilst a speedier diagnosis helped minimise immediate psychological distress it sometimes increased or sustained depressive and anxiety symptoms in those whom cancer was diagnosed [290]. It was suggested that this is due to loss of preparatory time for diagnosis [291].

In this study there was no correlation with pain scores of endometrial biopsies (VAS) and anxiety scores (GAD7). The International Association for the Study of Pain defines pain as "an unpleasant sensory and emotional experience associated with actual or potential tissue damage or described in terms of such damage". The sensation of pain is complex and may be exacerbated by anxiety [292]. It is possible that due to underpowering of this sub-study with only 23 women who completed the survey undergoing paired tissue samples no association was seen. However, it is more telling that all patients would have persevered with the procedure or agree to have it again as an outpatient; and corroborates patients overriding need to have a diagnosis quickly.

This study failed to show any agreement between GAD7 anxiety scores and self-reported stress scores. It was assumed that patients with more stress were more anxious, but the Kappa score, a measure of agreement was not significant. Looking at the distribution of scores in Table 5, patients who had moderate and severe anxiety scores using the GAD7 anxiety score were more likely to report high stress levels i.e. fairly congruent. However, normal/mild anxiety levels correlated more poorly with stress scores. Stress is multi-dimensional construct that is initiated when a person perceives that demands exceed resources mobilized by the individual. Anxiety itself is a response of the body to a perceived threat or stress which is triggered by an individual's beliefs, feelings, and thoughts and often accompanied by unpleasant feelings, behavioural, cognitive and physiological symptoms. There is a lot of overlap between the symptoms of stress and anxiety.

To help reduce anxiety in the waiting room, music has been shown to be effective [293]. It has also been suggested that a healthcare assistant present in the waiting room may also be used to help alleviate patients' anxieties and listen to patient concerns.

This study used the GAD7 scoring system for anxiety. In addition, a Likert, stress scale was used, based on Distress Thermometer [272]. Variations in methodologies and scoring systems make comparisons of anxiety levels in cancer patients difficult amongst different studies [294]. Table 7 outlines common anxiety scoring systems. Each scoring system has its own benefits and limitations.

Types of Anxiety Scoring Systems	**Key points**
Beck Anxiety Inventory (BAI)[295]	21 item self-reported scale assessing the severity of somatic symptoms of anxiety. Initially designed to discriminate between depression and anxiety symptoms. A score of > 10 is suggestive of mild anxiety; a score > 19 suggests moderate anxiety.
GAD 7[296]	7 item questionnaire. Scores of > 5, 10, and 15 suggest mild, moderate, and severe levels of anxiety respectively
Generalized Anxiety Disorder Questionnaire-IV (GAD-Q-IV)[297]	9 item questionnaire assessing symptoms of generalized anxiety disorder. Domains assessed include: uncontrollable worry, physical symptoms, functional impairment and subjective distress
Hospital Anxiety and Depression Scale (HADS)[298]	14 item self-reported scale, measures anxiety and depression. Physical symptom items are not included.
Penn State Worry Questionnaire (PSWQ) and abbreviated form (PSWQ-A)[299, 300]	PSWQ-A (8 items) and PSWQ (16 items) are self-reported scales assessing worry severity.
Spielberger State-Trait Anxiety Inventory [301]	20-item questionnaire assessing: ● State - how respondents feel right now / at this

	moment. ● Trait - how respondents feel in generally

Table 7. Types of anxiety scoring system currently used and their key features.

The Hospital and Anxiety Depression Scale (HADS) is one of the most widely used but has had poor sensitivity for anxiety in breast cancer [256, 302] with sparse studies in endometrial cancer. The GAD7 score was initially created to screen for the mental health condition Generalised Anxiety Disorder but is used ubiquitously as screening tool for anxiety in general, particularly in research studies [303]. The GAD-7 exhibits strong internal consistency, reliability and correlates positively with work absences and functional impairments [303]. It has been shown to have the best performance characteristics for identifying generalized anxiety disorder (GAD) in primary care [304, 305]. The GAD7 tool was validated with a cut-off score of 10, from the responses from 2739, primarily Caucasian patients (80%), but has been shown to be less accurate in other ethnic groups [303]. Using a threshold of 10, the GAD-7 has a sensitivity of 89% and a specificity of 82% for generalised anxiety disorder. It is also good at screening for other common anxiety disorders - social anxiety disorder (sensitivity 72%, specificity 80%), panic disorder (sensitivity 74%, specificity 81%), and post-traumatic stress disorder (sensitivity 66%, specificity 81%) [296] . The GAD7 scoring system was chosen as it was the shortest and easiest to fill, with minimum response burden. The general consensus has been that shorter questionnaires have lower response burdens and higher response rates, although this is somewhat contentious [306].

Strengths and limitations

One of the biggest benefits of this study is its large prospective nature. This study had a high response rates (85%) and sampled patients from a wide demographic within central London. Several studies have shown that waiting times and doctor-patient communication considerably influences anxiety levels [258]. As patients were asked to fill in the questionnaire prior to seeing any healthcare professional, there was no risk that the doctors or nurse's communication in clinic introduced bias. Future studies may focus on following patients journey through clinic and look at paired anxiety levels, pre and post review by the doctor and diagnosis in RAC. This will then ascertain whether

a quick diagnosis was beneficial in hindsight; or whether more preparatory time was important. In addition, future studies can help identify women with high anxiety and perception of cancer but with a final diagnosis of benign pathology, i.e. identify the 'worried well' and see if there is a way to target these patients.

As this is a questionnaire study, the main limitations include: reporting bias, and selection bias. The study relied on voluntary participation and it is possible there might be systematic differences between the patients who agreed to participate in the study and those who did not or were excluded from the study.

In addition, the classification of high and low stress levels and perception of cancer diagnosis was defined by a certain threshold on the Likert scale. The most frequent stress score cited in this study was 3 out of 5. Thus, defining high stress to be above 3, or 3 inclusive and above could impact the significance of correlation. For example, when analysing whether sufficient pre-clinic information influenced stress levels, if high stress was defined as 3 or more $p = 0.010$, whilst if high stress was defined as 4 and above $P=0.142$. There is no accepted cut-off in the literature for significant stress levels and perception of cancer diagnosis using these scales. In this study it was felt that a lower score for perception of cancer was still important so a cut off of 3 and above for high perception of cancer was used. Future studies may benefit from a Delphi survey to appropriately define this threshold. Alternatively, a more detailed stress questionnaire such as the perceived stress scale, stressometer or stress overload scale could be used, but may risk hampering uptake of the questionnaire [307-309].

Conclusion

In summary, this study supports the widely held belief that women attending RAC for suspected endometrial cancer are anxious and very keen to have a diagnosis as soon as possible. In addition, the presence disability and sufficient pre-clinic information can influence anxiety levels and perception of cancer diagnosis significantly.

3.3 Overall need for change

In a UK study, supported by the National Awareness and Early Diagnosis Initiative (NAEDI) programme, it was reported that over half of patients with endometrial cancer waited more than a month for a GP appointment. Furthermore, 30% of patients had more than a 2 weeks wait for a rapid access appointment and almost 20% patients had to wait for more than 62 days for their first treatment (surgery) [229].

Diagnostic and treatment delays are often blamed for poorer cancer survival rates in the UK [229, 310]. Evidence for improved prognosis with a shorter time from diagnosis to treatment was seen in this PhD. Furthermore, the psychological study provides strong evidence that women suffer from high levels of anxiety awaiting a diagnosis and want a quick result.

Thus, prognostic and psychological benefits to a faster diagnosis warrant an evaluation of the new technologies that might facilitate this. A clinical trial was therefore designed to investigate these novel technologies.

3.3.1 Clinical trial

I designed, set up and ran a multifaceted clinical trial looking at the diagnostic performance of novel tests in endometrial cancer diagnosis and assessment. As the research objectives involved the same patient population the trial assessed all the objectives and corresponding technologies together (see Figure 26). The patients, however, could choose to participate in all, or part of the trial.

Prior to commencement the clinical trial, a unified protocol (Appendix 12.2) with corresponding patient leaflets and consent forms were created. A Patient Public Involvement (PPI) group was created and used for advice on study design, and to check the leaflets and the study summary were easy to read and in lay-men terms. REC approval was sought and granted (June 2017). The clinical trials were registered separately on a publicly available independent website www.clinicaltrials.gov.

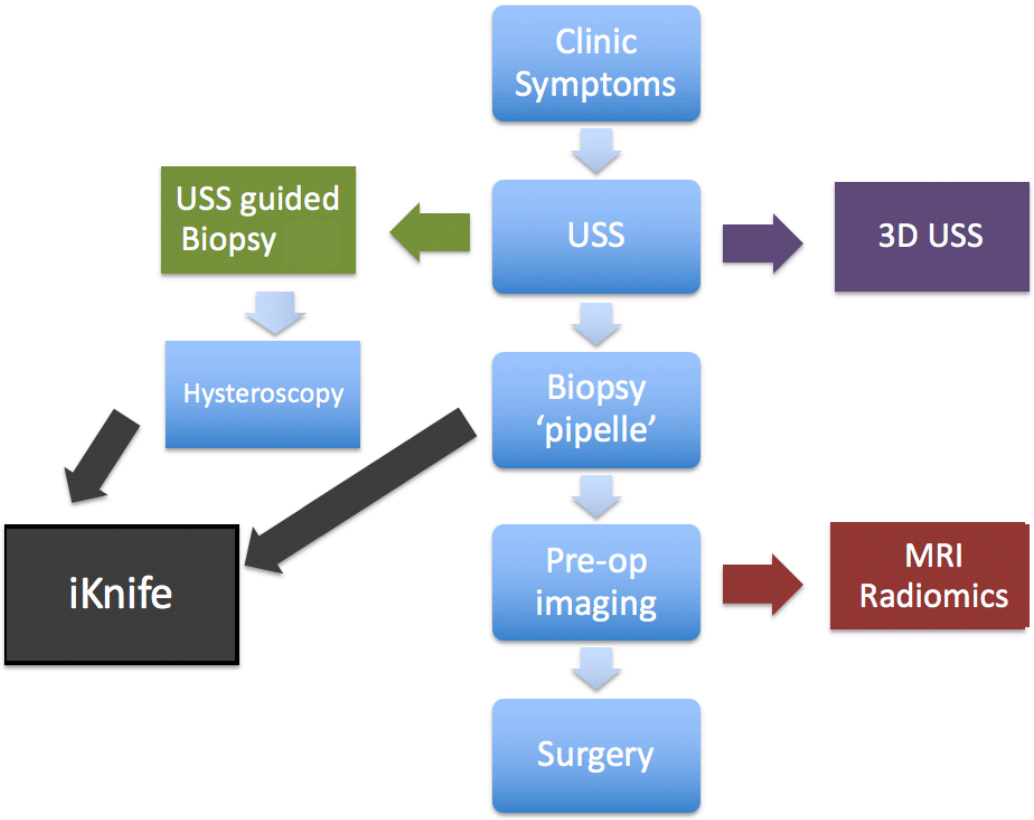


Figure 24. Clinical pathway with new technologies introduced.
The current pathway is shown in light blue boxes and the new technology is shown as a different box colour: USS guided biopsy, 3D USS, MRI radiomics and the iKnife.

A synopsis of each technological element evaluated within the trial will follow. After which, each of the chapters will describe in detail the methodology, results and interpretation of findings for each element. Each chapter begins with a short abstract summarising the key points and a brief introduction.

REIMS (iKnife)

Patients with suspected endometrial cancer undergoing an endometrial biopsy for a clinically indicated reason were invited to partake in the study by providing a tissue sample for research. The research tissue was analysed by REIMS and compared to the reference standard histopathology. The diagnostic accuracy was calculated.

USS guided biopsy

Women who would normally be advised to have a hysteroscopy and biopsy due to cervical stenosis or a focal lesion, were invited to participate in this part of the study by having an ultrasound guided biopsy in clinic instead. The sample was analysed with standard histopathology, and if insufficient or if the ultrasound guided biopsy was not successful then a hysteroscopy was performed. The success rate, pain and acceptability of this technique were calculated.

3D Ultrasound

Women with suspected endometrial cancer were invited to undergo a 3D ultrasound, and images saved. In those women who are later diagnosed with confirmed endometrial cancer the 3D images are rendered and an assessment of deep myometrial invasion was made by a blinded examiner. The diagnostic accuracy was compared to the reference standard of final histology. The diagnostic accuracy was also be compared to MRI.

A systematic review and meta-analysis of diagnostic performance of 3D ultrasound in diagnosing deep myometrial invasion was also performed.

Radiomics

All women with confirmed endometrial cancer underwent an MRI as part of routine standard of care. These images are anonymised, segmented as described in the introduction section 2.4.4. Texture analysis was performed and radiomics was created and validated for the prediction of grade, stage and prognosis.

3.3.2 Cost-effectiveness analysis

Having evaluated these new technologies, I performed a cost effectiveness analysis to assess whether these new innovations might be frugal, potentially minimising costs. The effectiveness figures I generated from the studies above formed the basis assumptions used in the cost-effectiveness model.

CHAPTER 4: THE iKNIFE

CHAPTER 4: THE iKNIFE

Collaborators:

Hiromi Kudo, histopathology technician mounted all the slides. Dr Francesca Rossi and Dr Roberto Dina provided histopathological validation of the samples.

4.1 Summary

Objective: Establish whether the iKnife could distinguish between normal and malignant endometrial biopsy samples based on differences in their lipidomic profiles.
Methods: Research pipelle biopsy samples were obtained for women needing biopsies for clinical reasons (samples concurrently sent to conventional histopathology). A Waters G2-XS Xevo Q-Tof mass spectrometer was used in this study in conjunction with a modified electrosurgical instrument (collectively coined the 'iKnife'). The resultant surgical aerosol containing ionic species produced during diathermy was then analysed with this technology; producing spectra that were background subtracted, lock mass corrected and in the phospholipid range. Principal component analysis (PCA) and linear discriminant analysis (LDA) were then performed to find the variance in spectral signatures. A leave one patient out cross validation was used to obtain diagnostic accuracy.
Results: A total of 150 pipelle biopsy samples (85 normal, 59 malignant, 4 hyperplasia and 2 insufficient) were obtained from 150 patients. Each tissue sample was processed as described; producing an individual spectrum per burn. The iKnife differentiated between normal and malignant endometrial tissues on the basis of differences in their unique phospholipid spectral signatures. Cross validation revealed a diagnostic accuracy of approximately 90%.
Conclusions: This study was the first to use the iKnife as a tool to differentiate between normal and malignant endometrial pipelle samples. These results are encouraging and suggest that the iKnife could be used as an adjunct in clinic to provide a point-of-care diagnosis.

4.2 Introduction

Endometrial cancer is the most common gynaecological cancer in the western world with 120,000 new cases diagnosed per year in Europe [1]. Diagnosis of endometrial cancer is confirmed by histological examination of endometrial curetting's or outpatient endometrial biopsies e.g. pipelle tissue samples. It can take up to two weeks for patients to get a result, causing extra anxiety for patients and delays time sensitive surgery, as discussed in chapters 2 and 3. To-date there is no point-of-care (POC) diagnosis available. The intelligent surgical knife, 'iKnife' is a novel mass spectrometry technique that combines REIMS with standard electrosurgery and analyses tissue real-time (see Introduction 1.4.3) but has never been used to diagnose endometrial cancer, thus far.

The surgical aerosol produced by electrosurgery produces an abundance of information about the phospholipid composition of cancer tissue. Phospholipids (PLs) are the main component in biological membranes [311]. They are generated by the coupling of a phosphate and a glycerol head group along with two, variable fatty acid chains, which make up the tails (see Figure 25). The cell membrane is formed by the aggregation of PLs into a bilayer, facilitated by the natural predisposition of the hydrophobic tails and hydrophilic glycerol head [312]. The most common phospholipid in cell membranes is phosphatidylcholine (PC), which gets its namesake through the incorporation of choline into the glycerol head group. Other common PLs include: phosphatidylethanolamines (PE), phosphatidylinositols (PI), phosphatidylserines (PS), phosphatidylglycerols (PG) and phosphatidic acid (PA) and these reflect the presence of additional head groups (such as ethanolamine, inositol, serine and glycerol) [311].

Lipid metabolism, including the biosynthesis, uptake, transport and degradation are complex processes [311]. Both the biosynthesis of PLs (via the Kennedy and CDP-DAG pathways) and degradation of PLs are regulated by multiple signalling pathways in response to cell needs and environmental changes [311] (Figure 25 adapted from [313]). During PL metabolism many bioactive lipid molecules are generated including: inositol trisphosphate, arachidonic acid and phosphatidic acid [311, 314] and these in turn regulate signalling pathways involved in cell growth, differentiation, survival, inflammation and apoptosis [311, 315, 316]. Many of these molecules are essential in normal cellular homeostasis but are also influential in the disordered cell signalling seen in cancer.

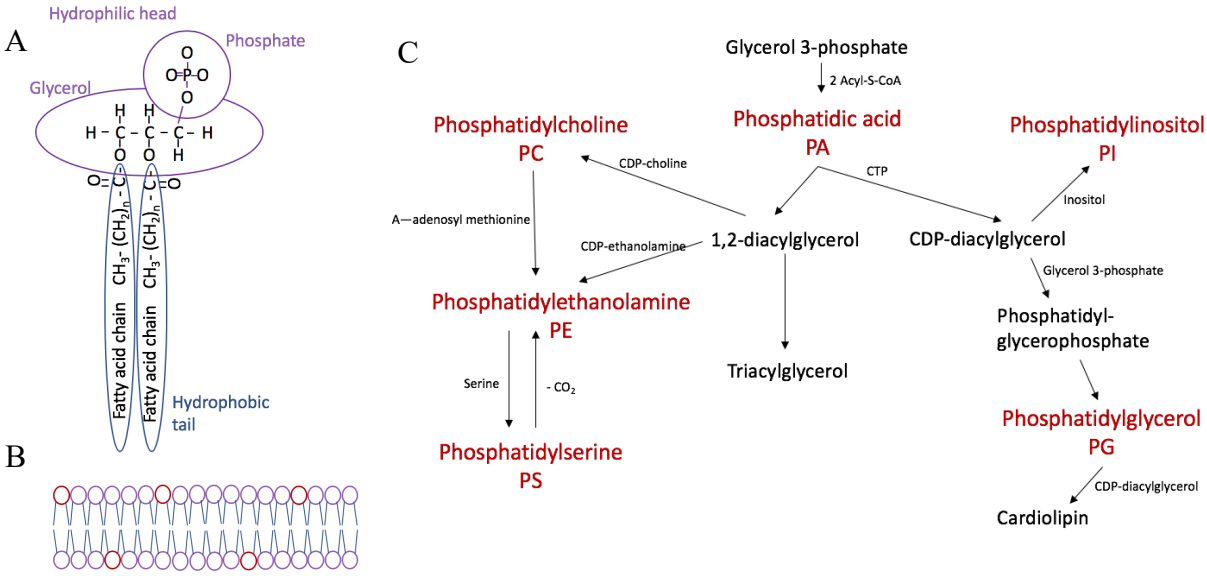


Figure 25. The phospholipid bilayer and lipid synthesis.
A) A phospholipid, comprising of a glycerol-3-phosphate head and 2 variable chain fatty acids. B) The phospholipid bilayer compromising a hydrophilic heads and hydrophobic tails. Head groups modified (red) according to the addition of additional head groups. C) Adapted illustration of the Kennedy pathway and CDP-DAG pathway for lipid synthesis, showing the biochemical pathways that generate the alcohol head groups. Annotations: H = hydrogen, C = Carbon, O = oxygen, P = phosphorous, CDP = cytidine diphosphate, CTP = phosphocholine cytidyltransferase. Figure adapted from Wickner 2011.

Cancer is characterised by uncontrolled cellular proliferation and reduced apoptosis. The most noticeable metabolic phenomena seen in cancer is an increase in glucose uptake and the use of aerobic glycolysis, known as the Warburg effect [317]. But aberrant lipid metabolism is also an important metabolic feature of cancer cells due to increased biosynthesis and the generation of bioactive signalling molecules during lipid catabolism [311]. Furthermore, the commonly mutated genes in endometrial cancer have important roles in lipid metabolism [21, 318]. *Phosphatase and Tensin Homolog* deleted on Chromosome 10 (*PTEN*) is a protein and lipid phosphatase in addition to being a tumour suppressor [319]. *PIK3CA* encodes for a subunit of phosphatidylinositol 3-kinase (PI3K), a family of lipid kinases that regulate growth and survival signalling [320]. *ARID1A* is involved in insulin sensitivity and lipid metabolism [321] and *p53* is both a tumour suppressor and regulator of lipid metabolism [322].

Cell proliferation requires duplication of all components of the cell. Therefore, cancer cells, much like normal cells will require duplication of PLs for the development of new cell membranes. Due to these raised metabolic demands, in addition to the normal supply of fatty acids from the diet, rapid de novo synthesis is also required [323].

Increased de novo synthesis is largely driven by overexpression of lipogenic enzymes regulated by lipid signalling pathways [324]. This is supported by evidence of increased cholesterol biosynthesis and fatty acid synthase activity in cancer cells [311, 312, 325, 326]. Indeed, studies have shown that inhibition of enzymes involved in cholesterol and fatty acid synthesis reduces tumour growth [311, 317, 324, 327-329].

A key enzyme in the biosynthesis of PCs, choline kinase activity, is upregulated by both growth factors and also oncogene coding proteins such as *ras* [311, 330]. In endometrial cancer, phosphocholine levels increase by 70%, which is mediated by increased expression of choline kinase [331, 332]. Interestingly, in a study looking for plasma biomarkers, Knific et al, identified 3 PCs which were significantly decreased in endometrial cancer patients [333]. PCs are themselves hydrolysed by the enzyme phospholipase D (PLD), and PLD has been shown to be involved in cell invasiveness [334]. In mice studies inhibition of PLD1, the isomer of PLD, suppresses the mitogen activated protein kinase (MAPK) signalling pathway and promotes tumour growth and metastases [335].

The shift in de novo lipid synthesis has been reported to increase membrane saturation, resulting in higher levels of saturated phospholipids, reducing membrane fluidity and potentially protecting cancer cells from oxidative damage secondary to peroxidation [317, 336].

Lipid synthesis has also been shown to promote cancer through its important roles in structural support, cell signalling, post translational modification of proteins, autophagy and angiogenesis [317]. Furthermore, it has been suggested that the accumulation of lipids can act as a source of nutrients for tumour cells [317].

Despite multiple studies showing lipidomic alterations in cancer, few studies have specifically addressed lipid metabolism in endometrial cancer. Upregulation of glucose transporters particularly GLUT6, and the lipogenic enzymes ATP citrate lyase (ACLY), acetyl-CoA carboxylases (ACC1 and ACC2), fatty acid synthase (FASN) and sterol regulatory element-binding protein 1 (SREBP1), a regulator of lipogenic gene expression have all been shown to be overexpressed in endometrial cancer [337, 338]. In addition, profound changes in sphingolipid have been demonstrated in endometrial cancer [339].

The aims of this study were to see if the iKnife can distinguish between normal and malignant endometrial biopsy samples based on differences in their lipidomic profiles and determine the main lipids involved in this separation.

4.3 Pilot study – Can iKnife distinguish between normal and cancer endometrial tissue bank samples?

4.3.1 Materials and methods

List of chemicals, solvents, materials and equipment (Table 8).

Item name	Supplier
Air displacement pipette (10, 20, 200,100µl)	Eppendorf
Argon gas cylinder, 7 bar pressure	BOC
Tissue Processing/Embedding Cassettes with Combination Lid and Base, blue	Fisher Scientific
Cassette Sponges, Blue	Fisher Scientific
Connectors – push in and straight for 6mm tubing	Camozzi
Conductive silicone return plate, CS 187cm	Erbe
CoolRack	Biocision
Dissection board, Cork	Thermoscientific
Electrosurgical ForceTriad generator	Covidien
Formalin, 10% Buffered	Sigma Aldrich
Formalin tubs, white, plastic 500ml	Various
Forceps	Various
Freezer, -80^0	Various
Gas line splitter, Y connector	AneticAid
Gas regulator for cylinder, 10 bars	BOC
Glass beakers	Fisher Scientific
Glass bottles, pyrex borosilicate, 50 and 100ml, phenolic cap and screw neck	Fisher Scientific
Glass Flasks, volumetric, 50ml, 100ml	Fisher Scientific

Glass vials	Various
Hamilton glass syringes, 5ml & 10ml	WWR
Histopathology cassette,	Sakura
Histopathology cassette printer, Histosette (M-498 6-Blue)	Simport
Iso-propanol, (IPA), LC-MS grade	Sigma Aldrich
Leucine enkephalin, 95% HPLC grade [L9133-25mg], 1ng/µl	Sigma Aldrich
Mass spectrometer, Xevo G2-XS Q-Tof	Waters Corporation
Methanol, LC-MS grade	Sigma Aldrich
Medical air cylinder, 7 bar pressure	BOC
Patient return diathermy electrode	Fannin
PEEK tubing	Sigma Aldrich
Plastic beakers	Fisher Scientific
REIMS ion source	Waters Corporation
Refrigerator, 2-8^{O}	Various
Scalpel, 10 blade	Swann-Matheson
Smoke extractor tubing, RapidVac	Covidien
Sodium Formate (4M) made up to 5mM [73932-10ml-F]	Sigma Aldrich
Sonicator, ultrasonic bath	Grant
Surg-N-vac handpiece and extraction system	Medtronic
Syringer driver and infusion pump	Chemyx
Venturi Chamber / IPA inlet and capillary	Waters Corporation
Water, LC-MS grade	Sigma Aldrich

Table 8. List of chemicals, solvents, materials and equipment

Clinical approval, ethics and funding

The iKnife system is a non-FDA approved device used for research in an academic setting. The handheld diathermy and laser used in the study are commercially available devices with built-in aerosol extraction tubing. The work of the iKnife was supported by Waters Corporation (P53626_WSSB).

One of the main facets of this study was to assess if the iKnife could correctly identify endometrial cancer from endometrial biopsy samples (pipelle samples) taken in clinic to provide true point of care diagnosis. After discussion with the histopathology consultants at Imperial College NHS trust, it was felt that all the tissue from the pipelle samples are essential for routine histopathological analysis. To this end an IRAS ethics application was submitted to gain consent for a second research pipelle biopsy in clinic. This prospective feasibility study used was approved by Bloomsbury research ethics committee (REC number:17/LO/0173) in May 2017.

Meanwhile, a REIMS database and model was built by analysing fresh and frozen solid tissue samples from Imperial College main tissue bank. This was approved by Imperial College London (ICL) research and ethics committee (REC 14/EE/0024). The acquisition, selection of tissue samples, quality control and processing will now be discussed in more detail.

The iKnife set up

The iKnife instrument

A Waters G2-XS Xevo Q-ToF mass spectrometer was used in conjunction with a modified diathermy, namely a monopolar electrosurgical hand piece (Surg-N-Vac) connected to a Covidien ForceTriad generator.

The embedded computer within the mass spectrometer (MS) and the compressed gas cylinder (medical air) connected to the gas inlet of the MS were both switched on. MassLynx is the software on the MS that enables access to the MS vacuum. Using MassLynx, the vacuum pump is initialised using the MS Tune tab and allowed to reach a time of flight pressure of $1.2e^{-6}$ mbar. After the appropriate vacuum is reached, the MS was switched to an operational mode, and the heated kanthal coil is switched on. The operation settings were set to negative ionisation mode, sensitivity resolution, MS mode, trap gas and a scan time of 1.0 scans.

iKnife Calibration

Regular calibration of the iKnife using chemicals of known and precise m/z vales facilitates correct mass accuracy. Before tissue processing, the iKnife was calibrated

using sodium formate solution (NaF). The gas supply was switched on and the instrument was taken out of standby. A 5ml Hamilton syringe was filled with 5mMol NaF solution and attached to PEEK tubing ensuring there were no air bubbles present in the syringe. The NaF syringe was placed in syringe pump at a rate of 0.15ml/minute. The free end of the PEEK tubing was connected to the REIMS interface capillary inlet using a ferrule. Once a good signal (see Figure 26) was seen the file was run for two minutes and the spectrum was created from the chromatogram (see Figure 28). Automatic peak detection and background subtraction was performed without a lock mass. The 'Calibrate TOF' function was then used to compare the acquired spectrum to a stored spectrum on the instrument. A root mean squared (RMS) residual at 95% figure is created from this and should be below 3ppm. The calibration files are saved and this updates the tuning and system settings. Finally, a calibration check is performed by running the NaF solution for a further one minute at 0.15ml/minute. The spectrum created from the chromatogram is processed with automatic peak detection, background subtraction and a lock mass correction of 724.872 m/z. The spectrum list is copied into Mass Difference software calculator to ensure the instrument passes quality control. Before processing tissue samples isopropyl alcohol (IPA) is then run through to clear out any NaF solution.

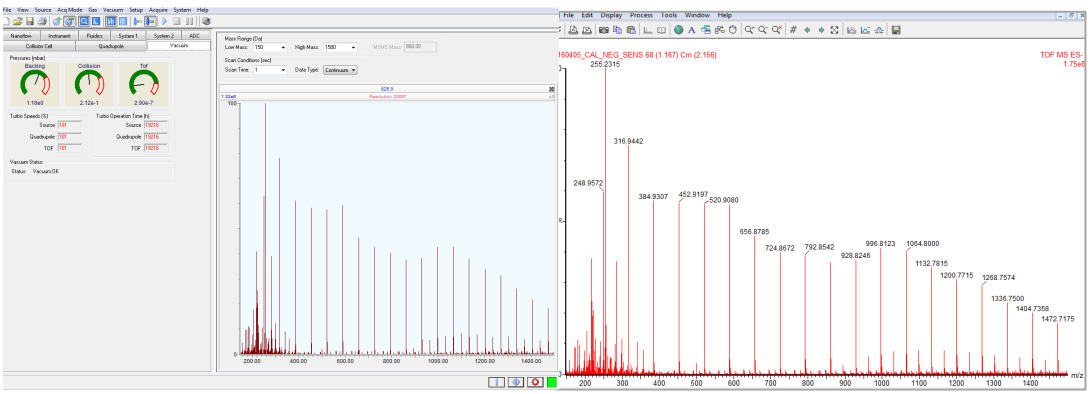


Figure 26. Left image - Calibration signal seen with Sodium formate. Chromatogram following 2 minutes of calibration

Lock mass

On any given day the environmental and experimental conditions will vary between minutes and days, and a degree of mass drift is inevitable. To compensate for small drifts in instrument calibration, a compound of known mass is often employed as a 'lock mass' which provides a mass standard in every spectrum. It can be internal or

external. Internal lock masses include ubiquitous cell membrane phospholipids with known masses such as: m/z 699.497 and 744.555. The m/z peak 699.497 is due to phosphatidic acid (36:2). External lock masses are compounds with known composition and m/z values that are added to the MS, often by an electrospray at the interface. Leucine enkephalin (LeuEnk) is a good example of an external lock mass, it is an endogenous opioid peptide with a well understood fragmentation pattern and was therefore used as an external lock mass in the iKnife experiments at a concentration of 1ng/µl of IPA. The average mass of LeuEnk is 555.623 Daltons and is seen at 554.262 m/z in negative ion mode.

Collection, storage and selection of tissue samples

Imperial College London (ICL) tissue bank database historically collected uterine tissue samples from December 1998 to September 2017. These samples were from patients consenting to storage of tissue for research purposes. All samples were snap frozen within 30 minutes of removal from the patient and then stored in a -80^{0}c freezer. Snap or flash freezing is performed to prevent degradation of metabolites. The ICL tissue bank database was searched for all uterine tissue (uterus, myometrium, endometrium) including: normal, benign, pre-malignant (hyperplasia) and primary malignant tissue. Endometrial hyperplasia samples did not specify whether they were simple/complex and whether atypia was present or absent. In total, 177 frozen samples were identified and requested, 154 samples, from 151 patients were released from tissue bank for analysis with the iKnife.

Table 9 illustrates the histological diagnosis of the 151 patients, from which the samples were derived. Normal and benign tissue samples were grouped together and classified collectively as 'normal'. Samples with hyperplasia were classified separate to normal and cancer specimens.

Type of specimen (and frequency of cancer cell type in population [340])	Number of patients (n=151)
Normal	3
Benign	44
Malignant endometrial primary:	
Endometrioid (75%)	59

Mixed (10%)	5
Papillary serous (10%)	9
Clear cell (4%)	10
MMT/Carcinosarcoma (3%)	11
Mucinous (1%)	0
Squamous cell (<1%)	0
Neuroendocrine (<1%)	2
Undifferentiated (<1%)	0
Indeterminate	2
Malignant primary elsewhere	
Cervical Cancer	1
Ovarian Cancer	2
Endometrial Hyperplasia*	3

Table 9. Histological breakdown of tissue samples obtained from tissue bank.

Frequency of histological subtypes within the general population on the left (%)

In addition, to frozen tissue bank samples fresh ex-vivo work included 21 uterine tissue samples from 21 patients undergoing gynaecological surgery, this was used for prospective validation. These patients read and signed a consent form for agreement of storage and processing of tissue for research. Post-surgery, the hysterectomy specimen was assessed by the histopathologist and a small piece of endometrium was excised with a scalpel by the histopathologist (Figure 27). The tissue samples were collected and processed within four hours of removal from the patient, all whilst at room temperature. Some tissue was snap frozen for later use by the iKnife.

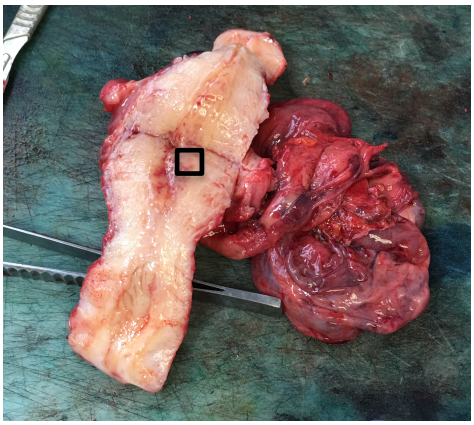


Figure 27. Photograph of cut open uterus following hysterectomy for ovarian cyst.
Small black box is the area surgically cut out by the histopathologist and donated for research.

Sample processing

A Xevo G2-S Q-TOF mass spectrometry machine based within Hammersmith Hospital was used to process the samples. Figure 28 illustrates the overall iKnife set up.

Tissue sample sizes varied significantly in size and texture but were approximately 0.25cm^3. The tissue samples acquired from the tissue bank were divided into 3 whilst frozen: the first was stored in a sub collection within the Institute of Reproductive and Developmental Biology, IRDB (-80^{0}c freezer), for potential later analysis. The remaining 2 pieces were thawed at room temperature for analysis by the diathermy iKnife, one using the cut setting and one using coagulation setting. Frozen tissue bank samples were analysed in batches of 15-25. Similarly, fresh ex-vivo samples were divided into 3, one for storage and 2 for analysis by the diathermy iKnife (cut and coagulation setting). Fresh ex-vivo samples were processed within four hours of collection.

The Covidien ForceTriad™ electrosurgical generator with a cautery finger switch was set to between 15-20 Watts for both cut and coagulation mode (depending on tissue type). As it is a monopolar device, a grounding pad was needed, this was attached to the rubber base on which the samples were processed. A tissue was placed directly beneath the samples and the samples were soaked in distilled water.

Following calibration of the instrument, the solvent in the syringe driver was changed to LeuEnk in IPA (1ng/µl) in a 10ml glass Hamilton syringe at a flow rate of 0.2ml/minute. IPA solution was sprayed across the heating coil (using a syringe driver).

Medical air pressure (7 bar) was regulated to 2 bar using the venturi chamber.

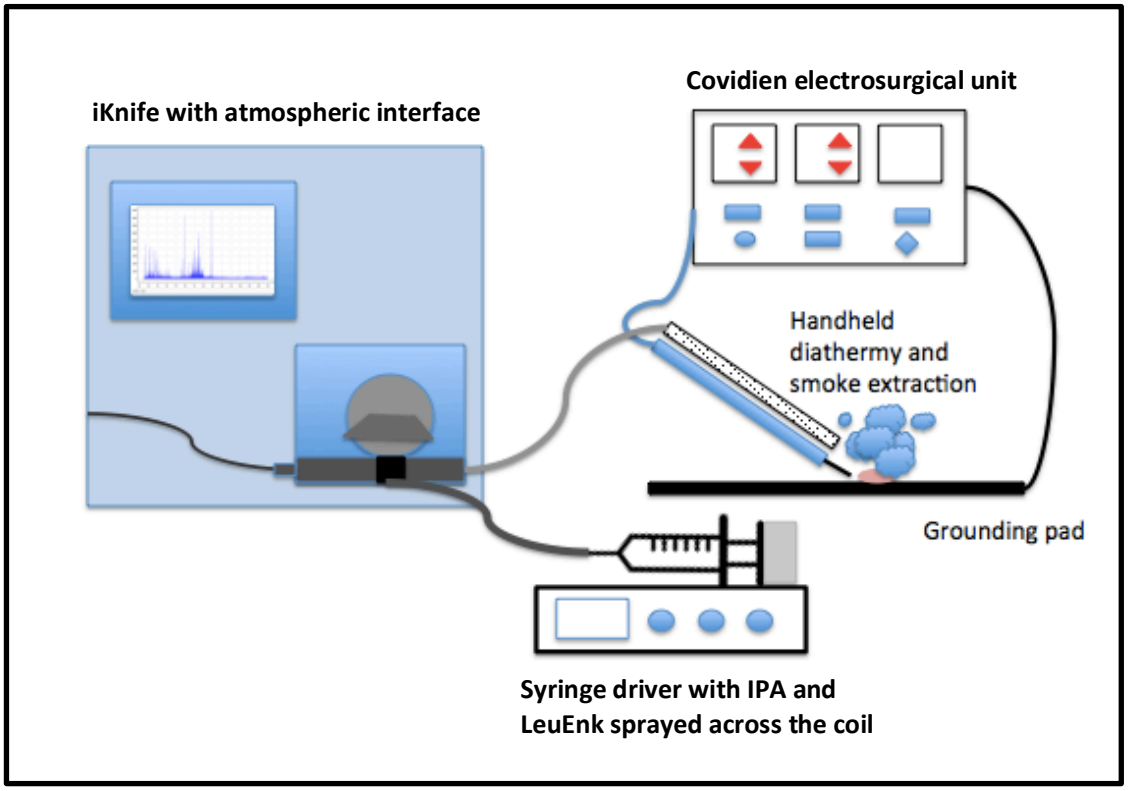


Figure 28. Pictorial diagram of the iKnife set-up.

Electrical current produced by the generator is applied to the tissue using a handheld diathermy. The charged aerosol produced is extracted through the handpiece and drawn into the iKnife interface and analysed by the G2-XS Xevo Q-ToF. IPA containing LeuEnk is sprayed across the heated coil.

Just prior to sample processing a file was created for the resultant sample's mass spectra. Each sample was burned with the monopolar diathermy, between 1 and 8 times depending on the size of the specimen (median 4), and for 1-2 second intervals to minimise charring. During each burn, the IPA solution mixed with the smoke extracted from the diathermised tissue. This aerosolised gas was introduced to a heated coil interface and then gas phase charged ion species accelerated via the Step Wave towards the MS, generating a mass spectrum in the 15-1500 m/z range.

After processing the samples with the iKnife, the burnt tissue was photographed, and then placed on top of a blue cassette sponge in a histopathology tissue embedding cassette (Figure 29). It was catalogued and then formalin fixed by placing it in a 500ml formalin tub filled with 10% formalin. The samples were then sent to histopathology for quality control and assessment of tumour content.



Figure 29. Tissue sample placed on blue cassette sponge prior to formalin.

Red arrow to represent size of sample

Histological handling, reporting and quality control

The ICL tissue bank provided information on the date of sample collection, the procedure undertaken, which organ the tissue was obtained from and the histological diagnosis. But, in order to ensure a robust dataset, it was essential to validate the samples and check that the spectral pattern stored for each tissue sample was correctly matched to accurate histopathology. This was particularly important for samples recorded as 'uterine', as it was unclear whether this was myometrial tissue or endometrial and this would have repercussions on the classification of the samples.

To this end, histopathological validation of all samples was performed, and histopathology was used as the reference standard. All formalin-fixed tissues were processed at Imperial College London NHS trust. A histopathology technician, Dr Hiromi Kudos embedded each sample into paraffin blocks and sectioned using a microtome to create 5µm formalin-fixed paraffin-embedded (FFPE) sections of the tissue. Each cross section was mounted onto a glass histology slide and stained with haematoxylin and eosin (H&E) stain. Each slide was scanned at high resolution using NDP.view2software (Hamamatsu Phonotics) and then catalogued for reference.

A histopathologist, Dr Francesca Rossi then manually reviewed each FFPE slide using a light microscope to confirm whether there was cancer present in the specimen and

to estimate the amount of cancer.

Statistical analysis

In-house software developed by Waters Corporation (Offline Model Builder, version Abstract model builder, AMX) was used initially for all pre-processing of spectra and model building. OMB software enables background subtraction, normalisation, peak alignment and selection of bining. The newer version of OMB (AMX) also removes poor quality spectra from the model.

Each file was firstly uploaded to OMB as a '.raw' file and then assigned a histological classification. Total ion chromatogram (TIC) peaks was used to identify each tissue burn (Figure 30). Each burn was then manually selected using the OMB software, which then displayed a representative spectrum. All tissue samples and burns were included within the original import. However, subsequent models were built using selective histological types e.g. endometrioid adenocarcinoma only versus carcinosarcoma.

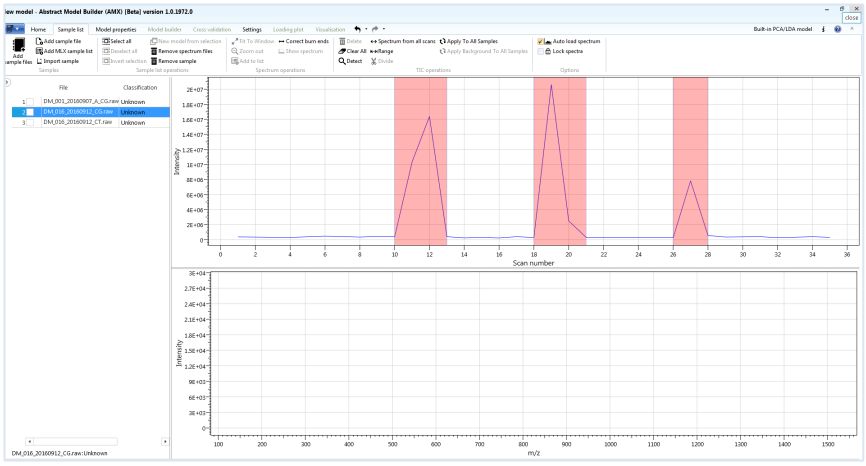


Figure 30. Chromatogram with peaks selected.
Chromatogram shows 3 obvious peaks in total ion count, which have been selected in red.

Mass spectral peaks were assigned to bins of 0.1 Daltons. Binning reduce the effects of minor observation errors and background noise. Background noise subtraction and lock mass correction were also performed. Spectra within 600-100 m/z range were included in the analysis.

Multivariate analysis and loading plots

Models were created based on either one spectrum per burn or one spectrum per sample (thus creating a representative spectrum of all the burns in a specific sample). The latter was used throughout. A multivariate analysis was performed to find the variance in spectral signatures between the tissues (normal and malignant endometrial tissue). This was 2 or 3-dimensional principal component analysis (PCA) and a linear discriminant analyses (LDA). The PCA is an unsupervised analysis to visually represent the tissue class separation based on 2 to 3 principal components respectively. The percentage of variance of each principle component was calculated and recorded. A supervised LDA was also performed, providing graphical 2D or 3D representations of the data. The 3-dimensional models could be rotated to find the best visual class separation. In OMB cancer is usually represented in a red colour and blue normal. If there are only 2 classes i.e. normal and cancer, a visual LDA is not possible in OMB AMX.

Loading plots were created to visualise principal components as a two-dimensional score plot. Each principal component loading plot illustrates all the spectral peaks and corresponding intensity that contributes to the separation in the model. The largest peaks in the loading plot correspond to m/z values which account for the most variance along that principal component. Visually this helped identity m/z values significant for class separation, however, as binning was 0.1 Da compound identification was not performed using loading plots alone.

Univariate analysis and tentative lipid assignment

The OMB data set was interrogated with the support of Dr Zsolt Bodai using R project for statistical computing and imported to Microsofft Excel. Analysis of variance (ANOVA) was performed to calculate the intensity of each m/z value and its contribution to the separation in the model (median fold change). P values were corrected to q values using the Benjamini Hochberg Yetuteli method (false discovery rate of 0.05). Peaks were significant for class separation if P and q values were <0.001.

These significant m/z values were then presented to LipidMaps structure bulk database (LMSD), on LipidMaps website to provide tentative lipid assignments. LipidMaps is the largest public lipid-only database in the world, it is also a free online

resource sponsored by the Wellcome trust [341, 342]. The database was searched with the exact mass and the following parameters: deprotonated [M-H]- glycerophospholipids and fatty acids with a mass tolerance of +/– 0.1m/z. Only even fatty acid chains were included in the search result.

Validation

Validation of the PC-LDA statistical model was performed two ways: cross validation and prospective validation of new tissue.

The OMB software was used to perform cross validation, of which two methods are possible. A '20% leave one spectrum out' and a 'leave one patient out'. The first method involves repeatedly leaving out 20% of random spectra and then rebuilding the model. Each spectrum is then individually presented to the new model to determine the accuracy of its classification. Similarly, a 'leave one patient out' (LPO) repeatedly leaves out one patient and all its corresponding spectra then rebuilds the model. The removed spectra are then classified to determine the accuracy of the model. Accuracy included: sensitivity, specificity, positive predictive value (PPV) and negative predictive value (NPV). All cross validations performed were 'a leave one patient out' unless otherwise stated.

The second method of validation was to collect new prospective endometrial tissue that was not analysed by the iKnife as part of the model and instead run the tissue through the recognition software (discussed below) to assess the models classification accuracy. This tissue was handled in the same way with respect to histological quality control to confirm that the spectral pattern stored for each tissue sample was correctly matched to accurate histopathology.

Based on these validation methods, correct classification, sensitivity and specificity rates were calculated and are presented in confusion matrices adjacent the models. A number of models were run, and the model with the best sensitivity and specificity was used subsequently.

Software recognition

The OMB recognition software allows for recognition of tissue real time, or post processing. Post processing analysis was used in this study. It enables spectra which have been created through analysis of tissue samples retrospectively, to be presented to the model for classification. Multivariate models were created in OMB and exported to the recognition software, to serve as a training set. Prospective samples introduced to the recognition software function as test sets. Lock mass and background correction are applied. A number of options in the OMB recognition software exist, including: outlier type, multiplier of standard deviation setting, intensity limit detection. For the purposes of this study the outlier setting was set to 'none' - this forces the programme to always report a tissue class even if unsure. For each burn, a spectrum is created, and the TIC will reflect the intensity of the signal; which inevitably varies. The intensity limit was set at the threshold approximately 25% above background noise, but below the peak maximum intensity of a burn. In order to capture all the burns with the recognition software, the intensity detection threshold was varied as the file ran through the recognition software.

4.3.2 Results

Collection of data - predominately frozen samples from tissue bank

In total, 151 patients provided 154 frozen solid tissue samples from tissue bank. Tissue was processed using the diathermy iKnife, initially with both cut and coagulations setting, see Table 10. This produced almost 1000 unique phospholipid spectra.

Tissue Samples (type & number)		Diathermy modality (n = number of burns)	
		Cut	Coagulation
Normal	50	179	92
Cancer	98	391	298
Total	148	570	390

Table 10. Breakdown of tissue samples analysed by each modality. Hyperplasia not shown in table. Tissue sample numbers reflect number of patients supplying a sample.

All spectra passed the quality control (QC) of the OMB AMX software. Histopathological validation was performed on all samples. Benign samples and normal samples were synonymous and classified together. Normal endometrial samples may have come from patients undergoing a hysterectomy for a different

primary (e.g. ovarian cancer) but have histologically confirmed normal endometrium. Benign samples were subclassified as endometrial tissue present, or no endometrial tissue present (myometrium only). All metadata was appropriately noted.

Cancer samples reported the percentage of tumour content visible within the specimen and was subclassified as: 0%-25%, 25-50%, 50-75% and ≥75%. If samples came from a known endometrial cancer patient, but under light microscope the histopathologist could not identify and cancer cells, the sample percentage tumour volume was recorded as 0%.

Interestingly, following quality control (QC) 40 samples were excluded as their classification changed (Appendix 12.4), this is described in more detail later.

Method optimisation

Only small quantities of solid tissue samples were received from tissue bank, as seen in Fig 31 with a range of 2mm to 15mm in maximal diameter. This reduced the volume of aerosol produced by diathermy substantially. The more tissue analysed, the more spectra produced and the more robust the statistical model; but, the less tissue available for histological validation due to surgical artefact. To this end, the size of the tissue dictated the number of burns, with smallest tissue only receiving a single processing point (burn), whilst larger tissue received up to 8 (with a median of 4).



Figure 31. Tissue samples on blue cassettes pre-formalin.
Red arrows to depict the small and variable size of samples.

The basic methodology of the iKnife was taken from Takats' group, including the addition of IPA to improve signal intensity [196, 199]. This also enabled the addition of the external lock mass LeuEnk by infusing it with the IPA. Despite IPA, the signal

intensity of the tissue bank uterine samples ranged from 10^4 to 10^7, substantially lower than seen in the ovarian and breast data.

The distance of the iKnife to the tissue, the size of the diathermy head, the rate of flow medical gas, rate of IPA and diathermy power were all adjusted to maximise signal intensity. The distance of the iKnife diathermy head to the tissue surface was increased by 1mm sequentially, and the maximal signal intensity was achieved when the diathermy was hovered 1-2mm from the tissue surface. The size of the diathermy head was tested - the shorter diathermy heads (2.5cm active electrode) and shorter total length, gave marginally higher signal intensity and were subsequently used, when available. Medical air flow rate was adjusted between, 1 and 4 bar using the venturi and 1.8-2.5 bar gave the best signal intensity, thus 2 was used throughout. The IPA solvent rate was adjusted between 0.1ml and 0.3ml per minute, high solvent rates caused droplets to form near the heated coil, and low rates lost the LeuEnk signal, thus 0.18-0.25ml/minute was the optimum range. Finally, the power setting on the monopolar device was altered, from 6 Watts to 50 Watts, in 2 Watts increments. The lower power settings produced insufficient surgical aerosol and no signal was detected. Higher voltages produced large amounts of tissue destruction. Thus, optimal rate was between 20 and 30 Watts, but this depended on the tissue type being burnt, therefore the power setting was altered between this range during tissue processing.

Both cut, and coagulation settings were used to process each tissue sample. It can be been seen in the figure 32 that the spectral signals of normal and malignant uterine tissues appear quite different - with different peak intensities for various ions. This forms the basis of the principal component analysis. It is apparent that the coagulation and cutting iKnife diathermy setting produced different spectra (Figure 32). Typically, coagulation burns produced spectra with very high levels of background noise. This meant that it was difficult to discern important low-level m/z peaks amongst the background noise. All statistical models going forward were based upon cutting diathermy setting only.

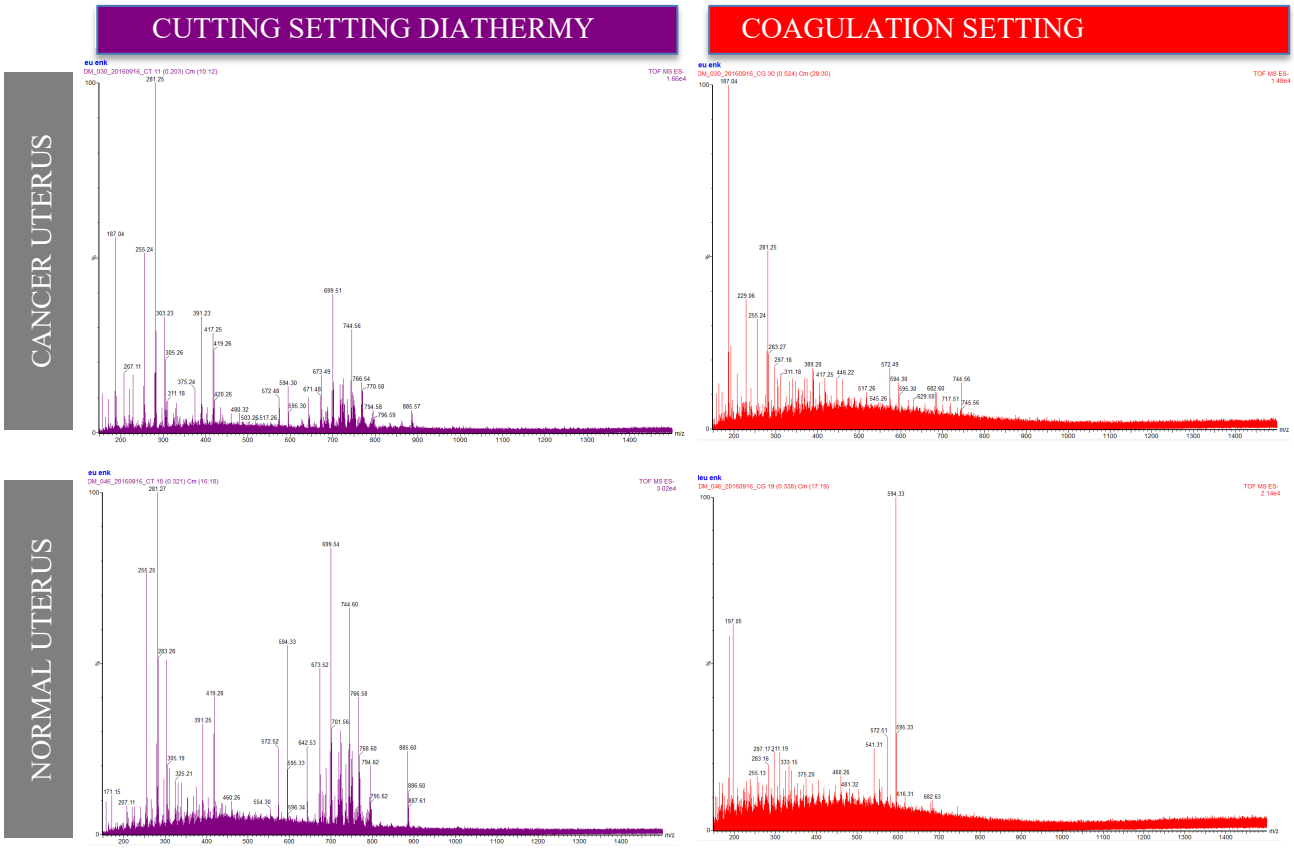


Figure 32. Four spectral patterns.

The purple spectra on the left are the less noisey spectra achieved using the cutting setting of the diathermy. The more noisey red spectra on the right are the same samples processed with the diathermy setting. The top row represents the cancer samples and the bottom samples are from normal endometrial tissue – all look distinct.

Histopathological validation enabled confirmation that the tissue was correctly classified into benign or malignant tissue. The histopathologist visually estimated the percentage of endometrial cancer within the tissue slide. If any cancer was present within the slide, the tissue was classified as cancer. However, one could alter this classification threshold. For example, if the model was built exclusively from cancer tissue with high percentage of cancer within it (>80% cancer cells), all tissue would be re-classified accordingly. Similarly, benign uterine tissue included both myometrium, endometrium (stroma and glands), to build a more robust model, one could build the normal cases entirely on tissue samples with endometrial tissue present. Normal and benign tissue (e.g. fibroids) were both classified as normal. Patients with a primary elsewhere (e.g. ovary) but had no abnormality of the uterus were also classified as normal.

Statistical modelling using tissue bank samples: normal vs cancer vs hyperplasia. Pre-Histopathological quality control

This model used 151 samples and only one sample per patient. Each dot on the PC/LDA plots represent the average spectra for a single sample. Red represents cancer samples, blue normal and purple hyperplasia (Figure 33). The confusion table is shown beneath the PC/LDA plots. All spectra passed the OMB quality control, so no spectra were removed. The overall sensitivity and specificity were: 60% and 74% respectively.

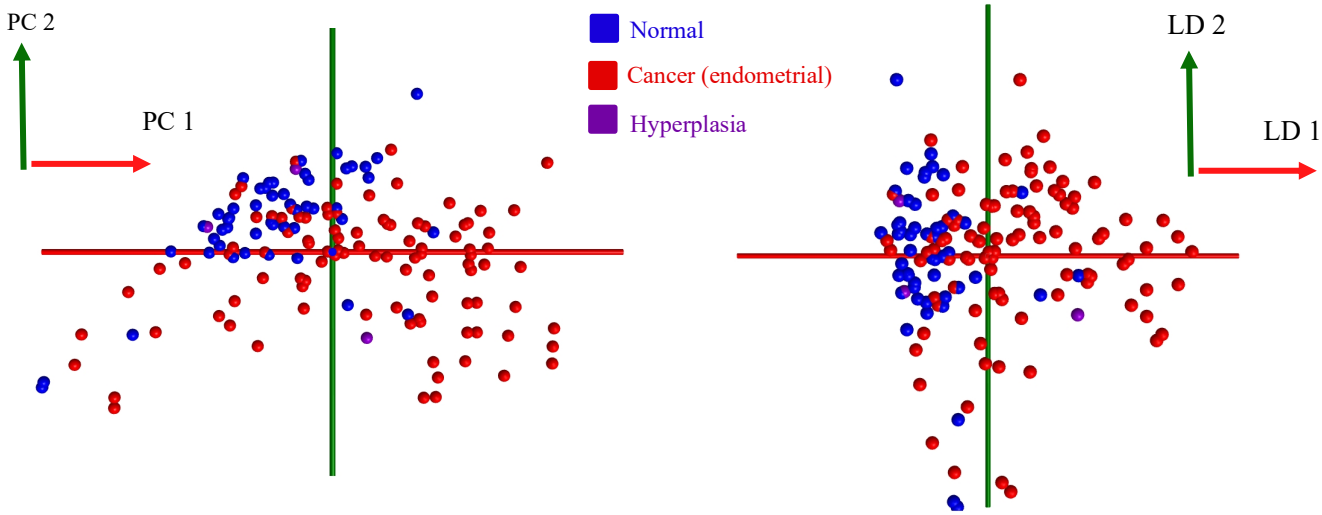


Figure 33. Multivariate analysis of normal vs cancer vs hyperplasia tissue bank samples pre-histopathological quality control. Red dots represent endometrial cancer samples, blue normal and purple hyperplasia. Each dot represents the average spectra of a single sample. The diagram on the left is a 2D PCA. Principal component one accounted 38.1% of the variance seen in the model and principal component two 11.9%. 2D LDA on the right. The confusion table is seen below.

		MODEL CLASSIFICATION n, (%)			TOTAL
		CANCER	HYPERPLASIA	NORMAL	
ACTUAL HISTOLOGY	CANCER	59 (60%)	22 (22%)	17(17%)	98
	HYPERPLASIA	1 (33%)	0 (0%)	2 (67%)	3
	NORMAL	3 (6%)	10 (20%)	37(74%)	50

Confusion table for Figure 33

Outlier assessment

As can be seen from the PC/LDA plots several outliers exist (either points distinctly further away from neighbouring points or mixing of normal data point within cancer area). These are illustrated in LDA plot below with yellow arrows (Fig 34).

The samples from which these data points were generated were analysed. All, bar two came from different processing batches.

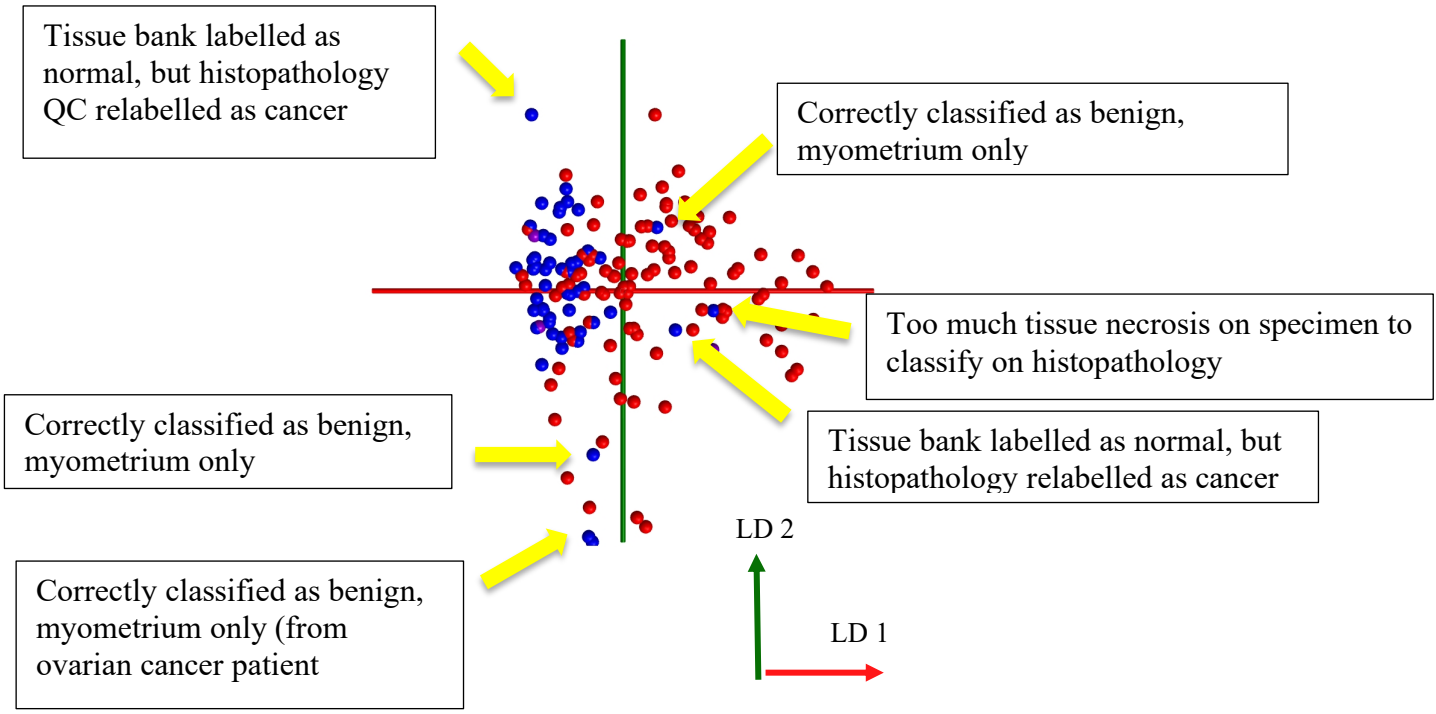


Figure 34. Investigation of outliers from the normal vs cancer vs hyperplasia LDA tissue bank model.
Each outlier is highlighted by a yellow arrow, and possible reasons for it, outlined.

Histopathological Quality check

All samples were checked to confirm correct tissue class classification. Following histopathological QC, 3 tissue samples which were classified as normal from tissue bank had cancer on histopathological check; this likely represents a transcription error during the tissue bank process. These samples were excluded. All 3 hyperplasia samples were excluded as histopathological assessment did not find any residual hyperplasia present. They were not reclassified as normal as it was unknown if the

iKnife picked up frameshift changes in phospholipids profiles on the spectrum between normal and cancer.

In 33 endometrial cancer samples, no cancer cells were seen on the tissue slide – it may mean the iKnife burnt through the cancer tissue already, or that the specific tissue sample did not contain any of the cancer to begin with. These patients were also excluded. Finally, one patient had complete necrosis of the tissue, so no assessment could be made by histopathology, this sample was excluded.

Thirty-five normal tissue samples on histological assessment only had residual myometrium. This may be the result of burning through the endometrial tissue during diathermy or that the tissue biopsy sampled was only myometrium. This would only leave 14 normal samples remaining, which is a very small number to run a meaningful analysis. To this end, the normal myometrium samples were kept within the dataset.

A summary of the tissue classification, pre and post histopathology is seen in the appendix 12.4.

Statistical modelling using tissue bank samples: normal vs cancer. Post-Histopathological quality control

After histological QC, the samples described above were excluded and the model was re-run. This model used 112 samples from 112 patients. All spectra passed the OMB quality control, so no spectra were removed. Red represents cancer samples, and blue normal (Figure 35). Good separation was seen on the unsupervised PCA model. The confusion table is shown beneath the PCA plot. LDA plot was not possible as there were only 2 classifiers. The overall sensitivity and specificity were: 80% and 98% respectively. Outlier assessment is shown in the appendix 12.5.

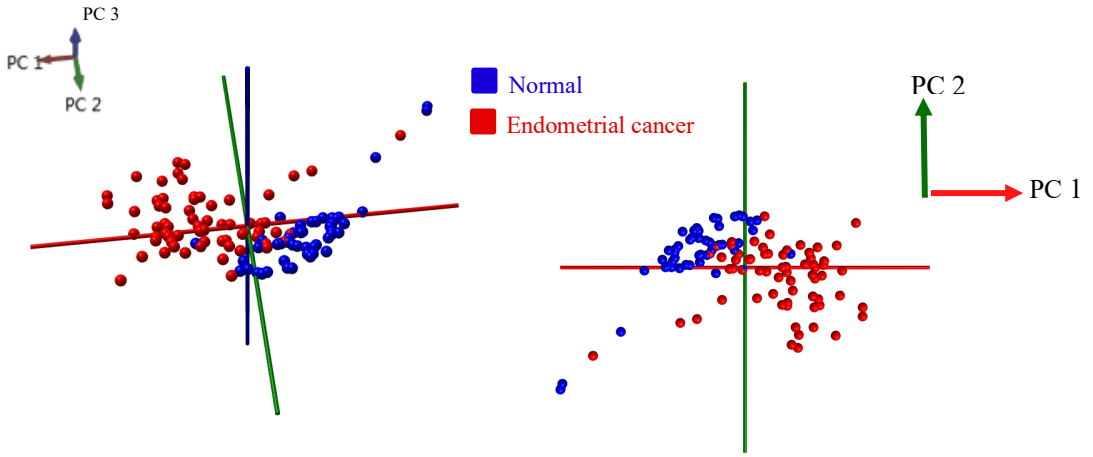


Figure 35. Multivariate analysis of normal vs cancer tissue bank samples post-histopathological quality control. Red dots represent endometrial cancer samples and blue normal. Each dot represents the average spectra of a single sample. The diagram on the left is a 3D PCA, and right 2D. Principal component one accounted for 39.7% of the variance in the model and principal component two 13.0%. The confusion table is shown below.

		MODEL CLASSIFICATION n (%)		TOTAL
		CANCER	NORMAL	
ACTUAL HISTOLOGY	CANCER	52 (80%)	13 (20%)	65
	NORMAL	1 (2%)	46 (98%)	47

Confusion table for Figure 35

Histological differentiation: Can the iKnife distinguish between Type 1 vs Type 2 vs normal?

Type 2 cancers are a heterogenous group of aggressive cancers, with different histopathological and molecular profiles. They are treated more aggressively with lymphadenectomy and adjuvant treatment. As discussed in the introduction, the ability to accurately distinguish tissue type enables optimal pre-operative planning. Thus, a model of normal versus type 1 and type 2 cancers was created to see if the iKnife is effective at distinguishing between these types.

All cancer cases were reclassified as Type 1 or Type 2 accordingly. The corresponding spectra from all 112 samples passed the OMB quality control. Each dot on the PC/LDA plots represent the average spectra for a single sample. Red and orange dots represent cancer samples (type 1 and 2 respectively), and blue normal (Figure 36). As

can be seen there is reasonable separation of the 3 groups, with type 1 and type 2 cancers clustering closer together. PC1 always explains the largest amount of variance, which suggests that type 1 and type 2 cancers phospholipid signatures align much closer together than normal tissue. This is demonstrated in the confusion table below. The model was able to distinguish between normal and cancer well but was unable to correctly discriminate between type 1 and type 2 cancer, (less than 50% accuracy).

This study was underpowered to build a model using the separate subtypes of type 2 cancer versus type 1 and normal, as there were too few samples of rare subtypes of type 2 cancers present within the dataset. Therefore, no further analysis on histological subtype was performed. An outlier assessment was also performed (see Appendix).

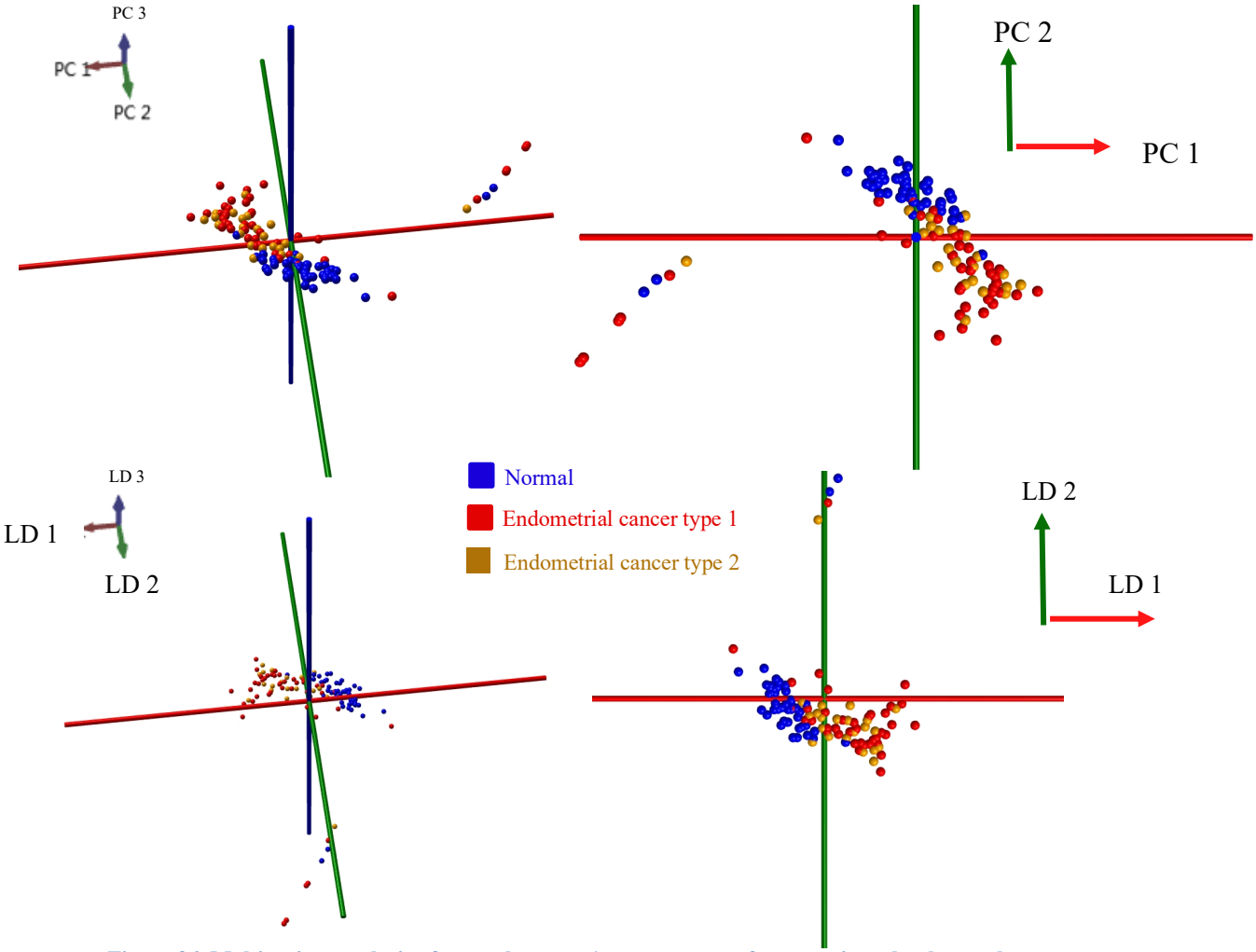


Figure 36. Multivariate analysis of normal vs type 1 cancer vs type 2 cancer tissue bank samples.
Red dots represent type 1 endometrial cancer samples, orange dots type 2 and blue dots normal. Each dot represents the average spectra of a single sample. The diagrams on the top are 3D PCA (left) and 2D PCA right. The LDA models are on the bottom, 3D left and 2D right. The confusion table is seen below.

		MODEL CLASSIFICATION, n (%)			TOTAL
		NORMAL	TYPE 1	TYPE 2	
ACTUAL HISTOLOGY	NORMAL	43 (91%)	2 (4%)	2 (4%)	47
	TYPE 1 CA	6 (14%)	19 (44%)	18 (42%)	43
	TYPE 2 CA	4 (18%)	7 (32%)	11 (50%)	22

Confusion table for Figure 36

Histology differentiation: Is Type 1 cancer vs normal a model better?

Model building is complicated by multiple tissues classes and diverse lipid profiles within tissue classes. Given the heterogenous nature of type 2 cancer, pooling together these phospholipid profiles using only a small dataset of 22 samples to look for separation between normal and cancer is difficult. It was hypothesised that a model consisting of only type 1 cancer vs normal would have a higher diagnostic accuracy.

An analysis was therefore performed consisting of 90 samples which consisted of normal and type 1 cancer only. All spectra passed the OMB quality control, so no spectra were removed. Each dot on the PCA plots represent the average spectra for a single sample. Red dots represented cancer samples and blue normal (Figure 37). The confusion table is shown beneath the PCA plots. Principal component one accounted 46.6% of the model and principal component two 15.1%. There was separation across PC1 and PC2, as the normal samples clustered top left and cancer bottom right. As there were only two classes an LDA plot wasn't possible using OMB. As expected, the overall diagnostic accuracy, particularly the sensitivity was higher (84%), with a specificity of 94%. The same samples from the model above persisted as outliers.

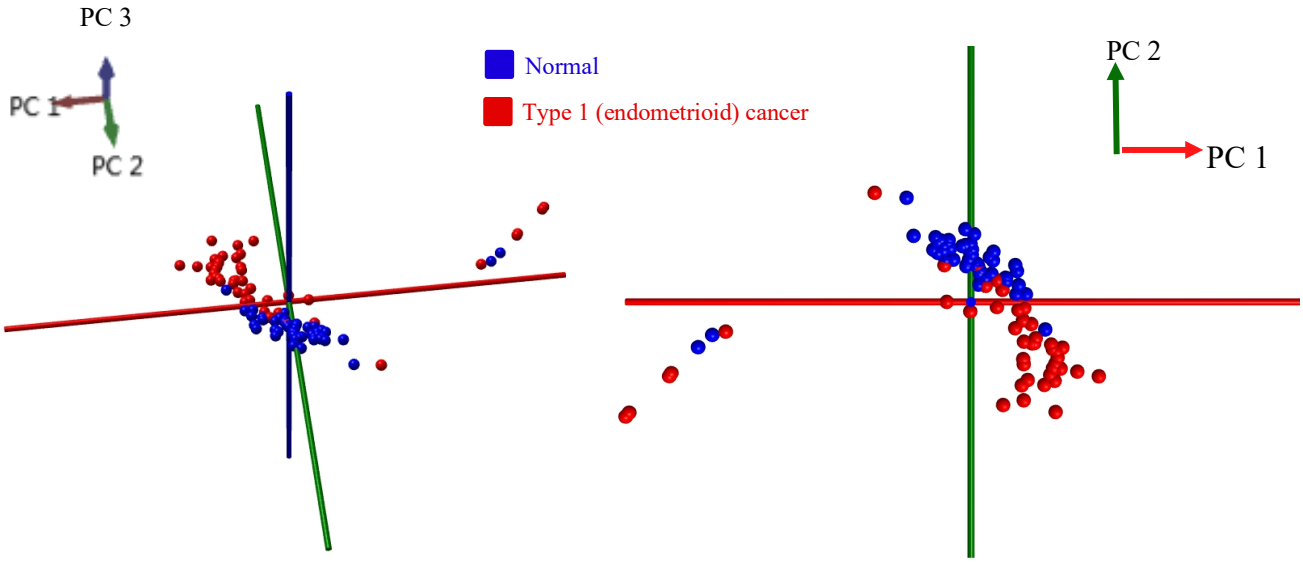


Figure 37. Multivariate analysis of normal vs type 1 (endometrioid) cancer tissue bank samples post-histopathological quality control.
Red dots represent endometrioid cancer samples and blue normal. Each dot represents the average spectra of a single sample. The diagram on the left is a 3D PCA, right 2D. The confusion table is seen below.

		MODEL CLASSIFICATION, n (%)		TOTAL
		TYPE 1	NORMAL	
ACTUAL HISTOLOGY	TYPE 1 CA	36 (84%)	7 (16%)	43
	NORMAL	3 (6%)	44 (94%)	47

Confusion table for Figure 37

Tumour cell content and tumour heterogeneity - removal of low volume tumour samples

In this study, the volume of cancer in the cancer samples varied from 0-100%. In other iKnife research groups, it was thought that the model would be more robust if cancer samples with low volumes of tumour (<50%) were excluded [199]. Thus, minimising the chance that cancer classified spectra came from non-cancer tissue. To this end, five type 1 (endometrioid) cancer samples which had cancer volumes of <50% on visual estimation of the slide and were excluded in this model, 84 samples remained.

All spectra passed the OMB quality. Each dot on the PCA plots represents the average spectra for a single sample. Red dots represented cancer samples and blue normal (Figure 38). The confusion table is shown beneath the PCA plots. Principal component one accounted 45.3% of the model and principal component two 15.7%. Good separation of cancer and normal is seen on the PCA. As there were only two classes an LDA plot wasn't possible using OMB. The overall sensitivity and specificity were: 78% and 94% respectively, worse sensitivity than models which included the low volume tumour samples.

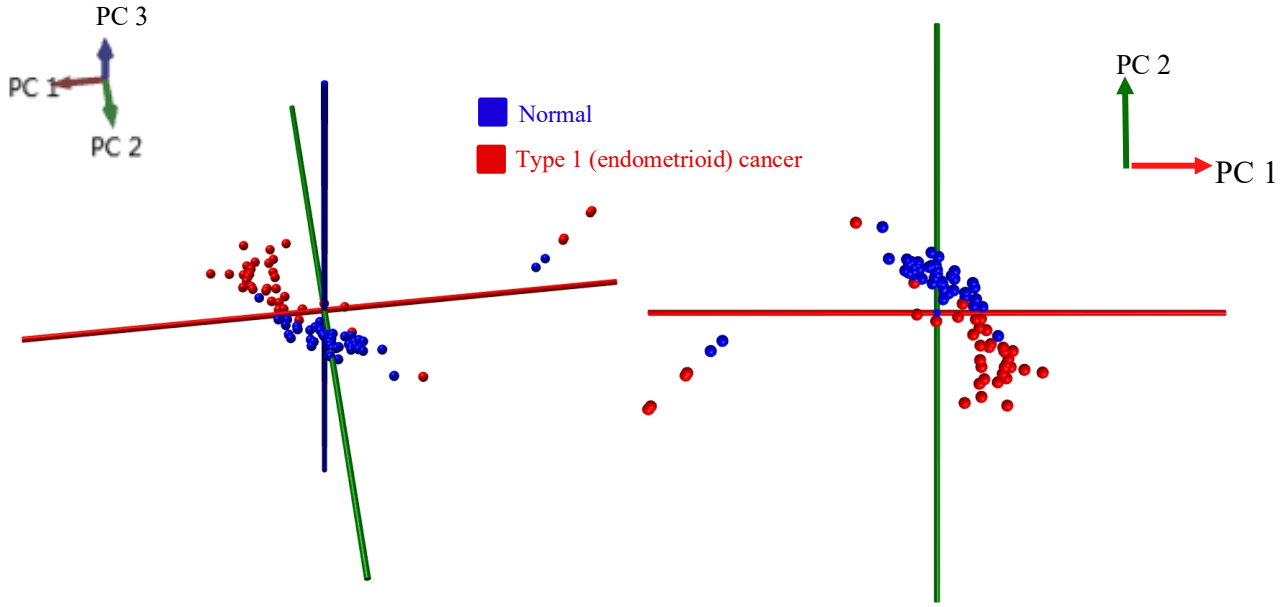


Figure 38. Multivariate analysis of normal vs high volume type 1 (endometrioid) cancer tissue bank samples.
Red dots represent endometrioid cancer with ≥50% cancer present and blue normal. Each dot represents the average spectra of a single sample. The diagram on the left is a 3D PCA, right 2D. The confusion table is shown below.

		MODEL CLASSIFICATION, n (%)			TOTAL
		NORMAL	TYPE 1	OUTLIER	
ACTUAL HISTOLOGY	NORMAL	44 (93%)	2 (4%)	1 (2%)	47
	TYPE 1 CA	6 (2%)	29 (78%)	2 (5%)	37

Confusion table for Figure 38

Tumour cell content and tumour heterogeneity – does % tumour volume make a difference?

As seen above, the removal of low volume tumour samples from the model did not improve the diagnostic accuracy of the iKnife. This might be a reflection of the iKnife burning through the cancer tissue, such that minimal residual cancer tissue remained for histopathological QC. Or, it could a be reflection of the iKnife detecting lipid change in the peri-tumoural micro-environment.

To assess the effect of tumour burden in the sample in more detail a model, all the cancer samples were re-classified according the percentage of tumour content visible on the specimen: 0%-25%, 25-50%, 50-75% and 75-100%. As before, each dot on the PCA plots represents the average spectra for a single sample (Figure 39). The confusion table is shown beneath the PCA plot.

There is good separation of cancer and normal, and indeed some suggestion that incremental increases in tumour burden increases the separation between those clouds of data and the clustering of normal samples. High tumour burdens (75-100%) cluster on the far right of the unsupervised PCA, normal tissue separates far left and moderate tissue burden (50-75%) seems to cluster between them. This is consolidated in the confusion table, which shows, in general that if the model's classification is incorrect for a specific sample, it usually classifies the tissue one category higher or lower than its actual group. Also, of note, there is a much higher number of outliers, samples which the model was unable to classify.

A big limitation of this model was the categorial classification of a tumour burden which a is a continuous variable. Such that samples with estimations of cancer volumes of 45% and 55% were in placed in different categories even though there is not much actual difference in tumour volumes.

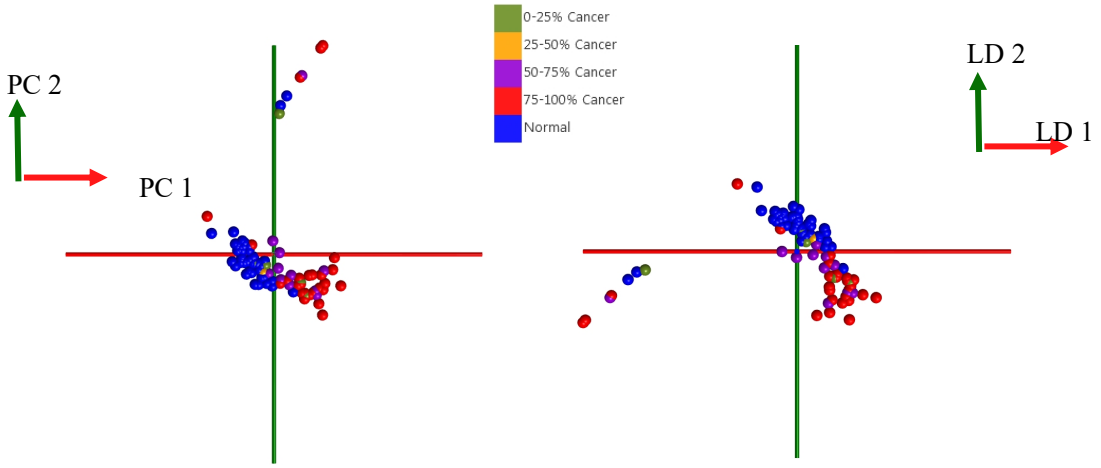


Figure 39. Multivariate analysis of cancer subdivided into % tumour burden vs normal tissue bank samples. Each dot represents the average spectra of a single sample. The left is 2D PCA and right 2D LDA. The LDA models are on the bottom, 3D left and 2D right. The confusion table is seen below.

		MODEL CLASSIFICATION, n (%)						TOTAL
		0-25%	25-50%	50-75%	75-100%	NORMAL	OUTLIER	
ACTUAL HISTOLOGY	0-25%	0	0	1 (20%)	2 (40%)	1 (20%)	1 (20%)	5
	25-50%	0	0	0	0	1 (100%)	0	1
	50-75%	5 (45%)	0	2 (18%)	3 (27%)	0	1 (9%)	11
	75-100%	2 (8%)	0	3 (12%)	19 (73%)	2 (8%)	0	26
	NORMAL	2 (4%)	0	1 (2%)	0	31 (66%)	13 (27%)	47

Confusion table for Figure 39 showing model accuracy with respect to percentage of cancer in the sample.

Selection of best model and prospective validation

A sensitivity analysis was performed (see Appendix 12.5). After this all the models were evaluated so as to select the model with the best performance. As seen in the confusion matrices beneath the PC/LDA plots, and the table below (Table 11) the best model with the highest combination of sensitivity and specificity using cross validation is *type 1 cancer vs normal* endometrial tissue. There is always a trade-off for sensitivity

and specificity, but for cancer diagnostic tests, it is important for have high rates of sensitivity, even if at the cost of a reduction in specificity.

MODEL	NUMBER OF SAMPLES	DIAGNOSTIC PERFORMANCE			
		SENSITIVITY (%)	SPECIFICITY (%)	PPV (%)	NPV (%)
Normal vs all cancer vs hyperplasia. Pre-histological QC	151	60	74	94	66
Normal vs cancer. Post-histological QC	112	80	98	98	78
Type 1 cancer vs normal	90	84	94	92	86
Removal of low volume cancers	84	78	94	94	88
Removal outliers	81	81	95	94	86

Table 11. Summary table diagnostic performance of all tissue bank models.

PPV = positive predictive value and NPV = negative predictive value

In addition to cross validation, prospective validation of the *type 1 cancer vs normal model* was performed using fresh endometrial tissue collected from women undergoing hysterectomies. Twenty one samples were obtained, two were excluded as the final histology was insufficient. Of the remaining 19 samples, 10 were from normal endometrial tissue and 9 from malignant tissue. Six of these samples were processed fresh (unlike the tissue used to build the model). These samples were presented to the OMB recognition software (version AMX), for the first time, using *the type 1 cancer vs normal endometrial tissue model*. The settings for software recognition were: 1 scan per spectra, three second time out and no outliers. The intensity limit was adjusted for each sample to ensure the burn was captured with minimal background noise.

For each burn, the model would classify the tissue class and specify the degree of certainty of that classification (see Figure 40). Afterwards, a final tissue classification and an overall degree of certainty for that tissue would be produced. The degree of certainty is a percentage of the final tissue classification burns, out of total number

burns e.g. 3 out of 4 burns classified as cancer, the overall certainty of cancer would be 75%. A threshold figure could be set manually to prevent reporting of any spectra where there was a low probability of certainty. In this dataset, none was used.

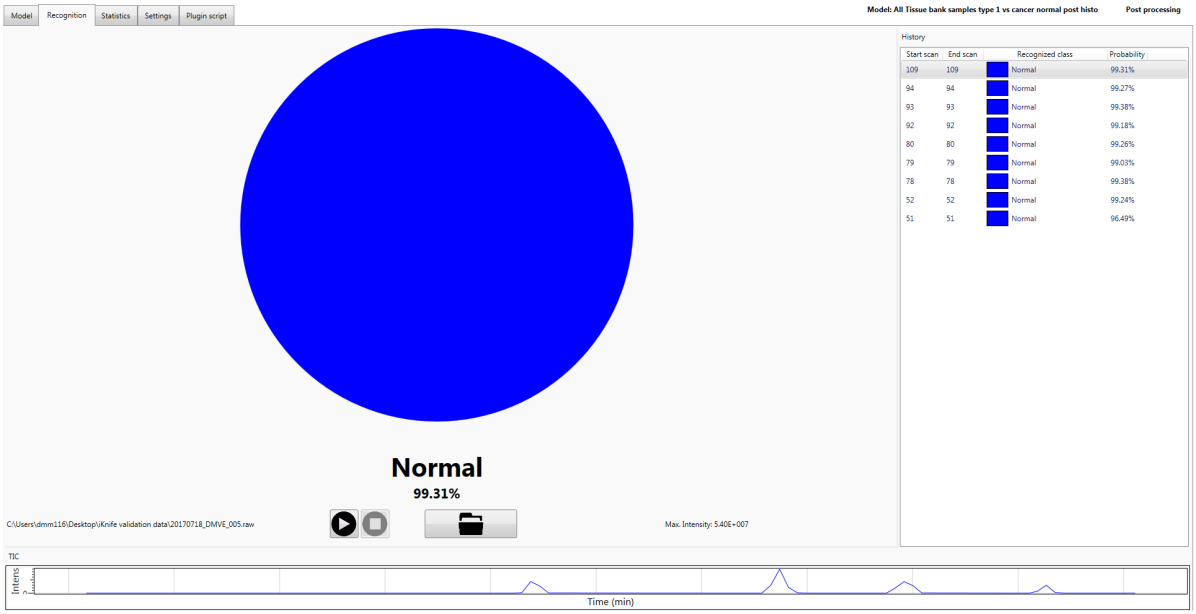


Figure 40. Recognition software analysing a tissue sample.

All the burns appear as peaks on the graph, seen at the bottom of the image. For each burn, a spectrum is produced. The software recognises the rise in total ion count and classifies the spectrum according to the model – either normal or cancer. It also specifies the degree of certainty of diagnosis, displayed on the right of the image. In this case, there were 4 burns. As the software refreshes every second, 9 spectra were recorded for the 4 burns, each were classified as normal with >90% certainty. As all the spectra were classified unanimously as normal, the overall diagnosis according to the model is normal tissue with 100% certainty.

The overall accuracy using this prospective validation was 95%. Only one case (cancer) was incorrectly diagnosed with 100% certainty. All other cases were diagnosed correctly with 85-100% certainty. This is in keeping with the high levels of accuracy seen on cross-validation model even with fresh tissue.

Loading plot and key m/z vales responsible class separation

The PC/LDA models have been shown to have excellent diagnostic accuracy in the diagnosis of endometrial cancer both on cross validation and prospective validation, as outlined above. They do not, however, provide any information on the lipid profile involved in the class separation. To understand this, it is crucial to study the m/z peaks that influence the class separation for the principal components in the model. Once the m/z peaks have been identified, a tentative lipid assignment can be made, and later confirmed using tandem MS.

The loading plots gives an instant visual assessment of the key m/z values responsible for the separation for a given principle component. As PC1 accounts for most of the variance (>45%) this is the loading plot illustrated for the best model. But, as can be seen in Figure 41 there is often separation along PC2 too. The m/z values with the highest peak are the most influential in class separation. In this case 699.5 and 744.5. The former is unsurprising, as lipids in that class are commonly observed in biological tissue, due to the presence in cell membranes.

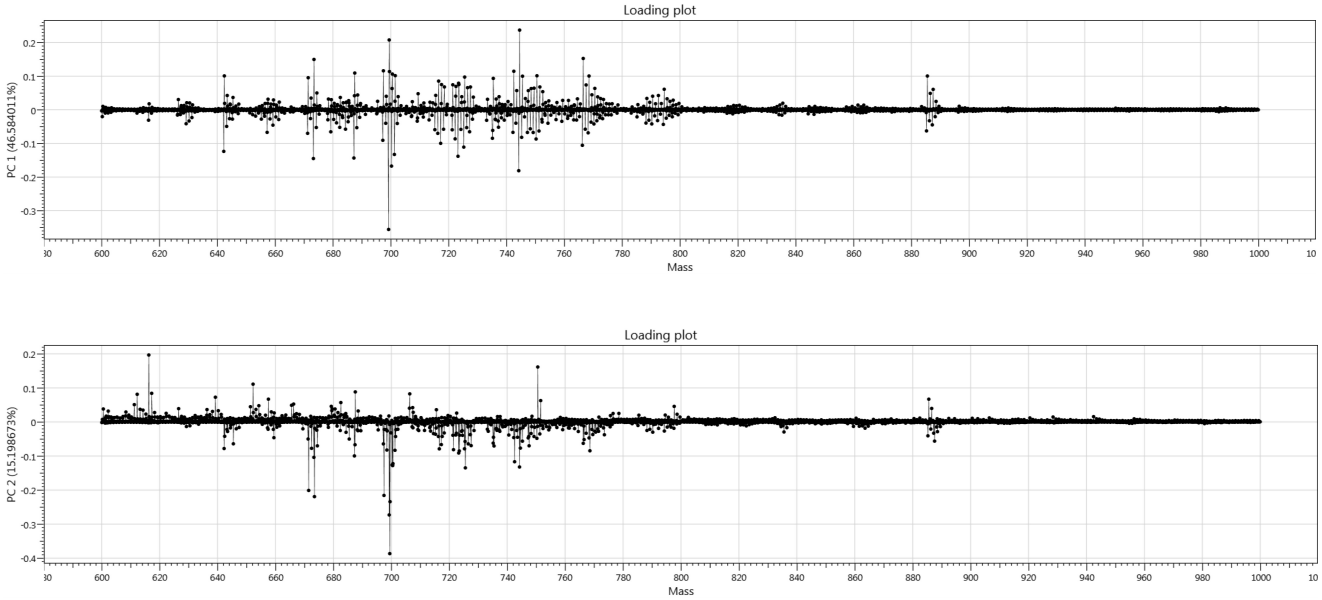


Figure 41. Loading plot of tissue bank model.

Top diagram is the loading plot of Principal component 1, for the tissue bank model: type 1 cancer versus normal, no hyperplasia. The bottom diagram is the loading plot of Principal component 2 of the same model.

After multivariate analysis using the PC/LDA models and loading plots, univariate analysis was performed to gain further information on individual m/z relative intensities and fold changes between classes. Figure 42 is an example box plot of one of the significant m/z values responsible for the separation of the tissue classes. Table 12 below shows the top 15 m/z values responsible for the separation of classes and the tentative lipid(s) involved. Only the m/z values which have been increased between cancer and normal were identified. The m/z peaks were shown to 2 decimal places and presented to the database in negative ion mode. LipidMaps proposes deprotonated ions [M-H]- and chlorinated ions [M+Cl]-, though deamnionated ions [M-NH3]- can also occur [196]. Approximately half of the lipids suggested were PAs.

These tentative lipid identifications can be confirmed with tandem mass spectrometry and will be discussed later in Chapter 4.6.

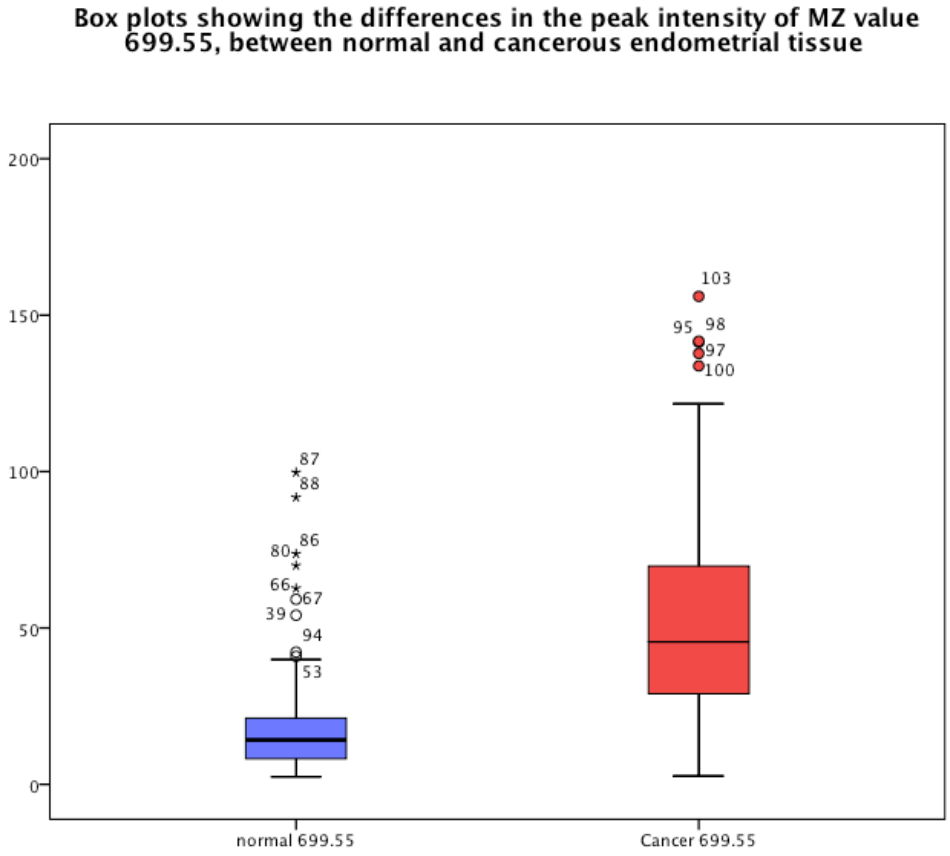


Figure 42. Box plot showing an example m/z value responsible for separation in the model.
In this case this box plot shows the difference in peak intensity between normal and cancerous tissue of m/z value 699.55. Endometrial cancer samples have significantly more of it present.

m/z value	Log2FC	Q value	Potential Lipids	Ion
645.45	1.42	6.70x10-7	PA 32:1	[M-H]-
669.45	2.12	6.47x10-6	PA 34:3	[M-H]-
671.45	1.94	3.45x10-7	PA 34:2	[M-H]-
672.45	2.22	2.70x10-7	PE O-32:2	[M-H]-
685.45	1.37	6.70x10-7	PG 30:4	[M-H]-
686.45	1.62	9.64x10-7	PE 32:2 PE 30:4;O2 PS 26:0	[M-H]- [M-H]- [M+Cl]-
697.45	1.58	9.54x10-7	PA 36:3	[M-H]-

			PI 24:0	[M-H]-
697.55	1.97	8.54x10-8	PA 36:3 PA O-34:0	[M-H]- [M+Cl]-
698.45	1.87	1.19x10-6	PE 30:0 PS 30:4 PC O-28:0	[M+Cl]- [M+Cl]- [M+Cl]-
699.55	1.28	3.40x10-7	PA 36:2	[M-H]-
714.55	1.82	3.58x10-6	PE 34:2	[M-H]-
740.55	1.81	2.19x10-6	PE 36:3 PC 30:0	[M-H]- [M+Cl]-
783.55	1.96	6.68x10-6	PG O-38:4 PG 34:1 PA 42:2 PA 40:6	[M-H]- [M+Cl]- [M-H]- [M+Cl]-
784.55	1.85	6.15x10-6	PS 36:3 PE 40:9 PC 34:6	[M-H]- [M-H]- [M+Cl]-
823.55	1.65	5.28x10-7	PG 40:5	[M-H]-

Table 12. Top 15 significant m/z values and tentative lipid assignments.

ANOVA was used to identify the most significant m/z values responsible for the separation on the model. The q value (adjusted p-value for multiple testing), along with log fold change score are recorded. The tentative lipid assignments or lipid differentials were derived from LipidMaps and are recorded alongside the m/z value.

The same process was applied to *type 1 vs type 2 cancer model* to ascertain if any specific m/z values were common in the more aggressive type 2 cancer compared to type 1. However, as the model had poor discrimination, when corrected to q-values using the Benjamini-Hochberg-Yekutieli method no m/z values remained significant.

4.3.3 Discussion

Key findings

The diathermy iKnife distinguishes between benign and malignant uterine tissue with a high degree of accuracy (89%). The binary models (*cancer vs normal / type 1 vs normal*) reduces the number of tissue classes and frequently, as in this case provides a superior diagnostic accuracy. But, in doing so, increase the chance that a correct diagnosis is made by chance. The model with the best diagnostic performance was

created from uterine samples containing either type 1 cancer or normal tissue only. This is unsurprising as type 1 cancer are more homogenous in nature, with a similar lipidomic profile, compared to the diverse profiles seen in type 2 cancers. Type 2 cancers include rare and mixed tumours and therefore building a robust model is more challenging, with fewer individual subtypes within the reference dataset.

Reassuringly, even though the iKnife could not distinguish between type 1 and type 2 cancer with good accuracy (both sample types clustered together on PC/LDA plot) they did separate very well from normal tissue; confirming a very different phospholipid signature between normal and cancer tissue.

The accuracy of the model was confirmed using both cross validation and prospective tissue validation of new tissue samples not included in the model. Both provided consistent high diagnostic rates. In the validation set, 32% were processed fresh to minimise the effects of autolysis of cells, anoxia and temperature changes. Encouragingly, prospective validation with a mixture of fresh and snap frozen samples made no discernible difference to the diagnostic rate. This suggests that whether samples are processed fresh or snap frozen and processed at a later date post thawing are both suitable methods of tissue processing. It also corroborates other studies in that the phospholipid composition is not grossly affected by the freeze thaw cycle [199].

Outliers in the models were analysed for reasons why those samples did not cluster appropriately. These reasons included: low volume tumour burdens and batch effect. Batch effect did not seem to be a big problem in this study. All samples used for model building were processed over 8 batches, only in one model (type 1 vs type 2 vs normal), was there any suggestion of batch effect.

Low tumour volume was another potential cause for outliers. Samples with little (<50%) viable tumour present could reflect that the iKnife destroyed the area of tumour, or that sample was taken from peri-tumoural tissue rather than the tumour itself. Consequently, a separate model was created, to ascertain if removal of all samples with low volume tumour improved the accuracy of the model, intriguingly it did not. This may be because, the iKnife already burnt through the cancer tissue, so little residual cancer remained for histopathological inspection, these ‘high volume cancers were then misclassified by the histologist as low volume. This is supported by the finding

that the iKnife identified spectral differences between samples of different tumour burdens, with progressive linear separation along PC1 (Fig 39), with high volume cancer samples separating more.

The alternative hypothesis for lack of improvement in the model after exclusion of low volume cancer samples is a 'halo effect'. Namely, there might be a peri-tumoural field change in the tissue [343], such that even if no microscopic disease is present in the biopsy the molecular profile and phospholipid signature of the remaining normal tissue aligns more with the surrounding cancer cells. In endometrial cancer, the stromal microenvironment, in particular, a macrophage response (CSF1) was associated with higher tumour grades, lymphovascular invasion, and PIK3CA mutations [344]. Other studies have reported that tissue adjacent to the tumour, in the microenvironment undergo metabolic transformations that prime the tissue for future malignant change and disease progression [119, 343, 345, 346].

Interestingly, removing all the outliers from the model did not improve the overall diagnostic accuracy. This may be due to the reduction in the size of the overall dataset. The iKnife, much like other learning models needs large datasets to provide reliable robust models. It may also be due to the type of statistics (PC/LDA) used by the software to create the models, some are more resilient to outliers.

The biggest improvement seen in the models was after histopathological quality control. This resulted in the exclusion of 26% of samples and their corresponding spectra. Sensitivity and specificity in the model increased by over 20%. This confirms the need to always histologically validate tissue samples used in the model building.

Of note, on histopathological review 71% of the 'normal' endometrial tissue samples did not contain any endometrium, only myometrium on microscopy. Endometrial cancer, unless more advanced is only present within the endometrium, thus, ideally, the model should be built with endometrial lining. However, procurement of only endometrial tissue by the histopathologist is very difficult and exclusion of all myometrial samples would result in too few normal samples to build a robust model. It is also possible that the small amount of endometrial tissue present on the normal samples was burnt through by the iKnife, leaving only residual myometrium.

Additionally, three normal samples came from cancer patients, with primaries of the cervix and ovaries. Whilst these samples appeared normal on histopathological QC and were therefore included in the model, it remains to be established whether there is any lipidomic change to adjacent tissue, from primaries elsewhere that might result in an incorrect classification. One of these normal cases derived from an ovarian cancer sample was a persistent outlier in each model. Whether it was due to this lipidomic field change or to the presence of myometrium only is debatable.

An important feature of malignancy is uncontrolled cell division, necessitating an increase in cell membrane lipid synthesis. This is reflected by an increase in phospholipid biosynthesis pathways and an alteration in the cellular phospholipid make-up of cancer cells. The iKnife interrogates these changes to distinguish between lipid classes. The loadings plot and univariate analyses suggested multiple m/z values were significant for the class separation, confirming that the entire lipid signature is important for class separation not just single m/z values. Therefore, despite each m/z value being highly significant (q value <0.001) none could be used in as an isolated biomarker. The tentative lipid assignments of the top 15 significant m/z values were predominately PAs and PEs. This is in keeping with other studies which found higher levels of PAs and PEs in breast, ovarian and bowel cancer [187, 195, 196, 199]. Tandem mass spectrometry is needed to confirm these lipid assignments and will be discussed more detail in section 4.6.

Strengths and limitations

The iKnife has been used in different tissue types with a high degree of diagnostic accuracy [187, 196, 199]. This was, however, the first study in the world to use the iKnife to process endometrial tissue and assess if it could be used to identify cancer.

Each tissue type has a different tissue consistency and fat content, which directly affects signal intensity. The iKnife research team working in the breast and ovarian group found the addition of a mobile phase solvent (IPA) improved signal intensity. Thus, IPA was used throughout my study. Overall, the signal intensity of the uterine tissue samples was much less than the ovarian group, which is a reflection of the tiny specimen size and tissue consistency of the uterine samples. Ovarian cancer usually presents at an advanced stage and there is copious tissue available for histological

assessment and research. Endometrial cancer conversely, presents earlier, and a significant proportion of the endometrial tissue is required for gold standard histological assessment, before donation to research.

Another limitation of the iKnife is its destructive nature, in the process of analysing the tissue, the cells and its architecture are ablated. This makes histopathological validation very challenging and leads to the exclusion of potentially correctly classified samples. Ideally, histological spatial identification of each burn and its corresponding spectra would be performed to ensure correct tissue classification for every burn. However, this is a very labour-intensive process and does not account for ablation of the tissue making histological QC impossible. One technique to overcome this would be to snap freeze each sample, cryosection the tissue to very thin 12 µm slices and then histopathologically validate and burn alternate slices. Alternatively, the CO2 laser iKnife or optical para- metric oscillator (OPO) laser iKnife could be used instead of the diathermy iKnife, as both cause much less tissue destruction. The CO2 laser energy is rapidly absorbed by water and has less thermal spread around the tissue. It reportedly burns to a depth of approximately 20 μm depending on tissue type, leaving ample tissue left for histological QC [347]. The CO2 laser has been found to produce cleaner cuts and higher quality spectral signals when compared with normal diathermy [348].

Electrosurgery used in the iKnife uses high-frequency, alternating polarity, electrical current to cut, coagulate, desiccate, and fulgurate tissue. Cut and coagulation setting on the monopolar diathermy are dictated by the high frequency waveform. In the cut setting the constant waveform vaporises tissue due to the rapid heat production and produces more aerosol with a higher peak ion intensity with less background noise. In the coagulation setting, the intermittent waveform caused by the generator produces less heat and a coagulum is formed. The ion intensity is relatively less, and much more background noise is apparent, as seen in Figure 32. As samples were small, cut was used in preference to coagulation if the tissue was insufficient to process with both.

Conclusion

In this pilot study the diathermy iKnife correctly identified endometrial cancer from tissue samples obtained from the histopathology department with a high degree of

accuracy. This is promising, but to be translational, the iKnife must be able to recognise cancer from tissue samples obtained in clinic using OEB devices such as the pipelle. The next part of this Chapter goes on to describe the implementation, performance and challenges of using the iKnife to process pipelle biopsies.

4.4 The pipelle

Can the tissue bank model identify cancer from pipelle biopsy samples?

4.4.1 Methods

The equipment, chemicals, iKnife set up, calibration, lock mass, sample processing and histological reporting are all the same as described in the materials and methods section 4.3, for the tissue bank model with the exception of a few modifications detailed below.

Pipelle biopsies were obtained from patients in clinic and theatre and these samples were presented to the recognition software using the *tissue bank type 1 vs normal model*. The acquisition of these pipelle samples was approved by Bloomsbury research and ethics committee (REC number:17/LO/0173). All patients provided written, informed consent. Only patients who had a clinical indication for a pipelle could participate in the study. In addition, to ensure gold standard clinical care, the sample obtained for research was from a second pass of the pipelle. The second research pipelle usually has less tissue than the first one. Patients who agreed for a research pipelle, but no tissue was obtained were excluded from the study.

Due to large variations in the quality of the tissue, a simple quality score was given for each sample: poor, moderate and good, which were according contemporaneously. Poor samples were defined by very bloody tissue / minimal amounts of tissue (less than 0.5cm in any of the diameters) / mainly mucus. Good samples were defined by large amounts of solid appearing of tissue (more than 1cm in any diameter). Moderate samples were moderate size with some solid tissue. See Figure 43.



Figure 43. Photographs of endometrial tissue obtained from pipelle biopsies.
Sample quality varied significantly; poor on the left to good on the right.

Tissue samples were processed as described in materials and method section 4.3.1 The samples were divided into 3, size allowing. Two for use by REIMS and one for storage in a -80^0 freezer for later use. As described in the discussion section 4.3.3, the cutting setting of the diathermy had much less background noise compared to coagulation setting. Due to the small sample sizes, and to minimise tissue wastage, the coagulation setting was not used again.

Instead, samples were burnt with the less destructive iKnife laser first (CO2 laser) followed by the diathermy cutting setting of the iKnife (with a median of 3 burns). The samples were not processed with laser in isolation, as it is not currently validated. The CO2 laser instrument is discussed below. Some samples didn't have any discernible solid pieces to burn using the diathermy iKnife, as such a liquid probe (Figure 44) was used instead of the conventional diathermy iKnife. In order to distinguish between these energy modalities, in the remaining thesis the CO2 laser iKnife is cited as CO2 laser, the standard diathermy iKnife is cited as iKnife and the liquid probe iKnife is cited simply as liquid probe.

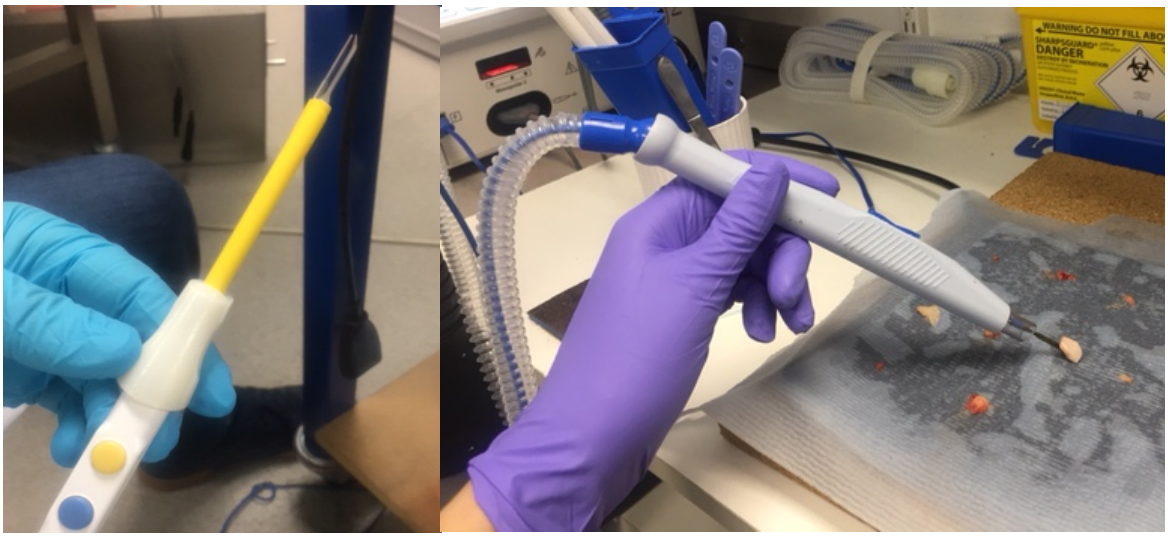


Figure 44. The handpiece attachments for REIMS.
Left is the liquid probe handpiece and right is the standard iKnife diathermy handpiece.

Tissues were processed fresh, within four hours of acquisition or snap frozen using the CoolRack and used at a subsequent date. The CoolRack enables freezing of samples to -78^{0}c in about 7minutes with dry ice alone. The reason for delayed processing was due to unavailability of the iKnife machine in Queen Charlottes hospital. In these cases,

the samples were snap frozen and stored in a -80^{0}c freezer and then analysed in Charing Cross hospital after thawing. If samples were only liquid and no signal was detected with either iKnife diathermy or CO2 laser they were processed with the liquid probe and G2-XS Xevo Q-ToF mass spectrometer in St Marys Hospital. A record was made of whether the tissue was processed fresh or snap frozen and which location (and mass spectrometer) the samples were processed.

The surgical CO2 laser

A CO2 LASER (l=10.6 μm, maximum power of 10 Watts, Omniguide,USA) and a Covidien ForceTriad generator was used for tissue sampling. The LASER fibre was connected securely to the laser machine and the free end inserted into the surgical handpiece equipped with a PTFE tube toward to the mass spectrometer (used for the `surgical smoke` extraction). The captured aerosol was connected to the same Waters G2-XS Xevo Q-ToF mass spectrometer. The laser can be operated in 4 energy modalities: continuous, single pulse, repeat pulses and super pulse. The continuous setting has a lower peak energy, with a more superficial impact and wider thermal zone [348]. Conversely, the pulse settings have a high peak energy, with deeper impact but less thermal spread [348].

Safety eyeglasses were worn for protection and a sign outside the door was placed whenever the laser was in use. The ICS-6 laser interlock system was enabled on the control panel and helium cylinder was opened. The laser was then switched on and placed into manual mode. The LASER settings were set to 3Watts for power, 40 PSI for gas flow and superpulse setting.

As using with the conventional iKnife diathermy, IPA with leuEnk was used as a matrix solvent to enhance the ionisation and for lock mass introduction.

Post processing analysis

After processing of the tissue, samples were histopathologically validated as described earlier. A senior histopathologist, Dr Roberto Dina manually reviewed the FFPE slides using a light microscope. He confirmed whether cancer was present in the sample or not, or if it was not possible to determine due to the charring effect of the diathermy.

The individual samples were presented to the OMB recognition software as discussed in materials and methods section 4.3.1.

4.4.2 Results

Collection of data from frozen samples

One hundred and fifty pipelle samples were obtained from 150 patients presenting to RAC or day surgery for hysteroscopic assessment (one sample per patient). Four patients had endometrial hyperplasia and 2 insufficient on histology due to atrophy. The remaining samples were either classified as either cancer or normal, with a fairly even divide of samples (59 versus 85 respectively) see Table 13 for breakdown. Patients with cancer tended to be older (median age 64 vs 54 years old). There was a higher proportion of patients presenting with postmenopausal bleeding (PMB) in the cancer group, as oppose to heavy menstrual bleeding (HMB), intermenstrual bleeding (IMB) or abdominal (abdo) pain. Most cancer samples were the more common endometrioid type 1 subtype.

	NORMAL (n = 85)	CANCER (n = 59)
Age	54 (22-80yo)	64 (35-85yo)
Presentation:		
PMB	36 (42%)	49 (83%)
HMB	26 (31%)	3 (5%)
IMB	10 (12%)	0 (0%)
Abdo pain	11 (13%)	5 (8%)
Other	2 (2%)	2 (3%)
Type of Cancer	N /a	Endometrioid Low grade: 30 (51%) High grade (G2/3) 19 (32%) Serous 7 (12%) Carcinosarcoma 2 (3%) Clear cell 1 (2%)

Quality pipelle:		
Small/Bloody	40 (47%)	14 (24%)
Moderate	22 (26%)	9 (15%)
Good/polyp	23 (27%)	36 (61%)

Table 13. Summary table of the patient demographic from which the pipelle biopsies were obtained, along with the sample quality.

All 150 pipelle samples were processed with REIMS. Four samples were too small to be processed with the conventional diathermy iKnife so were processed with the CO2 laser only. Five samples were purely liquid, with no solid tissue within in it. No signal was detected with the iKnife or CO2 laser and they were processed exclusively with the liquid probe. The remaining 141 samples were processed with the conventional diathermy iKnife producing 453 spectra. In addition, of the 150 original pipelle samples, 106 were also processed with the CO2 laser yielding 106 spectra.

The OMB software AMX utilises a spectrum analyser quality control feature. This reviews all spectra and removes any which have either a high signal to noise ratio (top 20 vs background). Following this, 52 diathermy iKnife spectra from 15 samples were removed. Three samples (all benign) processed with the diathermy iKnife were completely excluded from the analyses as all the spectra did not pass quality control (see Table 14). No laser spectra were removed due to poor quality.

Histological quality control excluded a large portion of samples (49/150 for diathermy iKnife and 42/150 CO2 laser). This was largely due to thermal artefact caused by the diathermy/CO2 laser. Some cancer samples also did not have any recognisable cancer tissue remaining; either because the tissue was burnt through, or because the pipelle sample missed the cancer. Of the 59 cancer samples, diathermy artefact also made estimation of tumour volume exceedingly challenging – more than 15 samples were inadequate and excluded from model building. More than 20 samples were confirmed as cancer but due to thermal artefact it wasn't possible to estimate the cancer volume. An assessment of the effect of tumour burden on the model wasn't possible with pipelle samples as the remaining numbers of samples in each classification group was too small to draw a meaningful conclusion.

TISSUE TYPE	Pre-spectrum QC		Post spectrum QC		Post histology QC	
	SAMPLES	SPECTRA	SAMPLES	SPECTRA	SAMPLES	SPECTRA
CANCER	59	210	59	189	43	145
HYPERPLASIA	4	12	4	12	1	5
NORMAL	78	231	75	200	45	131
TOTAL	141	453	138	401	89	281

Table 14. Summary table of pipelle samples processed with REIMS diathermy iKnife. The sample number and spectra generated for the tissues is shown. Each tissue sample was obtained from one patient, so the numbers seen represent both patient and sample number. It is also apparent that a significant number of samples were removed due to poor spectral quality or failed histopathological validation. Also note the total is 141, as not all 150 samples were processed with the standard iKnife diathermy.

The sample number and spectra generated for the tissues is shown in Table 14. Each tissue sample was obtained from one patient, so the numbers seen represent both patient and sample number. It is also apparent that a significant number of samples were removed due to poor spectral quality or failed histopathological validation.

Diagnostic accuracy of tissue bank model using pipelle samples.

The first 50 pipelle samples were presented to the OMB recognition software using the *type 1 cancer vs normal tissue bank* PC/LDA model. Of these, five samples were predominately mucus and were processed with liquid probe not the conventional iKnife. As the liquid probe is not a validated method these samples were ultimately excluded from this analysis. The settings for the software recognition were: 1 scan per spectra, three second time out and no outliers. The intensity limit was adjusted for each sample to ensure the burn was captured with minimal background noise. For most samples this intensity threshold was 10^7.

As described earlier, a final tissue classification and an overall degree of certainty for each sample classification was produced by the recognition software. This time a threshold figure of certainty was set to ≥75%, such that the model needed to be at least 75% confident of the tissue classification otherwise the outcome was not reported.

The overall accuracy of the conventional diathermy iKnife using the final patient diagnosis as reference standard and using the tissue bank model was 60% (27/45) (see Table 15). However, after histopathological QC 13 samples were excluded as the tissue was non-diagnostic due to thermal artefact or because the tissue class changed. The diagnostic performance of the model using the remaining 32 samples was 66%. Most samples were processed with a high degree of certainty, even if incorrectly classified. When the threshold figure for certainty of classification was reduced to 60%, the diagnostic accuracy increased to 72% (23/32), which is still far less than that observed in the tissue bank model.

Sample number	**Detection intensity threshold**	**Model classification**	**Degree of certainty**	**Actual classification**	**Histological classification**	**Correct diagnosis if 75% cut-off**
1	10^7	normal	100%	normal	Normal	Yes
2	10^7	normal	100%	cancer	Inadequate	no
3	10^7	normal	100%	normal	Normal	Yes
4	10^7	normal	75%	normal	Normal	Yes
5	10^7	cancer	100%	normal	normal	no
6	10^7	cancer	100%	normal	Normal	no
7	10^7	normal	67%	normal	Normal	n/a
8	10^7	cancer	100%	cancer	normal	no
9	10^7	cancer	100%	cancer	cancer	Yes
10	10^7	cancer	100%	cancer	inadequate	Yes
11	10^7	cancer	100%	cancer	cancer	yes
12	10^7	cancer	100%	cancer	cancer	Yes
13	10^7	cancer	100%	cancer	cancer	Yes
14	10^7	normal	100%	normal	cancer	yes
15	10^7	normal	100%	cancer	cancer	no
16	10^7	normal	85%	normal	Normal	Yes
17	10^5	normal	100%	normal	inadequate	Yes
18	10^7	cancer	88%	cancer	cancer	yes
19	10^5	normal	100%	normal	inadequate	Yes

20	10^7	normal	100%	normal	Normal	Yes
21	10^7	normal	100%	normal	inadequate	yes
22	10^7	normal	100%	cancer	cancer	no
23	10^6	normal	100%	normal	inadequate	Yes
24	10^8	normal	100%	cancer	inadequate	no
25	n/a	Not processed diathermy iKnife only liquid probe				
26	10^7	normal	100%	normal	normal	Yes
27	10^7	normal	81%	cancer	cancer	no
28	10^7	normal	100%	normal	normal	yes
29	n/a	Not processed diathermy iKnife only liquid probe				
30	n/a	Not processed diathermy iKnife only liquid probe				
31	10^7	normal	80%	normal	normal	Yes
32	10^7	normal	100%	normal	normal	yes
33	n/a	Not processed diathermy iKnife only liquid probe				
34	10^5	cancer	100%	normal	normal	no
35	10^6	cancer	96%	cancer	cancer	yes
36	10^7	normal	100%	normal	normal	yes
37	10^7	cancer	100%	normal	normal	no
38	10^7	normal	67%	normal	Normal	n/a
39	10^7	normal	100%	normal	Normal	yes
40	10^7	normal	85%	normal	normal	Yes
41	n/a	Not processed diathermy iKnife only liquid probe				
42	10^5	normal	100%	normal	inadequate	Yes
43	10^7	cancer	100%	Normal	inadequate	no
44	10^7	cancer	100%	Normal	inadequate	No
45	10^7	cancer	100%	normal	Normal	No
46	10^7	cancer	100%	normal	inadequate	No
47	10^7	normal	100%	cancer	cancer	no
48	10^7	normal	100%	normal	Normal	Yes
49	10^7	normal	100%	normal	Normal	yes
50	10^7	normal	100%	normal	normal	yes

Table 15. Summary table of pipelle sample classification according to the tissue bank model.

The first 50 samples were presented to the recognition model. The intensity threshold was varied according to the strength of signal detected. The model's classification (with % certainty) and the histological classification

(reference standard) were compared. When the histological classification was different to the model's classification the text is red.

4.4.3 Discussion

Key findings

Disappointingly, the tissue bank model had much worse diagnostic accuracy in endometrial tissue classification using pipelle biopsy samples as oppose to tissue bank samples (62% vs 89%). There are a number of reasons which may explain this. Firstly, 33/50 pipelle samples were processed fresh, and while the freeze-thaw process didn't appear to make a difference with the tissue bank samples, it might have had a significant impact with pipelle samples.

Secondly, the pipelle biopsy tissue is very different to the solid pieces of tissue acquired from tissue bank (Figure 29 and Figure 43). Pipelle biopsies only contain endometrium, and as discussed earlier a lot of normal myometrium samples were included in the tissue bank model dataset. The consistency of pipelle samples are very heterogenous (completely liquid to solid tissue), this posed technical challenges for the iKnife but also increased the complexity of model classification. For tissues which are very different, large reference data sets are even more important and it is likely that the 90 samples used in my model is insufficient.

Thirdly, the research pipelle is taken after the pipelle obtained for standard histopathology. The second pass pipelle inevitably has less tissue available for analysis. At present there is no way to overcome this, the iKnife is a research tool and it is essential patients receive standard level of care, even at the cost of research.

Fourthly, there were a variety of normal pipelle samples, including: inactive endometrium, normal secretory endometrium and benign polyps. Molecular profiling has shown differences in endometrial tissue dependant on the timing of the cycle, and also the presence of polyps or fibroids [349] and these changes may result in downstream phenotypic changes which are recognised by the iKnife. It is unclear what kind of normal tissue is including within the reference spectral library.

Intertumoral heterogeneity is well recognised with distinct morphological differences between type 1 and type 2 cancer [350]. One would expect these morphological differences would correlate with differences in spectral profiles. The best tissue bank model created was *type 1 cancer vs normal*, so processing of type 2 pipelle samples may be another possible cause for the poor performance of the model. However, on review, all 50 pipelle samples processed with the recognition software were all type 1 endometrial cancers, so the ineffective model was not due to the inclusion of type 2 samples. Intratumoral morphologic heterogeneity exists too, with evidence that molecular and morphologic features heterogeneously present in different tumour cell clones [350]. Thus, even if the model utilises type 1 cancer only, and if only pipelle type 1 cancers are presented to the model, intratumoural heterogeneity will mean not all samples are the same, and this may also be a contributing factor to the downfall in the model.

Histopathological validation only improved the performance of the model marginally (60 to 66%). This suggests that the reason for the poor performance is only partly due to tissue classification i.e. the lack of cancer in a cancer sample. As seen in the tissue bank dataset, histopathological validation removed a large number of samples, within the pipelle samples this was 29% (13/45). The ablative nature of the iKnife makes posthoc tissue classification exceedingly difficult.

Conclusions

Regrettably the tissue bank model performed average at best, with a diagnostic rate of 72%, which is insufficient due to be used in isolation in clinical setting. The diagnostic rate is also much worse than that seen using tissue bank samples predominately due to differences in tissue type. These findings suggest the need for the creation of a new pipelle model, made out reference spectra from pipelle biopsy samples only.

In the next part of this Chapter, the development, strengths and limitations of a new pipelle model are discussed.

4.5 A new pipelle model

4.5.1 Methods

All pipelle biopsy samples were processed as described in Materials and methods section 4.4.

Statistical analysis

The Offline Model Builder, version Abstract model builder (AMX) was used initially for all pre-processing of spectra and model building as described earlier. The newer version of OMB (AMX) removes poor quality spectra.

In addition, files were also imported to Matlab version 2016a (Mathworks), this enabled selection of method of classification of spectra, creation of Eigenvalues, univariate analysis and also the production of learning curves; all of which are described in detail below. No normalisation was required as the data had already been normalized by OMB.

Multivariate analysis using the unsupervised PCA was performed first to prevent overfitting of the model. Supervised models (like LDA) were then created using either partial least square regression (PLS) or maximum margin criterion (MMC). Matlab enables selection of the classification technique: Mahalanobis distance, nearest neighbours and centroid - these determine which class new observations belong to. Mahalanobis classification is based on the Mahalanobis distance, namely a measure of the distance between a point and the mean of a distribution (in terms of standard deviations). Nearest neighbours classify observations according to whichever 3 observations are closest to it. Centroid classifier determines the centroid of each class in the model and then calculates the distances between the observation and each class. Each classification technique has advantages and disadvantages. The model classifier with the best accuracy was used.

The 10 eigenvalues are also reported, these describe the percentage of variance explained by each of the first ten principal components. Loading plots were created.

Validation of these models were performed using a 'leave one patient out' (LPO) cross validation, unless otherwise stated. This is due to the small sample sizes of some of the groups which makes this a preferable approach.

Learning Curves

Learning curves are a pictorial way to plot the changes in classification rate as more samples are included in the training set of a predictive model. It shows a change in classification performance (y-axis) as a function of the number of observations (x-axis). Naturally, the expectation is for classification to improve as more observations are included, up to a finite number at which point the classification rate plateaus. It is useful in this context to estimate whether maximum diagnostic performance is reached, or if more samples are needed. The analysis can only be performed with binary models (e.g. cancer vs normal) and requires equal numbers of normal and cancer samples.

Univariate analysis

The data matrices were interrogated by Matlab; the intensity values and median fold change of each binned m/z values were analysed using ANOVA and Kruskal-Wallis to identify those discriminatory m/z values responsible for the separation in the model. P values were reported for each m/z value. The results are displayed as a volcano plot with log fold change on the x-axis and -log10(p value) on the y-axis (see Figure 45). Significant m/z values are shown as orange dots. As multiple univariate tests are performed, the likelihood of a false positive result becomes significant. As such, p-values are corrected to q-values using the Benjamini-Hochberg-Yekutieli method, with a false discovery rate, $\alpha = 0.05$. Altering the q value significance threshold makes more or less variables (m/z values) significant. Peaks were considered significant if the p and q values were <0.001. Individual boxplots and ROC can be produced for each m/z value.

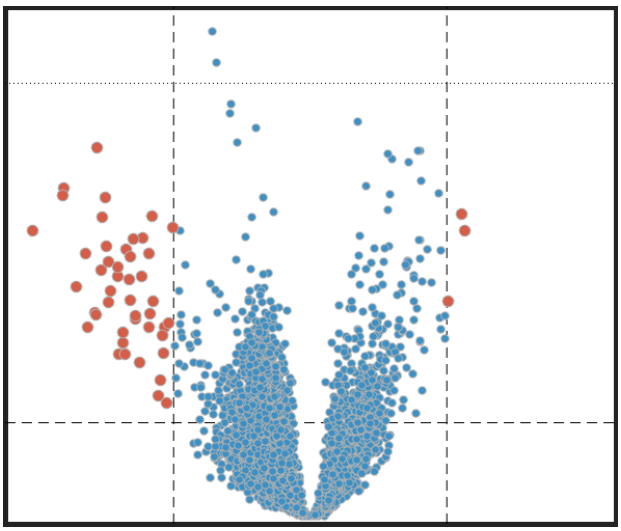


Figure 45. Example of a Volcano plot.
Each dot represents an m/z value. Log fold change is on the x-axis and p value (-log10) on the y-axis. The most significant m/z values are coloured red and appear in the top left and top right of the volcano plot.

Method optimisation

Pipelle samples varied significantly in consistency, the maximal intensity spectra were obtained when the samples were very wet. Large amounts of distilled water were sprayed across every sample prior to processing. Pipelle samples also, in general needed less power using the diathermy, (high power settings caused excessive charring) and the power setting was reduced to 15 Watts.

The purely liquid samples were transferred to a small vial, and the liquid probe was placed just under the surface of the liquid sample, care taken to avoid contact with the vial container wall. The cut setting was used and 2-3mm gap was maintained between the blades of the liquid probe.

Quality control

As described earlier, the OMB AMX software had automatic spectral quality detection and removed those spectra considered poor quality, based upon pre-defined metrics. Some spectra visually appeared poor quality with burn peaks not dissimilar to background noise, whilst other bad spectra were less obvious (Figure 46). Overall, 70 diathermy iKnife spectra were removed. Four samples (all benign) processed with the conventional diathermy iKnife were completely removed as none of the spectra passed

quality control. By comparison all spectra produced by the CO2 laser iKnife passed the spectral quality control, confirming the findings by Genangeli group – CO2 produces cleaner signal with less background noise [348].

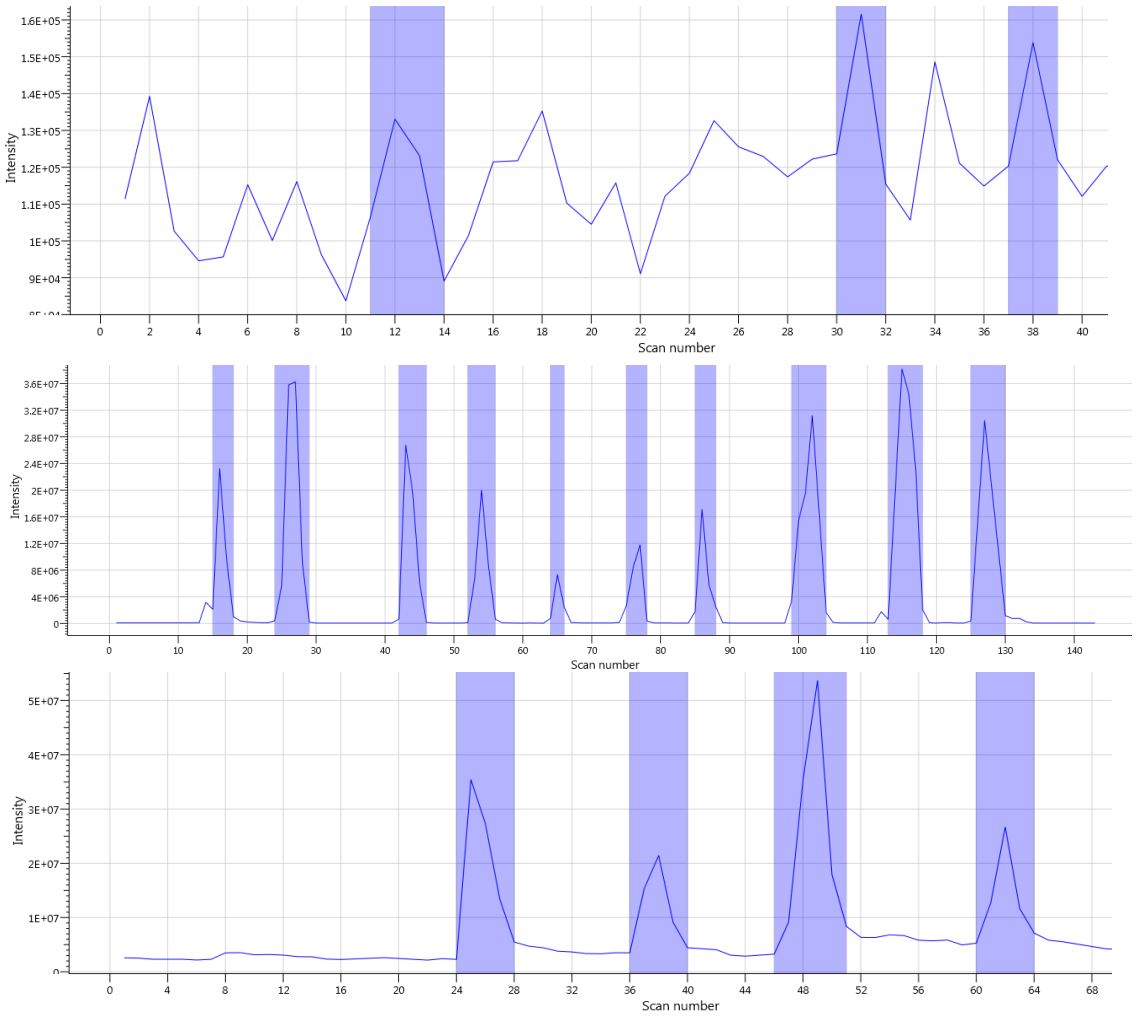


Figure 46. Chromatograms of different samples.
The top picture has a wondering baseline, with peaks hard to delineate and of low intensity (10^5) – it failed the spectral quality control. The bottom chromatogram has distinct peaks of good intensity (10^7) – it passed spectral quality control. The spectra in the middle looks good, but on closer inspection of each individual spectral peak, the noise: signal ratio was very high, and the sample was excluding after failing QC.

Similar to the tissue bank model, histopathology QC removed a large proportion of pipelle diathermy iKnife samples (36%) as they were inadequate due to thermal artefact. Thermal artefact makes cytological features more difficult to identify so class identification is predominately based on architectural features (Figure 47 to 49). A higher proportion of benign samples were removed. Of the 4 hyperplasia samples, only one sample confirmed hyperplasia on histopathological QC. One of the limitations of histopathological QC of the pipelle samples was the inability to perform the standard

immunohistochemistry profile which often helps distinguish between tissue groups. Table 16 outlines key features that distinguish between normal endometrium and endometrial cancer [351, 352], this can also be seen in Figure 47 to 49.

NORMAL		CANCER	
Cellular features	Histology architectural features	Cellular features	Histology architectural features
Epithelial cells either columnar or cylindrical – round nuclei and scanty dense cytoplasm	More stroma to glands.	Nuclei atypia and pleimorphism	> 3:1 glandular to stromal elements
Stromal cells spindle shaped with oval fusiform nuclei	Stroma present between glandular basement membranes	Prominent, enlarged nucleoli with irregular coarse chromatin with clumping	Irregularly shaped glands with back to back architecture
	Gland epithelial monolayer	Loss of polarity of cells with respect to basement membrane	Stratification of glands and cribriforming
	Small, round regular glands		Increase glandular complexity: gland fusion, loss of glandular contours, luminal infolding, budding, papillae (+- psammoma bodies), nests (epithelial cells fill gland)

Table 16. Summary table of cytological and histological features of normal and malignant endometrium.

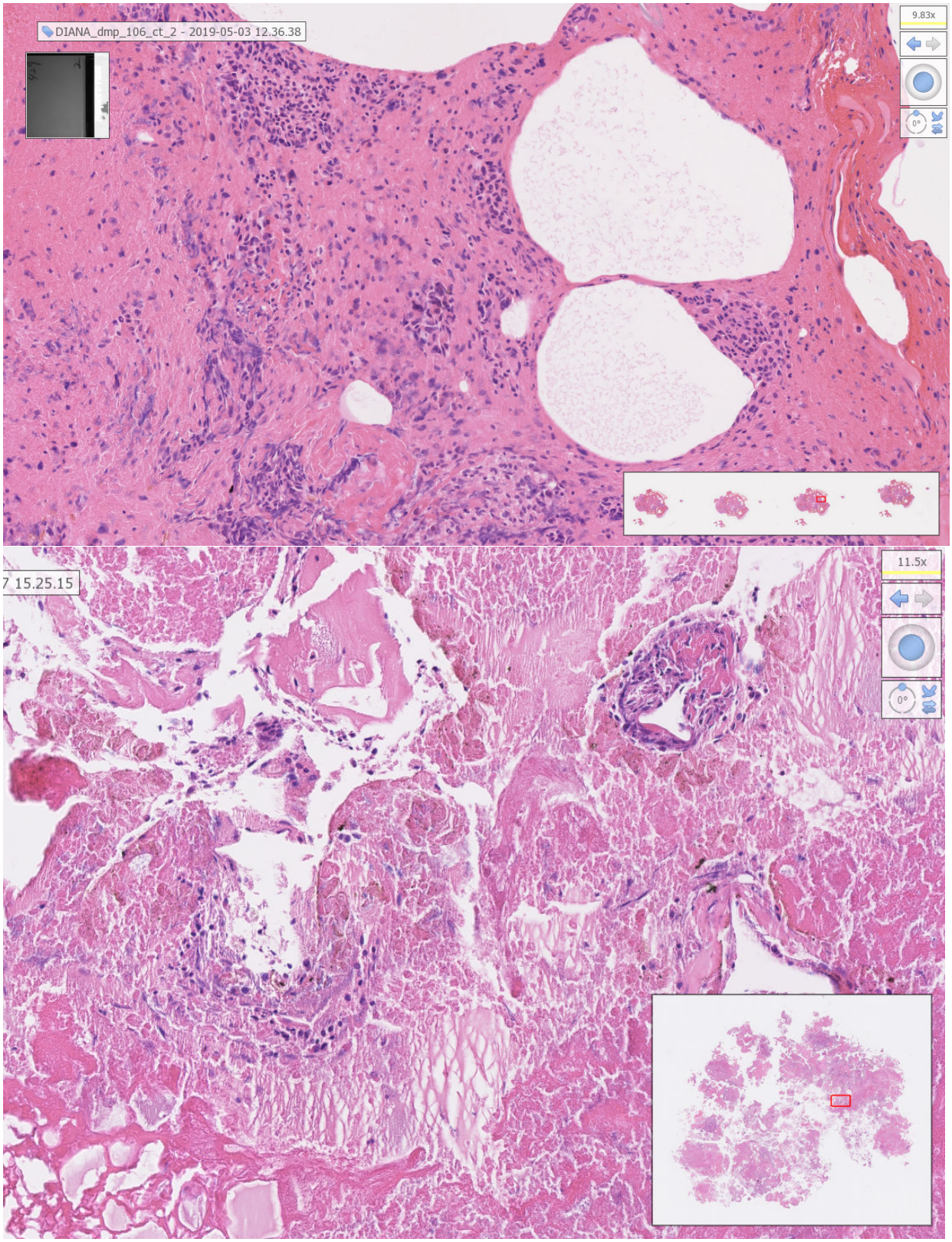


Figure 47. Endometrial cancer samples, heavily diathermised.
Bottom sample mainly clot and artefact. Impossible to provide confirmatory histological diagnosis

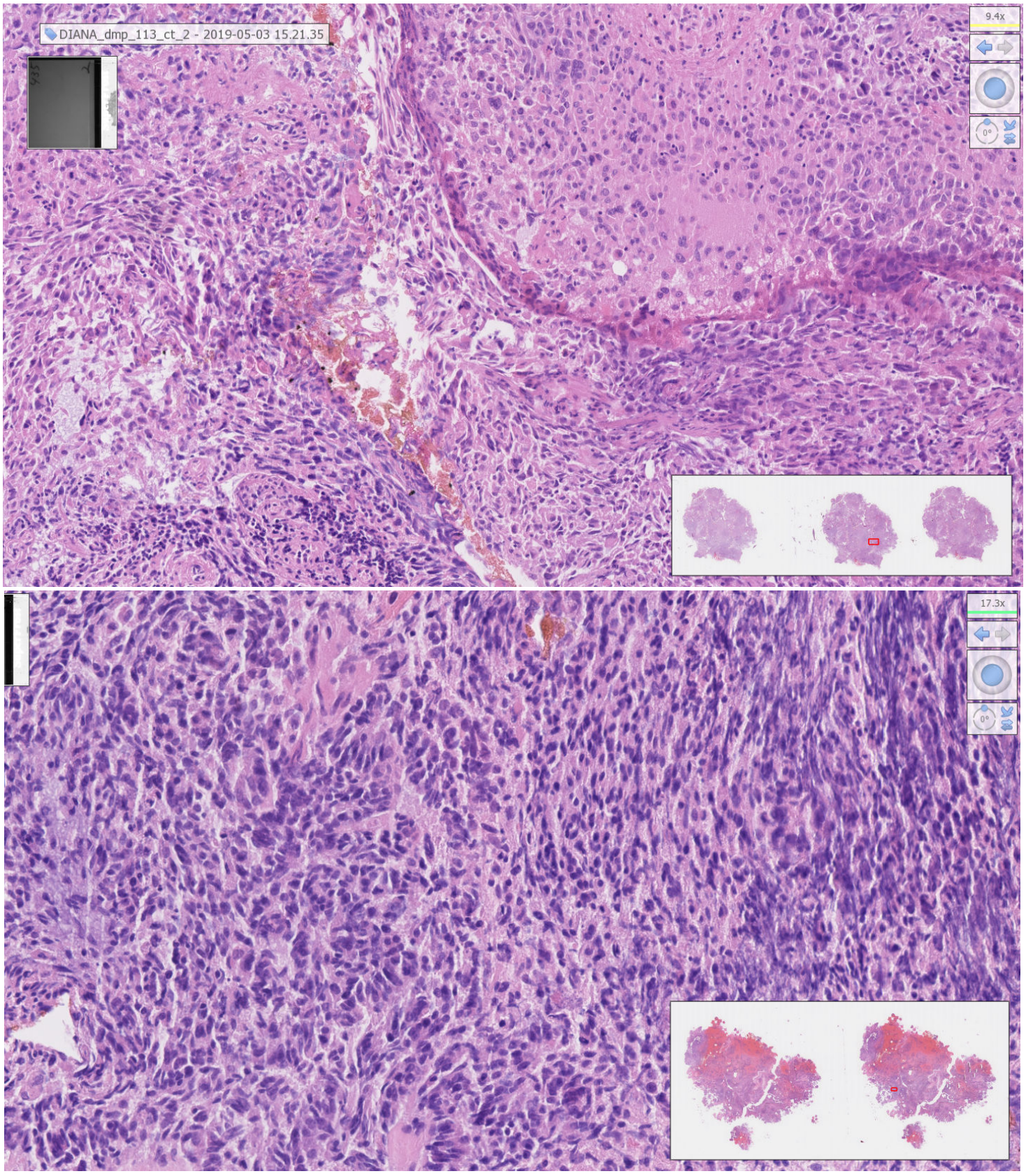


Figure 48. Endometrial cancer samples. Loss of cell polarisation.
Pleomorphic cells. Stratified glandular cells with some nests.

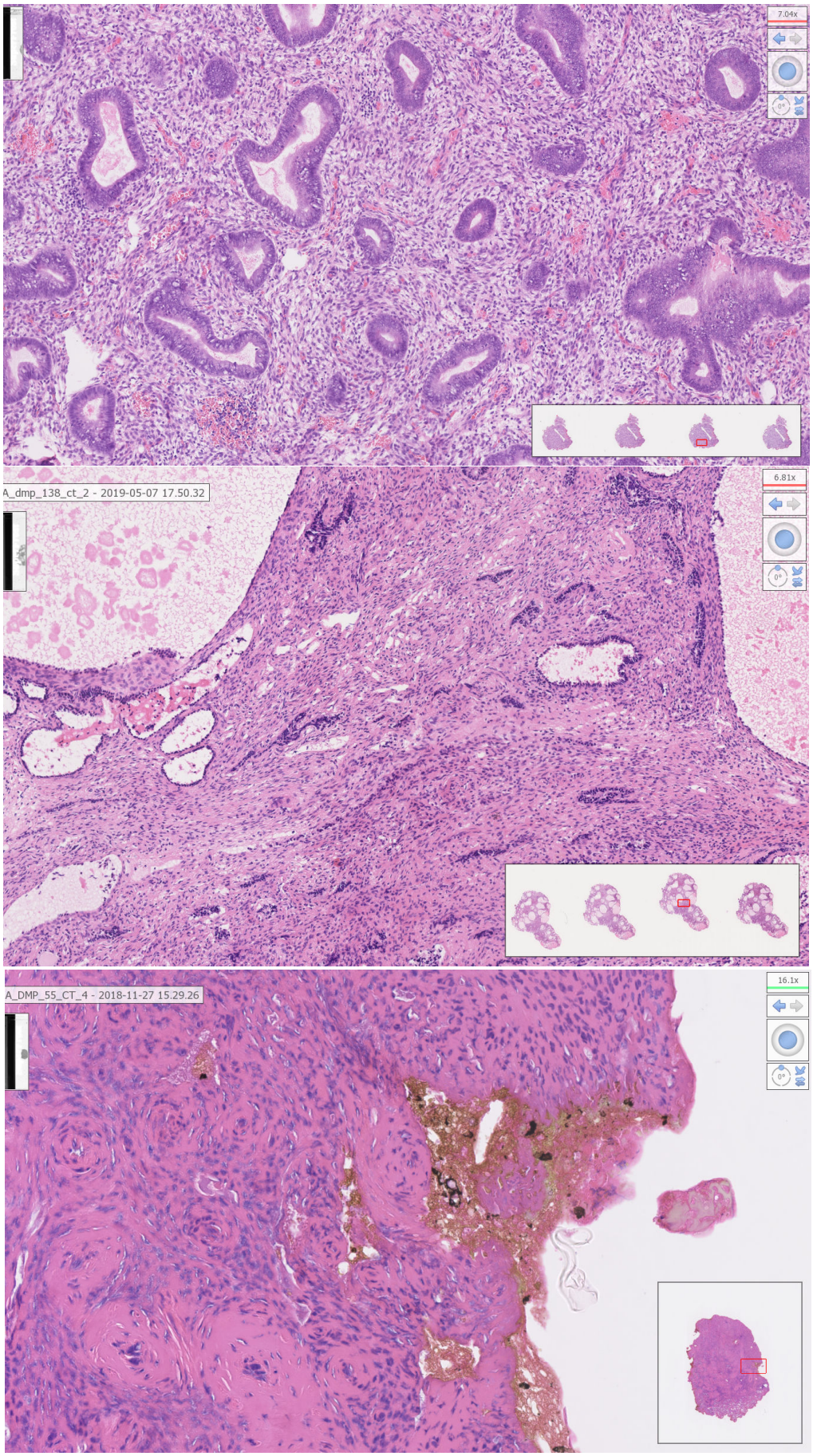


Figure 49. Benign endometrial pipelle samples.
Top oestrogenic effect with some disordered proliferation. Middle image cystic atrophy. Bottom image mainly myometrium with thermal artefact.

4.5.2 Results of conventional diathermy iKnife

Statistical modelling of diathermy iKnife using pipelle samples. Normal vs cancer pre-histopathological QC

The first model used 138 samples (one sample per patient), pre-histopathological QC. Each dot on the PC/LDA plots represented the average spectra for a single sample. Red represents cancer samples, blue normal and green hyperplasia (Figure 50). As can be seen on the PCA plot, no obvious separation is seen for the tissue classes. Hyperplasia samples were evenly distributed between normal and cancer. The confusion table is shown beneath the PC/LDA plots. The overall sensitivity for picking up cancer and specificity were: 63% and 69% respectively. There were no obvious outliers in the model.

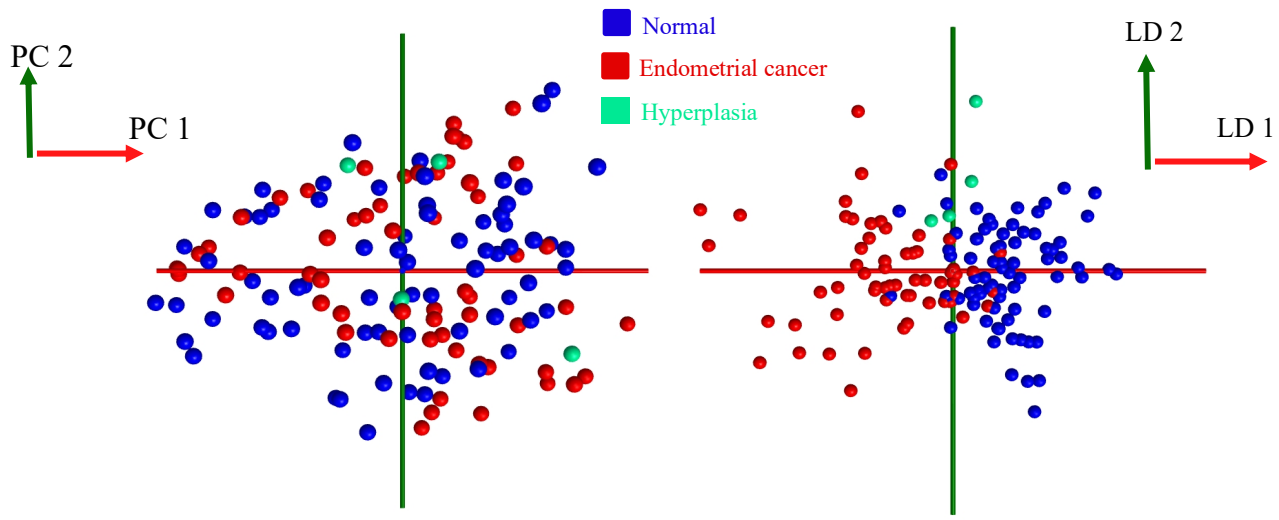


Figure 50. Multivariate analysis of normal vs cancer vs hyperplasia pipelle samples, pre-histological validation, processed with the diathermy iKnife.
Red dots represent endometrial cancer samples, green hyperplasia and blue normal. Each dot represents the average spectra of a single sample. The diagram on the left is a 2D PCA, and right 2D LDA. Principal component one accounted for 36.1% of the variance in the model and principal component two 19.2%. The confusion table is shown below.

		MODEL CLASSIFICATION, n (%)				TOTAL
		CANCER	HYPERPLASIA	NORMAL	OUTLIER	
ACTUAL HISTOLOGY	CANCER	37 (63%)	8 (14%)	14 (24%)	0	59
	HYPERPLASIA	1 (25%)	0	3 (75%)	0	4
	NORMAL	8 (11%)	13 (17%)	52 (69%)	2 (3%)	75

Confusion table for Figure 50

Statistical modelling of the diathermy iKnife using pipelle samples. Normal vs cancer post-histopathological QC

Following histopathological QC, a large number of samples (49) were excluded as histological examination was inadequate due to thermal artefact; 89 samples remained (43 cancer vs 45 normal and 1 hyperplasia). Only one sample per patient was used. Each dot on the PC/LDA plots represents the average spectra for a single sample. Red represents cancer samples, blue normal and purple hyperplasia (Figure 51). Again, no obvious separation is seen for the tissue classes on the PCA. As expected, good separation of tissue classes was seen on the LDA, even better than pre-histology QC. The single hyperplasia sample separated along the 2nd LDA dimension. The overall sensitivity for picking up cancer and specificity were: 79% and 87% respectively, much better than pre-histology QC. More outliers were seen on cross validation.

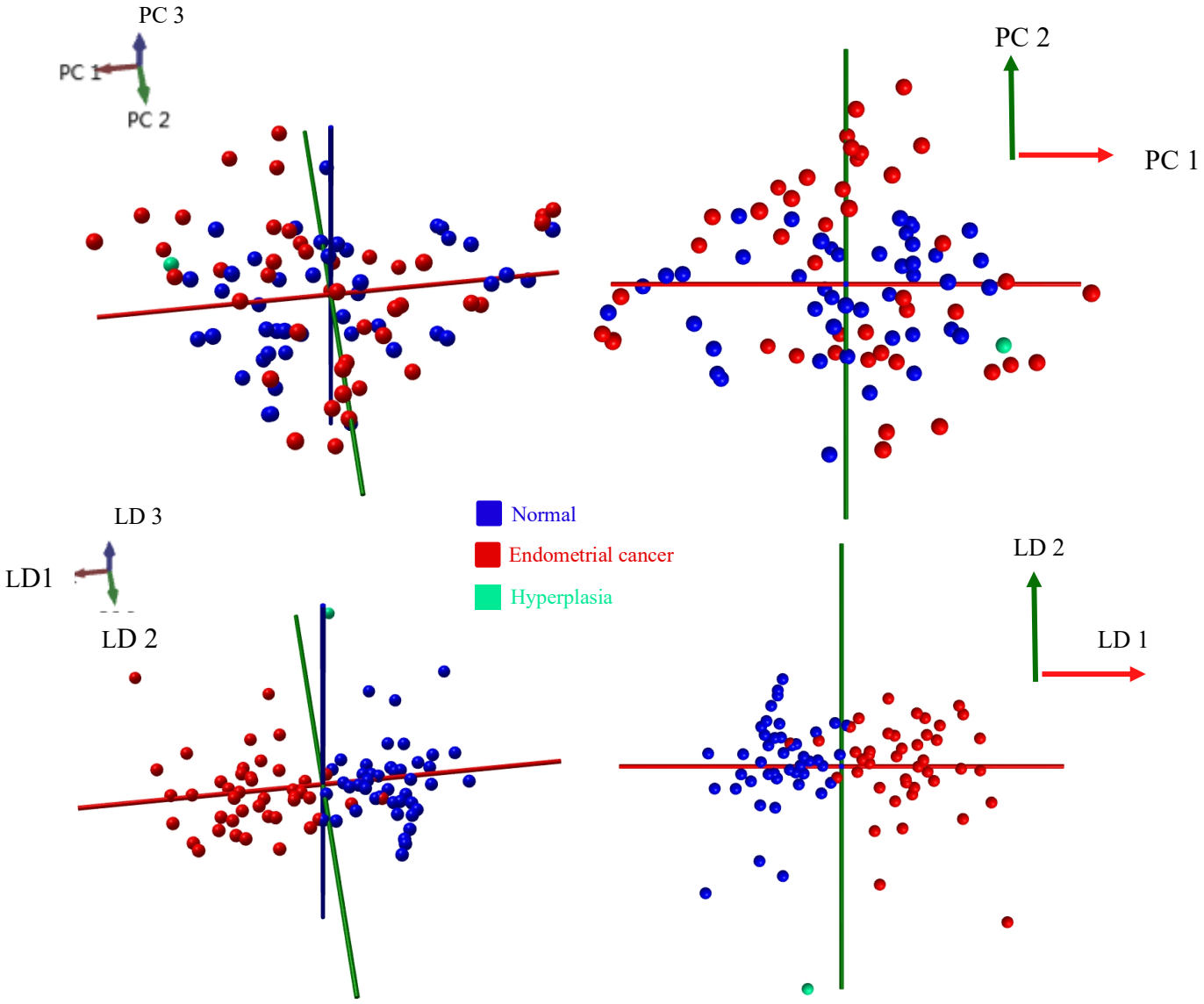


Figure 51. Multivariate analysis of normal vs cancer vs hyperplasia pipelle samples, post-histological validation, processed with the iKnife.
Red dots represent endometrial cancer samples, green hyperplasia and blue normal. Each dot represents the average spectra of a single sample. The diagram on the top left is a 3D PCA, and right 2D PCA. Principal component one accounted for 34.6% of the variance in the model and principal component two 18.7%. Bottom left is a 3D LDA and right 2D LDA. The confusion table is shown below.

		MODEL CLASSIFICATION, n (%)				TOTAL
		CANCER	HYPERPLASIA	NORMAL	OUTLIER	
ACTUAL HISTOLOGY	CANCER	34 (79%)	0	7 (16%)	2 (5%)	43
	HYPERPLASIA	0	0	1 (100%)	0	1
	NORMAL	4 (8%)	0	39 (87%)	2 (4%)	45

Confusion table for Figure 51

Cancer vs normal model. Does removal of the hyperplasia sample improve the accuracy of the model?

Models in which there is only one sample in a tissue class are suboptimal. Additionally, as described in discussion section 4.3 binary models usually have higher diagnostic accuracy. The model was therefore re-run excluding the single case of hyperplasia. Only one sample per patient was used. Each dot on the PCA plots represent the average spectra of a single sample. Red represents cancer samples and blue normal (Figure 52). Again, no obvious separation is seen for the tissue classes on the PCA. The overall sensitivity and specificity were: 81% and 91% respectively. In this model no outliers were seen on cross validation.

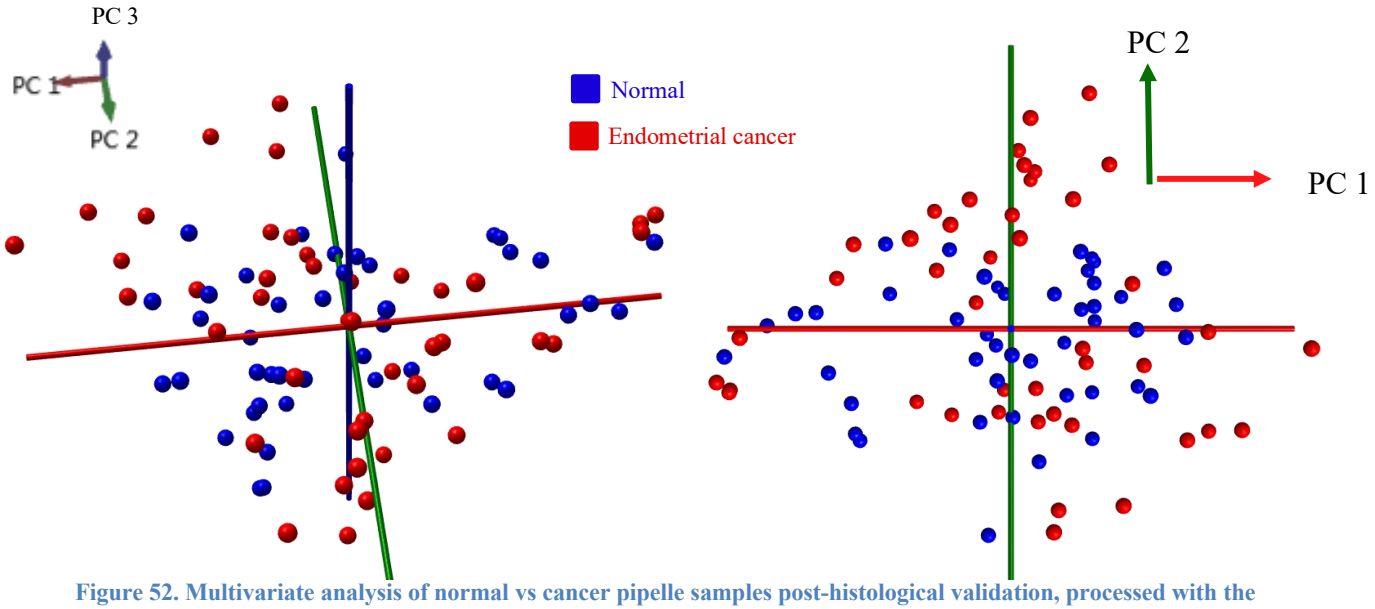


Figure 52. Multivariate analysis of normal vs cancer pipelle samples post-histological validation, processed with the iKnife.
Red dots represent endometrial cancer samples and blue normal. Each dot represents the average spectra of a single sample. The diagram on the left is a 3D PCA and right 2D PCA. Principal component one accounted for 34.1% of the variance in the model and principal component two 18.6%. The confusion table is shown below.

		MODEL CLASSIFICATION, n (%)		TOTAL
		CANCER	NORMAL	
ACTUAL HISTOLOGY	CANCER	35 (81%)	8 (19%)	43
	NORMAL	4 (9%)	41 (91%)	45

Confusion table for Figure 52

Histological subtype differentiation. Type 1 vs Type 2 vs Normal?

As outlined earlier, it is essential for any new technology to correctly identify cancer with a high degree of accuracy, but it is helpful for the type of cancer to be identified pre-operatively to enable better surgical planning. To this end, the samples were reclassified as type 1 and type 2. Almost 4 times as many type 1 cases were present in the model. This is a reflection of the general incidence of type 2 versus type 1 endometrial cancer, with type 1 representing approximately 75% of cases.

Only one sample per patient was used. Each dot on the PC/LDA plots represent the average spectra for a single sample. Red represents type 1 cancer, orange type 2 and blue normal (Figure 53). No clear separation is seen on the PCA plot, but the LDA separates the classes well along PC1. Interestingly, type 1 and type 2 cluster together on the left and normal tissue on the right. Only one cancer sample seems to cluster with the normal samples. This sample only had a low volume of cancer (10%) and the rest of the sample was blood. The overall sensitivity for picking up cancer was 88%, but the diathermy iKnife was not accurate at distinguishing between type 1 vs type 2 cancer.

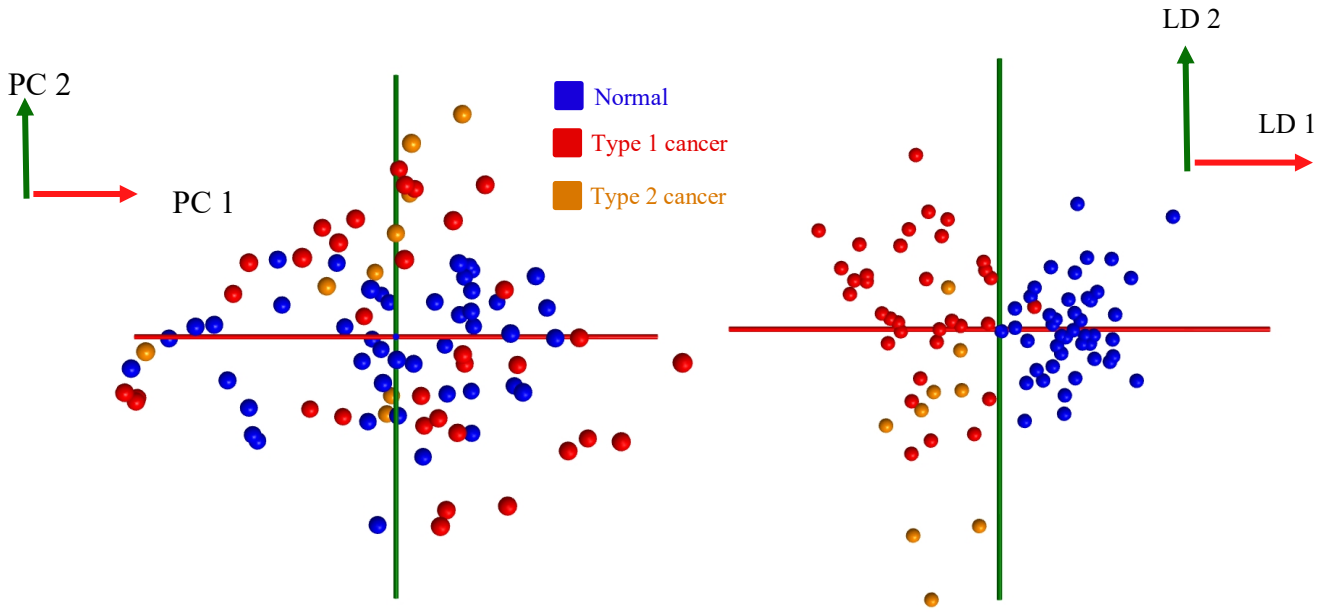


Figure 53. Multivariate analysis of normal vs type 1 vs type 2 cancer pipelle samples post-histological validation, processed with the diathermy iKnife.
Red dots represent type 1 endometrial cancer samples, orange type 2 and blue normal. Each dot represents the average spectra of a single sample. The diagram on the left is a 2D PCA and right 2D LDA. Principal component one accounted for 33.8% of the variance in the model and principal component two 18.9%. The confusion table is shown below.

		MODEL CLASSIFICATION, n (%)			TOTAL
		TYPE 1	TYPE 2	NORMAL	
ACTUAL HISTOLOGY	TYPE 1	22 (65%)	7 (21%)	5 (15%)	34
	TYPE 2	6 (67%)	3 (33%)	0	9
	NORMAL	3 (7%)	1 (2%)	41 (91%)	45

Confusion table for Figure 53

Model type 1 vs normal

In the tissue bank model, the overall model with the best accuracy was the binary *normal vs type 1 cancer*. In an effort to optimise the pipelle model type 1 vs normal samples were analysed. Only one sample per patient was used. Each dot on the PCA plots represents the average spectra for a single sample. Red represents type 1 cancer and blue normal (Figure 54). The overall sensitivity, specificity, positive predictive value (PPV) and negative predictive value (NPV) were: 79%, 96%, 93% and 86% respectively.

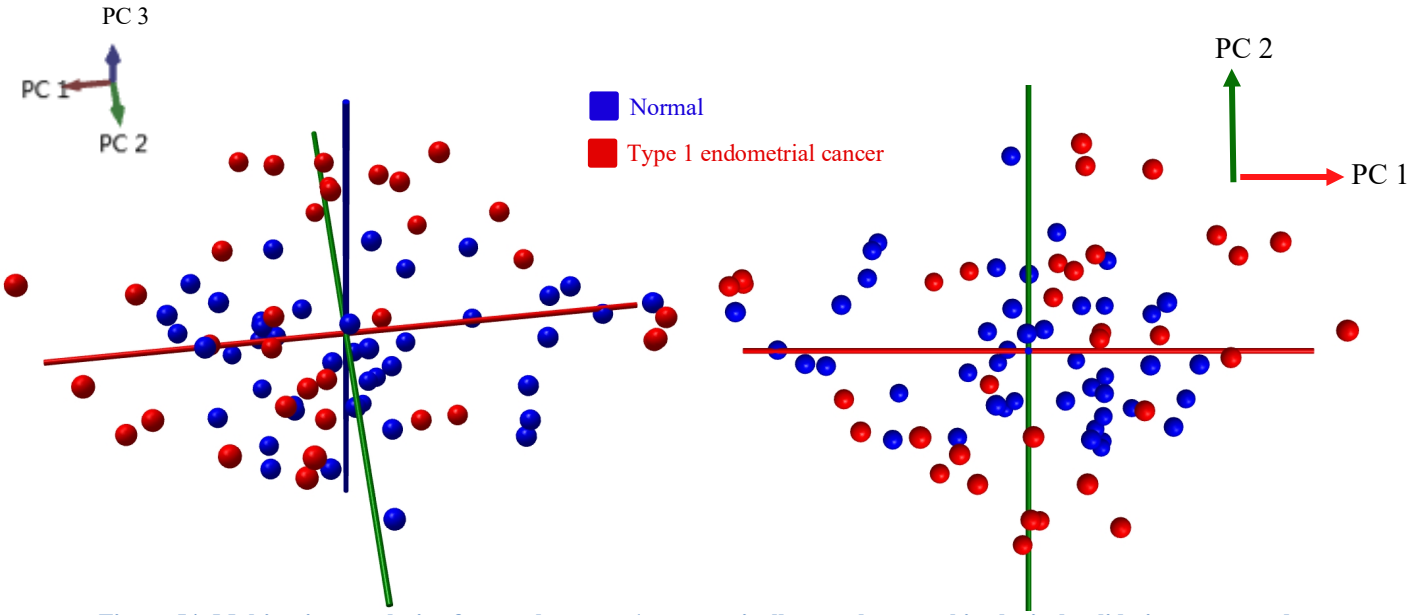


Figure 54. Multivariate analysis of normal vs type 1 cancer pipelle samples, post-histological validation, processed with the diathermy iKnife.
Red dots represent endometrial cancer samples and blue normal. Each dot represents the average spectra of a single sample. The diagram on the left is a 3D PCA and right 2D PCA. Principal component one accounted for 35.8% of the variance in the model and principal component two 16.7%. The confusion table is shown below.

		MODEL CLASSIFICATION, n (%)		TOTAL
		TYPE 1	NORMAL	
ACTUAL HISTOLOGY	TYPE 1	27 (79%)	7 (21%)	34
	NORMAL	2 (4%)	43 (96%)	45

Confusion table for Figure 54

Does fresh and frozen samples make a difference?

Overall, there has always been some contention as to whether the fresh-thaw cycle influences the phospholipid signature of cancer and normal tissue and consequently whether it is acceptable to combine both fresh and frozen samples into the same model. To answer this question a model was created with both cancer and normal samples reclassified according to whether they were processed fresh or snap frozen first. As can be seen on the PCA, there is no obvious separation of tissue classes (Figure 55). The samples are separated into tissue specific clouds of data on the LDA plot. Normal samples separated on the left and cancer samples on the right across LD 1, meanwhile fresh-frozen separated along the Y-axis (LD component 2). The confusion table also demonstrates a greater similarity between tissue class compared to fresh/frozen characteristic. For example, of the 28 frozen normal samples, the model classified 68% (19/28) correctly. Most of the incorrectly classified samples were fresh normal tissue (21%) not cancer. This is reassuring and confirms that it is reasonable to amalgamate both fresh and frozen tissue into the model.

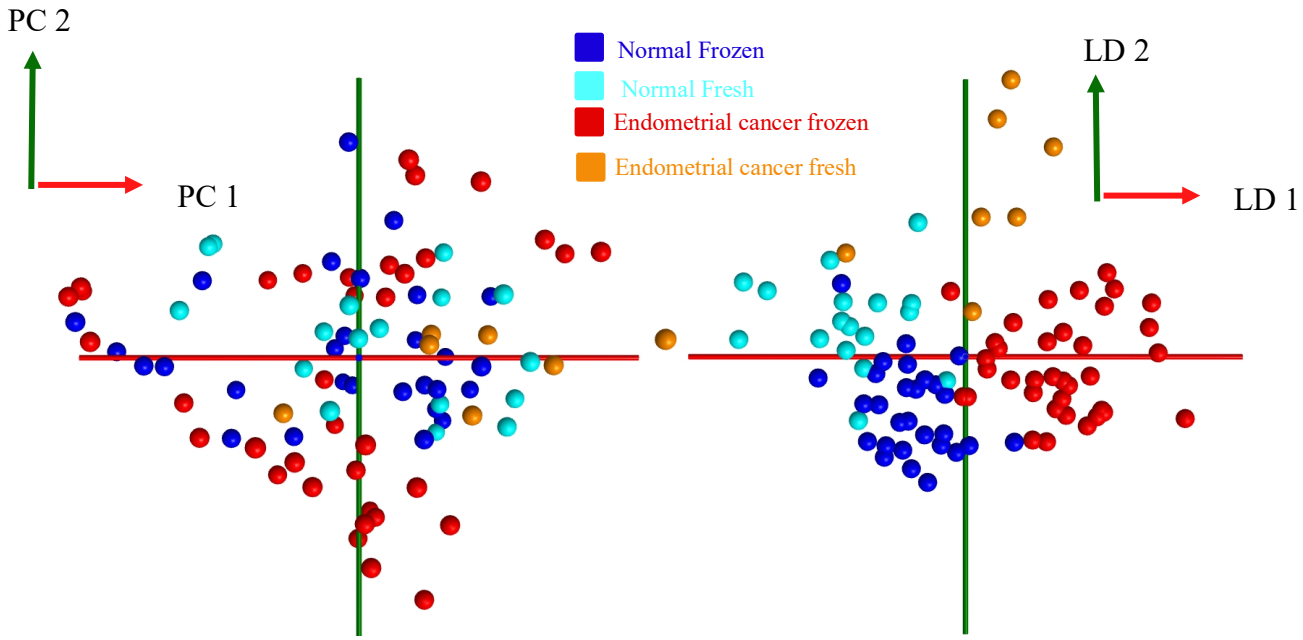


Figure 55. Multivariate analysis of normal vs cancer samples processed with the diathermy iKnife, separated according to whether processed fresh or snap-frozen initially and thawed.
Red and orange dots represent endometrial cancer samples and blue samples normal. Each dot represents the average spectra of a single sample. The diagram on the left is a 2D PCA and right 2D LDA. Principal component one accounted for 34.0% of the variance in the model and principal component two 19.2%. The confusion table is shown below.

			MODEL CLASSIFICATION, n (%)				TOTAL
			CANCER		NORMAL		
			FRESH	FROZEN	FRESH	FROZEN	
ACTUAL HISTOLOGY	CANCER	FRESH	4 (57%)	2 (29%)	1 (14%)	0	7
		FROZEN	1 (2%)	26 (58%)	1 (2%)	8 (18%)	45
	NORMAL	FRESH	1 (6%)	1 (6%)	13 (76%)	2 (12%)	17
		FROZEN	0	3 (11%)	6 (21%)	19 (68%)	28

Confusion table for Figure 55

In addition, 2 separate models for samples processed (1) fresh and (2) samples processed after initially being frozen were created. The frozen model had a sensitivity: 86% and specificity 89%; whilst the fresh had a sensitivity 57% and specificity 88%. Unsurprisingly, the number of samples were markedly reduced, particularly the fresh model, accounting for the reduced diagnostic rate. The frozen model had a comparable diagnostic accuracy to the *iKnife: normal vs cancer model*.

4.5.3 Results CO2 laser

CO2 Laser spectra

The CO2 laser was able to produce spectra of much better quality, and from much smaller tissue samples compared to the diathermy iKnife. For example, Figure 56 below depicts the spectra produced by processing the same tiny sample of normal endometrial tissue with the CO2 laser and the diathermy iKnife. The top image was processed with the iKnife and has a wondering baseline and no true discernible burn peaks (later excluded from all the models as it unsurprisingly failed the AMX spectrum analyser QC). Conversely, the CO2 laser spectra from the same pipelle biopsy sample had much less background noise and true burn peaks were identified, of higher intensity.

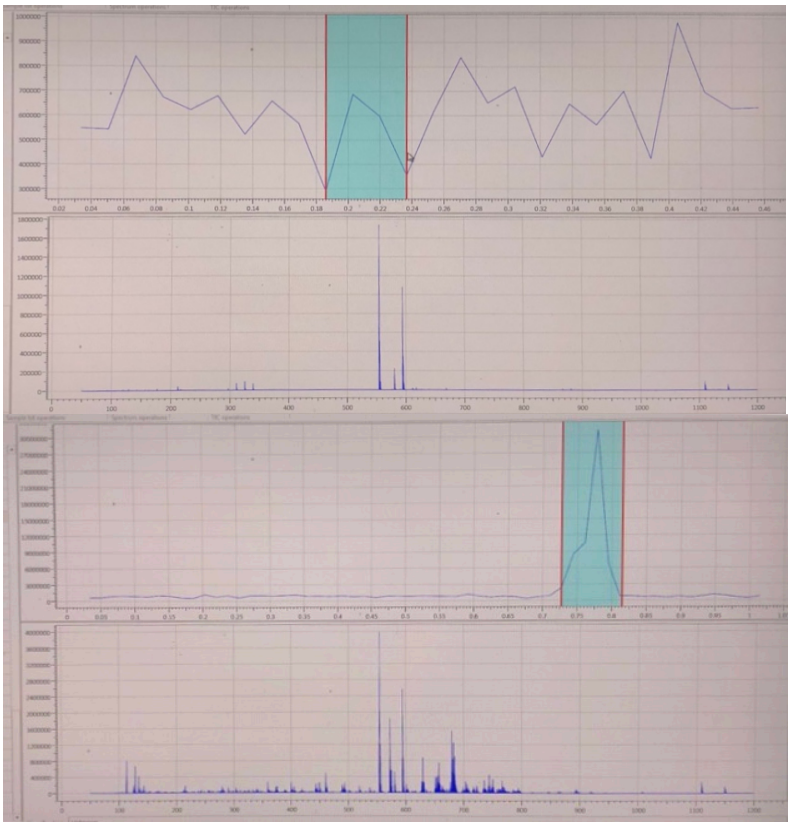


Figure 56. Chromatogram and corresponding spectra of the same sample processed with the conventional diathermy iKnife (above) and CO2 laser iKnife (below).

Statistical modelling using pipelle samples normal vs cancer pre-histopathological QC

The coupling of the CO2 laser with the REIMS interface is a relatively new development. As discussed in section 4.3, CO2 laser has more focussed energy, less tissue destruction, and a cleaner spectrum (as evidenced by the fact that all laser spectra passed quality control). A new model was created using samples processed by the CO2 laser only. PCA and LDA plots are shown below with each dot representing the average spectra of a single sample (Fig 57). The overall sensitivity and specificity were: 74% and 69% respectively. While only one outlier was seen on cross validation, multiple outliers appear on the PC/LDA plots which is thought to be due to incorrect tissue classification pre-histopathological QC.

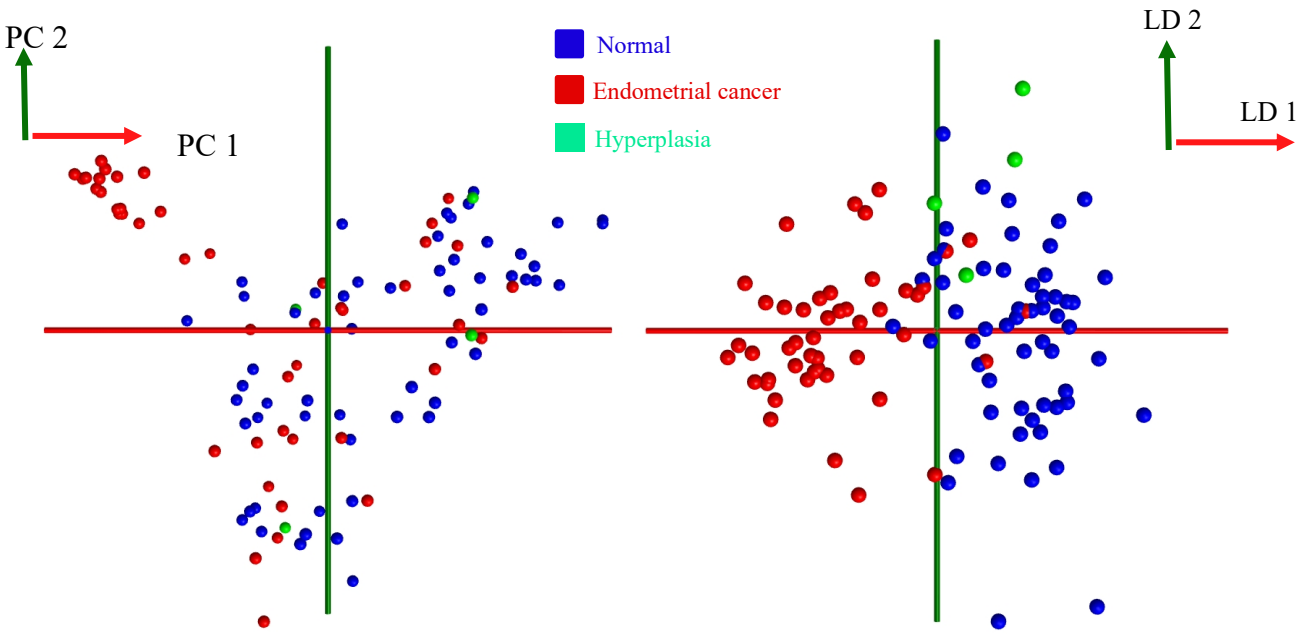


Figure 57. Multivariate analysis of normal vs cancer vs hyperplasia pipelle samples, pre-histological validation, processed with the CO2 laser.
Red dots represent endometrial cancer samples, green hyperplasia and blue normal. Each dot represents the average spectra of a single sample. The diagram on the left is a 2D PCA, and right 2D LDA. The confusion table is shown below.

		MODEL CLASSIFICATION, n (%)				TOTAL
		CANCER	HYPERPLASIA	NORMAL	OUTLIER	
ACTUAL HISTOLOGY	CANCER	35 (74%)	4 (9%)	8 (17%)	0	47
	HYPERPLASIA	0	1 (25%)	3 (75%)	0	4
	NORMAL	4 (7%)	12 (21%)	39 (70%)	1 (2%)	56

Confusion table for Figure 57

Statistical modelling using pipelle samples normal vs cancer vs hyperplasia post-histopathological QC

39% of samples (42/107) were excluded following histopathological validation. This is in keeping with the large number of samples excluded following histological QC in the tissue bank model. The 65 remaining samples were classified as cancer (all types), hyperplasia and normal. Each dot on the PCA plot represents the average spectra of a single sample. Red represents cancer samples, blue normal and green hyperplasia (Figure 58). Again, no obvious separation is seen for the tissue classes on the PCA.

The overall sensitivity and specificity were: 86% and 89% respectively. This model has the highest sensitivity compared to all models, including the iKnife models, despite its relatively small sized dataset and three tissue class groups.

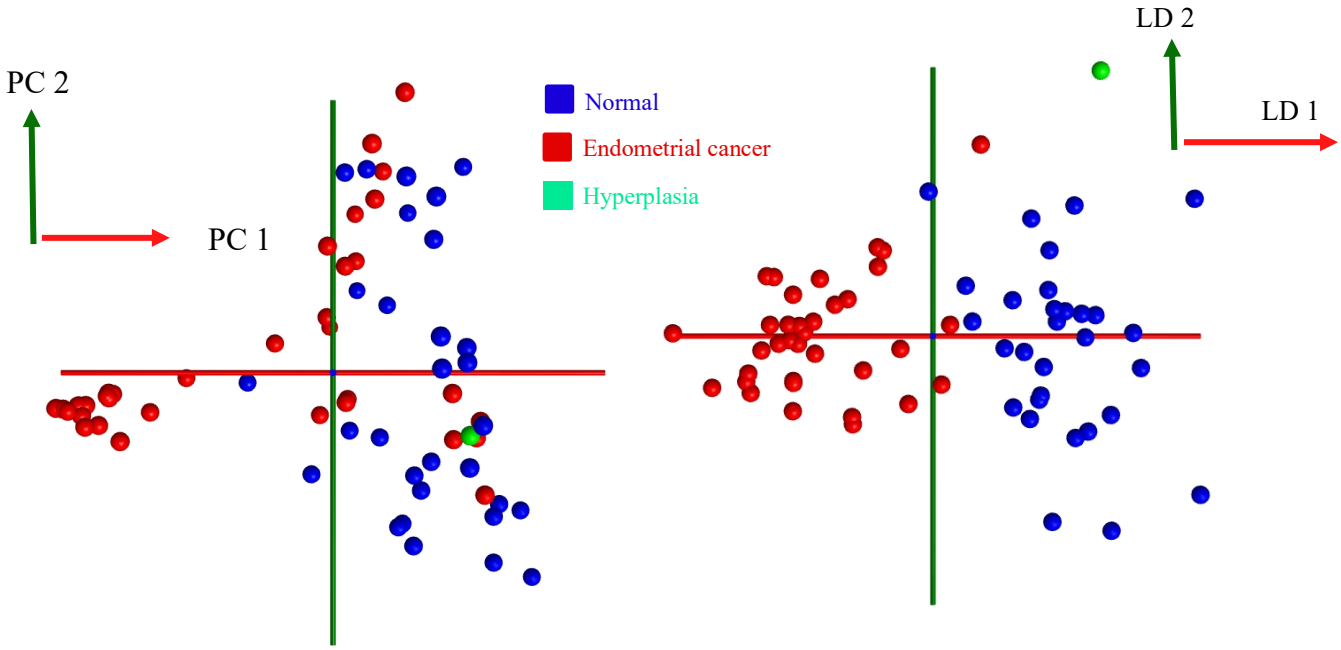


Figure 58. Multivariate analysis of normal vs cancer vs hyperplasia pipelle samples, post-histological validation, processed with the CO2 laser.
Red dots represent endometrial cancer samples, green hyperplasia and blue normal. Each dot represents the average spectra of a single sample. The diagram on the left is a 2D PCA, and right 2D LDA. Principal component one accounted for 42.9% of the variance in the model and principal component two 27.6%. The confusion table is shown below.

		MODEL CLASSIFICATION, n (%)				TOTAL
		CANCER	HYPERPLASIA	NORMAL	OUTLIER	
ACTUAL HISTOLOGY	CANCER	30 (86%)	0	4 (11%)	1 (3%)	35
	HYPERPLASIA	0	0	1 (100%)	0	1
	NORMAL	3 (10%)	0	26 (90%)	0	29

Confusion table for Figure 58

Statistical modelling using pipelle samples normal vs cancer post-histopathological QC, hyperplasia excluded

As can be seen above, only a single sample remains within the hyperplasia class. This inevitably reduces the robustness of the model. This sample was excluded, and the model rerun. Each dot on the PCA plot represented the average spectra of a single

sample. Red represents cancer samples and blue normal (Figure 59). The overall sensitivity, specificity, PPV and NPV were: 85%, 93%, 94% and 85% respectively.

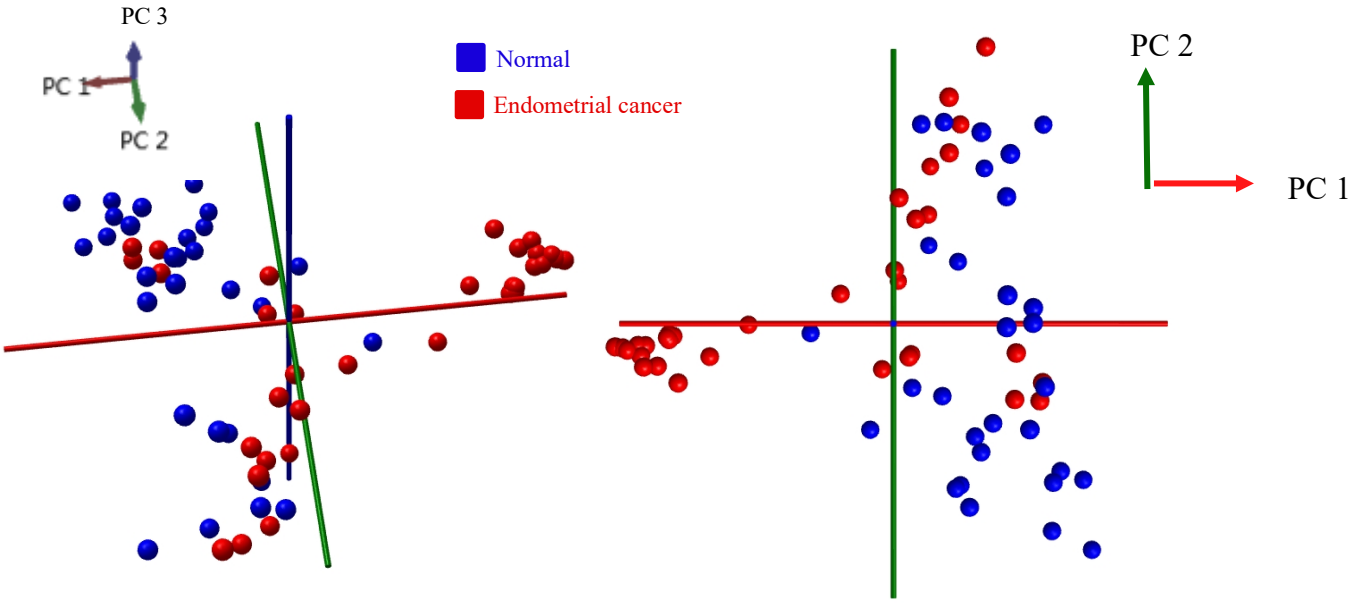


Figure 59. Multivariate analysis of normal vs cancer pipelle samples, post-histological validation, processed with the CO2 laser.
Red dots represent endometrial cancer samples and blue normal. Each dot represents the average spectra of a single sample. The diagram on the left is a 3D PCA, and right 2D PCA. Principal component one accounted for 42.7% of the variance in the model and principal component two 27.7%. The confusion table is shown below.

		MODEL CLASSIFICATION, n (%)		TOTAL
		CANCER	NORMAL	
ACTUAL HISTOLOGY	CANCER	29 (85%)	5 (15%)	34
	NORMAL	2 (7%)	28 (93%)	30

Confusion table for Figure 59

Following on from this CO2 pipelle model, a model was created to see if the different energy modalities (CO2 laser and diathermy iKnife) can be combined together. The results are shown in the Appendix. In summary, the conclusion is they cannot.

Furthermore, the results of the liquid probe are reported in the Appendix. As the dataset for the liquid probe is so small, no firm conclusions can be made. A model was also created to see if the different energy modalities (CO2 laser and diathermy iKnife and liquid probe) can be combined together, and they cannot either.

Finally, models were created to see if pipelle and tissue bank samples can be combined (in Appendix). Two models were created, the first with samples only processed with the standard diathermy iKnife, and the second pipelle samples processed with CO2 laser. In summary, the datasets are too different to combine.

4.5.4 Results - Learning curve of best model

The diagram below shows the learning curve, based on 35 normal and 35 cancer samples using the model *type 1 cancer versus normal (no hyperplasia).* The partition ratio was 90% which means that 32 samples (per class) was the size of the largest training set; all remaining samples formed the 'test' set.

The algorithm started with 5 observations per class and increased by increments of 1 sample per class each time. For each training set size, all of the observations are randomly partitioned 20 times ('resampled iterations') in order to get an estimate of the classification performance using different observations for training and testing. The mean accuracy, sensitivity and specificity were determined for each iteration and plotted on the learning curve (Figure 60). The pink boundaries represent ± 1 standard deviation of the accuracy. The 'curve' shows a gradual increase in diagnostic accuracy from 70±10% to approximately 80±10% when increasing the sample size from 5 to 32. It can also be seen that the curve has not plateaued yet, suggesting that an increase in sample size will increase the diagnostic accuracy further.

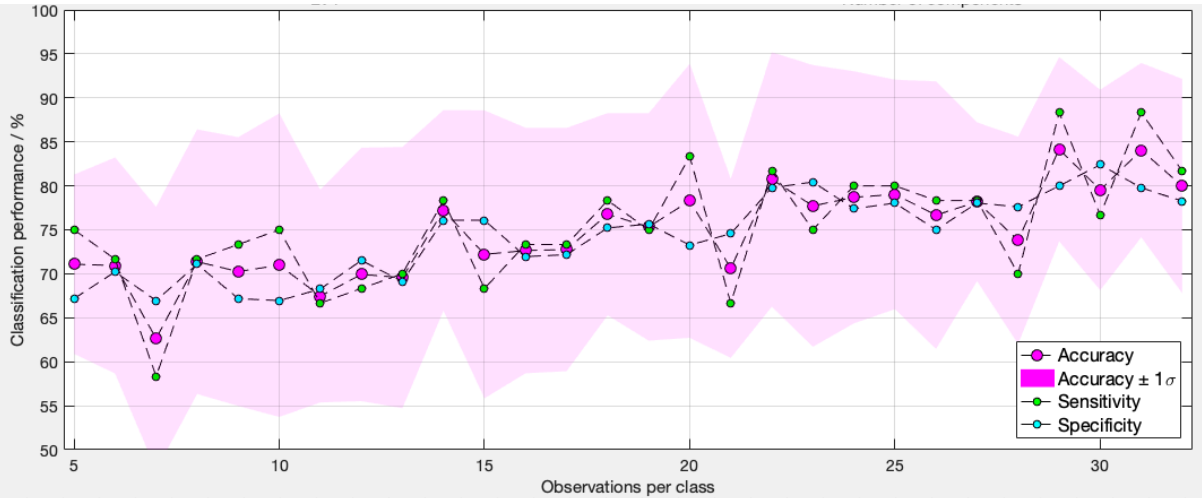


Figure 60. Learning curve of *type 1 cancer versus normal (no hyperplasia) iKnife model* based on 35 normal and 35 cancer samples.
The algorithm starts with 5 normal and 5 cancer samples and increases by increments of one. The overall diagnostic accuracy (pink dots) increase from 70±10% to approximately 80±10% when the sample size increases from 5 to 32.

4.5.5 Results - Choosing the best model

Table 17 below summarises the diagnostic performance of each PC/LDA model using LPO cross validation. The best conventional diathermy iKnife model is *type 1 cancer versus normal (no hyperplasia)* and the best CO2 laser iKnife model is *cancer versus normal (no hyperplasia)*. As always, there is a trade-off between sensitivity and specificity. The CO2 laser model has the highest sensitivity, ideal for cancer detection.

As mentioned in methods sections, after spectral QC, creation of PCA and LDA plots and cross validation using the PC/LDA model in OMB AMX, all the data was imported into Matlab. In Matlab the user can choose the mathematical algorithms used to separate samples e.g. MMC or PLS, and classification technique e.g. Mahalanobis, nearest neighbours and centroid. This produces models with slightly different diagnostic accuracies on cross validation. For example, the *type 1 cancer versus normal (no hyperplasia)* using LPO cross validation and MMC centroid model has an even higher sensitivity and specificity than the PC/LDA model (82% and 98% respectively). MMC models tended to improve specificity at expense of sensitivity, and PLS based models improve sensitivity at the expense of specificity, but overall had worse diagnostic accuracies.

As seen on the learning curve, more samples improve the accuracy of the model. Therefore, models that combined the tissue bank samples and pipelle samples had better diagnostic performance, purely a reflection of sample number. Samples tended to classify with sampling method (pipelle vs tissue bank) rather than malignancy status (see Appendix). Therefore, ideally, these two spectral reference libraries should not be combined, but, instead more pipelle samples would be needed to further improve the diagnostic performance.

MODEL	NUMBER OF SAMPLES	DIAGNOSTIC PERFORMANCE				OVERALL ACCURACY (%)
		SENSITIVITY (%)	SPECIFICITY (%)	PPV (%)	NPV (%)	
Diathermy iKnife: Normal vs cancer vs hyperplasia. Pre-histological QC	138	63	69	80	75	64
Diathermy iKnife: Normal vs cancer vs hyperplasia. Post-histological QC	89	79	87	89	83	82
Diathermy iKnife: Normal vs cancer (hyperplasia excluded)	88	81	91	90	84	86
Diathermy iKnife: Type 1 cancer vs normal	79	79	96	93	86	89
Diathermy iKnife Frozen: cancer vs normal	64	86	89	91	83	88
Diathermy iKnife Fresh: cancer vs normal	24	57	88	67	88	79
CO2 laser: Normal vs cancer vs hyperplasia. Pre-histological QC	107	74	70	90	78	70
CO2 laser: Normal vs cancer vs hyperplasia. Post-histological QC	65	86	89	91	84	86

CO2 laser: Normal vs cancer Post-histological QC	64	85	93	94	85	89
Combined pipelle CO2 and diathermy iKnife (cancer vs normal)	153	79	89	86	81	84
Combined pipelle diathermy iKnife (cancer vs normal) and tissue bank	178	83	97	96	86	90
Combined pipelle CO2 laser (cancer vs normal) and tissue bank	156	84	96	96	86	90

Table 17. Summary table diagnostic performance of all pipelle models.

PPV = positive predictive value. NPV =negative predictive value.

4.5.6 Results – which m/z values are important? Loading plots, univariate analysis and volcano plot.

The loading plots for PC1 of the two best models: the diathermy iKnife model (*type 1 cancer versus normal),* and the CO2 laser model (*cancer versus normal)* are depicted in Figure 61. These only provide an overall visual assessment of the significant m/z values and Kruskal-Wallis or ANOVA analysis must be performed to confirm these. Interestingly, very few m/z values after >800 m/z account for the variance in PC1, suggesting that the lipids most responsible for separation of cancer and benign samples are in the 600-800 range.

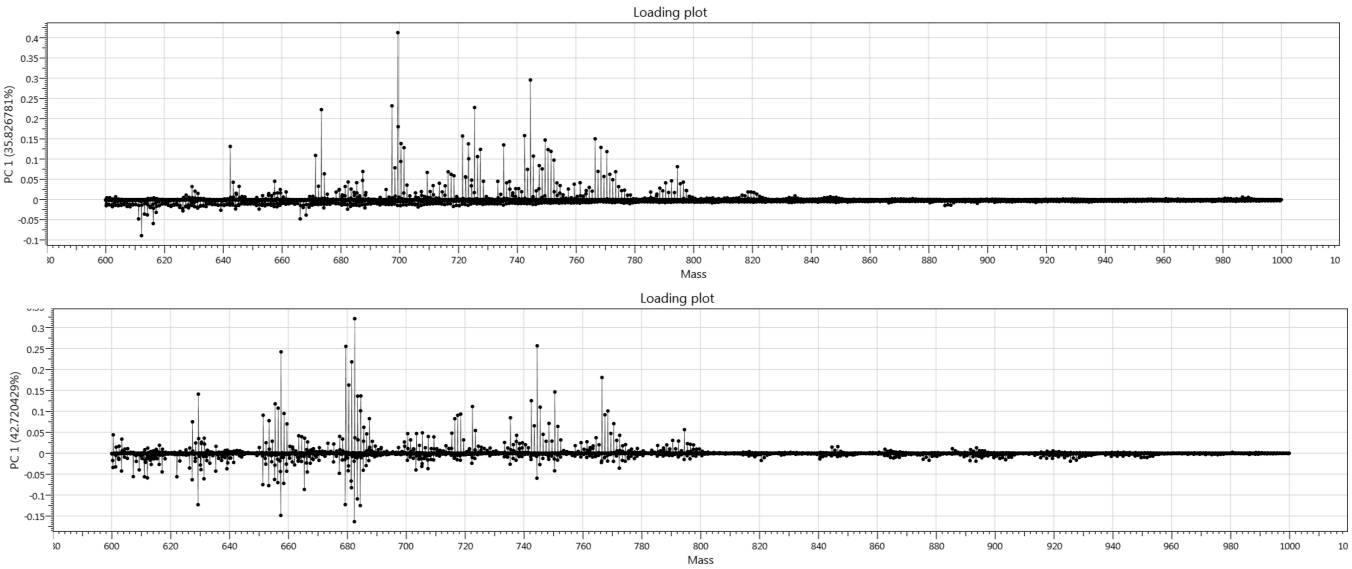


Figure 61. Loading plot of 2 best pipelle models.
Top diagram is the loading plot of Principal component 1, for the iKnife model: type 1 cancer versus normal, no hyperplasia. The bottom diagram is the loading plot of Principal component 1, for the CO2 laser model cancer versus normal, no hyperplasia.

Using, Matlab, Kruskal-Wallis analysis was performed to confirm the identify the specific m/z values responsible for the separation of cancer and normal samples on the LDA model. A -log2fold change of 1, in addition to a q value of 0.001 was used as a threshold to reduce the number of significant values. The m/z values can be seen graphically as a volcano scatter plot for both the two best models: diathermy iKnife *type 1 cancer versus normal (no hyperplasia)* and the CO2 laser iKnife model *cancer versus normal*, or individually as box plots for each m/z value (Figure 62). As can be seen in the volcano plots many more significant m/z values are present in the CO2 laser model compared to the diathermy iKnife model, with some overlap in between. There are also three m/z values with overlapping significance between the tissue bank model and the pipelle models, namely m/z: 671.45, 685.45 and 699.55.

Table 18 below shows the top 30 m/z values responsible for the separation of classes and the tentative lipid(s) involved. The m/z peaks were shown to 2 decimal places and presented the database in negative ion mode. LipidMaps proposes deprotonated ions [M-H]- and chlorinated ions [M+Cl]- and the deamnionated ion [M-NH3]-. As can be seen in the table, a number of different lipids have been upregulated in endometrial cancer including ceramides and the phospholipids: PAs, PEs and PSs. Meanwhile, PCs, PIs and PGs are more frequently downregulated in endometrial cancer.

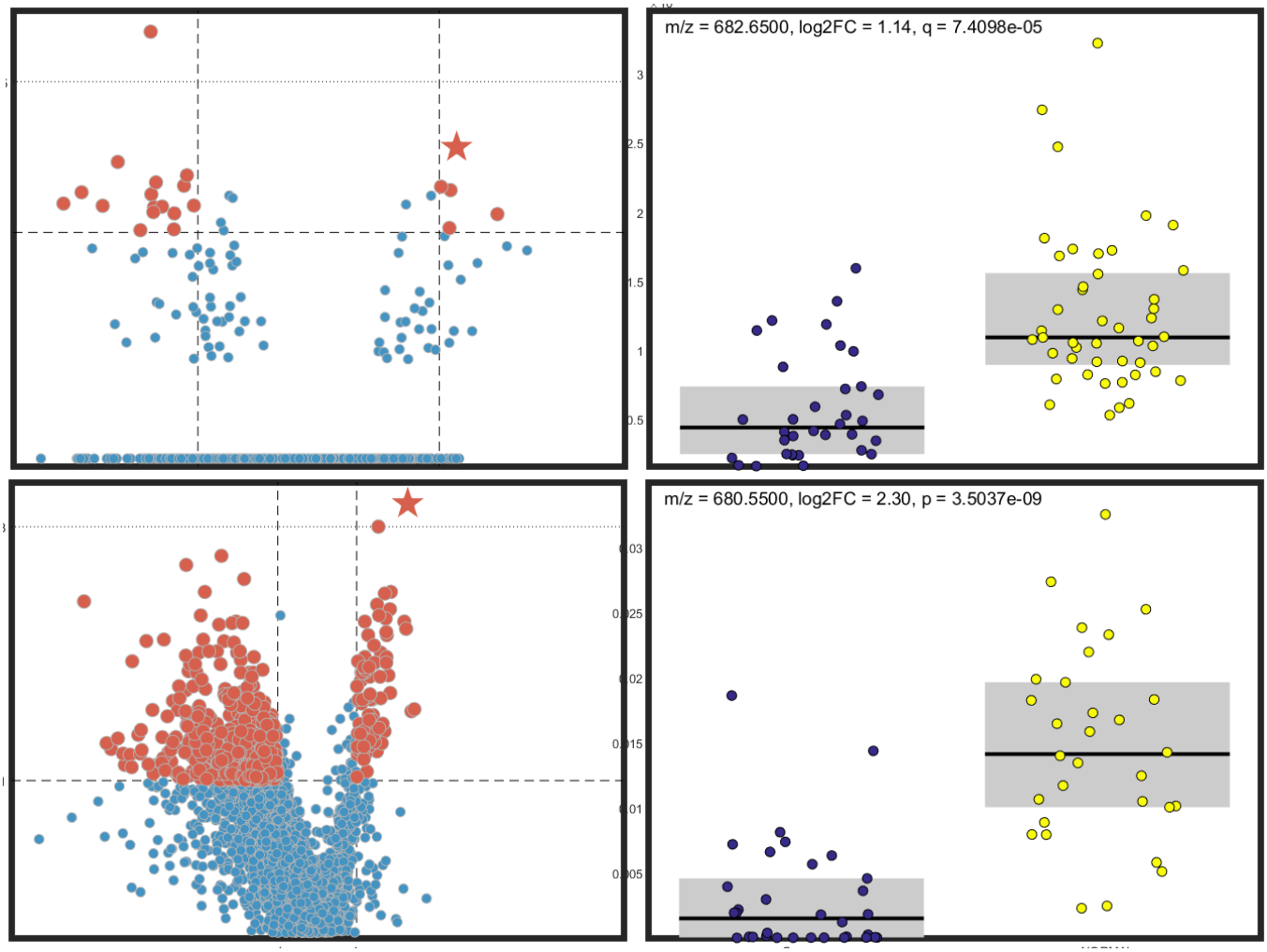


Figure 62. Volcano plot of iKnife (top) and CO2 laser models (bottom). Box plot to the right of each volcano plot depicts the single m/z value which is starred on the volcano plot.

Model used	m/z value	Log2FC	Q value	Potential Lipids	Ion
CO2 laser	600.55	1.29	1.37x10-6	Cer 36:1;O2	[M+Cl]-
	648.55	-3.33	5.66x10-5	PC 26:0	[M-H]-
	658.45	-5.92	1.32x10-4	PE 30:2	[M-H]-
	658.55	1.44	2.18x10-6	Cer 40:0;O2	[M+Cl]-
	670.55*	1.21	7.38x10-7	Cer 40:2;O3	[M+Cl]-

				Cer 42:0;O	[M+Cl]-
	671.45*	1.94	3.45x10-7	PA 34:2	[M-H]-
	678.45	1.87	1.92x10-7	PS 28:0 PE 28:2;O3	[M-H]- [M-H]-
	679.55	2.21	7.38x10-7	PG O-30:0 PA O-36:5	[M-H]- [M-H]-
	682.55	1.52	3.41x10-7	Cer 42:0;O4 Cer 42:2;O2 PE O-30:1	[M-H]- [M+Cl]- [M+Cl]-
	685.45*	1.37	6.70x10-7	PG 30:4	[M-H]-
	692.55	2.26	1.03x10-6	PS O-30:0	[M-H]-
	699.55*	1.28	3.40x10-7	PA 36:2	[M-H]-
	703.55	1.77	1.36x10-6	PA 36:0 PA O-38:7 PG O-32:2	[M-H]- [M-H]- [M-H]-
	725.45	1.75	1.19x10-6	PI 26:0 PA 38:3 PG 30:2	[M-H]- [M-H]- [M+Cl]-
	786.55	1.57	5.59x10-7	PS 36:2 PE 40:8	[M-H]- [M-H]-
	877.65	-3.89	2.48x10-4	PG 44:6	[M-H]-
	930.75	-4.74	4.07x10-4	PC 44:3	[M+Cl]-
Overlap CO2 laser and diathermy iKnife	680.55	1.48	5.72x10-4	Cer 42:1;O4 CerP 36:1;O2	[M-H]- [M+Cl]-
	706.55	2.47	3.94x10-5	PS 30:0	[M-H]-
	786.45	1.08	8.75x10-4	PE 40:8 PS 36:2 PC 34:5	[M-H]- [M-H]- [M+Cl]-

Diathermy iKnife model	682.65	1.14	7.41x10-5	Cer 42:0;O4 Cer 42:2;O2	[M-H]- [M+Cl]-
	683.65	1.09	2.75x10-4	FA 44:0	[M+Cl]-
	818.65	1.01	2.47x10-4	PS 38:0 PE 42:6	[M-H]- [M-H]-
	823.55	-1.48	9.04x10-5	PA 40:0 PG 40:5	[M+Cl]- [M-H]-
	859.55	-1.66	8.79x10-5	PG 42:1 PI 36:3	[M-H]- [M-H]-
	863.55	-1.88	1.64x10-4	PI 36:1 PG 40:3	[M-H]- [M+Cl]-
	864.55	-1.52	2.07x10-4	PC 40:8 PS 42:5	[M+Cl]- [M-H]-
	887.55	-1.79	4.08x10-4	PG 42:5 PI 38:3	[M+Cl]- [M-H]-
	888.55	-1.96	9.21x10-5	PC 42:10 PE 44:3	[M+Cl]- [M+Cl]-
	889.55	-2.11	2.62x10-5	PI 38:2 PG 42:4	[M-H]- [M+Cl]-

Table 18. Top 30 significant m/z values and tentative lipid assignments.

Kruskal-Wallis was used to identify the most significant m/z values responsible for the separation of the diathermy iKnife and CO2 laser model. The q value (adjusted p-value for multiple testing), along with log fold change score are recorded. The tentative lipid assignments or lipid differentials were derived from LipidMaps and are recorded alongside the m/z value. M/z values in black are more upregulated significantly compared to normal tissue, and m/z values in red are significantly downregulated in caner compared to normal endometrium. * = m/z value significant in tissue bank model too.

4.5.7 Discussion

Key findings

The overall diagnostic performance of the new pipelle model using REIMS technology is very good, with sensitivities of over 80% despite the relatively small sample size and corresponding reference spectral library. It can be seen on the learning models (Figure 60) that further increases in the size of the spectral library will increase the accuracy further, and that the greatest diagnostic performance has yet to be reached. The

diagnostic accuracies are now comparable to that of the tissue bank model. This also confirms that the tissue bank samples are very different to the pipelle samples with respect to the phospholipid signatures, and that the two datasets cannot be combined.

This study provides hope, that the iKnife could be used in the RAC to provide POC testing, possibly in combination with other risk factor and scan-based features as part of a multivariate model. The biggest advantage of the iKnife is its speed, able to provide a result within 1.8seconds as oppose to 2 weeks [196]. It also has a very high positive predictive value; which means, that in clinical practice, more than 90% of women who have a cancer diagnosis using the iKnife will indeed have cancer. This enables surgery to be booked and pre-operative investigations to be instigated straight away, minimising any treatment delays. Thereby reducing patient distress and unnecessary clinic appointments.

Approximately two thirds of samples were processed with the iKnife using the CO2 laser energy source. As this method had not been validated, where sufficient tissue remained, samples were also processed with the standard diathermy iKnife. As described in Genangeli group, the CO2 laser provided cleaner cuts, with higher quality spectra and less background noise [348]. Unlike the conventional diathermy iKnife which had 15% (70/453) of spectra removed due to poor quality; the CO2 laser had zero spectra removed.

Additionally, the CO2 laser burns are more superficial, with less thermal damage; making histological validation much easier. The diagnostic accuracy of the CO2 laser also appeared superior to the iKnife diathermy despite the smaller dataset and 3 tissue classes (normal / cancer / hyperplasia). The subtler differences in phospholipid signatures seen in the cleaner CO2 laser spectral library may be the reason for this. As seen in Fig 103 there is a large variation in the phospholipid pattern in the CO2 laser and diathermy iKnife spectra, even amongst the same sample set – thus it is not ideal to combine both sets of data into the same model. This is contrary to the data presented by the breast iKnife group, which tested the breast diathermy model with the CO2 laser using a modest 10 tissue samples [353].

Conversely, as observed in the tissue bank model, and in Fig 55, fresh and snap frozen tissue samples can be combined together in the same model. Fresh and snap frozen

samples of the same tissue group appeared to have similar phospholipid signatures and appeared close together on the LDA plots. In Fig 55 tissue class separated along the LD component 1 (x-axis), meanwhile fresh-frozen separated along LD component 2 (Y-axis). On breakdown of the cross-validation results, samples had a preference to classify with their correct tissue group as oppose to the fresh-frozen characteristic. This should be interpreted with caution as the dataset is small, also a moderate proportion of the frozen cancer samples classified with frozen normal tissue.

Histological validation improved the diagnostic accuracy of both the conventional diathermy iKnife and the CO2 laser pipelle models, but at the cost of excluding a large proportion of samples, 35% and 39% respectively. The CO2 laser would be preferable to use in future studies due to its improved diagnostic accuracy rate and less tissue destruction effect. The OPO laser might be another option which is less destructive, though may have insufficient energy to burn through the tissue samples. The PlasmaJet coagulator and Helica thermal coagulator use neutral pure argon plasma and helium gas respectively to achieve coagulation. While, they are ubiquitously used in clinical practice studies have shown that they coagulate to a depth of over 200μm [354, 355], almost 10x more than the CO2 laser. Alternatively, as suggested in section 3.3.3 the samples could be snap frozen and cryosectioned with a microtome. Immunohistochemistry could then be performed on some of slides to help with histological validation.

In addition to its diagnostic role, the iKnife can be used provide information about the phospholipid constitution of cancer versus normal cells. Interrogation of the key m/z values and phospholipids involved in class separation using Kruskal-Wallis, loading plots, univariate analysis and LipidMaps tentatively identified the lipid classes involved. Ceramides, PAs, PEs and PSs tended to be upregulated; whilst PCs, PIs and PGs were more frequently downregulated in endometrial cancer. Tandem mass spectrometry is needed to confirm these lipid assignments. This is described in more detail in the section 4.6. Interestingly, there was little overlap between the m/z values responsible for class separation between tissue bank and pipelle models which further confirms the differences in the models.

Strengths and limitations

One of the limitations observed in tissue bank model was the destructive nature of the iKnife, and the large amount of tissue samples that could not be histologically validated due to thermal artefact. The same phenomena were observed with pipelle samples, with the added challenge of even smaller samples and higher rates of inadequate samples.

Acquisition of pipelle samples was also challenging. Patients attending clinic were anxious and not always happy to participate in research, particularly in view of the painful nature of the procedure needed to obtain the sample. Those patients that agreed to research may not need a pipelle biopsy, and of those that need a sample there may not be enough tissue for research (insufficient volume or poor quality to process). The necessity of a separate research pipelle added to the challenge; these research pipelles were often smaller in volume with worse quality compared to the first clinical pipelle. In a study of endometrial biopsy samples taken in a hospital over one year and excluding cases in which the device could not be inserted into the uterine cavity due to pain intolerance or equipment failure, the pipelle biopsy was insufficient in 29% of cases [356]. Given that in this study a 2nd pass research pipelle was used, it is unsurprising that insufficient/poor quality samples accounted for a significant proportion of samples.

When this study was first conceived it was impossible to predict how many samples would be needed for the model to recognise differences in lipidomic profiles between cancer and normal tissue; or indeed if that was even possible. As seen on the learning curve (Figure 60) further improvements in diagnostic accuracy can still be reached with the inclusion of more samples in the model. Building of the reference dataset will be essential going forward.

Unfortunately, due to the limited number of samples, prospective validation with samples that were not already utilised by the model was not possible. Future studies would need to validate these models using prospectively collected pipelle samples. Care needs to be taken to ensure sample conditions are as uniform as possible, and to adopt a standard operating procedure for the acquisition, processing, utilization, storage of tissue to minimise confounding variables [357]. It is well recognised that endometrial physiology is highly complex and there are multiple source of biological

variability that can affect tissue composition, including: BMI, ethnicity, medication, timing of the biopsy in relation to the menstrual cycle [357].

The phospholipid range predominately investigated in this thesis is 600-1000, though future studies can focus on the entire range of m/z values, as some of these lower and higher m/z values might provide valuable clues to carcinogenesis.

Additionally, despite careful consideration to maintain the same processing conditions for each sample, and documenting any deviation, there inevitably will be subtle variations in TIC for each burn dependant on a number of conditions that cannot be controlled for e.g. temperature. Thus, there is an inherent limitation looking only for differences in phospholipid signatures without accounting for fluctuations in peak intensities due to these conditions. Peak ratios may a solution to this, by effectively correcting all peaks to the biggest peak. At the time of writing this thesis peak ratio software was being developed by the research group and would be an interesting avenue to explore in future studies.

Conclusion

The conventional diathermy iKnife and CO2 laser pipelle models perform as well, if not better, than the tissue bank models, thus paving the way for POC diagnosis for endometrial cancer. The learning models suggest that the diagnostic accuracy of the model can be further improved with the addition of more samples. Further work would therefore involve the acquisition of more pipelle samples, processed ideally with the CO2 laser in view of its superior diagnostic accuracy and reduction in tissue damage.

Interrogation of the unique phospholipid signatures of normal and cancerous endometrial tissue may help to understand the pathophysiology of cancer. Tentative phospholipid assignments suggest that endometrial cancer cells have higher amounts of ceramides, PAs, PEs and PSs; tandem MS will be performed to confirm these lipids.

4.6 Lipid identification – tandem mass spectrometry

4.6.1 Methods

Identification of MS peaks responsible for class separation

Based on the loading plots and univariate analysis in results section 4.5.6, m/z values which strongly contributed to the class separation in the PC-LDA models were selected for tandem mass spectrometry. In addition, m/z values with high intensity peaks (in either normal or cancer samples) were also selected for tandem MS. Due to limitations in MSMS technology m/z values which strongly contributed to the class separation in the PC-LDA models but have low signal intensity were not suitable for analysis.

MS/MS set up

Normal and malignant tissue samples of sufficient size were thawed from the -80^{0}c freezer. As sampling time required in MSMS is much longer, larger amounts of tissue were required, which limited which tissue samples could be used. Approximately 2-3 samples were used to determine a single ion.

Methods for tandem MS are similar to the materials and methods section 4.3.1. The Xevo G2-XS Q-ToF was set up and calibrated as described previously. In MS/MS tandem mass spectrometry, the collision gas argon was switched on (instead of medical air), MS/MS mode selected and the collision energy set to 30, but was varied according to the sample, range 30-45 (to ensure sufficient fragmentation of the mother ion, so biggest daughter ion peak remains about 1/3rd mother ion). The low mass and high mass range was set to 8 and 18.

A full long scan ('dry run') was performed on each tissue sample prior to m/z selection. The dry run entailed processing the tissue using the CO2 laser to confirm the normal internal lock mass peak (744.555) and peaks of interest were present in the sample.

MSMS was then performed by processing the tissue using the CO2 laser and selecting the specific m/z value of interest on the MassLynx interface. Tissue was sampled over 2-7 seconds per burn in order to achieve sufficient volume of aerosolised gas for analysis of each specific m/z value. These spectra were stored as described earlier.

LipidMAPS identification of lipids

MS/MS negative-ion-mode spectra were averaged and presented to the LipidMaps online tool. LipidMaps is also known as Lipid Metabolite and Pathways Strategy Lipidomic Gateway is a free online resource sponsored by the Wellcome trust [341, 342]. It provides a range of tools to enable lipid identification. The computationally-generated database of oxidized glycerophospholipid chain-composition masses was accessed for the m/z value precursor (to one decimal place) analysed with MSMS. The following search parameters were used: [M-H]- and [M+CL]-, intensity threshold 5, ion mass tolerance +/– 0.1m/z, any head-group. The output of lipidMaps suggested the lipids and chain configurations that could match. Only even fatty chain compounds were included. The main daughter ion was used to narrow down the exact lipid match.

The identified lipid was confirmed by using the product ion calculation tool for Glycerophospholipids (negative ion mode) toolbox, which produces the expected MSMS spectra for the mother ion and comparing it to the MSMS spectra created by the iKnife for an exact match.

4.6.2 Results

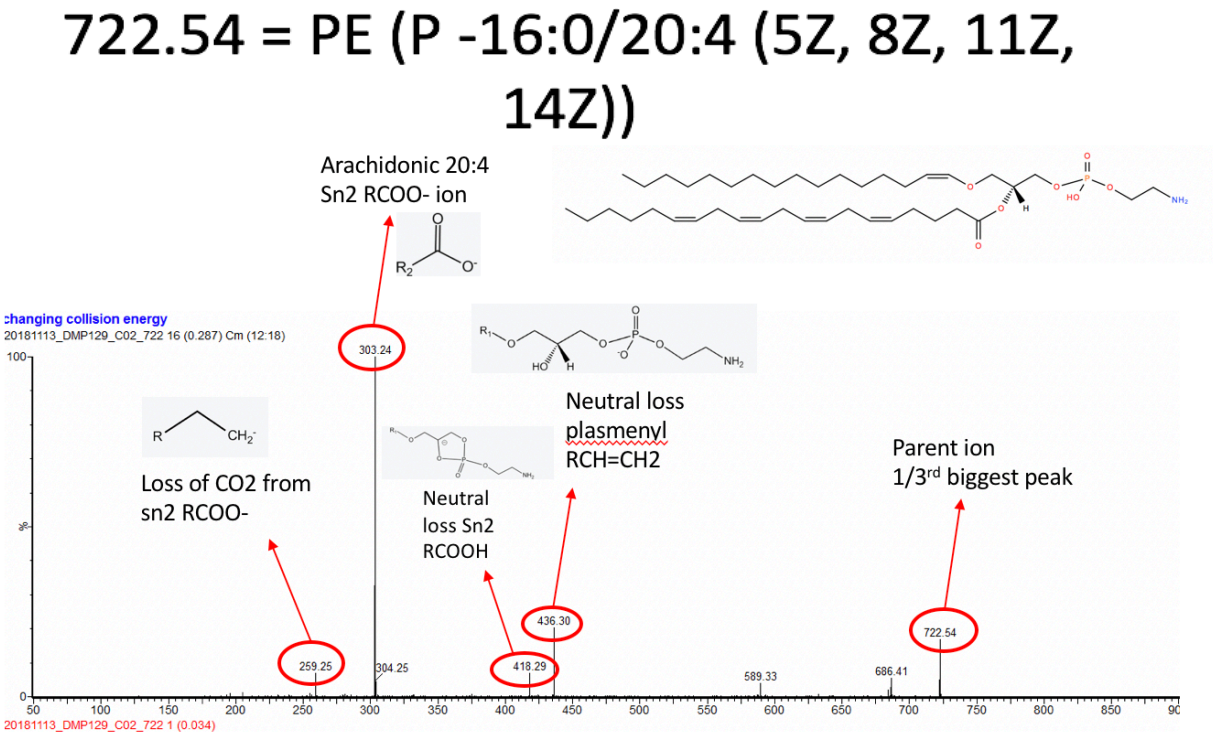
As described in section 4.5.6 a number of lipids contribute to the unique lipid signature that REIMs uses to distinguish between cancer and normal endometrium. Tandem MS was performed for all of the top 20 m/z values in Table 18. In addition, a full spectrum was run for normal and cancer endometrium and tandem MS was also performed on the 10 most abundant phospholipids found in normal and malignant endometrium (Table 19). Tentative lipid assignments were made using LipidMaps.

Tissue class	m/z value	P value	Potential Lipid
Cancer	679.55*	2.65x10-7	**PG(O-16:0/14:0)
	716.55	7.72x10-1	PE (16:0/18:1)
	722.54	6.00x10-4	PE (16:0/20:4)
	724.41	7.21x10-2	PE (P-16/20:3)
	766.56	2.82x10-2	PE (18:0/20:4)
	770.45	6.31x10-5	PE (20:0/18:2)
	794.65	3.63x10-3	PE (20:4)
	896.61	2.12x10-1	**PS(22:1/22:2)
Both normal and cancer	700.55	7.31x10-1	PE 16:0/18:1
	750.57	6.80x10-3	PE (18:0/20:4)
Normal	699.51	5.31x10-2	PA (18:1(9Z)/18:1(9Z))
	716.53	7.72x10-1	PE (16:0/18:1)
	722.52	9.74x10-2	PE (P-16:0/20:4)
	738.51	2.59x10-2	PE (P-16:0/20:4) (12OH[S]))
	766.54	2.82x10-2	PE (20:4/18:0)
	794.57	4.26x10-3	PC(O-18:0/20:4)
	864.57*	1.77x10-4	PI-Cer(d18:0/22:0)
	885.54	9.09x10-1	PI (20:4/18:0)

Table 19. Top 10 most abundant m/z values seen in normal and malignant endometrial pipelle biopsies, along with the confirmed lipid assignments following MSMS.

Double carbon bonds not reported. * = m/z value also responsible for separation of pipelle model. ** = tentative lipid assignment still as MSMS spectra inadequate.

The fragmentation pattern of each ion using tandem MS was interrogated using LipidMaps. A typical MS spectrum of m/z 722.54 is shown in Figure 63. The mother ion can be seen, approximately one third of the height of the biggest daughter ion (303.24), along with the other daughter ions: 259.25, 418.29, 436.30. Using LipidMaps, this confirms the lipid as a PE (P -16:0/20:4). Similarly, for m/z value 700.55 can be seen along with daughter ions. Confirmed lipids are seen in the Table 19. Most of the abundant lipids seen are PEs.



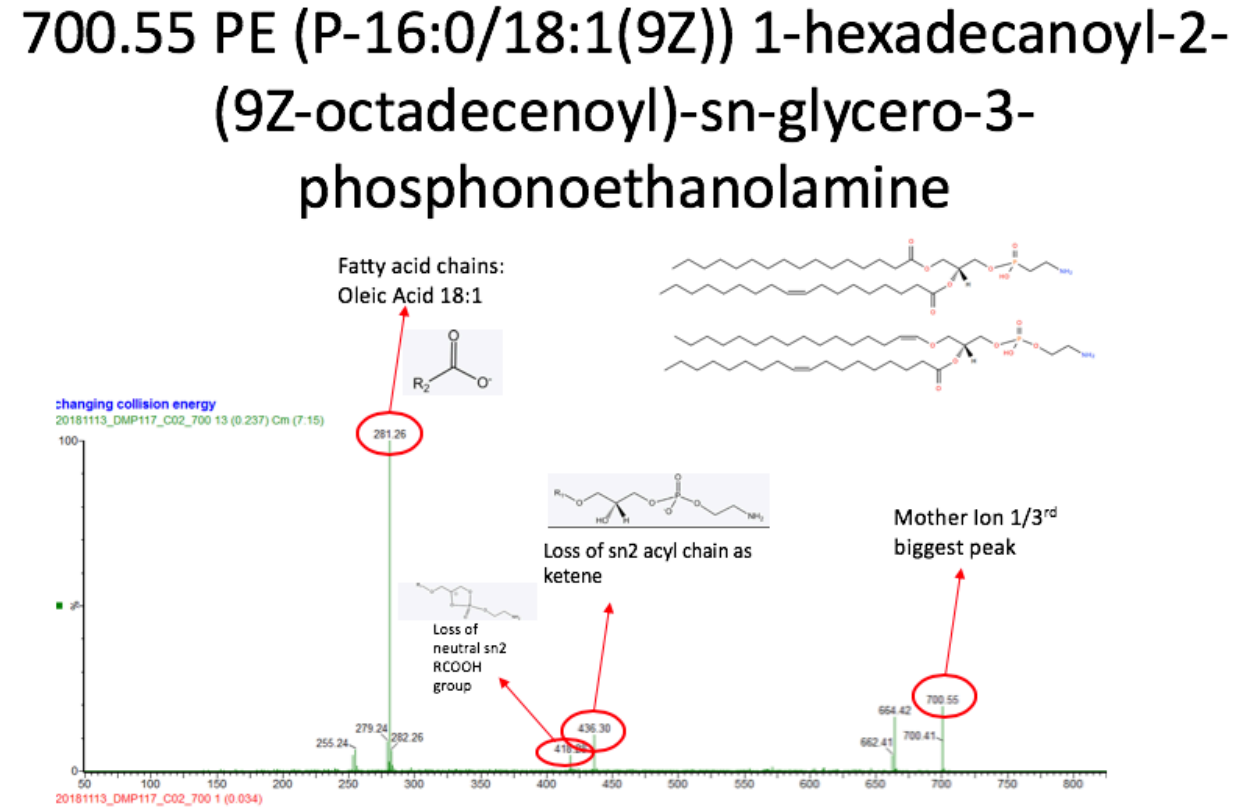


Figure 63. Tandem MS spectra of two m/z values: 722.54 and 700.55.
The mother and key daughter ion peaks are annotated along with a chemical illustration of the confirmed phospholipid.

Few m/z values were both abundant and responsible for separation in the models (Table 18 and 19). Most m/z values responsible for the separation were present in too small quantities for MSMS to be successful. Either no ion was detected, or the signal was too noisey e.g. m/z 679.55 and lipid confirmation was not possible (Figure 64).

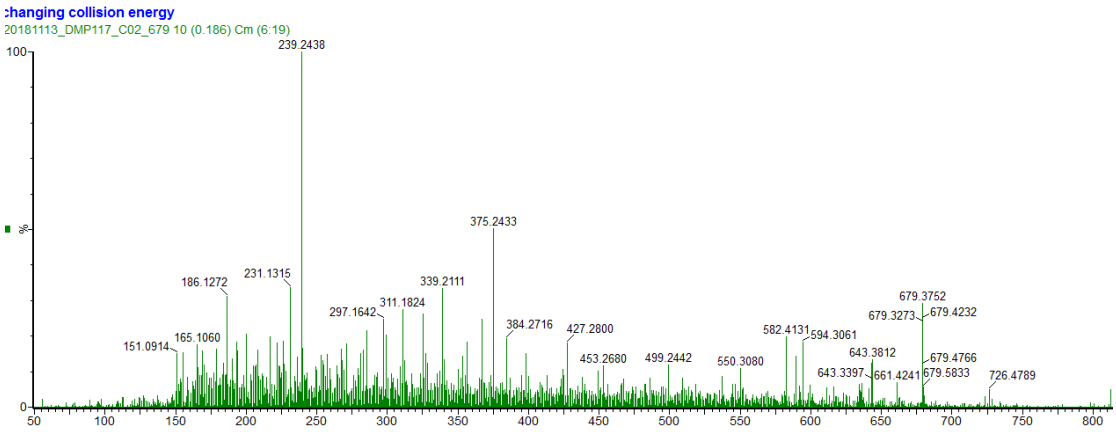


Figure 64. Inadequate MS/MS spectra of m/z 679.55

4.6.3 Discussion

Key findings

Lipids represent an important, albeit poorly understood class of molecule involved in carcinogenesis. Cancer lipidomics is a rapidly evolving field since the emergence of mass spectrometric techniques that can interrogate the lipidomic profile of tissues [357]. Lipidomics is defined as the identification and quantification of lipids within a specific biological system. Bioinformatic analyses of the data gathered by these techniques is likely to enable the discovery of new pharmacological and clinical targets.

In a normal pre-menopausal woman, the endometrium will fluctuate substantially during the course of a menstrual cycle. In order to replenish the endometrial lining, there will be large fluctuations in cellular synthesis and metabolism. Lipids play a pivotal role in biological membranes and are therefore essential for proliferating cells, associated with an upregulation in lipogenic enzymes such as fatty acid synthase and acetyl-CoA carboxylase. Lipid metabolism has also been linked to autophagy and in particular PEs are known to be involved in the initiating step of autophagy by covalent binding to autophagy-related protein Atg8 [317]. Understanding the key lipid variations which distinguish normal endometrium and malignant endometrium remains crucial to underpinning the pathophysiology of malignancy.

The work in this PhD involved the characterisation of lipid groups abundant in endometrial cancer pipelle samples using REIMS. As seen in Table 19, PEs were abundant in both normal and cancer tissue, with a different cluster of PEs more ubiquitous in each tissue group. In this study: PE (16:0/18:1), PE (16:0/20:4), PE (18:0/20:4), and PE (20:0/18:2) were all more common in endometrial cancer tissue. Whereas, PE (16:0/18:1), PE (P-16:0/20:4) and PE (20:4/18:0) were more common in normal endometrial tissue.

In Altadill study of 56 endometrial tissue samples they found significant dysregulation in lipid metabolism too, with a number of PCs, PEs, PIs and PAs upregulated in endometrial cancerous tissue. Interestingly, PE (16:1/P-18:1) was found to be upregulated in their study. One limitation of their study was the lack of clarity about how the tissue sample was obtained i.e. was it a pipelle sample or solid tissue from tissue bank. As discussed earlier, the tissue bank and pipelle models had different significant m/z values responsible for the separation.

Several studies have reported increased levels of PC in cancer [196, 358]. Indeed, one study in breast cancer found that PC (18:0/20:4) was associated with higher grade tumours and decreased survival [196, 359]. In endometrial cancer, Trousil's study found that PCs were present in 70% higher quantities within cancerous tissue [331]. However, in a targeted study of PCs and sphingolipids in EC patients' blood plasma, 3 PCs (C40:0, C42:5, and C42:6) were significantly decreased [333]. This was thought to be attributed to cell membrane synthesis exhausting substrates. The current study also suggests that PC, along with PIs and PGs are reduced in endometrial cancer. Due to the low intensity signal, tandem MS on the m/z values for these lipids was not possible, so the lipid assignment remains only tentative.

Multiple studies have suggested that glycerophospholipids can be used as a biomarker for cancer [360-363]. From the results of this study, it is unlikely that a single phospholipid can be used as a marker for EC, more likely a combination of phospholipids in EC can be used as part of a multivariate prediction model to diagnose EC.

Biomarkers in general can be used for screening, diagnosis, prognosis and treatment monitoring of cancer [364-367]. Biomarkers can be gene based (e.g. *PTEN, p53*, microRNAs, circulating tumour DNA), protein based (e.g. Ki-67), hormonal (e.g. Oestrogen receptor, HER2) or immunological (e.g. Tumour-associated macrophage density) [364, 368-371]. Whilst this study has shown that the iKnife is excellent at diagnosing endometrial cancer from pipelle biopsy samples by identifying differences in the phospholipid profiles of tissue; the requirement for tissue inevitably means it is invasive. Non-invasive blood biomarkers for EC represents an enticing avenue to explore.

Of the blood based biomarkers, those already studied in endometrial cancer are predominately protein based and include: human epididymis protein 4 (HE4) [372], CA125 [373, 374], Dickkopf-1 (DKK-1) [375] and DJ-1 [376, 377]; but these have been shown to lack diagnostic accuracy in isolation and most have not been validated [378]. Combination panels of serum biomarkers have also been studied [379, 380] and often perform superiorly compared to individual biomarkers. For example, apolipoprotein-1, prealbumin and transferrin levels were assessed in 433 women [381]. It distinguished normal samples and early stage endometrial cancer with a sensitivity of 71% and specificity of 88% [381].

A recent study by Paraskevaidi et al., using vibrational spectroscopy to look for endometrial cancer biomarkers in blood samples found a high diagnostic accuracy (71-100%) [382]. The study found also found an increase in lipid-related peak in the blood of women with endometrial cancer. The biggest disadvantage of their study was the inability to delve deeper and correlate the spectral peaks with the biomolecular, cellular changes underpinning carcinogenesis. Also, importantly, the group failed to correct for multiple testing and maintained a P-value of 0.05, despite testing hundreds of peaks with a high likelihood of a false positive results.

Strengths and limitations

This is the first study using REIMS to detect endometrial cancer from pipelle biopsy samples taken in clinic. The technology performed extremely well with a diagnostic accuracy of approximately 90%. The sensitivity and specificity of the best performing

models are sufficiently high to be used in clinical practice, following prospective validation. The result from REIMS is virtually instantaneous and can therefore provide a POC diagnosis for patients attending the RAC. Given the high PPV (93-94%), women who test positive are very likely to have endometrial cancer and could go on to have blood tests and pre-operative imaging that day while awaiting final histopathological confirmation, minimising any treatment delays.

Tandem MS helped assign some the key phospholipids present in higher quantities in endometrial cancer. The changes observed in phospholipid quantity can reveal changes in enzymatic activity and/or gene expression in cancer. Further cell line work will be needed to unravel the exact molecular pathways involved in endometrial cancer progression.

One of the limitations of tandem MS was the inability to confirm lipid assignments for many phospholipids significant in the separation of normal and cancer on the PC/LDA model, as the ions were present in too low levels to fragment and detect effectively. This also meant that all m/z values which were significantly downregulated in endometrial cancer samples could only have tentative lipid assignments.

Conclusion

In this pilot study, the iKnife could accurately distinguish between normal and malignant endometrial biopsy samples based on differences in their lipidomic profiles. This suggests that the iKnife can be used as an adjunct in clinic to provide a point-of-care diagnosis.

CHAPTER 5: ULTRASOUND GUIDED BIOPSY

CHAPTER 5: ULTRASOUND GUIDED BIOPSY

5.1 Summary

Objective: The aim of this study was to investigate the success rate, pain and acceptability of ultrasound-guided endometrial biopsy in the management of abnormal vaginal bleeding.

Methods: Prospective analysis of women with abnormal vaginal bleeding who underwent ultrasound-guided endometrial biopsy between June 2017 and April 2019 at the West London Gynaecological Cancer Centre, Imperial College NHS Trust, London, United Kingdom. Indications for procedure under ultrasound were cervical stenosis and focal lesions. Diagnostic performance was calculated. Patients were also asked to rank pain on a 0-10 visual analogue score (0 no pain and 10 unbearable) and acceptability on a 0-5 Likert scale (0 not acceptable and 5 very acceptable).

Results: We evaluated 10 patients, with a median age 68 (range 46-84 years). The main indication for USS guided biopsy was cervical stenosis (80%). All women underwent uncomplicated USS guided endometrial biopsy in clinic. Biopsy was successful with sufficient tissue in 90% of cases. VAS was high (median 7.5) but despite this acceptance was 100% (Likert 5).

Conclusions: Ultrasound can be used safely, with good success rates to facilitate endometrial biopsy under vision. It is a painful procedure, but patients stated they were willing to have a second procedure under the same conditions.

5.2 Introduction

Postmenopausal bleeding is the most frequent presentation of endometrial cancer. Transvaginal ultrasound followed by endometrial biopsy when indicated by endometrial thickness of > 4mm has been shown to be the most cost-effective strategy [383]. There are a number of outpatient endometrial biopsy (OEB) sampling methods available, such as: pipelle, vabra, accurette, endorette and novak. These are used in outpatient gynaecological clinics with a speculum examination and without anesthesia; the most ubiquitous OEB being the 3mm Pipelle de Cornier.

Studies have shown that OEB have a high diagnostic accuracy for the detection of global endometrial pathology [94, 384]. In a recent meta-analysis by van Hanegem 12 studies compared blind outpatient biopsy techniques against a reference standard of either hysteroscopy or blind dilatation and curettage (D&C) for assessment of the endometrium [385]. The weighted sensitivity of endometrial sampling with hysteroscopy as a reference for the diagnosis of endometrial cancer and atypical hyperplasia was 90%, 82% respectively with high specificity. The failure rate of blind outpatient endometrial sampling was 11% and insufficient tissue samples were found in 31% [385]. Risk factors for failed biopsy include postmenopausal status, history of previous failure to biopsy endometrium and inexperience of the operator [104]. Interestingly, in those women with insufficient or failed outpatient biopsy samples, endometrial cancer or pre-cancer was found in 7% [385].

Despite being minimally invasive, outpatient biopsy procedures are still associated with a variable degree of pain, which can limit the success rate of performing a biopsy [386, 387]. While most patients experience moderate to severe levels of biopsy-associated pain on a visual analog scale (VAS), they will still tolerate the procedure [387]. A large number of studies have evaluated pain and analgesia in outpatient hysteroscopy [388-396] but comparatively fewer studies have assessed pain with office endometrial biopsy techniques [397-402]. Those that have, have predominately assessed the use of intrauterine lidocaine [403-409]. A greater need for analgesia is also required in cases of cervical stenosis which can increase the difficult of performing a biopsy and is associated with significant iatrogenic patient morbidity [410].

Cervical stenosis is defined as a narrowing of the endocervical canal that prevents the passage of a 2.5mm dilator [410-412]. The true incidence is unknown, however, in Betocchi's series of more than 31000 women receiving outpatient hysteroscopy it was present in 32.7% cases and was more common in postmenopausal women [413]. In their case series, pain and cervical stenosis were the main reasons of incomplete and failed procedures. Even more worryingly cervical stenosis was associated with uterine perforation. In Jansen et al study of over 13600 receiving hysteroscopies they reported a uterine perforation rate of 0.76% [93]. Techniques to overcome cervical stenosis include: preprocedural use of cervical-ripening agents such as misoprostol, hydrodilation of the cervical canal, manual dilatation, vaginoscopy, and hysteroscopic resection of the obstructed endocervical canal [410].

A handful of studies have suggested the use of concomitant ultrasound to assist in cases of cervical stenosis [410, 414]. Hammoud's case report showed that an endometrial biopsy could be obtained in women with cervical stenosis using transvaginal ultrasound and a biopsy needle passed through the vaginal vault to the anterior uterine wall into the endometrium [103]. Meanwhile, Hunters' study describes using gradual dilation of the cervix under ultrasound guidance in a case series of 21 women receiving D&C [415]. More recently Dua, described a similar technique of abdominal ultrasound and biopsy through the cervix in 113 women referred for an USS guided biopsy [104]. The main indication was failed biopsy (35%) and fibroids (31%) [104]. They report an 84% success rate but did not comment on tolerability or pain perception. Moreover, as inexperience of the operator is a key factor in failure to achieve a biopsy in clinic and given the assessment of cervical stenosis can be somewhat subjective, multiple operators in the study reduced the quality of data.

One of the other limitations of outpatient endometrial biopsies is the inability to sample focal lesions such as polyps. Endometrial polyps are very common, with a prevalence of 10-40% in women with abnormal uterine bleeding [416-420]. They are also more common in postmenopausal women, with a prevalence over 20% [419]. In a large meta-analysis of 35,345 women approximately 2.7% of endometrial polyps were found to malignant (95% CI 2.57–2.91) [421] with rates above 5% in postmenopausal symptomatic women [421, 422]. To this end, endometrial sampling of polyps and polypectomies in symptomatic postmenopausal women is recommended. This cannot be achieved with outpatient blind biopsy techniques such as pipelle biopsy which has a low accuracy compared to hysteroscopy and guided biopsy [100, 423-426]. Blind techniques frequently miss small or pedunculated polyps and can complicate histological assessment due to tissue fragmentation.

The preferred alternative for localised pathology is hysteroscopy. However, this is also not without risk, with an incidence of serious complications such as perforation, false tracts and vasovagal collapse between 0.1- 1% and a failure rate of 4%, during diagnostic hysteroscopy, and higher still for postmenopausal women [89].

Historically there has also been some concern that hysteroscopy might disseminate malignant endometrial cells into the peritoneum, thereby potentially upstaging cancer

and decreasing survival. Indeed, positive peritoneal cytology is considered an adverse prognostic factor [427, 428] and several studies have confirmed strong association between hysteroscopy and positive peritoneal cytology [112, 116, 429-432]. Whether this worsens prognosis is more controversial.

A meta-analysis by Chang et al found that hysteroscopy before surgery in patients with endometrial cancer does increase the risk of dissemination of malignant cells into the peritoneal cavity, particularly if liquid medium is used [114]. However, there was no evidence to support an association between preoperative hysteroscopic examination and a worse prognosis [114]. A limitation of this meta-analysis was the short follow up and lack of accounting for confounding variables that might affect prognosis. As normal saline hysteroscopy is so widely used as part of the investigative work up, until recently, there was no way to answer this question with certainty.

The aim of this study was to demonstrate if ultrasound guided endometrial biopsy could be used safely and effectively as an alternative to hysteroscopy in cases of cervical stenosis or in cases where there are focal lesions.

5.3 Methods

Consecutive women presenting to the rapid access clinic in West London Gynaecological cancer centre with post-menopausal bleeding (PMB) or intermenstrual bleeding were approached for consent for inclusion into this study between June 2017 and April 2019. The study was approved by the local ethics committee and patients provided written informed consent. Women were excluded if they lacked capacity, were under 18 years old, pregnant or if there were any contra-indications to a biopsy. Patients initially underwent routine standard of care with a pelvic ultrasound scan and outpatient tissue biopsy (pipelle) if clinically indicated. Only women who had an indication for an endometrial biopsy were invited to participate in the study.

Women were seen by a single expert clinician (JY). If the outpatient biopsy was not tolerated due to cervical stenosis, or if there was insufficient material, an ultrasound (USS) guided biopsy was offered in the first instance during the same clinic consultation as an alternative to hysteroscopy. If there was a focal lesion an USS guided biopsy was offered prior to a blind pipelle biopsy.

Patients were asked to assess tolerability and pain perception of the procedure using a 10-point visual analogue scale (VAS), ranging from 0 (no pain) to 10 (unbearable pain) by a clinical fellow. see Figure 65. The score was taken immediately after the procedure.

The secondary outcome of the study was patient acceptability i.e. would the patient have the outpatient procedure again should they need it, instead of a hysteroscopy. This was recorded by the clinical fellow on a 5-point Likert scale (0 not acceptable, would never have it again, and 5 very acceptable and would have again). Patients were also given the opportunity to comment, and state if they would recommend the procedure to family or friends. If the results of the USS guided biopsy were inadequate patients were sent for hysteroscopy and biopsy. The success rates and diagnostic accuracy of tissue sampling using USS were calculated.

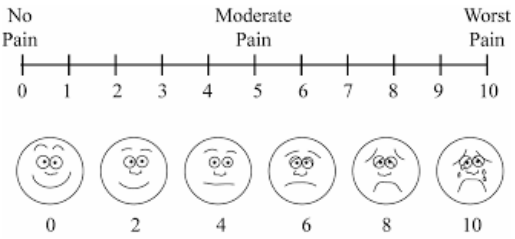


Figure 65. Visual analogue scale used for the assessment of pain

5.3.1 The technique

Patients underwent a standard pelvic examination in lithotomy position, and a cusco speculum was inserted into the vagina to visualize the cervix. Concurrently abdominal ultrasound was performed by a single expert clinician. The USS guided biopsy was performed using either fine forceps such as Bettochi or using a pipelle passed through the cervix under abdominal ultrasound guidance (see Figure 66). The sampling device was passed into the uterus and the tip was guided to the fundus or focal lesion. The biopsy device was passed at least twice to ensure an adequate quantity of tissue. A tenaculum and/or cervical dilators were also used at the discretion of the clinician, as were paracervical blocks. The specimen was placed into a formalin-filled box for standard histopathological examination. In those cases where there were insufficient tissue patients were sent for a hysteroscopy under general anaesthesia.

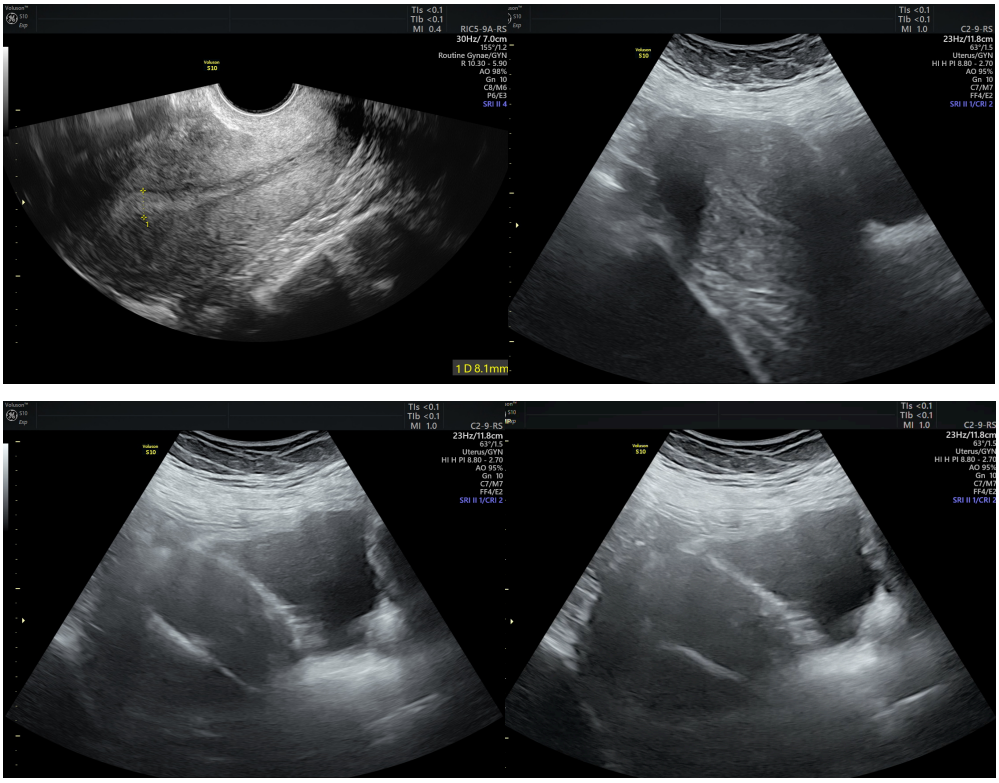


Figure 66. Image of ultrasound guided biopsy.
Top left image shows 2D TV ultrasound assessment of the endometrial lining. Top right image shows the endometrial lining of the uterus in sagittal section using abdominal scan. The bottom two images show the uterus in sagittal section with hyperechoic pipelle sampler inside the cavity.

5.3.2 Statistical analysis

Data were analysed using the Statistical Package for Social Sciences, version 26.0 (SPSS Inc., Chicago, IL, USA). Visual analogue scale results were classified as ordinal data (ranked), so range and interquartile range were calculated, and box plots were created. Severity of pain was categorised as: mild if VAS <4.5, moderate if VAS is 4.5-7.4 and severe pain if VAS ≥7.5 [390, 433]. All P values were 2-sided and a P <0.05 was considered statistically significant.

5.4 Results

Ten patients underwent ultrasound-guided tissue biopsy between June 2017 and April 2019, with a median age 61 (range 45-84 years old). The median BMI = 25 and 66% of women were multiparous. Seven women presented with postmenopausal bleeding, 1 with menorrhagia, one with intermenstrual bleeding and one patient was referred due to concerns on a CT scan for abdominal pain. The endometrial thickness on USS

varied between 2.2 - 42mm. Two women had polyps. The main indication for USS guided biopsy was cervical stenosis. The main method of biopsy was a pipelle. The procedure was successful in 100% of cases and provided sufficient tissue in 90% of cases. In the one case of insufficient tissue, the patient underwent a hysteroscopy under general anaesthesia (GA) and was ultimately diagnosed with endometrial cancer. No complications occurred during this study. The pathologic findings are seen in Table 20. The data of all 10 patients is summarised in the Table 21.

Pathological Findings	**Number of patients (%)**
Benign	4 (40%)
Pre-malignant	1 (10%)
Malignant	5 (50%)

Table 20. Breakdown of final histology for women undergoing ultrasound guided biopsy.

The tolerability of the procedure is shown is illustrated in the stem and leaf graph below (Figure 67). The median VAS score was 7.5 (range 4-10). All patients said they would have the procedure again if indicated without hesitation, as oppose to a hysteroscopy under GA. This was documented as 5 on the Likert scale i.e. very acceptable. Similarly, patients would all recommend the procedure to family and friends.

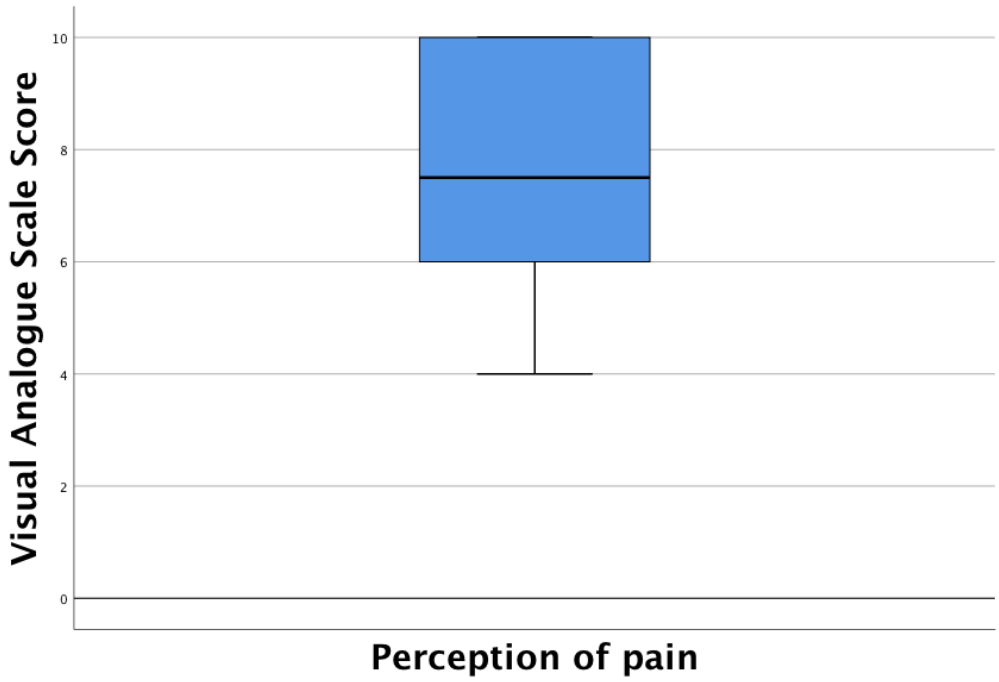


Figure 67. Box and whiskers plot of patient's perception of pain using VAS.

5.5 Discussion

5.5.1 Main findings

This study demonstrates the safe use of USS guided biopsy in the investigation of abnormal bleeding in cases of cervical stenosis or focal lesions. In this study no complications occurred, and all procedures were completed successfully. The main indication for USS guided biopsy was cervical stenosis (80%). One patient had insufficient tissue and subsequently underwent a hysteroscopy under GA, giving a performance accuracy of 90% which compares favourably to diagnostic hysteroscopies.

Importantly, the present study showed moderate to high pain scores on the VAS during the USS guided biopsy. This is slighter higher than other studies which reported a VAS of 4-6 [396, 401, 403, 404]. This is likely due to a combination of patient selection and variations in recording of VAS (timing, methodology and significance threshold). In this study most of the patients recruited had cervical stenosis which is key factor in procedural pain and failure to perform the procedure, which is unlike all the other studies. In addition, there are a plethora of scoring mechanisms and interpretations of these scoring methods used [434]. For example, Perrone study used VAS but on a 100-point scale, Siddle used the McGill pain score in addition to VAS and verbal rating scale and described their data using mean values despite lack of normally distributed data [396, 402]. There was also variation of thresholds of 'significant pain', with some studies using 4.5 and others used ≥6 [435]. To mitigate these high pain scores, paracervical blocks, anaesthesia or Entonox may be useful adjuncts.

Pain itself is difficult to compare as is it is affected by various environmental, ethnic and cultural influences. Anticipatory pain might also contribute to overall pain scores. In Kosus' study they used pain on speculum insertion as a surrogate marker for a patient's overall tolerance of pain and/or anxiety and excluded patients with high pain on speculum insertion [405]. Anxiety itself is a well-recognised confounder for pain. Studies have shown that an assistant explaining the procedure can moderate patients' pain and anxiety levels [436, 437].

Interestingly despite severe pain scores, all patients unanimously agreed to have the procedure again, if needed, instead of a hysteroscopy under anaesthesia. This was in keeping with a study by Iaco who assessed 1144 consecutive women undergoing a diagnostic hysteroscopy [435]. The median pain score in their study was moderate (4.7) and despite this, acceptance of the procedure was high (83%) [435]. This suggests that patients are either overreporting pain or are willing to accept a reasonable amount of suffering. This may be driven by fear of uncertainty, fear of cancer diagnosis, unwillingness to displease the clinician or the desire to maintain self-esteem.

Furthermore, there has been some suggestion that hypersensitivity of endometrial nerve endings of oestrogen-dependent gynaecological pathologies, may contribute to the biopsy associated pain [387]. Some studies have reported higher VAS pain score and or reduced acceptance of endometrial biopsies in menopausal as oppose to pre-menopausal women. It has been suggested that this due to genital atrophic changes. Due to the small case series it is not possible to assess this factor.

Given USS guided biopsy appears a safe and effective alternative to hysteroscopy, it may now be possible to finally determine whether preoperative hysteroscopy effects disease prognosis as there is a viable alternative to hysteroscopy that patients can be randomised to.

5.5.2 Strengths and Limitations

The main strengths of this study are the assessment of the success rate of USS guided endometrial biopsy in addition to patient centred outcomes: pain scores and acceptability. Also, importantly, the diagnosis of cervical stenosis and therefore decision for inclusion into this study was made by a single expert operator, instead of the judgement of less experienced clinicians. It is well documented that experience of operator is a big factor in success of biopsy and pain scores. In addition, all endometrial biopsy procedures were performed by the same expert gynaecologist to maintain consistency and limit confounding variables. These factors are an improvement from Dua study which had multiple operators making the decision for failed biopsy and also performing the USS guided biopsy [104]. Of note, the failure rate In Dua study was

15%, with a similar age of population but a much higher rate of benign pathology (96% vs 50% in this study).

It is known that transabdominal USS can be challenging in patients with a high body mass index. In this study, unlike most patients with endometrial cancer, the average BMI was normal. This can limit the generalisability of the conclusion to the general population.

One of the other strengths of this study is the use of validated method of pain measurement and having a different member of the research team explain the VAS and receive the score. This minimised any bias that the patient may have to please the clinician.

In this study, only the pain perception immediately post procedure was recorded. Other studies also recorded pain during the procedure and 30 minutes after, which might be interesting aspects to explore. Moreover, the educational status of the patients, which may affect the patient's ability to identify perceived pain on the visual analogue scale was not recorded.

The main limitation in this study is the small sample size. Whilst patients were recruited consecutively, the clinical fellow (me) recruiting patients was only available on certain clinic days thus it took a long time to recruit patients. Also, not all patients agreed to the procedure so there may be a selection bias.

Ultrasound scanning is exceedingly user dependant and requires expertise. Thus, the single expert operator may also be seen as a limiting factor and can affect the generalisability of the results.

5.5.3 Conclusion

In summary this small study supports the use of USS guided endometrial biopsy as an effective way to perform targeted biopsies of a polyp and enable safe entry to the uterine cavity. The procedure is minimally invasive and can be used with a high degree of safety. Whilst associated with high pain scores, it is well tolerated and accepted by patients. Further studies, on a larger scale would be helpful to confirm these findings.

The technique uses standard transvaginal ultrasound equipment that is universally available in most practices. Though expertise in ultrasonography are required, these skills are now integral components of the gynaecology curriculum, making this technique readily accessible.

Case number	Prior History			Main symptom	USS findings	Indication USS guided Biopsy	The procedure			Final histology
	Age	Parity	BMI				Device	VAS	Successful	
1	72	3	29	PMB	ET 12.2mm ?polyp	Polyp	Pipelle	7	Yes	Endometrioid carcinoma grade 2
2	68	3	ND	PMB	ET 6.6mm	stenosis	Forceps	4	yes	Benign
3	84	0	21	PMB	ET2.2mm ?pyometria	stenosis	Pipelle	10	yes	Endometrioid carcinoma grade 1
4	54	0	25	menorrhagia	ET 29mm with vascularity	stenosis	pipelle	8	No insufficient	Endometrioid carcinoma grade 1
5	71	2	30	Incidental abnormality CT	ET 42 mm, fluid in cavity	stenosis	Pipelle	9	yes	Clear cell carcinoma
6	52	0	21	PMB	ET 6.6mm cystic	stenosis	Pipelle	6	yes	Atypical hyperplasia
7	46	2	24	PMB	ET 15mm ?polyp	polyp	Pipelle	10	yes	benign

8	70	1	26	PMB	ET 42x32x41mm mass	stenosis	Pipelle	4	yes	Endometrioid carcinoma grade 2
9	45	1	31	IMB	ET 14.7mm	stenosis	Pipelle	7	Yes	Benign
10	49	2	ND	PMB	ET 8.1mm	stenosis	pipelle	10	yes	Benign

Table 21. Summary table of patients who underwent ultrasound guided biopsy. Acronyms: ET = endometrial thickness, ND = not documented, PMB = post-menopausal bleed

CHAPTER 6: 3D ULTRASOUND

CHAPTER 6: 3D ULTRASOUND

6.1 Summary

Objective: To evaluate diagnostic accuracy of 3D ultrasound in the pre-operative assessment of deep myometrial invasion in endometrial carcinoma.
Methods: Design - A prospective observational study. Setting - University teaching hospital. Population – 25 patients diagnosed with endometrial carcinoma and undergoing surgery were seen preoperatively and had MRI and 3D USS examinations performed by an expert. The depth of myometrial invasion was assessed subjectively and objectively using shortest distance from tumour to serosa (TDS) and compared to the final histopathology report after surgical staging.
Results: In detecting deep myometrial invasion the sensitivity and specificity was 80% and 67% respectively for subjective assessment, 80% sensitivity and 80% specificity for objective assessment TDS using 5mm cut-off and 80% sensitivity and 83% specificity for MRI.
Conclusion: 3D ultrasound had moderate performance in detecting deep myometrial invasion, but larger studies are needed.

6.2 Introduction

Endometrial cancer is the most common gynaecological cancer in developed countries. Surgical staging is essential for both treatment and inferring prognosis. Surgical treatment involves a total hysterectomy and bilateral salpingo-oopherectomy. Lymphadenectomy is also performed in high risk cases, as it is not without inherit risk. One of the most important factors which determine risk and influence surgical staging is the assessment of deep myometrial invasion (MI) [129, 438, 439]. The presence of deep myometrial invasion alone increases the risk of lymph node metastasis from 4-5% to 15-30% in low grade endometrioid cancers [128, 438].

Thus, non-invasive selection of cases pre-operatively, based on an assessment of MI will enable better surgical planning and avoid unnecessary lymphadenectomy. This is currently performed by MRI, which is reported to have a sensitivity, specificity, positive predictive value, and negative predictive value of 80.7%, 88.5%, 77.6%, and 89.5%

respectively for the assessment of deep MI [440]. MRI is limited by resources, costs, patient acceptability and patient size.

Ultrasound (USS) is ubiquitously used in gynaecological imaging due to its low cost, accessibility and high tolerability. But the most recent meta-analysis by Alcazar found that standard 2D USS only had a moderate pooled sensitivity and specificity for detecting MI, 75% (95% CI, 67%-82%) and 82% (95% CI, 75%-93%) respectively [135].

More recently, 3D ultrasound has gained traction in recent years. It is being used more commonly in cervical cancer, in the assessment of invasion, tumour volume and planning of brachytherapy [441-445]. Three dimensional ultrasound enables enhanced tissue demarcation and valuable coronal views enabling assessment of MI in the uterine corners [446, 447]. A few studies have now investigated the accuracy of assessing deep MI using 3D with promising results [136, 137, 142, 448, 449]. All the studies have limitations in quality, reporting. Most are small retrospective studies, often with more than one expert assessors. The 3D ultrasound scan was performed only after a diagnosis of endometrial cancer was made. Additionally, the method of assessment of MI in these studies are not always defined [142].

Both subjective and objective assessments to predict MI exist and are described by Alcazar [137, 446, 450], with subjective assessment performing superiorly [137]. There are number of objective assessment techniques available, the most common is calculating the shortest tumour distance to serosa (TDS). A cut-off of <9mm is usually used for predicting deep myometrial invasion (≥50% MI). Subjective assessment involves looking for asymmetry in the myometrial-endometrial interface in the tumour and supposedly tumour-free myometrial wall.

This study will prospectively evaluate the diagnostic accuracy of 3D ultrasound and MRI in the detection of deep myometrial in endometrial cancer patients, using both subjective and objective techniques and comparing it to final histopathology.

6.3 Methods

The STARD guidelines were adhered to during the undertaking of this prospective study [451]. Consecutive patients with suspected endometrial carcinoma at Queen Charlotte hospital London between May 2015 and April 2020 were seen by one of 2 experts in clinic and underwent a 3D transvaginal USS as part of their assessment. Only those patients who had histologically confirmed (by dilatation and curettage, hysteroscopy or outpatient endometrial biopsy) endometrial cancer were included in the final analysis. Patients were excluded if no cancer was detected, if surgery was not performed, if neoadjuvant treatment was performed, or if there was an incomplete pathological report.

All patients provided written informed consent, and the study protocol was accepted by the ethics committee. All patients underwent a hysterectomy, bilateral salpingo-oophorectomy +- pelvic/para-aortic lymphadenectomy if clinically indicated. The patients were staged according to the FIGO 2009 recommendations by a specialist gynaecological histopathologist who was blinded to the 3D USS result. The histopathological variables assessed included histological type, grade and pathological stage. As per FIGO, Stage IA was defined as myometrial invasion<50%, Stage IB as myometrial invasion>50%. This defined the reference standard.

The MRI examination was performed approximately 2 weeks after diagnosis, and the ultrasound examination was performed on the day of attendance at the rapid access clinic, before a diagnosis of endometrial cancer was made.

6.3.1 Ultrasound assessment

All of the ultrasound examinations were performed by one of 2 experts with at least 2 years' experience in 3D ultrasound (JZ, CL) using a Voluson S10 or E6 (GE Medical Systems, Zipf, Austria) with a multifrequency endovaginal probe (5–9 MHz). Women were examined in the lithotomy position and with an empty bladder. A 2D USS exploration of the uterus and adnexa was initially performed. The following measurements were then taken, endometrial thickness at the level of maximal thickness in the sagittal plane. After which, at 3D volume box was activated and was manually altered to include a view of the entire uterus. With patient remaining still, a sweep angle of 90°, a 3D image was acquired. Acquisition time lasted from 5 to 10

seconds. Rotations were performed so that transverse, sagittal, and coronal planes were placed on the screen and stored for analysis at a later date (see Figure 68).

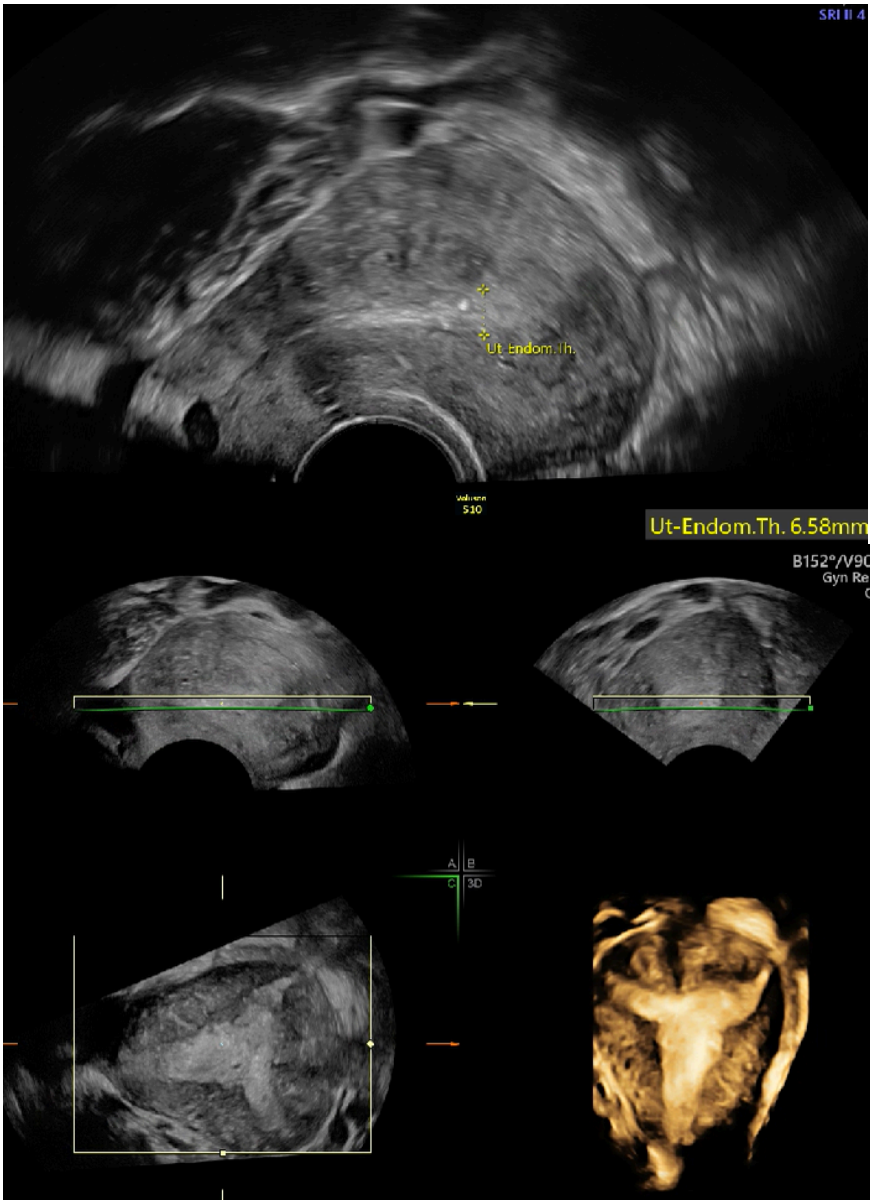


Figure 68. Three-dimensional ultrasound image.
Top image shows the endometrial lining using standard 2D TV USS. The subsequent images depict the process of creating a 3D coronal image of the uterus.

6.3.2 Image analysis

Stored images were rendered and evaluated, 12-60 months post acquisition, by single expert operator with more than 5 years' experience in 3D ultrasound (JY) blinded to the patients' identity, histology and prior imaging results. Sequential virtual navigation through the uterus then was performed by sweeping through the 3D scanned images.

First by going through the sagittal plane, from anterior to the posterior uterine serosa, followed by the coronal plane, were the images were navigated from one uterine cornu to the other, followed by transverse.

Myometrial infiltration depth was estimated subjectively by the examiner according to their impression of depth of invasion. The point in which the myometrial-endometrial interface was not clearly defined was compared to the supposedly tumour free opposite myometrial wall. In cases of marked asymmetry, deep myometrial infiltration was documented, and if the myometrial thickness appeared the same on both myometrial walls superficial infiltration was documented. Hence, if the tumour was confined to the endometrium (endometrial–myometrial junction was intact) no invasion was documented. If invasion of less than half of the myometrium (thinnest part of normal myometrium on sequential sagittal, axial or coronal planes was more than half the myometrial thickness) superficial invasion was documented. Finally, if invasion of half or more than half of the myometrium (thinnest part of normal myometrium on sequential sagittal, coronal or axial) then deep MI was documented.

6.3.3 Statistical analysis

A power calculation demonstrated the need for 56 patients with endometrial cancer (anticipated mean diagnostic ability 90% standard deviation 10%, error rate (alpha) 5%, 80% power).

Cases in which histopathological results (reference standard) were indeterminate or missing were excluded from all analyses. The statistical analysis was performed using SPSS version 24.0 (SPSS Inc., Chicago, IL, USA). Continuous data were presented as mean, standard deviation and range. Categorical data were presented as percentages. The Sensitivity, specificity, positive predictive value (PPV), negative predictive value (NPV) were calculated. Summary receiver operating characteristic (ROC) curves were created along with area under the curve (AUC) measurements. Histopathological findings were considered the reference standard.

6.4 Results

Over 100 patients underwent 3D ultrasound scans in the rapid access clinic for suspected endometrial cancer during the study period. Of these, 36 patients had

endometrial carcinoma proven by histological diagnosis and 9 patients were later excluded as the patients never received definitive surgery (hysterectomy), as such, no final histology were available. The remaining 25 patients met inclusion criteria for the study. The patient demographics and histologic features are presented in Tables 22. The mean age was 61 years old with standard deviation 13. There were no cases of myometrial invasion diagnosed in women who did not have cancer.

Parameters	**Patients n (%)**
Histological type:	
Endometrioid	20/25 (80%)
Carcinosarcoma	2/25 (8%)
Serous papillary	2/25 (8%)
Clear cell	1/25 (8%)
Histologic grade:	
G1	12/25 (48%)
G2	4/25 (16%)
G3	9/25 (36%)
FIGO Stage	
1A (<50% MI)	15/25 (60%)
1B (≥50% MI)	4/25 (16%)
2	3/25 (12%)
3/4	3/25 (12%)
Cervical invasion	5/25 (20%)

Table 22. Histological summary of patients who underwent a 3D ultrasound.

Example images of superficial and deep invasion assessed using the subjective technique are demonstrated in Figure 69. The diagnostic accuracy of subjective assessment and objective ultrasound measurement techniques and MRI in predicting deep myometrial involvement are shown in Table 23 and Table 24, along with summary ROC curve (Figure 70). Of note, only 16 patients (64%) had an MRI scan.

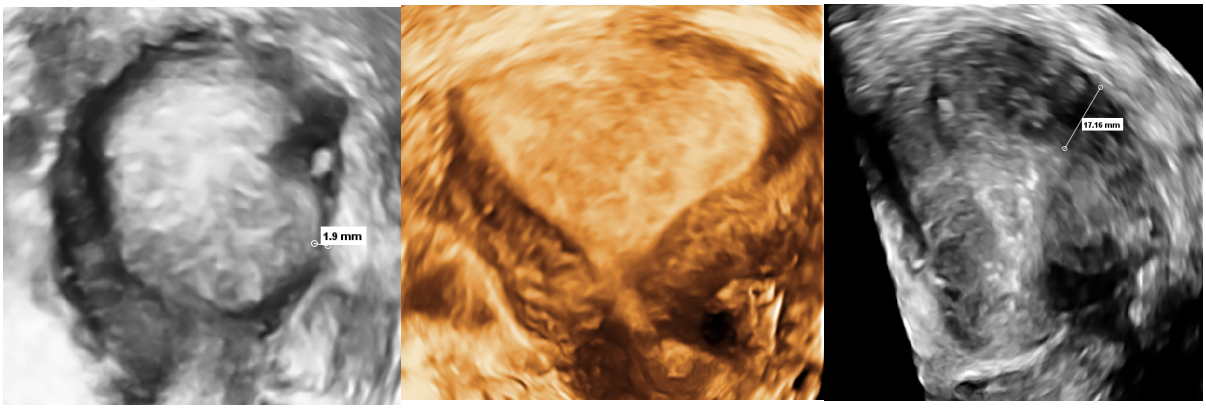


Figure 69. 3D scan images.
Left and middle image show deep myometrial invasion. Image on right shows superficial myometrial invasion. In some of the images the TDS = the distance from tumour to serosa is shown.

	3D USS show deep MI using subjective assessment		
Deep MI in Final histology	**+ve (≥50% MI)**	**-ve (<50% MI)**	**Total**
+ve (≥50% MI)	8	2	10
-ve (<50% MI)	5	10	15

Table 23. Results of subjective assessment in the diagnosis of deep myometrial invasion (MI).

	Subjective assessment	**Objective assessment TDS**			**MRI**
		9mm	**7mm**	**5mm**	
Sensitivity	80%	89%	89%	80%	80%
Specificity	67%	50%	56%	80%	82%
PPV	62%	50%	53%	73%	67%
NPV	83%	89%	90%	86%	90%
Overall accuracy	72%	64%	68%	80%	81%
AUC	0.818	0.727	0.773	0.809	0.809

Table 24. Summary table of diagnostic performance of 3D ultrasound using different threshold for deep myometrial invasion (9mm, 7mm and 5mm) along with MRI scans.
PPV = positive predictive value, NPV = negative predictive value. AUC = area under the curve

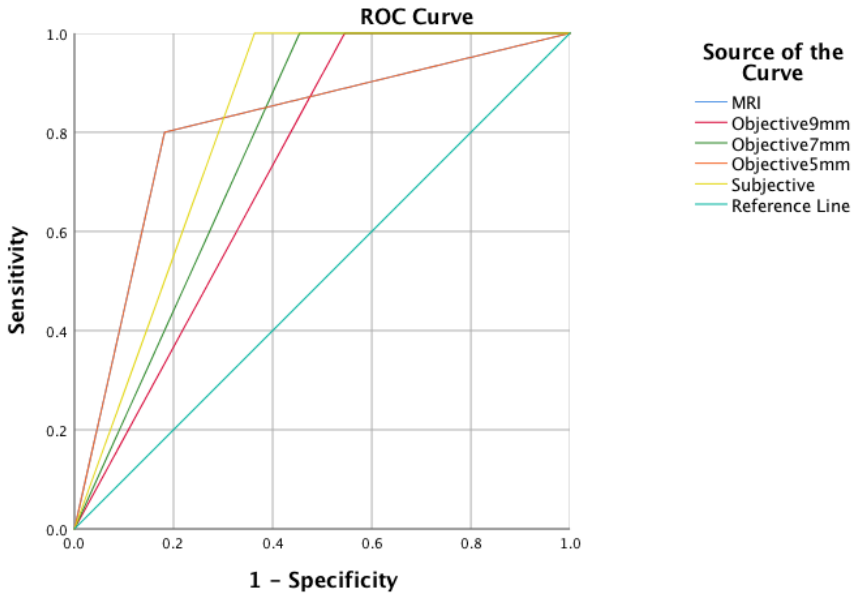


Figure 70. Summary ROC curve showing diagnostic performance of 3D ultrasound using different threshold for deep myometrial invasion (9mm, 7mm and 5mm) along with MRI scans.
The line for MRI overlaps objective assessment using 5mm threshold.

The time taken between 3D ultrasound imaging and surgery was a median of 34 days (range 1-264 days, interquartile range 47). The patient who took 264 days to from imaging to surgery underwent egg freezing first, thus delaying definitive surgery. No adverse events occurred.

6.5 Discussion

6.5.1 Main Findings

This study demonstrates moderate performance of 3D ultrasound in the assessment of deep myometrial invasion in women with endometrial cancer; performing favourably compared to MRI, the current gold standard. Of the techniques employed subjective assessment had the highest overall AUC, marginally better than objective techniques using the shortest tumour distance to serosa (TDS) and a 5mm cut off. Non-invasive methods that accurately determine myometrial invasion are essential to enable adequate pre-operative surgical planning and appropriate surgery. Ultrasound is a relatively cheap technology which is well tolerated by patients. Three dimensional scans enable multiplanar imaging, which can be saved and rendered by an expert at a later date. They are particularly useful to visualise the cornu of the uterus. The technique is simple to learn, and acquisition of 3D images takes seconds. The findings

of this study add weight to the role of 3D USS in pre-operative imaging of women with endometrial cancer.

Previous recent meta-analyses have found that pelvic MRI has, in general lower sensitivities (79-83%) than specificities (82-88%) [135, 440, 452]. In this study the sensitivity and specificity of MRI are consistent with previous research. MRI is not without limitation; it is expensive, claustrophobic and not always possible (due to patients' weight/presence of a pacemaker). Artefacts such as abdominal wall movement and peristalsis can also affect image quality [140, 453]. In addition, patient related factors may cause misdiagnosis, such as: tumour isointensity with the myometrium, myometrial thinning, polypoid tumour and the presence of adenomyosis and fibroids [140, 454].

In keeping with other studies subjective techniques outperformed objective techniques in the present study [141, 449, 455]. This might be attributed to all the subtle signs seen on subjective assessment including size, blurring of endo-myometrial junction which are not accounted for in the objective methods. In this study the sensitivity for subjective technique was good (80%) but with low positive predictive value (62%) and thus high false positive rate (38%). From a clinical oncological perspective, high sensitivities are required, and false positive results are less clinically important as it is beneficial to perform surgery only once (and avoid a separate operation for lymphadenectomy).

Interestingly, the overall diagnostic accuracy of objective technique using TDS improved as the threshold of deep myometrial invasion reduced from 9mm to 5mm, increasing the number of cases reported as superficial. This is contrary to Alcazar study which suggested the use of 9mm as cut off [136]. The improved accuracy with a 5mm cut-off may be just a reflection of the study population and relatively fewer cases of deep myometrial invasion (9/25). Lindauer et al found that the shortest distance of tumour to serosa (TDS) was more important for predicting endometrial cancer recurrence than the depth of cancer invasion [456].

6.5.2 Strengths and Limitations

One of the strengths of this study was the its prospective nature and recruitment of consecutive patients, to reduce selection bias. Indeed, all scans were performed before a diagnosis of endometrial cancer was even made. All scans were also performed by an expert and then reported by a blinded expert at least one year from the date the scan was performed, minimising any bias.

Another advantage of this study was the lack of exclusion criteria on the basis of the presence of fibroids and adenomyosis, unlike Ergenoglu study [449]. Fibroids, and particularly adenomyosis can cause disruption of the endo-myometrial junction and makes interpretation of the images difficult, thereby affecting the reliability of the results and the frequency of false positives. High risk cases such as more advanced and aggressive tumours (serous/clear cell) were also included in my dataset. No cases were excluded on the basis of suboptimal 3D images. Inclusion of all these cases help to ensure that the results of this study are generalisable to the wider population.

This study only used the shortest distance from tumour to serosa (TDS) as its objective method and did not assess cervical invasion, which is a limitation of the study. With TDS, it is known healthy women may have a thin myometrium and the cut-off value for deep myometrial invasion has yet to be thoroughly validated. Mascilini et al found that tumour/uterine antero-posterior diameter had similar performance to subjective techniques [141]. It may be that other objective techniques are superior and require further investigation.

Whilst 3D scans are simple to perform there is a learning curve for the procedure and the interpretation of images. To this end, in order for this technique to be widely used, upskilling of staff is required.

The biggest disadvantage of this study was the small sample size. As mentioned in the methods section, the power calculation revealed that a minimum of 56 patients with endometrial cancer needed 3D scans performed, but this study fell short. Recruitment was difficult due to resource and time limitations during my PhD. Whilst many patients with suspected cancer underwent a 3D scan in clinic, only a minority of these had a final diagnosis endometrial cancer and were included in the analysis. My ethics approval will enable continued recruitment over the next year to increase the sample size further. To this end, this project has been handed over to another clinical

fellow to continue this work. However, in the interim, to reliably establish if 3D USS has sufficient diagnostic ability to be used to diagnose deep myometrial invasion a meta-analysis needs to be performed, which can then pool the results from multiple studies. In the next chapter of my PhD I perform a systematic review and meta-analysis on this topic.

6.5.3 Conclusions

In summary, in this small study, 3D ultrasound particularly using subjective assessment performed comparably against MRI at identifying deep myometrial invasion. But, with added advantage of being cheaper, more accessible and better tolerated than an MRI. Due to the small sample size a systematic review and meta-analysis are required to confirm these findings.

CHAPTER 7: 3D ULTRASOUND SYSTEMATIC REVIEW AND META-ANALYSIS

CHAPTER 7: 3D ULTRASOUND SYSTEMATIC REVIEW AND META-ANALYSIS

7.1 Summary

Objective: Three-dimensional ultrasound is becoming more accessible and widely used in gynaecology. The aim of this meta-analysis were to evaluate the diagnostic accuracy of 3D ultrasound in the pre-operative assessment of deep myometrial invasion and cervical invasion in endometrial carcinoma. Both subjective and objective techniques for deep myometrial invasion were assessed.

Methods: Electronic searches were conducted using PubMed, EMBASE, Google Scholar and Cochrane database to the end of March 2020. Studies included needed to specify the use 3D ultrasound in women with endometrial cancer and the method of evaluation of deep myometrial invasion. Study quality was assessed using the QUADAS-2 tool.

Results: 2971 studies were retrieved; 49 full text studies were selected for detailed assessment and 9 studies were included in the final analysis. Using subjective assessment, the pooled sensitivity, specific, positive likelihood ratio (LR+) and negative likelihood ratio (LR–) for detecting deep myometrial infiltration using 3D ultrasound were 81% (95% CI, 72–87%), 84% (95% CI, 79–88%), 5.1 (95%CI, 3.6–7.1) and 0.22 (95%CI, 0.22–0.34) respectively. Significant heterogeneity was found, with an I^2 of 59.0% (95% CI, 28.8 - 89.2%) for sensitivity and I^2 of 45.2% (95% CI, 3.0 – 87.4%) for specificity. Due to the limited number of studies it was not possible to pool the studies assessing objective assessment of deep myometrial invasion and cervical invasion.

Conclusion: Three-dimensional ultrasound has comparable diagnostic performance in detecting deep myometrial infiltration in women with endometrial cancer, when compared to MRI. Differences in methodologies hampers any comparison of objective techniques in the assessment of deep myometrial invasion.

7.2 Introduction

Endometrial cancer is the 6th most common cancer in women worldwide. The key prognostic features of endometrial cancer are the FIGO stage (International Federation of Gynecology and Obstetrics), histological type and grade of differentiation, and the

presence of lymphovascular space invasion (LVSI). Indeed, most of these are independent predictors of outcome [44, 457, 458]. Depth of myometrial invasion (MI) is pivotal in the assessment of stage 1 disease and correlates strongly with prognosis and nodal spread [129, 438, 439]; with stage 1A defined as no, or less than half myometrial invasion and 1B with invasion equal or more than half of the myometrium. The risk of lymph node metastases and extension into the parametrium increases significantly in those with MI ≥50% [438, 459]. Conversely, in early, well differentiated or moderately differentiated stage 1A disease the benefit of routine lymphadenectomy in is not evident [162]. Thus, selection of low risk cases pre-operatively, based on assessment of MI will enable better surgical planning and avoid unnecessary lymphadenectomy, which is not without its complications.

Different modalities have been applied to assess the depth of MI pre-operatively or intra-operatively. Studies using intra-operative gross evaluation and frozen section have had mixed findings and overall it is not thought to be sufficiently reliable to be used in isolation [460-467].

Several imaging techniques are also currently employed, including: transvaginal ultrasound (TV USS), computed tomography (CT) and magnetic resonance imaging (MRI) [455, 468-470]. Since 1989 when the first paper citing the use of TVS to assess MI, TVS has been used extensively [471]. Both subjective and objective measurements have been used. The latter have been proposed by Gordon and Karlsson respectively [472, 473]. Gordon's approach is the ratio of distance between maximum tumour depth and the total myometrial thickness. Karlsson's approach is the ratio between maximum anteroposterior diameter of the endometrial lesion, and the uterine anteroposterior diameter, both in the sagittal plane. A systematic review and meta-analysis by Alcazar found the pooled sensitivity and specificity for TVS detecting MI was moderate, 75% (95% CI, 67%-82%) and 82% (95% CI, 75%-93%) respectively [135].

More recently, three-dimensional ultrasound (3D USS) has been studied for detection of deep myometrial invasion, with promising results [446, 447]. It enables, calculation of 3D volumes and review of images in multiple planes, in addition to enhanced assessment of vasculature using power Doppler, 3D-power Doppler angiography (3D-PDA). Additionally, the coronal view may add valuable information about myometrial

invasion in the uterine corners and 3D rendering techniques may enhance tissue demarcation [138, 139]. Images can be stored for comparison and rendering at a later point. Two studies have also reported less user dependant findings with 3D versus 2D USS [450, 474].

The first few studies examining 3D USS and endometrial cancer looked at whether mean endometrial thickness (ET), tumour or endometrial volume and vascularity was higher in women with ≥ 50% MI [447, 475, 476]. In Galvan study endometrial volume (EV) and vascularization index were independently associated with myometrial infiltration with EV: odds ratio (OR), 1.119 (95% CI, 1.025–1.221), but they did not use these metrics to predict MI [477]. Further studies, similar to 2D ultrasound, used subjective and objective assessments to predict MI , as described by Alcazar [137, 446, 450], with subjective assessment performing superiorly [137]. Objective assessment involved calculating the shortest tumour distance to serosa (TDS). A cut-off of <9mm was used for predicting ≥50% MI. Meanwhile, subjective assessment involved looking for asymmetry in myometrial-endometrial interface in the tumour and supposedly tumour-free myometrial wall. If marked asymmetry was found, deep (≥50%) infiltration was diagnosed; if myometrial thickness was similar in both myometrial walls, superficial (<50%) infiltration was diagnosed.

MRI, however remains the gold standard imaging modality in the UK for assessment of myometrial and cervical stromal invasion, as well as lymph node metastases [3, 453, 468, 478-483]. Though not without limitations, it provides excellent soft tissue contrast resolution, with multiplanar capabilities [484]. A meta-analysis by Luomaranta found a pooled sensitivity, specificity, positive predictive value, and negative predictive value of 80.7%, 88.5%, 77.6%, and 89.5% respectively for the assessment of deep MI [440].

This meta-analysis will evaluate the preoperative accuracy of three-dimensional ultrasound for deep myometrial invasion in endometrial carcinoma.

7.3 Methods

7.3.1 Search Strategy

Electronic searches were conducted using PubMed, EMBASE, Google Scholar and Cochrane database to the end of March 2020. The search was limited to studies in humans and English language text. The only exclusion for study design was case studies. The following search terms were used: (((Ultrasound) OR (Imaging) OR (Ultrasonography)) AND ((endometri*) OR (uterine)) AND ((3D) OR (three) OR (dimensional))) AND ((cancer) OR (malignancy) OR (neoplas*))). All article abstracts were reviewed for relevance, and the reference lists and bibliographies of included studies were then searched. Furthermore, a manual search of published cases was performed to identify any additional relevant cases.

7.3.2 Study selection and Data extraction

Following removal of duplicate publications, I examined the electronic search results, checking the titles, abstracts and full text for further detail. Figure 71 adapted from the PRISMA checklist illustrates the study selection process.

Published trials were eligible for inclusion if they assessed depth of myometrial invasion using three-dimensional ultrasound and compared it depth of invasion from the histological specimen (reference standard). Studies required adult participants with biopsy-proven primary carcinoma (or hyperplasia) of the endometrium, at any stage of the disease, undergoing preoperative staging prior to surgery. Hyperplasia patients were included as it is known that up to 40% of patients with hyperplasia will have a concurrent endometrial cancer on histology following hysterectomy [29]. Studies using both subjective and objective assessments of MI were included, but studies needed to specify the method of assessment. Studies not predicting MI, and any studies looking at cervical cancer or uterine myomas were excluded. Studies were also excluded if they did not use 3-D ultrasound for their assessment, or if the study population was not confined to endometrial cancer patients. Following the search query, it was not necessary to contact any authors to retrieve missing data.

7.3.3 Quality assessment and risk of bias assessment

All studies were assessed for quality using predetermined criteria based on the QUADAS-2 tool (Quality Assessment of Diagnostic Accuracy Studies-2) [485]. The

QUADAS-2 tool includes four areas: patient selection, index test, reference standard, flow and timing. For each domain, the risk of bias and concerns were analysed.

7.3.4 Statistical analysis

The diagnostic performance of 3D USS for diagnosing deep myometrial invasion in endometrial cancer patients was extracted from all the studies. All studies used the same reference standard of at least 50% MI representing deep invasion on histopathology. The primary outcome was the pooled sensitivity, specificity, positive and negative likelihood ratio (LR). The analyses were pooled separately for subjective and objective (TDS) approaches. Pooled results were only possible if 5 or more studies were included in the meta-analysis. A randoms effect model was used. A P-value <0.05 was considered as statistically significant.

The thresholds used for LR are of 0.2-5.0 providing weak evidence for confirming or ruling out MI, 5.0-10.0 and 0.1-.02 providing moderate evidence to either confirm or rule out MI, and LR >10 or <0.1 providing strong evidence of confirming or ruling out disease [135, 486]. Additionally, prevalence of deep MI (pre-test probability) was calculated for each group and plotted on Fagan nomograms.

Secondary outcomes were pooled sensitivity, specificity, positive and negative likelihood ratio for the assessment of cervical infiltration subjectively using three-dimensional ultrasound compared to final histology. Similarly, pooled results were only possible if 5 or more studies were included in the meta-analysis.

Statistical heterogeneity amongst the studies was examined by checking for overlap in confidence intervals on the forest plots of sensitivity and specificity. In addition, it was tested formally using both the Cochran's Q test and the I2 index. The null hypothesis for the tests state that all studies evaluated have the same effect; thus, a low P-value <0.1 indicates heterogeneity. The Cochran's Q test is calculated by summating the squared deviations of each study's estimate from the overall meta-analytic estimate and weighting each study's contribution in the same way as the meta-analysis. Meanwhile, the I2 index describes the percentage of total variation across all the studies that is due to heterogeneity as oppose to chance; such that the lower the

% the less the heterogeneity. Higgins study suggests that low, moderate, and high heterogeneity have I2 values of 25%, 50%, and 75% [487].

Summary receiver–operating characteristics (sROC) graphs were created to illustrate the relationship between sensitivity and specificity for both subjective and objective 3D approaches. Deeks funnel plot asymmetry test for publication bias was also performed.

Analyses were performed using MIDAS (Meta-analytical Integration of Diagnostic Accuracy Studies) command in STATA version 16.1 for Mac (Stata Corporation, College Station, TX, USA), Review Manager 5.3 (Revman version 5.3; Nordic Cochrane Center,) for Forest plots and nomograms and R 3.4.1 software for SROC.

7.4 Results

7.4.1 Literature search and study selection

After the initial search, 2971 studies were retrieved, and abstracts reviewed. Forty nine studies were selected for detailed assessment. The main reasons for exclusion were lack of use of 3D ultrasound (15 studies only used 2D) and the lack confirmed endometrial cancer in the study population (19 used 3D in suspected endometrial cancer patients and evaluated whether it could be used to diagnose endometrial cancer). Four studies did not use 3D ultrasound to predict MI involvement, but instead looked at features which discriminate deep MI from superficial, these studies were excluded [140, 447, 477, 488]. Greens study was excluded as it assessed interrater user reliability as focus [489]. The most recent study by Yang et al was also excluded as it did not satisfactorily specify method of assessment of myometrial infiltration [142]. Finally, 9 studies that assessed myometrial involvement using 3-dimensional ultrasound compared to histopathology were included in the meta-analysis. A flowchart of the studies included is shown in Figure 71.

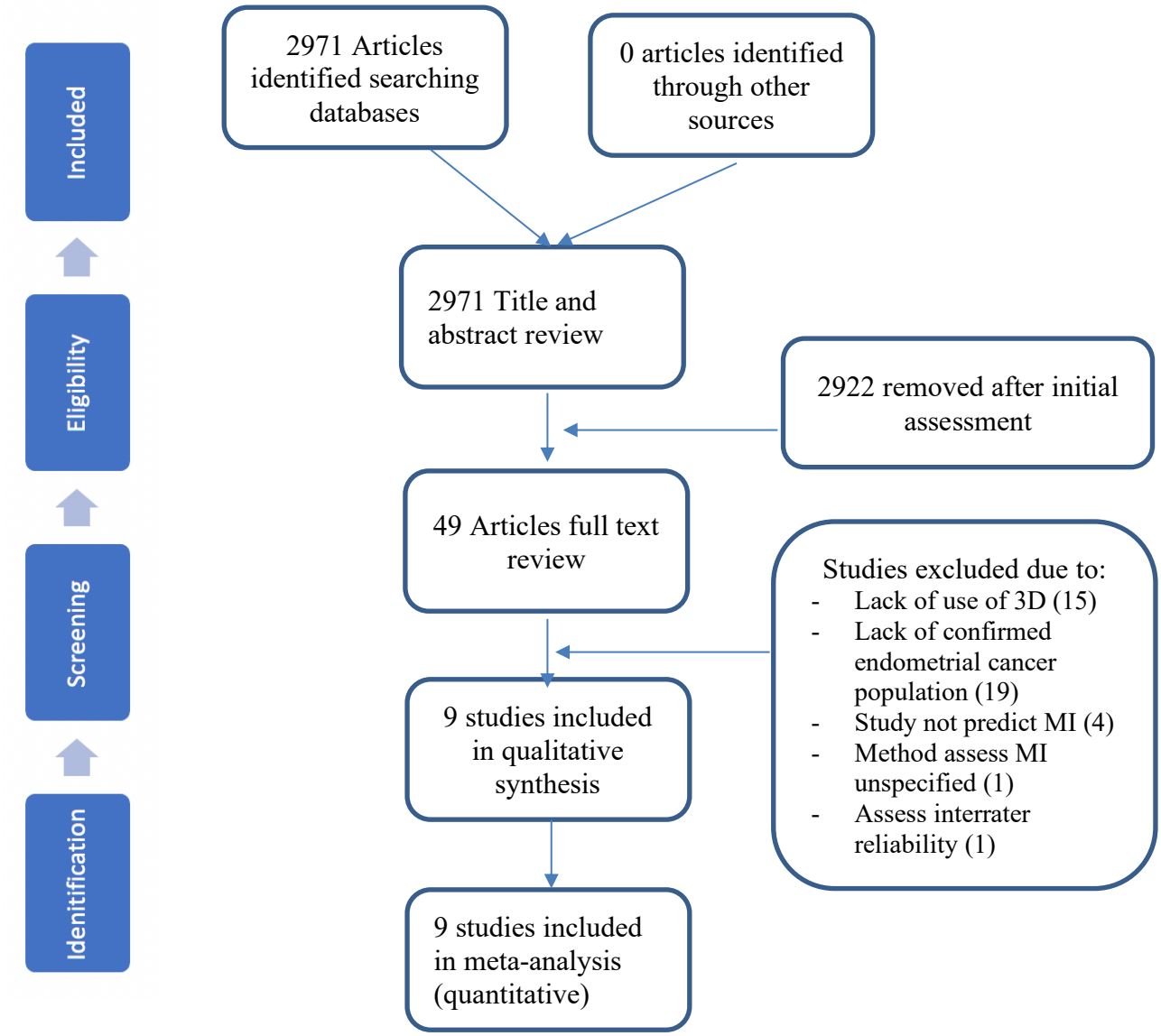


Figure 71. Flowchart of studies included in 3D ultrasound meta-analysis.

7.4.2 Trial Characteristics

The PICOS (Patients, Intervention, Comparator, Outcomes, Study design) criteria used for inclusion and exclusion of studies is shown in Table 25.

Overall, the 9 included studies accounted for 627 women with confirmed endometrial cancer or hyperplasia between 1995 and 2016. These women were aged 31 to 91 years old and 299 women (48%) had MI ≥ 50%. Of these studies 8 were performed in Europe and 1 in Asia.

A pictorial display of the evaluation of the risk of bias and concerns regarding applicability of the selected studies, according to predefined QUADAS-2 criteria, is shown in Figure 72.

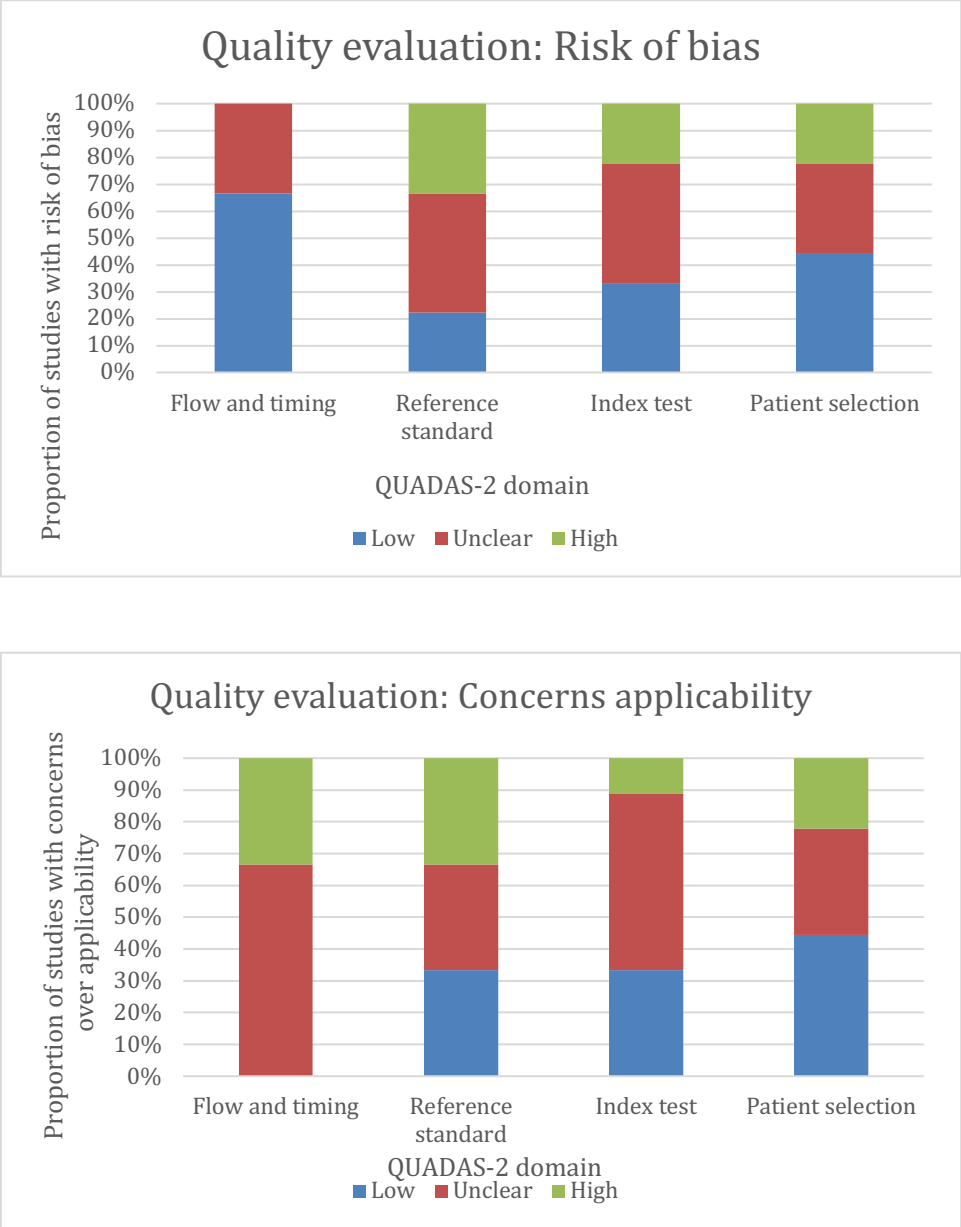


Figure 72. Graphs depicting quality evaluation of included studies. Top looking at risk of bias and bottom looking at concerns over applicability.

Study and year	Number patients	Setting	Consecutive recruitment	Method assessment	Inclusion / Exclusion	Number Observers	Cases ≥50% MI (n)	Comments
Alcazar 2009 [136]	96	Two centres	yes	Subjective and objective TDS	Excluded: - surgery performed elsewhere or not performed -incomplete pathologic report or 3D volume with exclusion of uterine serosal margins	2	69	Blinded observers
Saarelainen 2012 [490]	20	Single centre	yes	Subjective and vascularity index	Nil specific	2	12	Blinded observers Accuracy MRI comparison too
Mascilini 2013 [141]	144	Four centres	yes	Subjective and	Nil specific	3	73	No MRI performed

				objective TDS				
Jantarasaengaram 2014 [139]	40	Single centre	yes	Subjective	Excluded: - Surgery not performed Or >7 days after volume acquisition - patients undergoing neoadjuvant treatment - non-primary endometrial cancer; - suboptimal image resolution - patients with high-risk histological cell types, including Grade 3 endometrioid adenocarcinoma	1	11	Observer not blinded
Alcazar 2015 [137]	169, of which	Single centre	yes	Subjective and	Include:	unclear	21	Not blinded

	74 3D USS			objective (TDS)	- G1 and G2 endometrioid adenocarcinoma			- 3 cases no cancer no cancer and 3 cases sarcoma but both included
Christensen 2016 [138]	110	Single centre	yes	Subjective	Excluded: - Women with known stage 3–4, serous, clear-cell or grade 3 carcinomas	1	47	Cases include hyperplasia with atypia SIS performed
Ergenoglu 2016 [449]	45	Single centre	unclear	Subjective and Objective (TDS)	Excluded: - Patients with intramural leiomyoma >3 cm and submucous leiomyoma	1	9	Blinded observer
Rodriguez Trujillo 2016 [491]	98	Single centre	no	Subjective	Included: - Tumours confined to the corpus uteri	1	39	Compare with Diffusion weighted MRI

					- scans and surgery performed in their hospital Excluded: - patients who received neoadjuvant treatments - Diagnosis of Sarcoma			
Yildirim 2018 [448]	40	Single centre	no	Subjective	Excluded: - advanced stage which were not operable	unclear	18	Blinded observer

Table 25. Summary table of key features of included studies.

Patient selection:

Regarding patient selection, 2 studies did not document whether the patients were consecutive or random, which is concerning that inappropriate exclusions may have been made. Three studies excluded high-risk groups such as Grade 3 endometrioid adenocarcinoma and sarcomas, and 2 excluded advanced cancers. But three studies did not clearly report inclusion and exclusion criteria. No patient underwent oncological treatment between imaging and surgery.

Index Test:

All studies described clearly the index test, how it was performed and interpreted. Six studies did not blind the sonographer/observer to the histopathological/MRI diagnosis which may bias their interpretation of MI.

All 9 studies used subjective assessment of myometrial invasion and 4 used the objective metric TDS. Although, it should be noted, that even with 'objective approaches' a subjective measurement of tumour and serosal margin is made by an individual examiner.

Reference standard:

All studies used histopathology as reference standard and used the FIGO staging for depth of invasion, defining deep MI as ≥50% myometrial thickness. Most studies did not describe the details of how this was done. Only 2 studies stated clearly that the histopathologists were blinded to the TVS result. Two studies compared the diagnostic performance of 3D ultrasound to the reference standard (histopathology) and MRI.

Flow and timing:

Three studies did not report the interval between USS and surgery, or this information was unclear. The other cases were performed between 24 hours and up to 15 days from the date of surgery. No studies were excluded from this meta-analysis on the basis of methodological flaws.

7.4.3 Overall Diagnostic performance of 3D Ultrasound for myometrial invasion

The overall performance of the different diagnostic tests is depicted in the table below (Table 26).

Parameter	For Myometrial Invasion
	Subjective
Sensitivity %, (95% CI)	81 (72–87)
Specificity %, (95% CI)	84 (79- 88)
LR+ (95% CI)	5.1 (3.6-7.1)
LR- (95% CI)	0.22 (0.15-0.34)

Table 26. Summary table of diagnostic accuracy using 3D ultrasound to assess myometrial invasion. LR = likelihood ratios

7.4.4 Diagnostic performance of 3D Ultrasound using subjective assessment for the detection of deep myometrial invasion

Overall, for the 9 studies included in this meta-analysis, the pooled sensitivity, specificity, LR+ and LR– of 3D ultrasound in detecting deep MI using subjective measures were 81% (95% CI, 72–87%), 84% (95% CI, 79–88%), 5.1 (95%CI, 3.6–7.1) and 0.22 (95%CI, 0.22–0.34). Forest plots illustrating the individual studies sensitivities is shown in Figure 73 along with the summary ROC curve In Figure 74 (AUC = 0.89 [0.86 - 0.92]).

Heterogeneity was moderate for sensitivity and specificity with I^2 of 59.0% (95% CI, 28.8 - 89.2%) and I^2, 45.2% (95% CI, 3.0 – 87.4%) respectively. Deeks funnel plot for publication bias is illustrated in Figure 76.

The number of cases of deep myometrial invasion out of the total in this subgroup, gave a prevalence of 0.35 (267/762). Based on this, Fagan nomograms were created, (Figure 75). This shows that a positive test significantly increased the pre-test probability of deep myometrial invasion, while a negative test significantly decreased it.

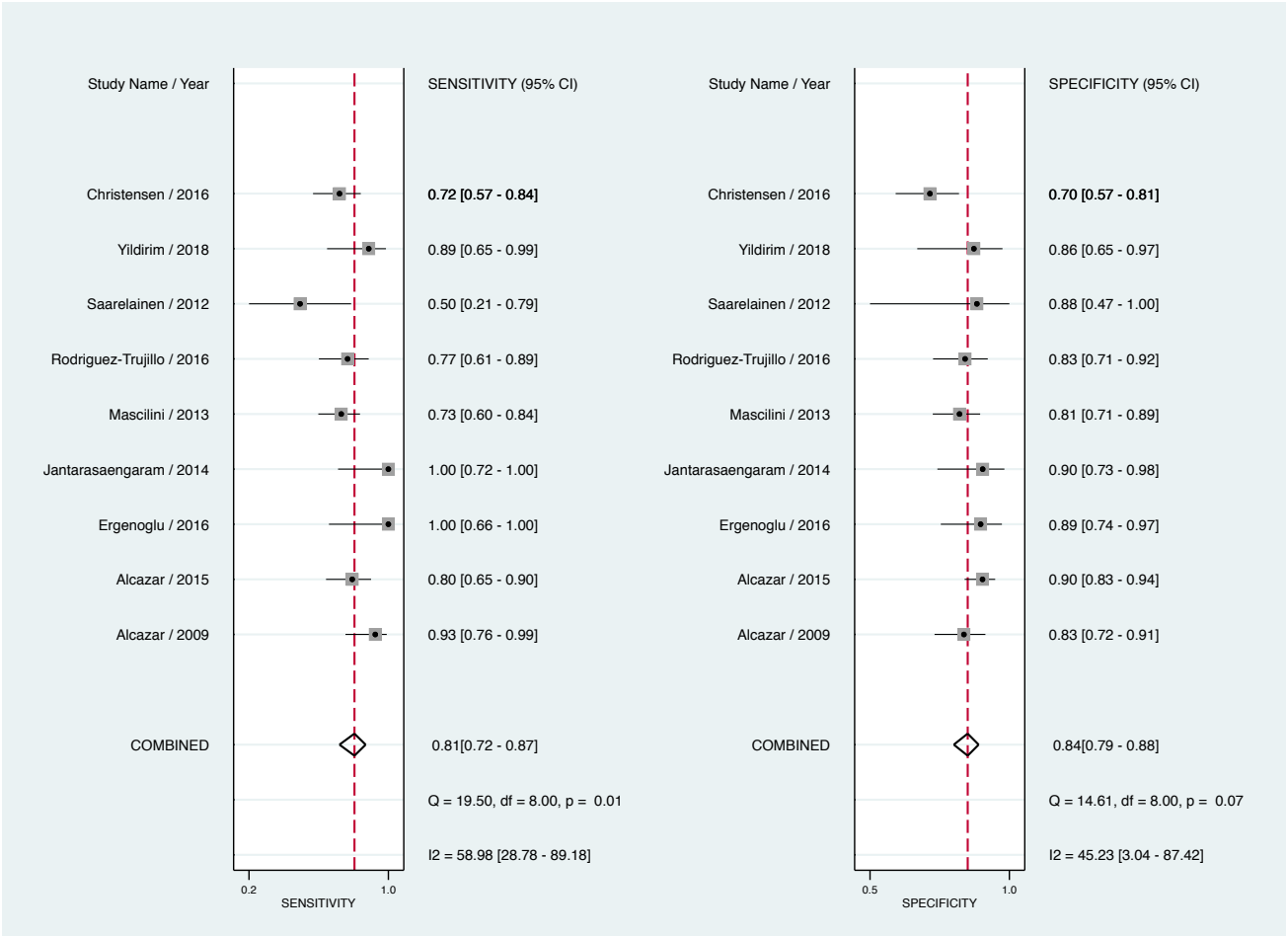


Figure 73. Forest plot of included studies in meta-analysis looking at accuracy of subjective assessment of deep myometrial invasion using 3D ultrasound.

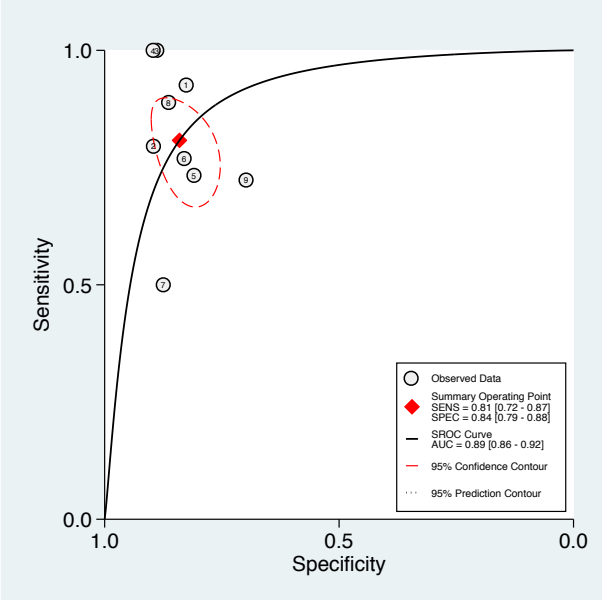


Figure 74. Summary ROC curve of pooled studies in meta-analysis looking at accuracy of subjective assessment of deep myometrial invasion using 3D ultrasound.

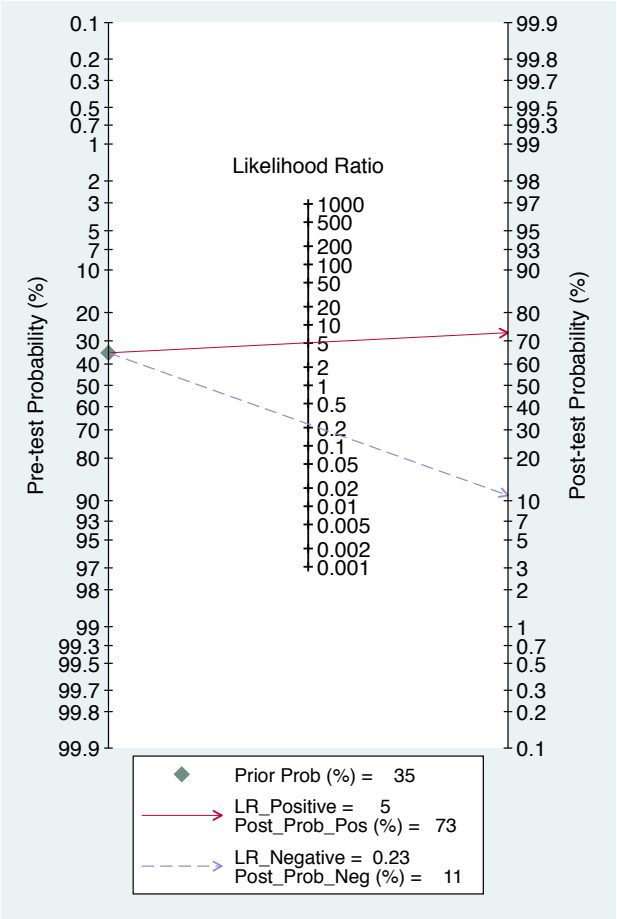


Figure 75. Fagan nomograms, showing likelihood ratios based upon pooled results from meta-analysis.

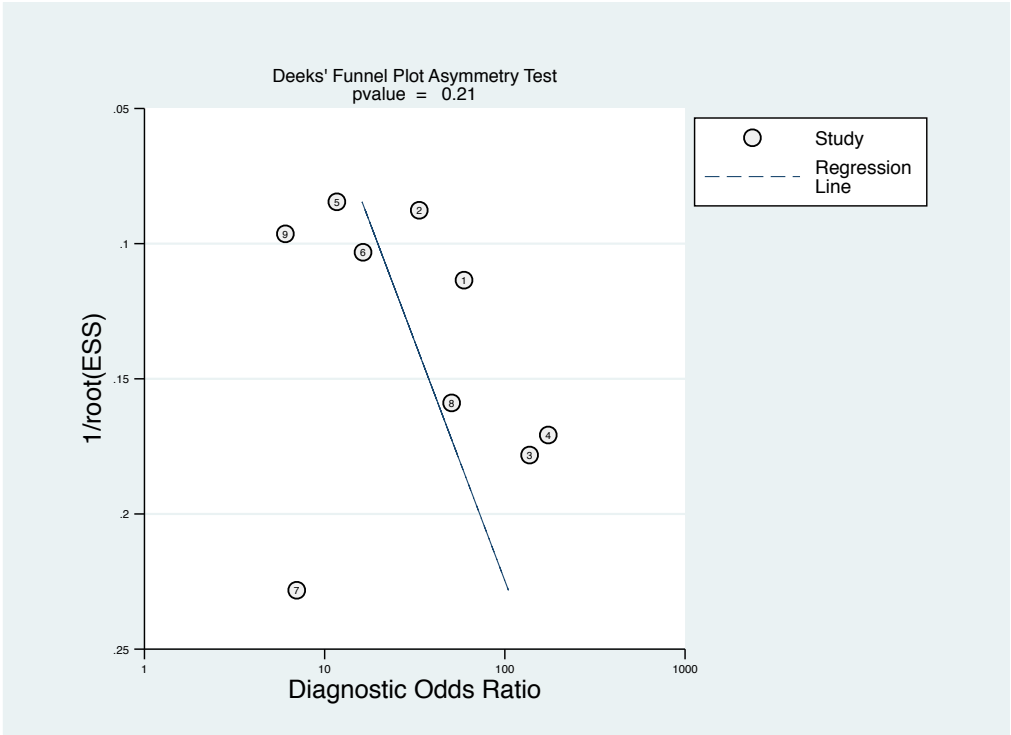


Figure 76. Deeks funnel plot for publication bias.

7.4.5 Diagnostic performance of 3D Ultrasound using objective assessment for the detection of deep myometrial invasion

Overall, 4 studies evaluated the performance of using objective measure TDS in 3D to diagnose deep MI. Pooled sensitivity, specificity, LR+ and LR– of 3D ultrasound in detecting deep MI using objective measures was not possible due to the lack of studies available. Forest plots illustrating the individual studies sensitivities is shown in Figure 77.

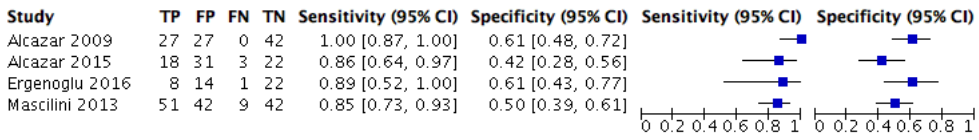


Figure 77. Forest plot of included studies in meta-analysis looking at accuracy of objective assessment of deep myometrial invasion using 3D ultrasound

The number of cases of deep myometrial invasion out of the total in this subgroup, gave a prevalence of 0.35 (164/469).

7.4.6 Diagnostic performance of 3D Ultrasound using subjective assessment for the detection of cervical invasion

Only 3 studies assessed cervical invasion subjectively. No pooled sensitivity, specificity and sROC are possible due to limited number of studies. The sensitivities varied widely between studies: 54-100%, but with overall much more homogenous specificity: 86-97% (Figure 78).

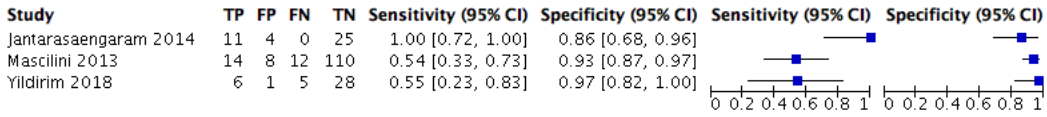


Figure 78. Forest plot of included studies in meta-analysis looking at accuracy of subjective assessment of cervical invasion using 3D ultrasound

7.5 Discussion

7.5.1 Main findings

Myometrial invasion is a key factor determining lymph node metastasis. Even in low grade endometrioid cancers lymph node metastatic risk increases from 3-5% to 15-30% when there is deep myometrial invasion present [128, 438]. Thus, non-invasive methods of diagnosing MI enable accurate planning of surgery and adjuvant treatment. Lymphadenectomy surgery itself has inherent risk, particularly in patients with co-morbidities such as diabetes, advanced age and obesity [491, 492]. Studies have reported rates of lymphoedema in the lower limbs (28-38%), lymphocele formation (9-17%), thrombosis (3.5-5%) and ileus (1.4-6%) [491-494]. It is worth noting that in the UK, lymphadenectomy is offered only in high-risk cases (MI, high grade or type 2 tumours). As can be seen in Table 27 taken from the GOG study [129], by not offering lymphadenectomy to all women with endometrial cancer, approximately 3% of women with lymph node metastasis will be missed, and this is current accepted practice.

	Depth of myometrial invasion	
	Inner third	Outer third
Grade 1	3%	11%
Grade 2	5%	19%
Grade 3	9%	34%

Table 27. Risk of lymph node metastasis from GOG study.
621 patients with a lymphadenectomy were evaluated for lymph node metastasis and classified with respect to grade of tumour and depth of myometrial invasion as part of GOG study.[129]. .

This meta-analysis is the first to assess performance of 3D ultrasound using subjective assessment for deep myometrial invasion in endometrial cancer. It shows an overall high diagnostic rate, with a sensitivity and specificity of 81% and 84% respectively. This compares slightly better than studies using conventional 2D USS which have a pooled sensitivity and specificity of 75-82% and 81-82% [135, 455] and is in keeping favourably with studies using MRI which have sensitivity of 79-90% and specificity 81-91% [135, 440, 452, 484, 495, 496]

The positive and negative likelihood ratio of detecting MI using subjective assessment in this study was 5 and 0.23 respectively. As the diagnostic accuracy of a test is strongly dependent on the prevalence (or pre-test probability) of a diagnosis it is important that the prevalence of deep MI in this study reflects that of the general population, in order to be applicable. Within this cohort the prevalence of deep MI was 0.35. It is known at presentation in the UK, approximately 74% of endometrial cancers are stage 1 [497]. Of those stage 1, approximately 31% are 1b and 69% are stage 1a, which is in keeping with prevalence found in this meta-analysis [484]. These likelihood ratios provide moderate evidence that subjective assessment using 3D USS can confirm deep MI but weak evidence that subjective assessment using 3D USS rules out deep MI. Given the cost, accessibility and limitations of MRI, 3D USS maybe a good option. It has the advantages of being cheaper, well tolerated, possible in women with pacemakers and severe obesity and enables multiplanar sequential imaging which can be stored.

At present, lymphadenectomy is already recommended for high risk cases (grade 3/type 2 tumours), the main advantage for both 3D and MRI are to accurately predict those patients with myometrial invasion (Stage 1B) and recommend lymphadenectomy for these cases too. Despite this, even if we assume 100% accuracy of the imaging modality we will still effectively ‘miss’ 4-5% of cases with lymph node involvement. In

addition, the extra trade-off for using 3D ultrasound versus MRI for pre-operative imaging is lack of imaging for other areas of the pelvis (such as cervical invasion and lymph nodes themselves). It will also require a cultural shift in the norm within the multi-disciplinary meetings, with more emphasis on the clinician with expertise on 3D ultrasound interpretation of the images.

Although many techniques for objective assessment of MI exist such as Karlssons criteria, endometrial thickness, tumour/uterine 3D volume ratio [446]. The measurement of the myometrial tumour-free distance to the serosa (TDS) is the most widely reported. Histopathological TDS has also been shown to be predictive of recurrence risk and survival in multivariate models [456]. Subsequently, in this meta-analysis TDS was used. But interestingly, of the objective techniques evaluated in Mascilini study tumour/uterine AP diameter ratio and minimal tumour-free margin/uterine AP diameter ratio seem to be the best, not TDS [141]. It is possible, therefore that alternative objective assessment techniques might have superior diagnostic accuracy, but the lack of studies using these other techniques hindered pooling of results and drawing any conclusions. It is also worth noting, that even while using TDS within this meta-analysis there is some variation amongst the cut off value used. Mascilini analysed the data using two different cut-offs; 7.1mm and 5.1mm, meanwhile Ergenoglu and Alcazar used 9mm as cut off deep MI [136, 137, 141, 449]; these differences may impact strength of any conclusion.

In Mascilini study, subjective assessment outperformed objective measures using (TDS). One of the reasons why subjective assessment of deep MI might be more accurate is that it encompasses multiple features as part of the assessment including: size, regularity of border and vascular pattern.

Various studies have examined the role of 3D-PDA in detecting the presence of deep invasion, using a multitude of different techniques and indices. The diversity of imaging techniques hampers any comparison in the present study. Galvan, Merce and Saarelainen studies reported a correlation between different vascular indices and the depth of myometrial invasion [447, 477, 498].

In the current meta-analysis, only 3 papers met the inclusion criteria for evaluation of cervical invasion using 3D USS. These studies reported a sensitivity of 54-100% and

specificity 86-97%. Only 48 patients within these studies had cervical invasion out of 224 (21%). The lack of studies and low prevalence of cervical invasion makes meaningful conclusions unreliable. Historically cervical invasion was diagnosed with cervical curettage, however due to low rates of accuracy (51%), this has been superseded by MRI [499, 500]. However even with MRI the sensitivity and specificity are suboptimal, 33–69 % and 82–96 % respectively [165, 500-502]. It is worth noting that prior to the FIGO 2009 guidelines cervical mucosal infiltration was counted as cervical infiltration. Whilst nowadays cervical infiltration refers specifically to cervical interstitial infiltration. This does mean that older studies using the old definition of cervical infiltration cannot be included in any future analysis.

It is known that 3D ultrasound requires expertise and a learning curve is warranted. Indeed, as obesity is a strong risk factor for development of endometrial cancer, many women who require a scan will be obese; and this can impact on the clarity of the ultrasound image, as obesity often causes the uterus to take an upright position. In experienced hands, alterations in positioning of the patient and probe can mitigate this problem to some extent. The accuracy of 3D scan findings is also related to the number of cases the clinician see annually [489]. Thus, ideally, all studies should have a limited number of expert observers to ensure they have adequate case load per annum. Within this meta-analysis, there were 1-3 observers per study.

There have also been some concerns about reproducibility of 3D ultrasound findings and their interpretation. Two studies have addressed this. Green et al assessed the presence of deep MI from 58 patients with endometrial cancer using 15 different expert observers. Median accuracy for diagnosing deep MI varied from 59-84% between the observers. They also found interrater reliability was better for 2D-USS than for 3D-VCI [489]. Alcazar reported high intra-observer and inter-observer reproducibility for TDS measurements [136].

7.5.2 Strengths and Limitations

The main strength of this study is that is the first meta-analysis using 3D ultrasound to assess deep myometrial invasion. Over 600 women are included in the pooled analysis. Additionally, this meta-analysis was performed using a thorough search for

articles on the diagnostic accuracy of 3D ultrasound in women with endometrial cancer. By searching with all synonyms for 3D USS and endometrial cancer, I think I selected all the articles on this subject. Only one study was excluded on the basis of language.

The main limitation of this meta-analysis is the small number of studies and small number of patients within each study. This is particularly true for the objective assessment of MI and the subjective assessment of cervical infiltration which only had 3 or 4 studies included. Whilst theoretically a minimum of 2 studies are needed for a meta-analysis, the standard error using a random effects model will be very large giving wide confidence intervals and low power. The low number of studies in these analyses did not allow for more standard statistical analyses recommended for diagnostic test accuracy reviews, such as pooling sensitivity and specificity using the bivariate model or estimating summary ROCs.

Moreover, the small number of studies can lead to publication bias, namely the results of meta-analysis do not reflect the actual performance of 3D USS. There is a risk of underreporting studies with poor performance outcomes. Reassuringly, the statistically nonsignificant P value of 0.2 for the slope coefficient on Deeks funnel plot suggests symmetry in the data and a low likelihood of publication bias. However, the test is known to have low power due to only inclusion of only 9 studies.

One, recent large study examining 314 women with endometrial cancer and comparing 3D USS to both MRI and histopathology was unfortunately excluded on the basis on the absence of any details regarding the method of assessment of MI [142]. Their findings for diagnostic accuracy of 3D-TVS for MI were 86.36%, 91.07%, 79.17% and 94.44%, for sensitivity, specificity, PPV and NPV respectively [142]. Given the size of this study it would add significant weight to the current pooled analysis.

Significant heterogeneity was observed between the studies in terms of sensitivity and specificity. The most common reason for this in diagnostic studies is the threshold effect. In this systematic review it is likely that the collected data will be a mixture of different positivity thresholds. When using objective metrics such as TDS, this can be easily understood. As per Mascilini study altering the TDS cut off from 5.1mm to 7mm had a big impact on changes in sensitivity and specificity. When using subjective

assessment there is a binary cut off for assessment of deep MI, either the patient has it or not. However, even on this subjective assessment, each examiner will have their own internal threshold for a positive result based on judgement rather than measurement. Additionally, there will also be some variation between equipment and implementation of tests.

Another limitation of the meta-analysis is variations in the inclusion criteria of each individual study. Three studies excluded high-risk patients such as grade 3 endometrioid adenocarcinoma and sarcomas, and 2 excluded advanced cancers. Presumably because the assessment of deep MI is unlikely to affect surgical management. Including high risk cases risks overestimating the diagnostic performance as the probability of deep MI is higher in this population. However, the presence of high-risk features will not affect the ability to diagnose superficial or deep MI and including these cases would add to the case number, increasing the confidence of any accuracy measurement.

Of note, Christensen study included patients with hyperplasia and atypia on the assumption that most will have cancer (indeed more than 80% did) but this did mean that the 8 women analysed within the final analysis did not actually have cancer [503]. Additionally, Alcazar study compared both subjective and objective techniques, but only 74 out of the 169 patients in the study received a 3D scan too [137]. Their data didn't separate the subjective impression of deep MI by the examiner into 2D and 3D impression, instead included both. Thus, unfortunately in this meta-analysis a minority of patients in the subjective analysis group using Alcazar et al., data only received a 2D scan.

Interestingly Christensen et al. study included patients with inadequate or suboptimal scans as they wanted to assess the clinical applicability of 3D USS in real life [138]. Conversely, Jantarasaengaram, and Alcazar excluded patients with suboptimal quality images and Ergenoglu also excluded cases where fibroids might have affected quality of assessment [136, 137, 139, 449].

In this meta-analysis the final histopathological result was considered the gold standard reference with 100% accuracy, as used Rutter and Gatsonis HSROC model for the sROC. However, no test is 100% accurate and many studies failed to report the

reference standard with much detail. Two studies did not report consecutive recruitment, risking patient selection bias. Future studies would benefit from improved quality metrics being reported. It is likely that as time advances and improvements in technology continue the diagnostic performance can continue to advance.

7.5.3 Conclusions

In summary, this is the first meta-analysis to assess the diagnostic performance of 3D ultrasound in the assessment of deep myometrial invasion for endometrial cancer. The overall pooled sensitivity and specificity for subjective assessment was 81% and 84% respectively. Too few studies are available to ascertain, the diagnostic performance of 3D ultrasound in assessing cervical invasion and more quality studies are needed.

CHAPTER 8: RADIOMICS

CHAPTER 8: RADIOMICS

Collaborators:

Mr Ioannis Lavdas and Mr Xingfeng Li did all the statistical analyses and modelling. Dr James Russell and Dr Nishat Bharwani and Prof Rockall provided the segmentations and VOI. Prof Rockall, Dr Bharwani and Dr Eric Aboagye and provided advice and guidance on the project.

8.1 Summary

Objective: To identify imaging signatures that predict high risk histology and survival in women with endometrial cancer using baseline T2 weighted MR images.

Methods: A total of 464 retrospective patients were enrolled and divided into a training cohort and validation test (80:20). All patients underwent preoperative MRI, had final histopathology and had at least 3-year survival data. Imaging features and radiomic features were extracted and delineated to predict (i) type, grade and stage of tumour (ii) overall survival and recurrence of endometrial cancer. Twenty-one machine learning algorithms were then used to classify the features. Feature selection used a combination of methods including: PCA, cross correlation, least absolute shrinkage and selection operator logistic regression (LASSO), BestSelect and univariate methods. Stratified 5-fold cross validation was used to calculate accuracy and determine the best model.

Results: In total 990 features were extracted. Prediction of high-risk endometrial cancer was 0.74 using Gaussian Process Classifier (GPC) model. Prediction of endometrial type, grade and LVSI was 0.76, 0.78 and 0.73 respectively. Five year survival was predicted with almost 80% accuracy.

Conclusion: Radiomics has moderate prediction of high risk histologies. Prospective validation of this model will be required with larger datasets.

8.2 Introduction

Tumour heterogeneity and alterations in tumour microenvironment greatly impacts cancer behaviour and survival [504-510]. Methods of objectively quantifying tumour heterogeneity and correlating this with outcomes has yet to be standardised and

validated. Invasive biopsy can provide a microscopic snapshot of tumour heterogeneity but does not evaluate the whole tumour. Imaging can therefore provide a non-invasive way of interrogating the global tumour over multiple time points.

Radiomics is a rapidly expanding field of research and describes the extraction of information from medical images using quantitative features [200, 202]. It was first introduced to decipher genomic expression of tumours although it works on a macroscopic level it has been shown to be useful in oncological imaging [511-513]. Extracted features are often based on tumour shape and textural features and have been used to predict clinical stage, histology and outcome [207, 511, 514-520]. Tumours with high spatial heterogeneity exhibit worse prognosis, which is likely a reflection of more aggressive tumour biology [521].

Research studies in cervical [515], brain [522], lung [518, 523], breast [524, 525] and prostate [526] radiomics have shown promising results in the prediction of oncological outcomes. Most studies in endometrial cancer have evaluated the use of radiomics in the prediction of lymph node metastasis [208-210, 527]. Initial studies, have also found it helpful in the prediction of myometrial invasion and preoperative stratification of patients [211-215, 528, 529]. But radiomics necessitates large amounts of data and these studies are limited by small sample sizes, between 27 and 180 patients.

As described in Chapter 6 and 7, MRI has been shown to accurately delineate both local and regional spread of the tumour and currently remains the gold standard in pre-operative imaging in endometrial cancer [478, 479, 530]. Additionally, advances in MRI have enabled quantitative and functional imaging. For example, diffusion-weighted imaging (DWI) reflects tumour microstructure and dynamic contrast-enhanced MRI reflects tumour metabolism [468, 481, 482]. This helps reduce the subjectivity inherent with imaging interpretation [213]. Humans are not able to appreciate the subtle patterns of tissue alterations (textural features) which can be detected by computer models. In this study MRI was the modality chosen due to its key role in pre-operative surgical planning.

This retrospective study aims to explore if textural features can predict high risk histological features, overall survival and recurrence in endometrial cancer patients.

8.3 Methods

Ethics was approved by the national health research authority and Imperial College NHS trust. To ensure quality of radiomics science and radiomics reporting, the RQS (radiomics quality score) guidance [531] and the TRIPOD (Transparent Reporting of a multivariable prediction model for Individual Prognosis Or Diagnosis) guidelines respectively were adhered to [532]. In brief, a retrospective database of anonymised endometrial cancer patients with their corresponding MRI images were created. Each image was segmented, and textural analyses were performed. Each step is outlined in more detail below.

8.3.1 Patient characteristics and study centre

All patients with endometrial cancer who were reviewed at the specialist gynaecology oncology MDT in West London Cancer network, between October 2011 and 2017 and underwent a pelvic MRI were included in this study. Fifteen hospitals form part of this cancer network. Patients were identified from the cancer registry database. The remaining inclusion criteria were: (1) Histologically confirmed endometrial cancer on final histology, with histology available for review (2) pre-operative T2 sagittal MRI's available for review (3) minimum of 36 months follow-up information available. Patients were excluded if: the MRI imaging had severe motion artefacts, inadequate histopathologic report, follow up duration of less than 3 years. Clinical parameters were obtained from CERNER the online electronic medical records. Survival and recurrence data were updated on the 1st August 2020. Cases with missing data were omitted from the analyses that required the missing data.

The outcome measures that radiomics was used to predict were divided into short-term and long-term outcomes.
Short-term outcomes:

1. Risk classification (described below)
2. Tumour type (type 1 vs type 2)
3. Stage (1,2,3,4), also presence of deep myometrial invasion and stromal invasion
4. Grade (1,2,3)
5. Lymphovascular space invasion, LVSI (positive or negative)

Long-term outcomes:

1. Overall survival
2. Recurrence

8.3.2 Histological analysis

All patients underwent surgical hysterectomy as routine standard of care. The specimens were analysed by dedicated gynaecological histopathologist per standard protocol using the 2009 FIGO staging system. Deep myometrial invasion referred to more than 50% myometrial invasion. Patients were classified into one of 4 risk categories, low, intermediate, high and advanced (Table 28).

Risk classification	Criteria
Low	Stage 1A endometrioid grade 1–2
Intermediate	Stage 1A endometrioid grade 3 Stage IB (Grade 1 and Grade 2) with endometrioid type
High	Stage IB Grade 3 endometrioid type Stage 2 endometrioid type Stage 1 or 2 non-endometrioid type.
Advanced	Stage 3 or 4 any type

Table 28. Risk classification used for radiomics patients

A binary classification of risk was also evaluated, this constituted Low risk endometrial cancer versus all other categories (intermediate/high/advanced) [530].

8.3.3 MRI acquisition

Before undergoing surgical staging, all patients received a pelvic MRI. The images used for quantitative analysis were the matched sagittal T2-weighted pre-contrast images.

8.3.4 Image segmentation and analysis

All images were downloaded from PACS software and anonymised. Voxel size of (0.5x0.5x5mm) was used as this was the most common size used by the images, and therefore minimised artefact caused by image interpolation. Voxels are discussed in more detail later. Tumour volume of interest (VOI), of the all visible the tumour on each

the T2 weighted sagittal MR image were manually segmented using the segmentation tool on ITK-SNAP software (www.itksnap.org, version 3.6.0). This was then checked by two radiology consultants (NB and AR) who provided the VOI ground truth. The radiologists were not blinded to the outcome measure. Each VOI appears as 'mask' - a superimposed image on top of the original MRI that outlines the tumour. This mask can have basic amount of greyscale detail (2gl) or can be complex (256gl). An example segmentation and mask are illustrated in Figure 79.

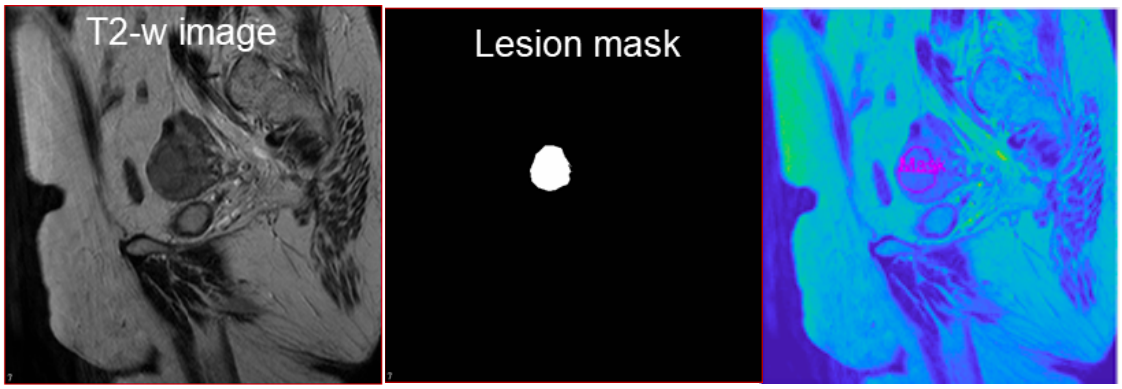


Figure 79. Segmentation process illustrated. Left is a T2 sagittal image of the pelvis. The area of the the tumour (VOI) is outlined as in the right image, and this creates a mask (middle picture).

8.3.5 Radiomic features, selection and statistical analysis

Radiomic features can be classified into: qualitative and quantitative features. Qualitative features are used as descriptors of the lesion [533]. Quantitative features are derived from mathematical algorithms from a computer programme [534, 535]. They vary in complexity and can be extracted directly from the image or after applying transformations or filters. Quantitative features can be further subcategorised into: shape/structural, first-order (FO), second-order (SO) and higher-order (HO) statistical features [535].

The VOI can be thought of as a collection of voxels. Each voxel is an array of elements that represent a 3D object. Shape features (SNS) are the most basic and describe the shape and geometric properties of the VOI, for example, the degree of compactness and surface-to-volume ratio [536]. First-order statistics features describe the distribution of individual voxel values but without concern for spatial relationships. They give a central tendency which can be described with a mean, median, mode, along with a dispersion (and thus standard deviation and range of intensities). They are often

described using histogram images [537]. Histogram images are a graphical depiction of intensity distribution of an image [537]. Statistical measures on the histogram include: voxel intensities, symmetry (skewness), randomness (entopy) and kurtosis (flatness) [535, 537].

Second-order statistics features include textural features and obtained by calculating the inter-relationships between neighbouring voxels, thereby providing a measure of the spatial arrangement of voxel intensities and intra-tumour heterogeneity [535]. Grey level co-occurrence matrix (GLCM) and grey level run length matrix (GLRLM) quantify the incidence of voxels with same intensity along a fixed direction [535, 538]. In GLRLM these voxels are consecutive, and in grey level size zone matrix (GLSZM) the size of each area with pixels of the same intensity level is taken into account [539]. Size zone matrix (SZM) and neighbourhood grey tone difference matrix (NGTDM) and fractal dimensions (FD) are also second-order statistical features [540].

Finally, higher-order statistics are obtained by applying transformations or filters e.g. wavelet transformation, fractal analysis, Minkowski functionals and Laplacian transformations [535].

Many of the radiomics features extracted are redundant. Therefore, following feature extraction, initial efforts focus on reducing dimensionality and feature selection (usually via an unsupervised approach) and associating it with clinical outcomes [535]. In this study a multivariate statistical model was built using TexLAB tool version 2.0 on Matlab R17a (Mathworks).

In the first pilot study Mr Ioannis Lavdas used the endometrial cancer dataset, dividing cases approximately 50:50 into a training set and a validation test set. Textural features were identified, and then classification of features was based on random forest decision trees. Feature selection used a combination of filter methods, wrapper methods and embedding methods that identified the most informative features with maximum relevance and minimal redundancy. Training and fine-tuning occurred using the training data, ultimately creating supervised PC/LDA models. K-fold cross validation (in this case 5-fold) was used initially used to create classification accuracy measurements based purely from the test data. In this, the test dataset is divided into 5 equal proportions. All the training data from one of these 5 proportions was removed,

and then those MRI images were re-introduced into the model to see whether it correctly classifies the outcomes correctly, this is repeated a further four times, and the score of all 5 proportions is averaged. Final classification accuracy measurements are then determined by using this PC/LDA model and introducing the validation test data, which has not been presented to the model before. Confusion table and receiver operating characteristic (ROC) curves were then created for classification performance. The model was used to predict only endometrial type (type 1 and type 2 cancer), endometrial cancer grade (1,2,3) and the presence of lymphovascular space involvement (LVSI). A summary of the radiomics pipeline is illustrated below (Figure 80).

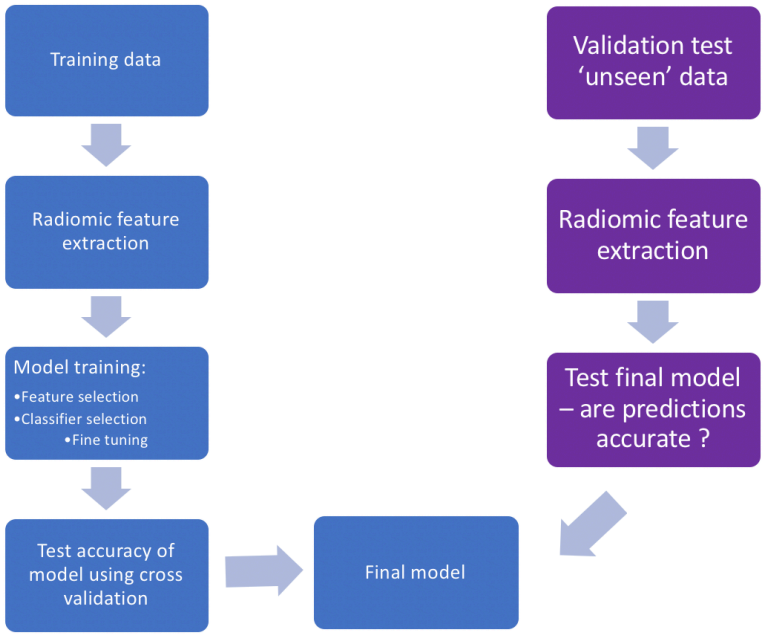


Figure 80. Radiomics workflow, showing test and validation data.

In the larger study, Mr Xingfeng Li, used radiomics to predict the outcome measures described in Section 8.3.1. In addition to TexLAB, PyRadiomics [541] and Scikit-image [542], both in Python [543] were used. Pre-processing and normalisation were performed. N4 image bias correction was performed to remove artefacts due to inhomogeneity of MRI fields [544]. The pelvic MRI images obtained were derived from 15 different hospitals, all part of the West London Gynaecological Cancer Centre network. As a result of variations in MRI machines, the image intensity was subtly different with differences in contrast. Normalisation of intensities was thus required in order to compare all the images on the same scale. This normalisation step was

performed in TexLAB. Textural features were then identified, and feature normalisation performed. As the feature data are not of the same scale, they must be normalised in order to be used for analysis. This is especially important for the PCA method of classification. For example, the feature SNS_area, has a value of around 2900, while for the feature of SNS-S2v, has value of approximately 1. They are not on the same scale for comparison. StandardScaler and MinMaxScaler were used to normalise these features.

Twenty-one machine learning algorithms were then used to classify the features. In addition to the random forest classifiers used earlier, logistic regression (LR), linear discriminant analyses (LDA) were used. Figure 81 lists all the classification algorithms evaluated.

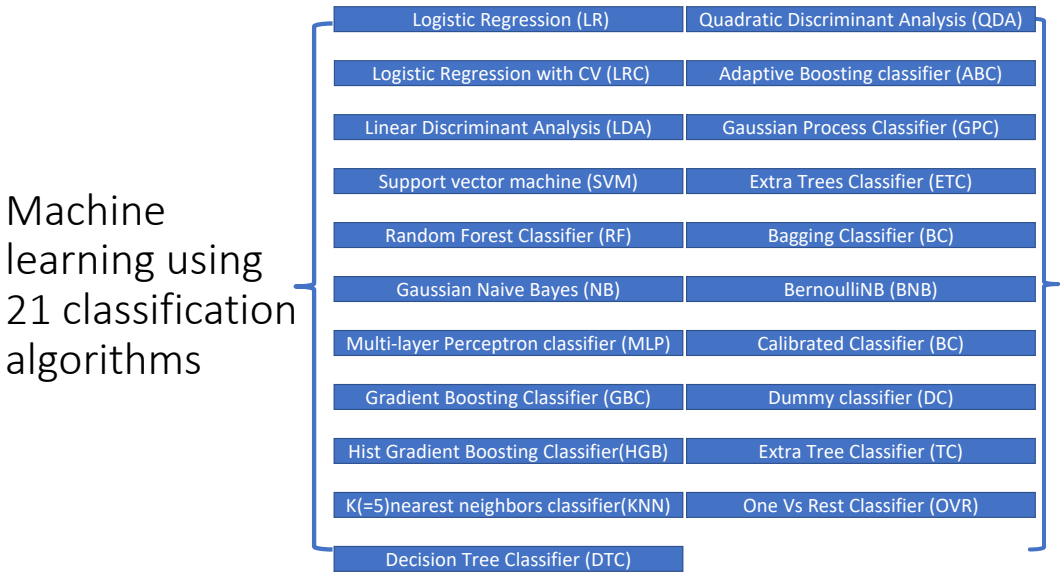


Figure 81. All machine learning classification algorithms used. Calibrated classifier is also known as the abbreviation CCC.

A feature correlation matrix was used in the feature selection process, to remove highly correlated features and avoid the problem of co-linearity. Correlation coefficients adjustment method were also used to reduce the total number of features. Feature selection used a combination of methods including: PCA, cross correlation, least absolute shrinkage and selection operator logistic regression (LASSO), BestSelect and univariate methods. The false discovery rate method was used to adjust for multiple testing.

All data was used to train the model i.e. all data was used as test data, unlike Mr Lavdas analyses. To ensure robustness of the model and avoid overfitting of the data, accuracy was obtained using stratified 5-fold cross validation, as described earlier [542]. Therefore 4 folds for training, and 1 for testing were used, i.e. an 80:20 split for training and test data. A random number generator was used to stratify the splits of the data but preserve the percentage of samples in each class. Figure 82 outlines the cross-validation technique used. A series of boxplots were created for each outcome variable (e.g. survival) using all the classification learning models and using the accuracy derived from 5-fold cross validation. The average accuracy from each split result is represented as a small blue triangle on graph.

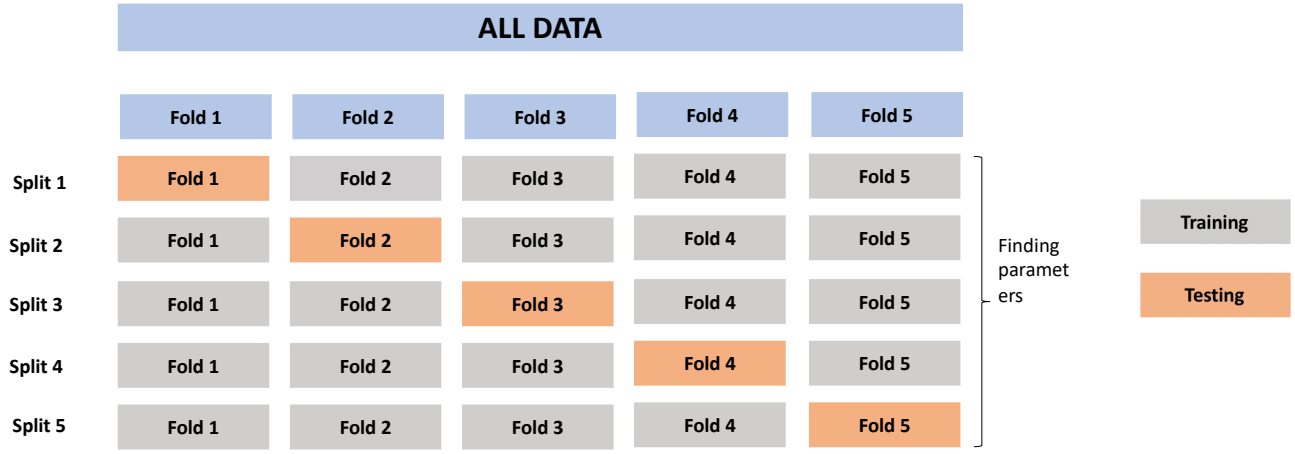


Figure 82. 5-fold cross validation.
All data was used to train the model. The data was divided into 5 folds (proportions). One-fold (20% of the data) was removed and then reintroduced into the model to determine accuracy (test set in orange). This was repeated a further four times. The accuracy was then averaged to determine the final accuracy. This figure was adapted from [542].

8.4 Results: Pilot study – 60 cases analysed by Mr Ioannis Lavdas

Between February 2012 and March 2014, 382 women were diagnosed and treated for endometrial cancer. Of these, 107 patients met the inclusion criteria for the study and their MRI images were segmented. The region of interest (ROI), also known as volume

of interest (VOI) of the tumour and corresponding normal myometrium was manually drawn.

Patient histological and clinical breakdown

Overall, 54% of patients in the pilot dataset had stage 1A disease, 15% had stage 1B, 7% stage 2, 18% stage 3 and 6% stage 4. Low risk cancer i.e. either grade 1 or 2 endometrioid cancer, was found in 62% of patients (with a fairly even split between grade 1 and 2) and 38% of patients had either type 2 cancer or grade 3 endometrioid. LVSI was positive in 33% of cases, negative in 54% and not documented 13% At the time of analysis, 14% of patients were deceased and 19% had disease recurrence.

Textural analysis and feature selection

Analysis was performed by Mr Lavdas. During analysis a further 12 cases were excluded due to technical errors. As described in the methods section the dataset was divided into a training set (30-35 cases) and validation set (30-34 set). All cases used the same voxel size (0.5×0.5×5 mm^3), thus reducing the size of the dataset further. In total 656 textural features were identified. Eighty textural features (FO, SNS, GLSZM, NGTDM, GLRLM, FD, GLCM) were selected along with 6 grey-levels (8, 16, 32, 64, 128, 256). No wavelets were used.

Outcome

Using the PC/LDA models Type 1 and type 2 endometrial cancer lesions were predicted accurately in 60-74% of cases depending on the amount of detail in the grey scale mask, but this accuracy fell to only 50% of cases during final validation (Table 29 and Figure 83). The model could predict the grade of endometrioid cancer and lymphovascular space invasion accurately in only 50% and 44% of cases respectively. The ROC curve has an acceptable area under the curve (AUC) at 0.71 and is illustrated in Figure 84.

	Accuracy (%)		
	Type 1 vs Type 2 cancer	Grade 1 vs Grade 2 vs Grade 3	LVSI involvement

8gl	73.3	51.4	62.5
16gl	63.3	51.4	62.5
32gl	60	48.6	65.6
64gl	66.7*	54.3	59.4
128gl	66.7	51.4	65.6
256gl	66.7	51.4	65.6

Table 29. Accuracy of radiomics model to detect type and grade of endometrial cancer and presence of lymphovascular space involvement (LVSI).

In this small pilot sample only 30-35 patients were used in the test data set which is presented in the table. After which, the validation set was used to confirm the accuracy of the model. On the left-hand column, the grey scale level (gl) represents the detail used in the mask/VOI, the higher the number the more the detail. *The confusion table for the starred box is shown in the Figure below.

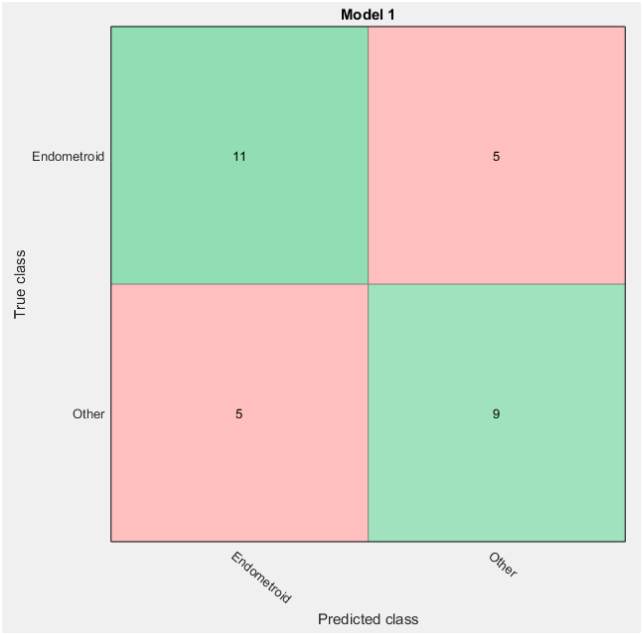


Figure 83. Example confusion table for test data using 64gl and seeing if the model can predict type 1 vs type 2 cancer, see * in Table 29.

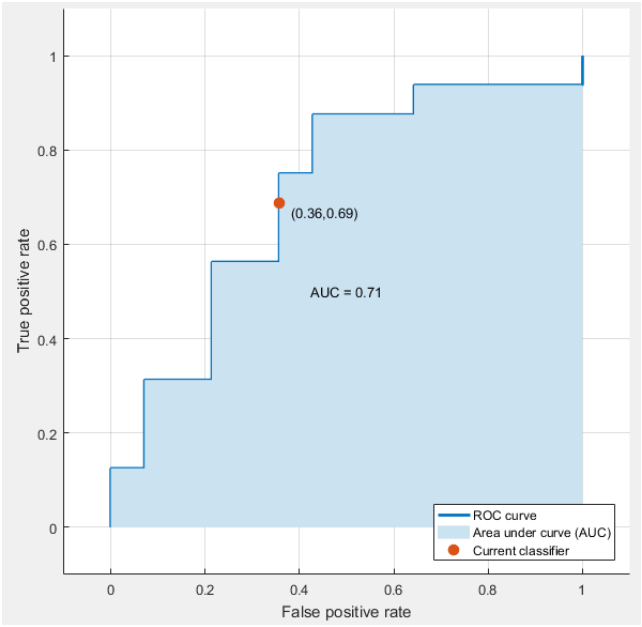


Figure 84. Summary ROC curve showing the performance of the radiomics pilot model. Note, true positive rate refers to sensitivity and false positive rate equates to 1-specificity.

8.5 Discussion of pilot study results

Overall, the results are disappointing. However, there might be scope to improve the accuracy of the model. In the small pilot study, higher order features such as wavelets were not interrogated during feature identification and selection. Furthermore, complex computer learning models were not used including non-linear algorithms such as: k nearest neighbour and support vector machines, ensemble methods like bagged and boosted decision trees. These might improve the diagnostic accuracy. Moreover, various data preparation methods (e.g. data scaling, different dimensionality reduction methods) might improve the model.

The biggest limitation of the pilot study is the relatively small sample size. Radiomics and computer learning models need very large datasets to look for subtle differences in voxels between cancer and normal tissue. Previous successful models, such as Aerts study had more than 1000 separate patients [203]. As data continued to be collected in my study, the larger dataset was re-analysed by Mr Xingfeng Li.

8.6 Results: Larger study – 464 cases analysed by Mr Xingfeng Li

8.6.1 Patient characteristics

A total of 611 consecutive patients were treated for endometrial cancer between February 2012 and September 2017. Overall, 468 met the inclusion criteria for the study and were suitable for segmentation. The region of interest (ROI) of the tumour and corresponding normal myometrium was manually drawn. The median voxel size was 0.52mm x 0.52mm x 5.00mm. All analysis was performed by Mr Xingfeng Li. Pre-processing of the data including normalisation was performed. Four images failed pre-processing and normalisation due to malfunctions in Matlab. The remaining 464 T2 weighted MR images and corresponding paired clinical data was then used for analysis. As described in the methods the dataset was divided into a training set and validation set with an 80:20 split. A total of 990 imaging features were identified using texLAB, SkImage and pyRadiomics. A feature correlation matrix presented as a heat map was used in the feature selection process to remove highly correlated features

(Figure 85) and avoid the problem of co-linearity. Twenty one machine learning classification algorithms were evaluated.

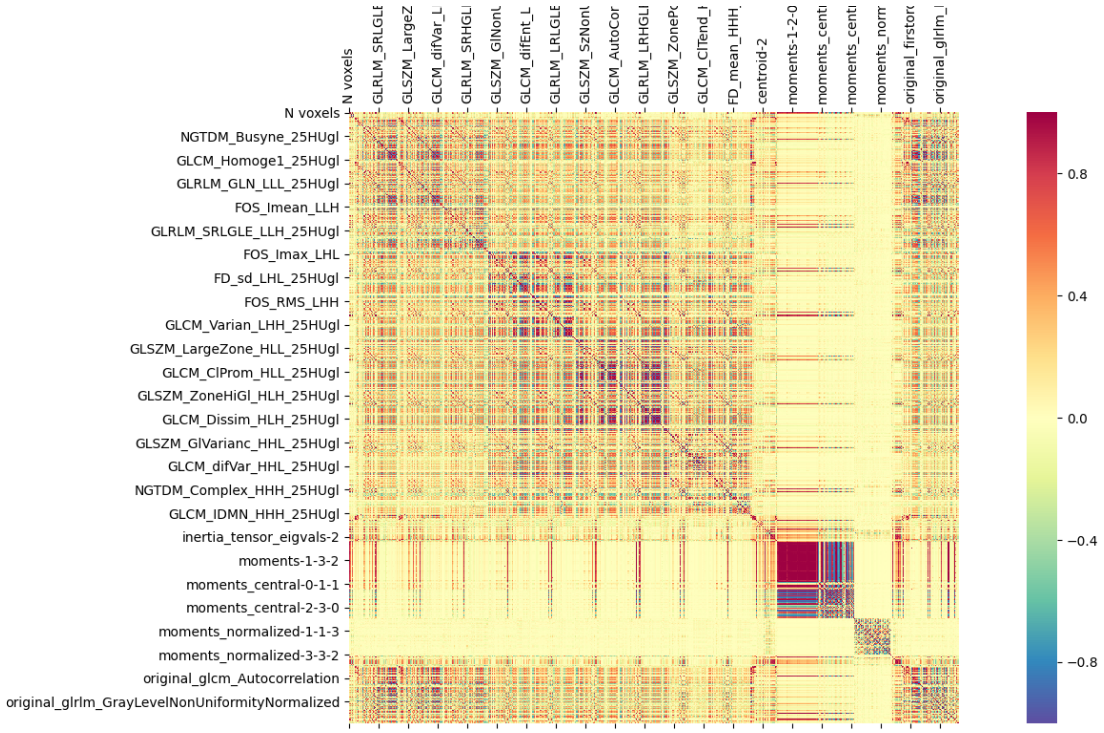


Figure 85. Unsupervised feature correlation matrix presented as a heat map.

Overall, 70% of tumours were type 1 endometrioid tumours and 33% had LVSI involvement. Approximately 33% were grade 1, 33% grade 2 and 33% grade 3 tumours. In the dataset 69% had stage 1 disease, 7% had stage 2, 16% stage 3 and 8% stage 4. The percentage of women with deep myometrial invasion and cervical stromal invasion were 30% (97/299) and 15% (63/425) respectively. In terms of risk score: 37% were classified as low, 17% intermediate, 23% high and 23% as advanced. At the time of analysis 115 patients had died (25%), and 98 patients (21%) had recurrence/disease progression.

8.6.2 Prediction of risk classification

Using the 4 groups of risk (low/intermediate/high/advanced), the best method evaluated to determine risk score was logistic regression with cross validation (LRC) with an accuracy was 0.54 (Figure 86). StandardScaler was used for feature normalization and BestSelect was the best method for feature selection, with 6 features used, namely: GLCM_IDN_LLH_25HUgl, equivalent_diameter, major_axis_length, minor_axis_length, original_shape_LeastAxisLength and original_shape_Maximum2DDiameterRow.

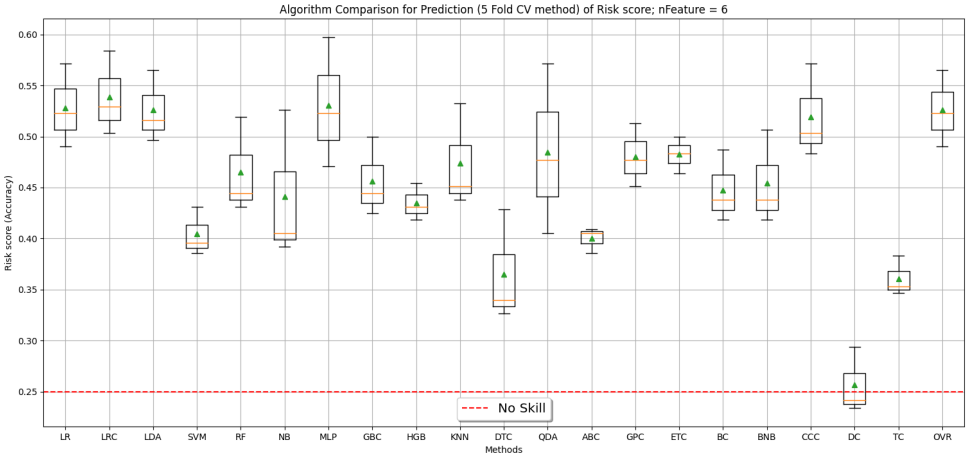


Figure 86. Accuracy of prediction of risk score using various classification methods.

Using 2 groups of risk classification (low versus all others), the best method evaluated to determine risk score was Gaussian Process Classifier (GPC) with an accuracy of 0.74 (Figure 87). StandardScaler was used for feature normalization and BestSelect was the best method for feature selection, with 6 features used, namely: GLCM_IDN_25HUgl, GLCM_IDN_LLL_25HUgl, GLCM_IDMN_LLH_25HUgl, GLCM_IDN_LLH_25HUgl, FOS_Imedian_HLL and minor_axis_length,original_glcm_Idn.

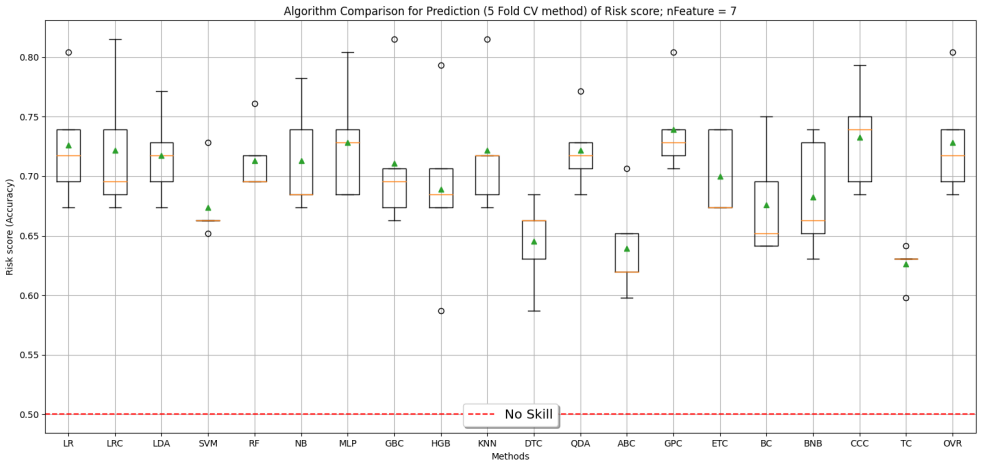


Figure 87. Accuracy of prediction of binary risk score using various classification methods.

8.6.3 Prediction of high-risk histology: type, grade and lymphovascular space involvement

The best method evaluated to determine the type of endometrial cancer was Calibrated Classifier (CCC), using univariate method for feature selection and

Standard StandardScaler for feature normalization (Figure 88). The mean accuracy with this method mean is 0.76 and used the features: GLRLM_LRHGLE_LLL_25HUgl and original_gldm_LargeDependenceHighGrayLevelEmphasis. The mean AUC is 0.66+-0.10.

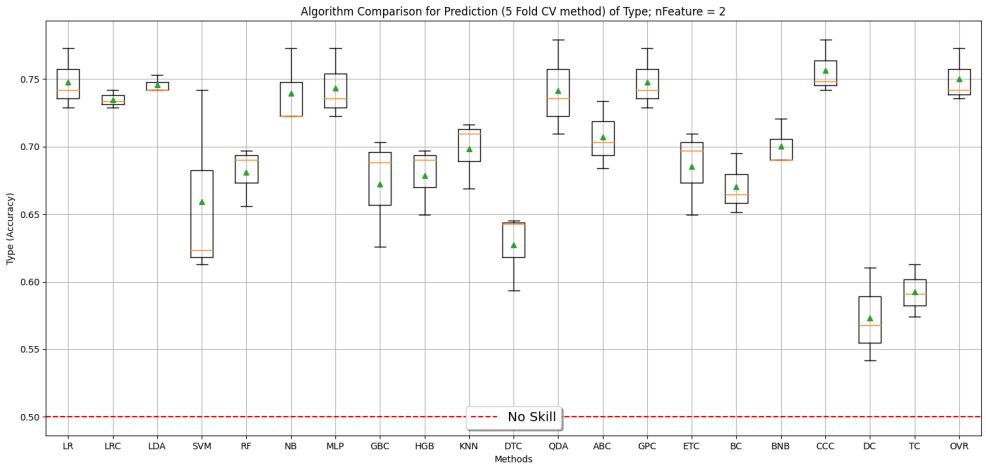


Figure 88. Accuracy of prediction of type of endometrial cancer using various classification methods.

The best method evaluated to determine the grade of endometrial cancer (grade 1 versus 2 versus 3) was linear discriminate analysis (LDA) using univariate method for feature selection and Standard StandardScaler for feature normalization (Figure 89). The mean accuracy with this method mean is 0.56. The 12 features used include: SNS_com_1, GLRLM_LRHGLE_25HUgl, GLCM_IDN_25HUgl, GLCM_IDMN_LLH_25HUgl, GLCM_IDN_LLH_25HUgl, original_shape_LeastAxisLength, FractalDimension, equivalent_diameter, original_gldm_LargeDependenceHighGrayLevelEmphasis and minor_axis_length, original_glrlm_LongRunHighGrayLevelEmphasis and original_glcm_Idn.

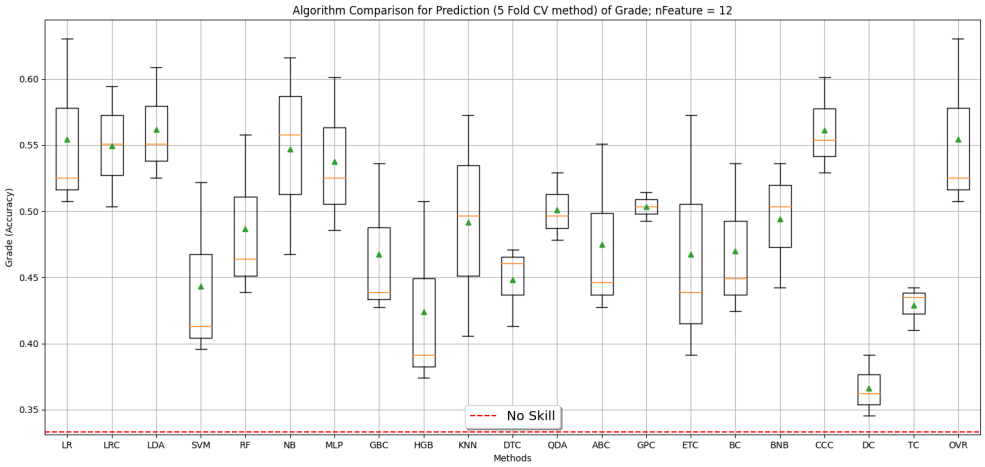


Figure 89. Accuracy of prediction of grade of endometrial cancer (3 groups) using various classification methods.

By comparison, predicting of endometrial grade using 2 group classification: low grade (1 and 2) versus high grade (3) had a much higher accuracy of 0.78 using Gaussian Naïve bayes (NB), BestSelect for feature selection and Standard StandardScaler for feature normalization (Figure 90). The 6 features used include: SNS_com_1, GLRLM_LRHGLE_25HUgl, original_glrlm_LongRunHighGrayLevelEmphasis, equivalent_diameter, minor_axis_length and original_shape_LeastAxisLength.

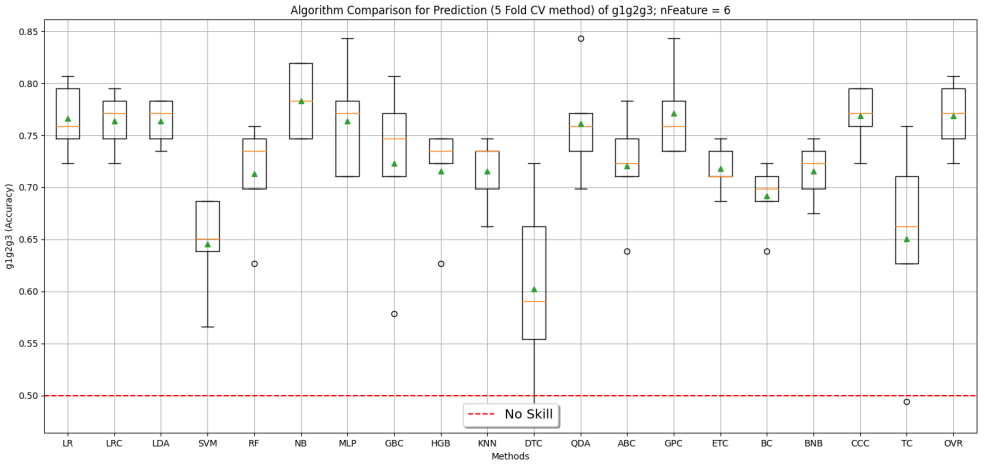


Figure 90. Accuracy of prediction of grade of endometrial cancer (2 groups, high grade and low grade) using various classification methods

The best method evaluated to determine the presence of lymphovascular space invasion (LVSI) was Multi-layer perception classifier (MLP) using LASSO method for feature selection and Standard StandardScaler for feature normalization (Figure 91).

The mean accuracy with this method mean is 0.73. The 2 features used were: GLCM_IDN_LLH_25HUgl and original_shape_LeastAxisLength.

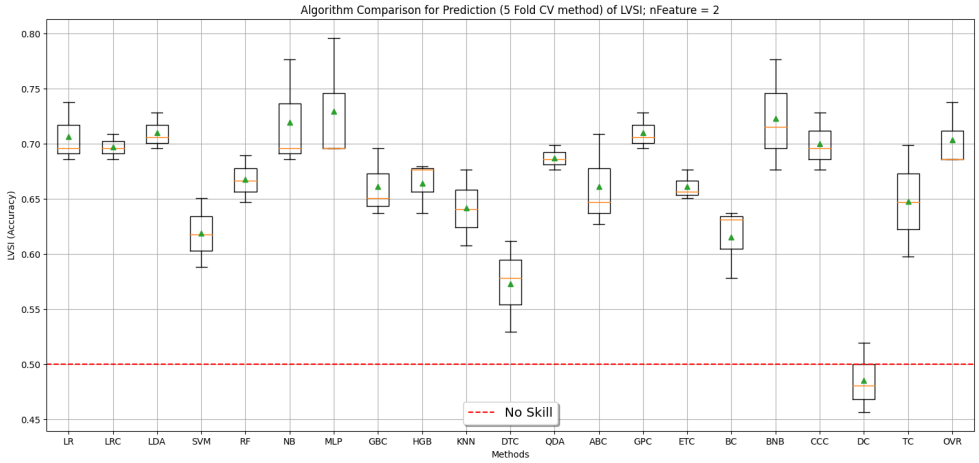


Figure 91. Accuracy of prediction of presence of lymphovascular space involvement using various classification methods.

8.6.4 Prediction of stage including deep myometrial and stromal invasion.

The best method evaluated to determine the stage of endometrial cancer was logistic regression (LR) using univariate method for feature selection and Standard StandardScaler for feature normalization (Figure 92). The mean accuracy with this method mean is 0.73, and used 5 features including: SNS_area, major_axis_length, original_shape_MajorAxisLength, original_shape_Maximum3DDiameter and original_shape_SurfaceArea.

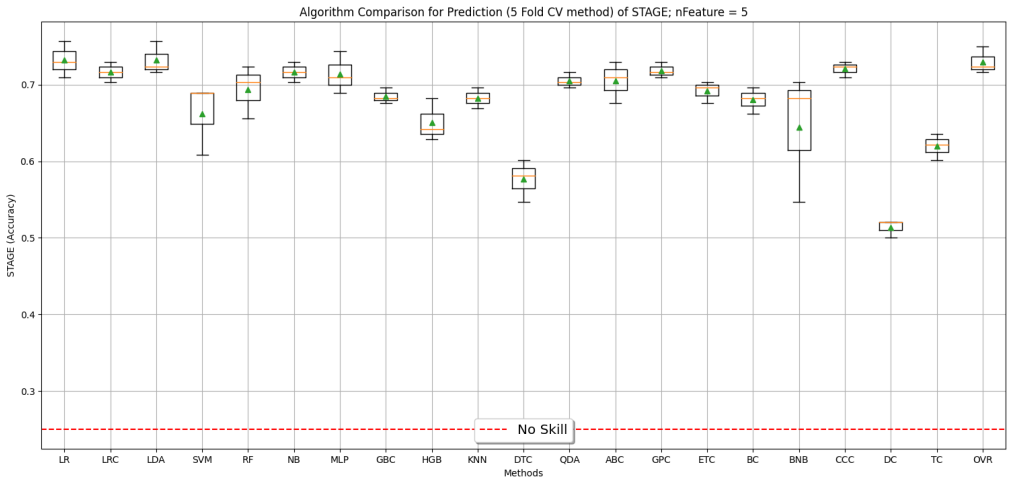


Figure 92. Accuracy of prediction of stage of endometrial cancer using various classification methods.

The best method evaluated to deep myometrial invasion was Multi-layer Perceptron Classifier (MLP) using LASSO feature selection and Standard StandardScaler for feature normalization (Figure 93). The mean accuracy with this method mean is 0.77 and used 5 features including: GLSZM_LzoneLogl_25HUgl, FOS_Kurt_LLH, FOS_Imean_HLL, original_shape_Flatness and original_firstorder_Skewness.

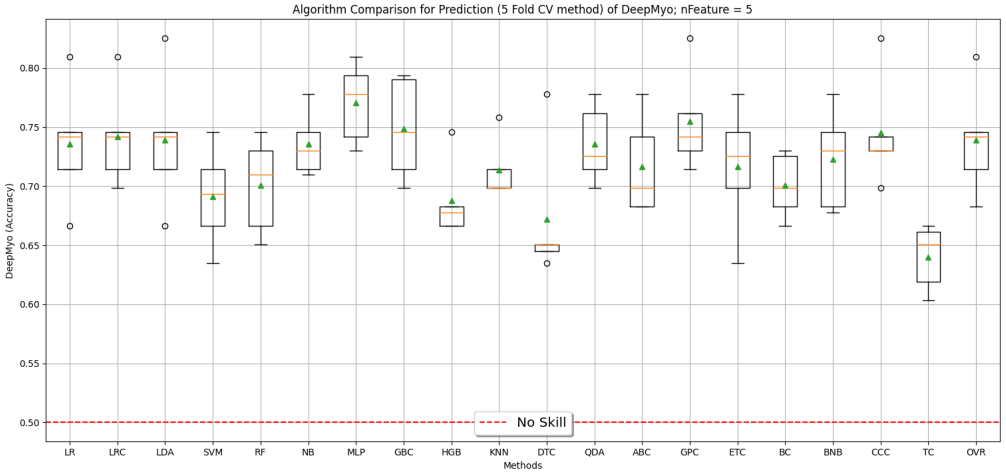


Figure 93. Accuracy of prediction of deep myometrial invasion using various classification methods

The best method evaluated to predict stromal invasion was Linear Discriminant analysis (LDA) using BestSelect feature selection and Standard StandardScaler for feature normalization (Figure 94). The mean accuracy with this method mean is 0.87 and used 6 features including: inertia_tensor-2-2, inertia_tensor_eigvals-0, inertia_tensor_eigvals-1, major_axis_length, original_shape_MajorAxisLength and original_shape_Maximum2DDiameterSlice.

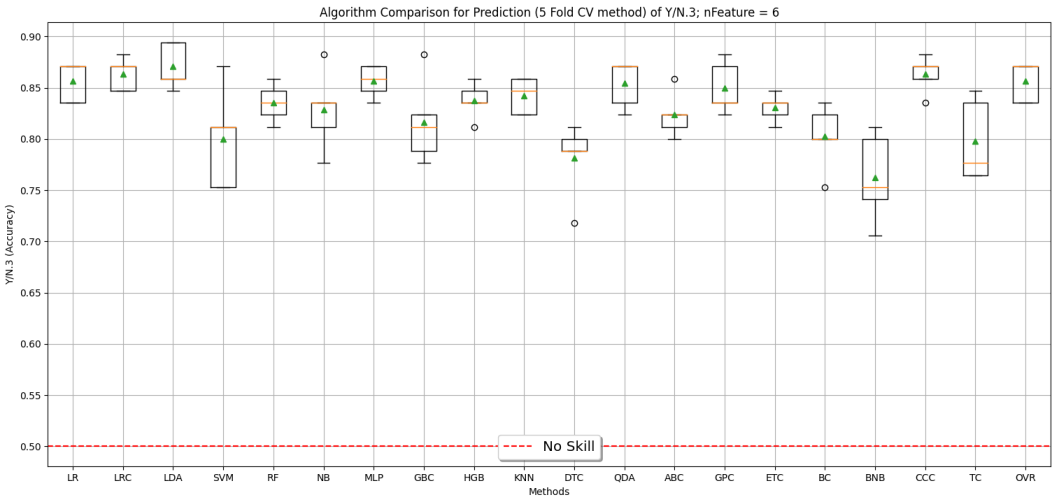


Figure 94. Accuracy of prediction of cervical stromal invasion using various classification methods

8.6.5 Prediction of survival and recurrence

The optimal method evaluated to determine the overall survival of women with endometrial cancer was Gaussian Naïve Bayes (NB) using univariate method for feature selection and Standard StandardScaler for feature normalization (Figure 95). The mean accuracy with this method mean is 0.78, and used 7 features including: original_shape_Maximum2DDiameterRow, GLRLM_LRHGLE_LLL_25HUgl, equivalent_diameter,minor_axis_length, original_shape_MinorAxisLength, original_shape_LeastAxisLength and original_gldm_LargeDependenceHighGrayLevelEmphasis. Accuracy was 1.00 if all deaths were accurately predicted and 0.00 if none. The single feature which discriminated most between dying in the first 3 years versus living beyond 5 years was: GLCM_difEnt_LHH_25HUgl.

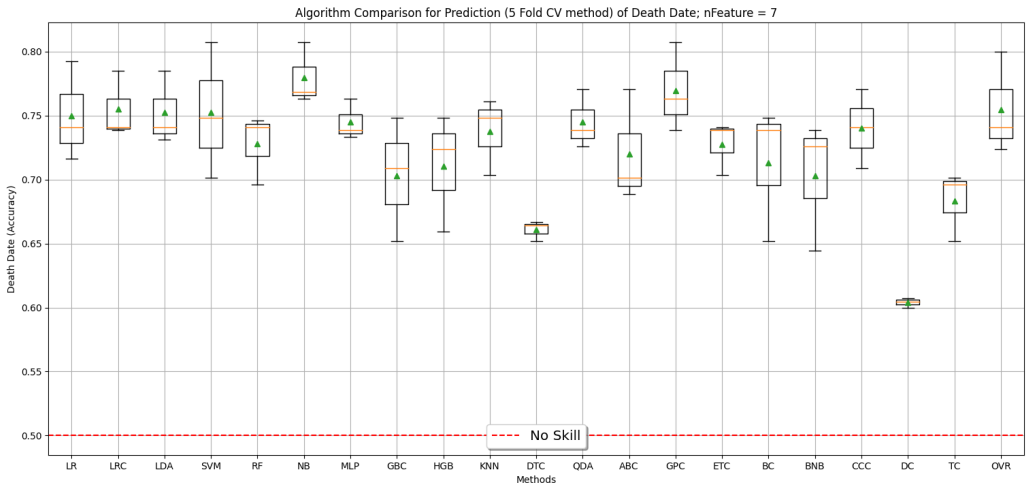


Figure 95. Accuracy of prediction of overall survival using various classification methods.

The optimal method evaluated to determine recurrence of endometrial cancer was linear discriminant analysis (LDA) using LASSO method for feature selection and Standard StandardScaler for feature normalization (Figure 96). The mean accuracy with this method mean is 0.68, and used 6 features including: SNS_sph, FD_mean_25HUgl, FD_sd_25HUgl, GLRLM_LRHGLE_LLL_25HUgl, NGTDM_Busyne_LHL_25HUgl and GLSZM_LzoneLogl_HLL_25HUgl. The single feature which discriminated most between recurrence and no recurrence was GLCM_IDMN_LLH_25HUgl,

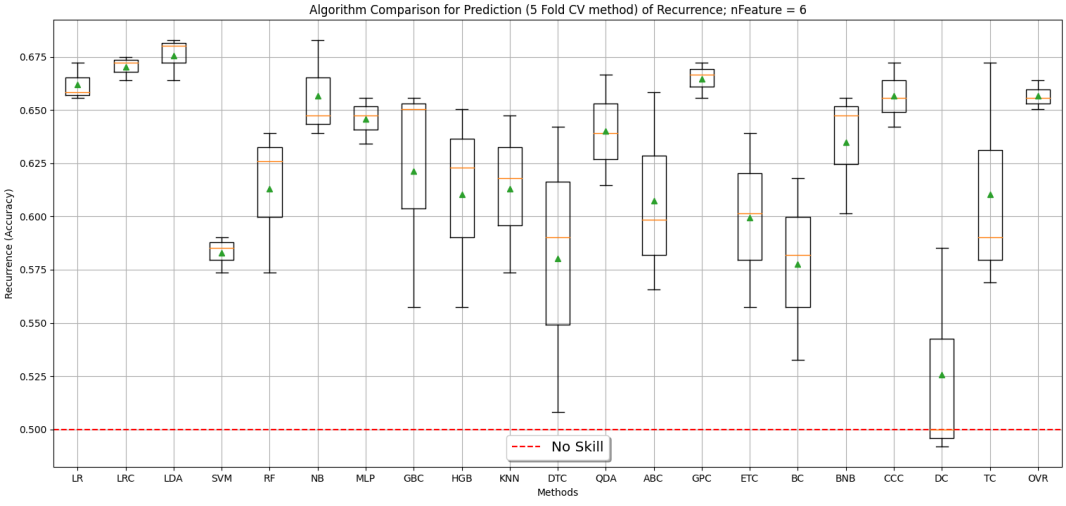


Figure 96. Accuracy of prediction of recurrence of endometrial cancer using various classification methods.

8.7 Discussion

8.7.1 Main findings

Textural features describe the properties of an image in a quantitative manner, with an emphasis on pixels (voxels) spatially, as oppose to focussing on the intensity of a single pixel [516]. This enables investigation of heterogeneity within the tumour and between tumours [516, 545]. Regional variations in gene expression, metabolism and oxygenation contribute to these observed changes [540, 546-549] and it is these variations that are interrogated through textural features and then correlated to short term outcomes such as histological grade and tumour type, and, more importantly long-term outcomes such as survival.

Using the larger dataset in the current study, radiomics was able to predict overall 5-year survival with moderate accuracy (78%). Prediction of survival is highly advantageous, enabling personalised medicine. The only other study to utilise radiomics to predict study survival in women with endometrial cancer was Ytre-hauge et al [213]. They reported that high kurtosis in T1 weighted MR images predicted reduced recurrence and progression-free survival (hazard ratio [HR] 1.5, $P< 0.001$), but only after adjusting for MRI-measured tumour histology and volume [213]. Their study used only 180 patients, compared to over 400 in this study. Furthermore, they used T1 weighted MRI images (not the current gold standard). Despite variations in methodology, which hampers comparison, it was interesting to note that kurtosis was not a feature selected in the present model to predict survival but was key in theirs.

The current study was able to predict the presence of LVSI involvement with over 70% accuracy. This is comparable to Ueno et al., study [212] with an accuracy of 78%, albeit using a study cohort consisting of a much higher prevalence of LVSI (47% vs 33% in this study). The results from the present study are also superior to Bereby-Kahane et al., which reported a sensitivity of 71% but a specificity of only 59%; their poorer results may be attributed to the limited number of patients (n= 73) included within their analysis [215]. LVSI is a histological diagnosis, made by confirmation of tumour emboli within microvessels. It has been shown to be a strong prognostic factor in recurrence and lymph node metastasis [44, 457, 458], but is not perceptible to the naked eye on MR images. Accurate prediction of LVSI involvement pre-operatively

using MR images, as observed in this radiomics study, can therefore reduce the chance of repeat surgery to confirm lymph node spread.

Tumour type and stage were predicted with moderate accuracy 76% and 73% respectively. This fared slightly worse compared to other studies that showed accuracies of 80-90% in the prediction of tumour type and presence of deep myometrial invasion [211, 212, 529]. Intriguingly, all these studies had smaller sample sizes ranging from 27-137 patients but used a higher number of extracted features for their machine learning models (3-11). Ghosh et al., study found those patients with superficial myometrial invasion tended to have lesser skewness, energy, entropy, variance, and kurtosis and greater uniformity of mean diffusivity [529]. Radiomics had a relatively high accuracy for identifying cervical stromal invasion (87%), which is unsurprising given that this a feature identified by the radiologist using MRI pre-operatively.

Interestingly, risk classification and grade were comparatively poorly predicted, 54% and 56% respectively, in the current study. Despite risk classification itself being dependant on type, grade and stage of tumours; all of which correlate strongly with survival data, and type/stage tumour being well predicted individually using the current radiomics model. One of the reasons for this maybe the higher number of groups. In both risk classification and grade classification the models had at least 3 groups, thereby reducing the overall number of samples in a single group. When comparing high risk endometrial cancer to low risk endometrial cancer the overall accuracy was 74%, worse than the largest endometrial cancer radiomics study using the data from 717 patients with combined clinical parameters. They had reported an AUC of 0.877 [550].

Of note, and unsurprisingly, the radiomics models from the larger dataset (464 cases) provided much better correlation with outcomes compared to the smaller pilot dataset (60 cases). For each variable, such as survival, and recurrence, a different radiomics model (classification method, feature selection method and normalisation method) provided the optimal result. It appears, therefore that no all-encompassing model can be used to predict all outcomes effectively.

8.7.2 Strengths and Limitations

This study had several strengths. It included the study data from the north west London cancer network, of which 15 hospitals participate. This makes the radiomics model more reliable and reproducible. Furthermore, this is one of the largest radiomics models in endometrial cancer with over 400 patients, and one of only 2 studies to explore whether textural features in endometrial cancer correlate with survival. Multiple modelling techniques were evaluated, and substantial feature selection was utilised to avoid overfitting of the model. Moreover, unlike most studies, volumetric measurements (using the whole tumour) were performed, as oppose to the more common two-dimensional method using the largest cross-sectional area only; thus, mitigating the chance of 'missing' key textural features. Most importantly, the RQS and TRIPOD guidelines were adhered too to ensure quality of both scientific method and reporting [532]. Park et al., demonstrated overall poor radiomics scientific quality and reporting of studies in general [532].

This study also had several limitations. Firstly, it was retrospective and therefore at risk of bias and missing data. This study only included patients who received surgery and had MR imaging with paired clinical data available. Secondly, external validation has yet to be performed and accuracy measurements were obtained using 5-fold cross validation only. In order to enable applicability worldwide, it is important to confirm that radiomics model can be applied to different imaging systems and software.

A problem, though not intrinsic to this study is the standardisation of images and algorithms. MR scan parameters vary, resulting in variations in imaging quality; thus, reducing the stability of any radiomic features identified. Textural features are highly dependent on image acquisition, pre-processing, segmentation, and modelling, standardisation of techniques is essential.

Thirdly, inter and intra-observer variability for textural values were not evaluated, and these values were based upon manual segmentation of images. Manual delineation of images is one of the most challenging steps, it is time consuming and prone to inter-observer variability [526, 551]. Automatic segmentation in the future may make volumetric analysis more feasible.

Finally, survival outcomes can't be taken out of context and survival outcomes represent not only the effect of the disease itself, but also of patient factors (such as age, co-morbidities) and treatment factors (such as whether the patient underwent neoadjuvant radiotherapy or chemotherapy). Adjuvant treatment predictably improves survival. Regional and national differences in patient demographics along with treatment options offered and delivered will impact survival disparities.

In this study only T2-weighted MR images were used, future work could evaluate the use of alternative MR images such as: diffusion weighted, dynamic contrast material–enhanced images and apparent diffusion coefficient maps [212]. Indeed, endometrial cancer radiomics could be evaluated using CT or USS, given that in many less developed countries due to cost, MRI is not available.

Since the initial draft of this manuscript data collection and analysis has remained ongoing. The focus of the subsequent analysis has been to find a radiomic signature that can predict survival. In addition, a fresh set of data has been segmented to present to the model to provide external validation.

8.7.3 Conclusions

The ability to predict treatment outcomes of patients, particularly those who respond poorly to standard treatment is hugely beneficial. This is one of the only studies to utilise radiomics to predict overall survival of women with endometrial cancer, with an accuracy of just under 80%. Radiomics also had reasonable prediction of stage and high risk histologies. Unfortunately, there was no single model that could predict all these outcomes measures instead multiple models were needed. Further work will need to be carried out to develop a unifying model along with prospective validation.

CHAPTER 9: COST – EFFECTIVESNESS ANALYSIS

9. Economic effect: cost-effectiveness analysis

Collaborators:

Dr Mark Pennington and Dr. Elena Pizzo, health economists who both provided help on an advisory capacity.

9.1 Summary

Objective: To determine the cost effectiveness of introducing new technology including: the iKnife, 3D ultrasound and ultrasound guided biopsy into the clinical model for investigating and managing endometrial cancer in women with postmenopausal bleeding.

Methods: A decision analytical model was created to reflect the current patient pathway using ultrasound (4mm and 5mm cut-off). This was compared to the new pathway using the iKnife, 3-dimensional ultrasound and ultrasound guided biopsy. Diagnostic probabilities were derived from systematic reviews and cost estimates were taken from national datasets were possible. The main outcome measures were the ICER, incremental cost per unit of effectiveness (additional woman alive at the end of 5 years).

Results: Models using 5mm cut-off were the cheapest, as was the use of 3D ultrasound. Ultrasound guided biopsy provided the lowest ICER.

Conclusions: Based on cost-effectiveness, women presenting with post-menopausal bleeding should undergo initial evaluation with ultrasound guided biopsy instead of outpatient hysteroscopy.

9.2 Introduction

Endometrial cancer is the most common gynaecological malignancy in the UK. The age standardised incidence and age standardised mortality of endometrial cancer has increased between 1999-2012 [552]. The presentation of endometrial cancer is typically with postmenopausal bleeding and treatment is primarily surgical but will vary with stage. The stage of disease will significantly impact the cost of treatment, with the cost of 5 years for stage 1 and stage 3 disease ranging from £9,475 to £26,080 respectively over 5 years [553]. Most of the treatment cost for early stage cancer is

incurred within the first 6 months post diagnosis, whilst late stage cancer accrues most costs after the first 6 months [553].

The majority of cost and effectiveness studies on endometrial cancer, are American and focus of the costs is hysterectomy with limited follow up data [554-562]. Moreover, there has been a shift towards studies looking specifically at the cost effectiveness of lymphadenectomy [563-567] and robotic surgery [568-575]. There is, however, a paucity of studies looking at the cost analysis of the patient pathway from management of women referred with suspected endometrial cancer up until surgery.

In Clark et al 2006 modelling study of initial diagnostic strategies, the cost per additional life year gained (£/LYG) and incremental cost-effectiveness ratios were calculated for each method (ultrasound, endometrial biopsy and hysteroscopy including combinations). They concluded that women presenting for the first time with symptoms should undergo initial evaluation with ultrasound assessment or endometrial biopsy [383]. The authors made a number of assumptions in the model, including failure rates, complication rates, true positive rates, prevalence of cancer, mortality from surgery and 5-year survival. Whilst they cite a number of published studies there was no report on validity or relevance of primary studies, which were chosen selectively, and some estimates were derived from an expert panel. There is, therefore, much scope for error.

It has been shown in breast cancer than one-stop clinics provide timely, cost-effective and accurate diagnosis [576]. Could the new technologies enhance the patient pathway in endometrial cancer, add effectiveness and/or reduce cost?

In this study I will outline the patient pathway and costings based on current best evidence. I will then look at speculative costs following introduction of the new technologies (iKnife, USS guided biopsy and 3D ultrasound) to speed up the patient pathway.

9.3 Methods

The consolidated health economic evaluation reporting standards (CHEERS) were observed during the undertaking of this study [577]. A decision analytic approach was employed to evaluate the cost and effectiveness of the new technologies for women

with suspected endometrial cancer. By calculating the value of all possible events and weighing the uncertainty of each result using the probability of each outcome, it is possible to identify the sequence of decisions that will maximise value and minimise costs. Amua 2019, open source modelling framework was used to specify the models [578].

The current patient pathway was first outlined, using best practice from presenting symptoms to the point of surgery and adjuvant treatment. Input parameters and model assumptions were based on earlier work by Clark et al and Breijer et al [383, 579]. Current best practice is to perform a pelvic ultrasound. If abnormal, an endometrial biopsy is performed (either OEB or outpatient hysteroscopy, OPH depending if focal pathology). If the outpatient procedure is unsuccessful than a diagnostic hysteroscopy and biopsy under general anaesthesia is performed. The morbidity and failure rate of all these procedures were included in the model. Both 4mm and 5mm cut offs were used to define abnormal endometrial thickness to reflect variations in clinical practice (with 5mm as base strategy). The new technologies (3D ultrasound, iKnife and USS guided biopsy) were also evaluated. Thus, the overall strategies evaluated in this study were:

1. USS (4mm cut off) standard pathway
2. USS (5mm cut-off) standard pathway
3. USS (4mm cut off) using ultrasound guided biopsy instead OPH
4. USS (5mm cut-off) using ultrasound guided biopsy instead OPH
5. USS (4mm cut-off) using the iKnife for tissue processing
6. USS (5mm cut-off) using the iKnife for tissue processing
7. USS (4mm cut-off) using 3D ultrasound for pre-operative assessment
8. USS (5mm cut-off) using 3D ultrasound for pre-operative assessment

The decision tree path for option 2, USS using a 5mm cut off, is illustrated in Figure 97. Decision tree paths for all 8 strategies were created.

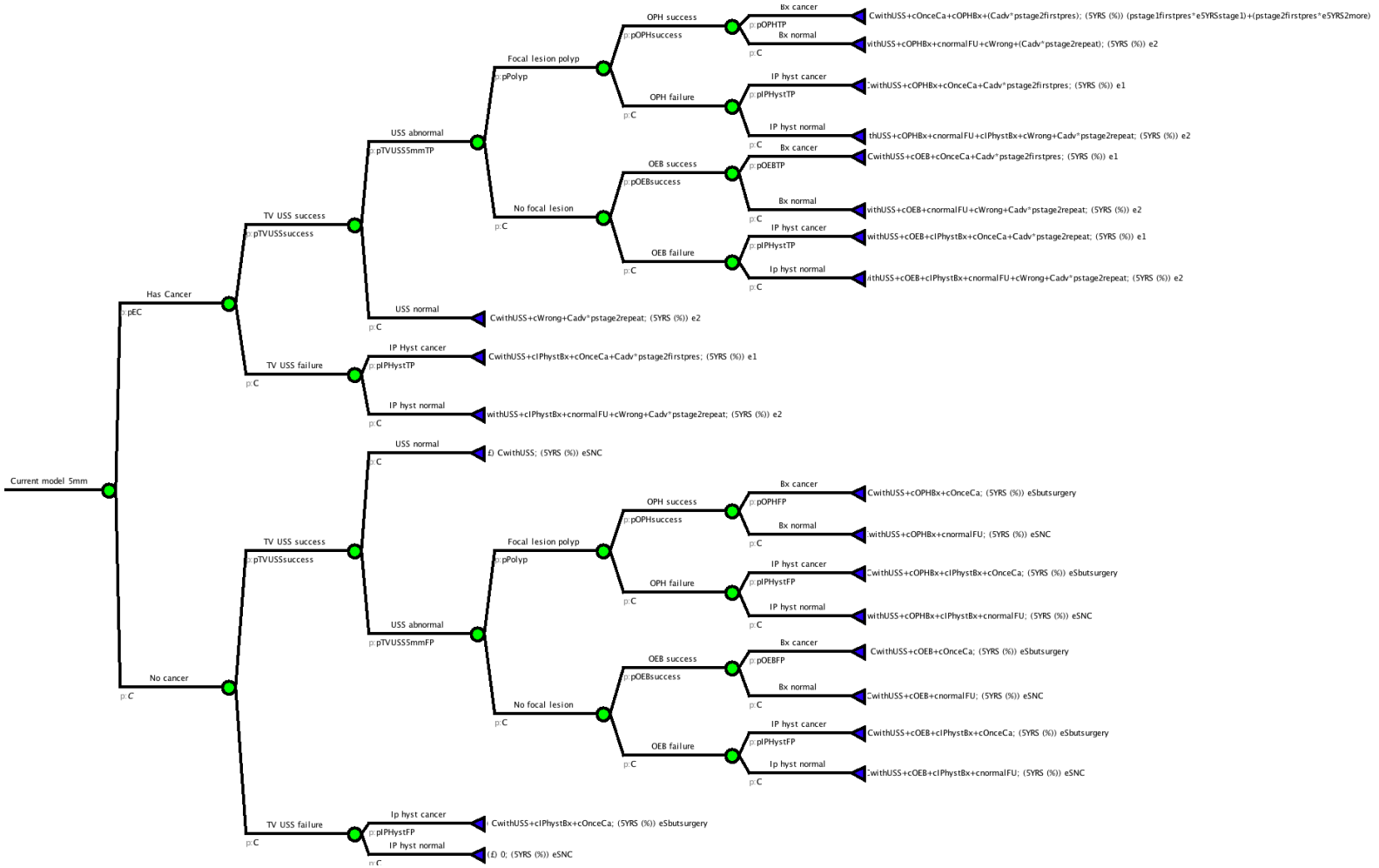


Figure 97. Decision tree for 5mm USS pathway. The scenario starts with the probability of a cancer diagnosis and then goes through the following steps of investigation and treatment with their respective costs, risks and benefits. At the end of the pathway all outcomes; their likelihood and costs are outlined.

Probabilities: Assumptions and input parameters

This decision analytic model begins with a woman presenting with postmenopausal bleeding (PMB). The probability of endometrial cancer in women with PMB varies according to age, between 3-13% [42, 383, 580]. It is assumed in this model that the woman is 65 years old and is otherwise healthy, with a normal life expectancy for her age. The prevalence of endometrial cancer was defined as 9% (see Table 30) with a prevalence of endometrial polyps of 20% [419]

A realistic one stop clinic was used as the model, with the pelvic ultrasound and OEB taking place during the initial consultation. If outpatient hysteroscopy (OPH) or day case hysteroscopy were required, these were assumed to occur at a later date. If the pelvic scan findings were normal the patient was discharged. If the biopsy sample was normal the patient received a telephone follow-up appointment with a nurse. If the biopsy showed cancer, the patient was seen in a combined gynaecology oncology clinic and the case was discussed in an MDT. Following this, pre-operative work-up including bloods, CT scan and pelvic MRI were performed. Surgery was assumed to be a hysterectomy (laparoscopic or open). The peri-operative mortality of surgery ranges between 0.7%-5% [158], in this model it was taken as 1%.

Endometrial cancer was classified as localised (stage 1) and more advanced (stage 2 or more), according to FIGO. It was assumed that 70% of women had stage 1 disease and 30% had more advanced disease [497]. In cases of advanced disease, radiotherapy and chemotherapy were provided by a medical oncologist. Standardised radiotherapy regime of external beam radiotherapy with a total dose 50-55 Gy in 20-28 fractions over 5 weeks was the default. The standard cytotoxic chemotherapy and/or hormonal treatment were given. Compliance was assumed to be 100%.

The time horizon for the model was 5 years post referral with symptoms. Future benefits (women alive at 5 years) were appropriately discounted after accounting for false-positive results, and immediate mortality due to unnecessary hysterectomies.

Diagnostic accuracy and failure rates of the diagnostic procedures were based on a number of studies including Clark et al [45, 47, 88, 94, 383, 419, 579, 581]. Most of

these studies were large systematic reviews and meta-analyses providing synthesis-based estimates. All the diagnostic tests were assumed to have negligible mortality rates. For those women who were erroneously discharged i.e. a false negative, it was assumed that they remained symptomatic and represented to clinic.

The diagnostic accuracies and success rates of the new technologies (iKnife, USS guided biopsy and 3D ultrasound) are based upon data presented later in the thesis. The iKnife is performed on the tissue ex-vivo and therefore has zero additional complication rate.

Parameter	**Probability**	**Source**
Success rate		
TV USS	1.00	TC
OEB	0.88	TC
OPH	0.95	TC
IP Hyst	1.00	MC
USS guided Bx	0.90	Thesis
3D USS	1.00	Thesis
iKnife	1.00	Thesis
Failure rate		
TV USS	0.00	TC
OEB	0.12	TC
OPH	0.05	TC
IP Hyst	0.00	MC
USS guided Bx	0.10	Thesis
3D USS	0.00	Thesis
iKnife	0.00	Thesis
Complication rate		
TV USS	0.00	TC
OEB	0.00	TC
OPH	0.00	TC
IP Hyst	0.014	TC
USS guided Bx	0.00	Thesis
3D USS	0.00	Thesis
iKnife	0.00	Thesis
True positives		
TV USS 4mm	0.99	TC

TV USS 5mm	0.97	TC
OEB	0.94	TC
OPH	0.86	TC
IP Hyst	0.96	MC
USS guided Bx	0.95	Thesis
3D USS	0.85	Thesis
iKnife	0.93	Thesis
False positives		
TV USS 4mm	0.51	TC
TV USS 5mm	0.45	TC
OEB	0.01	TC
OPH	0.01	TC
IP Hyst	0.01	MC
USS guided Bx	0.01	Thesis
3D USS	0.10	Thesis
iKnife	0.86	Thesis
Probability polyp	0.20	FN
Prevalence Endometrial cancer	0.09	AC
Peri-operative mortality surgery	0.01	KG
Surgical stage at Hysterectomy 1st presentation	0.7	MC
Stage I	0.3	MC
Stage II-IV		
Surgical stage at Hysterectomy representation	0.65	MC
Stage I	0.35	MC
Stage II-IV		
5 Year survival		
Stage I	0.95	Seer
Stage II-IV	0.60	Seer

Table 30. Estimated probabilities for each parameter.

Codes: TC = Clark et al [383], MC = Briejer et al [579], thesis = data taken and extrapolated from thesis. Seer = SEER dataset [5], KG = Gupta et al [158], AC = Clarke et al [42] and FN = Nagele et al [419].

Acronyms: OEB = office endometrial biopsy, TV USS = transvaginal ultrasound, Bx = biopsy, OPH = Outpatient hysteroscopy, IP Hyst = inpatient hysteroscopy.

Costs: Assumptions and input parameters

Estimate costs of inpatient and outpatient episodes using national schedule of reference costs for the UK 2017-2018 and Unit Costs of Health and Social Care 2018 were used [582, 583]; these are illustrated in Table 31. Costs for inpatient investigations included the hospital costs for a day-case surgical procedure in addition to the consultant gynaecologist and anaesthetist. Drug costs were derived from the British National Formulary 2019. Only direct medical costs in the UK were used.

It should be noted that 3D USS does not appear in the national reference costs, so outpatient ultrasound scan without contrast lasting less than 20minutes was used as a surrogate cost (in addition to the cost of TV USS).

Similarly, REIMS and the iKnife are new technologies and the exact cost per patient will vary widely depending on the amount the iKnife is used. Much like an MRI, the capital costs of REIMS are high, approximately £200'000, depreciating over about 10 years, with large benefits of economies of scale. Within Imperial alone, approximately 30 biopsies for suspected endometrial cancer are performed a week, so over 1500 per annum. The iKnife (currently used for research only) is currerntly trialled in other cancers, so assuming that it is used in 5 other malignancies/specialities with an equivalent amount of use, this will mean >10000 samples are processed per annum. A technician will be needed to maintain the machine (approximately £30'000 per annum) and consumables will cost about £2.5 per sample. This will give a unit cost of £7 per sample.

The cost of re-investigation after initial erroneous misdiagnosis were included in the model. The treatment for most endometrial cancer cases is surgery, and the cost associated with this was coded for as 'complex, open or laparoscopic upper or lower genital tract procedure for malignancy'.

Step in patient pathway	Costings	
	Unit cost	**Range**
GP appointment	£32*	£28-38
Rapid access appointment with Gynae oncology team	£133	
Ultrasound (TV USS) OUTPATIENT	£165 averaged £155	£155-£1272
Ultrasound (TVUSS) and biopsy OUTPATIENT	£239 averaged £233	£233- £1650
Pipelle (Minimal Genital Tract Procedures)	£247 averaged	£205-£1570
Diagnostic hysteroscopy OUTPATIENT DAYCASE	£201 £960	£192 - £1502 £396 averaged
Diagnostic Hysteroscopy and biopsy OUTPATIENT DAYCASE	£239 £1073	£233 - £9321
Biopsy processed: - Histopathology - iKnife	£33 £7	
Gynae onc clinic - non-admitted face to face (FU, 1st) - non-admitted no face to face (FU, 1st) - Multiprofessional non-admitted face to face appt (FU, 1st) - Multiprofessional non-admitted non face to face appt (FU, 1st) - Nurse led non admitted non face to face	£116- £161 £87- £107 £166 -194 £152-£180 £60	
MRI pelvis Magnetic Resonance Imaging Scan of One Area, with Post-Contrast Only, 19 years and over	£165	
3D Ultrasound - USS <20min without contrast	£54	
CT - Computerised Tomography Scan of Three Areas, without Contrast	£110	
Gynae cancer MDT	£120	
Bloods –		

Phlebotomy Processing sample	£3 £4	
Surgery	£6164	
Radiotherapy - preparation - deliver fraction	 £435 £111	
Chemotherapy - drugs - delivery	 £260 £312	

Table 31. Cost for each step during the patient pathway.

*=Price of patient contact lasting 9.22 minutes including carbon emissions but excluding cost of pre-registration and post graduate medical education. New technology steps highlighted in red.

Outcomes: survival

In this model, much like, Breijer et al. paper, 5-year survival data based on FIGO stage [5, 128, 579] was used. In those women who had a delay in cancer diagnosis due to a false negative result, it was assumed that the cancer was upstaged in 5% of cases and the 5-year survival was reflective of that (Table 30).

Outcomes: cost-effectiveness.

The effectiveness of the standard diagnostic strategy (USS 5mm cut-off) was compared to the diagnostic strategies using the new technologies using the outcome measure percentage of women alive at 5 years.

In this model cost-effectiveness was expressed as incremental cost-effectiveness ratios (ICERs) – these reflect the costs needed to obtain one extra unit of health benefit (in this case, one extra woman survives 5 years). When a diagnostic model is more effective or less costly than the reference standard it has a negative sign.

Each diagnostic strategy is depicted graphically as a cost-effectiveness plane with effectiveness on the x-axis and cost on the y-axis. Diagnostic strategies which fall in the bottom right side of the graph are more effective and less costly, whilst those in right upper quadrant are less cost effective. Often there is a trade-off between cost and effectiveness. No universal cost-effective threshold exists, but £30'000/LYG was used by Clark et al. study and several others [383, 584-586].

Sensitivity analyses

Sensitivity analyses are used to examine the potential impact of a parameter assumptions. Probabilistic sensitivity analysis incorporates all parameter uncertainties. One-way sensitivity analyses were performed for disease prevalence, diagnostic success rates. In this, the estimates of costs and effectiveness are repeated with varying parameters, the results are shown on a graph with cost-effectiveness on the y axis and the parameter being assessed on the x-axis.

9.4 Results

Cost, effectiveness and ICER

The baseline strategy used for comparison against all other models was strategy was the current pathway with an USS cut-off of 5mm. Table 32 shows the costs, effectiveness and ICER for each of the 8 diagnostic strategies evaluated. The cost for investigating and treating a woman with postmenopausal bleed (irrespective of final diagnosis) was £1207.37 and ranged from £1196.92-£1236.22 depending on the strategy used. Similarly, the number of days gained or lost depending on the strategy used varied between 8 days lost and 5 days gained; overall fairly minimal benefit in terms of survival. Strategies using USS guided biopsy were the cost-effective overall.

Strategy	**Cost (£)**	**Incremental cost (£)**	**Effectiveness (% alive at 5 years)**	**Average days extra survival /women**	**ICER (£/%alive at 5 years)**
USS (5mm cut-off) standard pathway Reference	1207.37	0.00	97.871	0.00	D
USS (4mm cut off) standard pathway	1231.95	24.58	98.005	2.45	D
USS (4mm cut off) using ultrasound guided biopsy instead OPH	1234.53	27.16	98.128	4.69	103.59
USS (5mm cut-off) using ultrasound guided biopsy instead OPH	1209.42	2.05	97.992	2.21	103.59

USS (4mm cut-off) using the iKnife for tissue processing	1236.22	28.85	97.541	-6.03	D
USS (5mm cut-off) using the iKnife for tissue processing	1211.97	4.6	97.417	-8.29	D
USS (4mm cut-off) using 3D ultrasound for pre-operative assessment	1221.44	14.07	98.005	2.45	D
USS (5mm cut-off) using 3D ultrasound for pre-operative assessment	1196.92	-10.45	97.871	0.00	D

Table 32. Summary results of costs (diagnosis and treatment, in £ per patient) and effectiveness (% of women surviving 5 years), based upon most likely assumptions.

D represents strategy dominance by USS guided model (i.e. USS guided biopsy was cheaper and more effective than the other models). ICER = incremental cost-effectiveness ratio.

Additionally, a cost-effectiveness plane was generated (Figure 98). As can be seen the strategies using 4mm cut-off were generally more expensive and strategies using 3D ultrasound were cheaper. Ultrasound guided biopsy was marginally more expensive, but also more effective and represented the best compromise between cost and effectiveness.

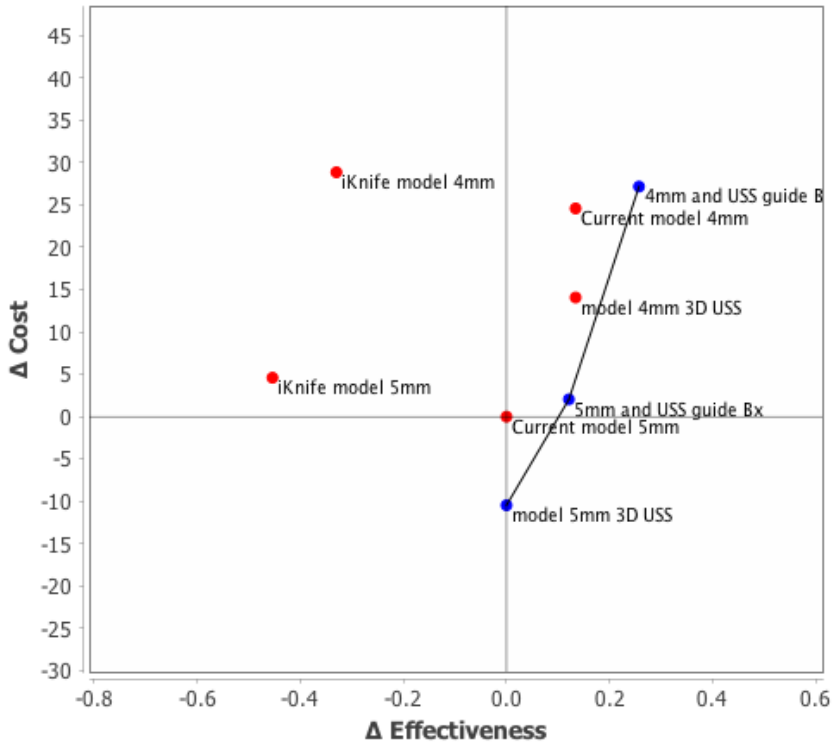


Figure 98. Incremental cost-effectiveness plane.
The x-axis represents the relative effectiveness and y-axis relative cost. The current model using 5mm ultrasound cut-off represents the baseline to which the other strategies were compared. Each dot represents a strategy.

Sensitivity analyses

The results of the sensitivity analyses are show in Figure 99. It should be noted that only the baseline strategy and 'best alternative strategy' are depicted on the sensitivity analyses. As the prevalence of endometrial cancer increases from 3-13% the ICER falls, quite markedly for the baseline strategy and less so the strategy using USS guided biopsy. Similarly, the ICER falls as the prevalence of finding a polyp on scan increases, Furthermore, the ICER falls for the baseline strategy as the success rate of outpatient diagnostic procedures (OEB and USS guided biopsy) increases but appears to plateau at 10%.

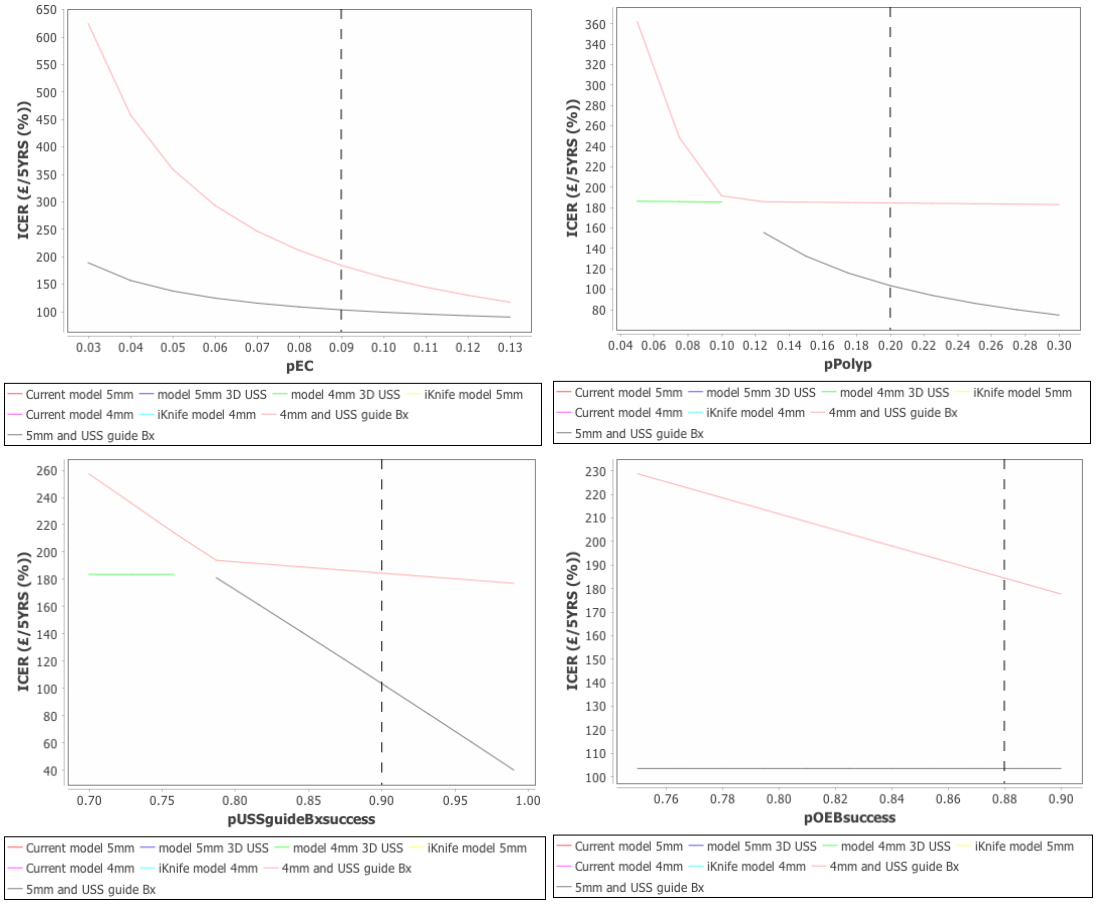


Figure 99. Sensitivity analyses.
Changing ICER reflected by changes in a given parameter: prevalence endometrial cancer top left, prevalence endometrial polyp top right, success rate of ultrasound guided biopsy bottom left and success rate of OEB bottom right.

9.5 Discussion

9.5.1 Strengths and Limitations

This study demonstrates that all models using an endometrial thickness of 4mm are comparatively more effective than using 5mm; however, the trade-off is a higher cost per unit. This in keeping with Clark et al., findings [383]. It is also unsurprising, given that transvaginal ultrasound is a useful screening test with very high negative predictive values, but low positive predictive values (14.8% at 4mm and 54% at 5mm) necessitating additional investigation [97, 587, 588]. The lower the endometrial thickness threshold used, the higher the number of unnecessary additional procedures required and the higher the cost.

In this health economics analysis USS guided biopsy has the lowest incremental cost effectiveness ratio (ICER), i.e. the most benefit for the least cost. It can be performed during the initial consultation and saves money by omitting an additional outpatient appointment. It also speeds up the patient pathway minimising patient distress due to diagnostic certainty observed in the psychological study (Chapter 3.2). It should be noted that in this strategy the success rates and diagnostic rates of USS guided biopsy were assumed to be similar to OEB and OPH. This economics study fails to take into account the tolerability and acceptability of the procedures.

The iKnife is a novel technology which offers near-real time diagnosis for patients. In this health economics study, the overall the cost was higher than the current standard of care. This is explained by the reduction in effectiveness compared to standard care. It was assumed that the iKnife has a high diagnostic accuracy (93% true positives and 86% false positives), but the standard of care is assumed to have 100% diagnostic accuracy, therefore any false positive will incur unnecessary cost. In addition, as it is currently only used for research purposes the cost is speculative and depending on the amount of use, the cost could vary between £4-£100 per unit. It is worth highlighting that ICERS do not take into account all the qualitative and quantitative aspects of patient's health. Indeed, the main benefit of the iKnife lies in its diagnostic speed, and therefore reduction in patient's psychological anxiety due to uncertainty. An incremental cost to psychological benefit ratio would therefore be interesting avenue to explore.

In this study the replacement of a pelvic MRI with 3D ultrasound was the most cost saving measure. Three-dimensional ultrasound scans can be performed by most modern scan machines with the addition of a specific probe and basic training. In this model, the diagnostic accuracy was considered similar to a pelvic MRI. In either case the proportion of women surviving at 5 years is unlikely to vary significantly irrespective of modality used to plan surgery, and a standard cost of complex surgery was applied in both models. As 3D ultrasound scans are not currently routine standard of care, the costs were overestimated, and were based on the cost of a 20min additional non-contrast scan, when in fact it usually takes less than 5minutes and is performed during the initial scan. In addition to its cost-effectiveness other considerations may support the role of 3D ultrasound scan including tolerability and accessibility. Conversely, it should also be appreciated that an MRI scan can often provide additional information

such as enlarged lymph nodes or extra-uterine disease that an ultrasound may not, so even if there is significant cost saving, the benefits of an MRI may not be seen with this cost-effectiveness analysis.

The sensitivity analyses showed that the ICER of the current model (and USS guided biopsy) decreased as prevalence of endometrial cancer increased. Given that the prevalence of endometrial cancer increases with age, it suggests that different models may be tailored to patient risk factors including age. Breijer et al.; commented on the cost-effective benefits of model selection based on patient characteristics [579].

In this study the focus of the cost-effectiveness strategies is based upon a woman presenting with post-menopausal bleeding. It is therefore not applicable to women having screening for endometrial cancer, or who have a confirmed diagnosis already.

9.5.2 Strengths and Limitations

This is the first study to assess the cost-effectiveness of these novel technologies in the management of women with post-menopausal bleeding. An analytic approach was used to quantify decisions made within the current diagnostic framework [383, 584, 589, 590]. These were based upon best estimates of accuracy and safety and were obtained from high-quality systematic review where possible with survival data taken from national datasets. It is also the first study to include the costs of GP and rapid access clinics too within the cost-effective framework.

The validity of any model-based approach is the dependence on the parameters used. Thus, despite using best estimates for diagnostic accuracies and failure rates, these parameters can only ever be estimates, and this limits this strength of any inferences drawn. In this study one limitation was the lack of context for diagnostic studies. In real life clinicians will evaluate risk based upon both history and exam, thus there is a risk of overestimating usefulness of diagnostic tests and increasing cost-effectiveness [579, 580, 591].

A number of assumptions were made within the models. The outpatient diagnostic strategies were assumed to have short recovery times, with no significant mortality. Indirect costs (such as patient transportation and time off work) nor the costs of

treatment of recurrent or terminal endometrial cancer were not accounted for in this study. The costs of the new technologies were also estimated as no national or local data existed. The iKnife's costs in particular will vary substantially depending on economies of scale. Sensitivity analyses were not performed for cost estimates as variations in cost are likely to overestimate uncertainty related to the economic evaluation because cost components are unlikely to be well correlated [383, 592].

In this study, it was assumed that women erroneously discharged remained symptomatic and therefore represented. To take into account the delay in diagnosis 5% of these women were upstaged, in line with other studies [383, 593]. This is an extrapolation of a clinical outcome and represents uncertainty in the evaluative process [585]. The costs of litigation for women erroneously discharged were not included within the models.

Another limitation for this study is the generalisability, the costs are based on UK data and are unlikely to be applicable to the wider population. Also, the effectiveness metric used in this study was the proportion of women surviving the first five years. Although life expectancy and quality-adjusted life years (QALYs) are the most common outcome measures, 5-year survival is not uncommon outcome and was relevant to the clinical framework [579].

9.5.3 Conclusion

The introduction of 3D ultrasound and ultrasound guided biopsy are frugal innovations providing effectiveness at low cost. Postmenopausal bleeding is a frequent symptom with a high use of resources [594], so whilst the incremental effectiveness and cost reduction is modest, at a population level this can still represent significant savings. External validation in future studies will be important to confirm the generalisability of these findings and confirm the costings of the new technologies.

CHAPTER 10: CONCLUSION AND FUTURE WORK

CHAPTER 10: CONCLUSION AND FUTURE WORK

10.1 Achievements

This thesis marks many firsts; it is the first study to assess whether time to surgery influences survival in women with endometrial cancer in England. It is the first study in the world to look at anxiety and stress in women with suspected endometrial cancer. It is also documents the world's first use of REIMS technology and the iKnife in the differentiation of malignancy versus benign endometrial tissue.

At the commencement of this thesis, few studies addressed the benefits of an earlier diagnosis. In Chapter 3 a clinical needs assessment and technological gap analysis was performed. Looking at survival data over 5 years from Queen Charlottes Hospital, a deleterious impact of prolonged waiting times was demonstrated, especially in type 2 cancer. Furthermore, the large observational and survey study I performed confirmed high levels of anxiety and stress in women attending rapid access clinic with suspected endometrial cancer. Whilst, this result was not entirely surprising, the study also showed a strong association between patients' belief of cancer and GAD7 anxiety scores ($P < 0.00001$) i.e. the more anxious the patient is, the more likely they are to think they have cancer. Furthermore, adequate pre-clinic information was shown to make a significant difference in anxiety and stress levels. I hope this study provides impetus for hospital trusts and GPs to improve pre-hospital information.

The next two Chapters discussed the role and introduction of novel technologies to speed up a tissue diagnosis. These novel technologies were assessed using a clinical trial I set up. Chapter 4 described the performance of the iKnife in the diagnosis of endometrial cancer using endometrial biopsy samples. In this pilot study a model was built initially using tissue bank samples, followed by 150 pipelle biopsy samples. With an accuracy of approximately 90%, with potential for improved accuracy, this could easily be translated into routine clinical practice. Similarly, Chapter 5 evaluated the role of USS guided biopsy as an alternative to hysteroscopy, to provide a quicker tissue sample. In a case series of 10 consecutive women, the biopsy was successful with sufficient tissue in 90% of cases. Despite the high pain score using VAS, it had a high acceptance rate.

Chapter 6 and 7 addressed the introduction of 3D ultrasound in pre-operative imaging, eliminating the need for an expensive, resource limiting MRI, which can add to delays in surgical treatment. In a study of 25 women, 3D ultrasound was able to detect deep myometrial invasion with a sensitivity and specificity was 80% and 67% respectively for subjective assessment, and with 80% sensitivity and 80% specificity for objective assessment TDS. The accuracy of this technology was then assessed on a larger level by performing a systematic review and analysis. This confirmed moderate diagnostic accuracies in the assessment of deep myometrial invasion with a pooled sensitivity and specificity of 81% (95% CI, 72–87%), and 84% (95% CI, 79–88%) respectively.

In Chapter 8 radiomics, was assessed to see if quantitative features in imaging can help prognosticate patients. In a small test sample of 464 patients it was able to predict type, stage and prognosis of patients with moderate accuracy.

Finally, in Chapter 9, an economic analysis was performed which suggested that some of these innovations (particularly 3D ultrasound and ultrasound guided biopsy) might be frugal, potentially minimising costs too. Thus, there are prognostic, psychological and economic benefits to a faster diagnosis.

10.2 Future work

10.2.1 Extension of psychological and survival impact of delayed diagnosis and treatment

Whilst, it was widely thought that there is a negative psychological and survival impact with delays for an endometrial cancer diagnosis, evidence was lacking. To this end, my survival analysis confirmed survival benefits for earlier treatment and the psychological study confirmed patients desire for a rapid diagnosis. As an extension to this work, it would be interesting to see the effect of co-morbidities, in particular an assessment of frailty on the survival analyses. A number of studies have shown worse outcomes in minority groups and it would be interesting to confirm these findings within the London population, but also do some qualitative work to establish reasons why this might be the case in order to better rectify the disparities.

With regard to the psychological study, it would be fascinating to see whether the final diagnosis (be it benign or cancer) correlates with patients' self-perception of cancer diagnosis, and also how quickly, if at all, their anxiety levels diminish post diagnosis. This would be best performed by doing a paired survey pre and post diagnosis.

10.2.2 Development of the iKnife as diagnostic tool

The iKnife was successfully used to analyse the lipidome of the endometrium and utilise differences in lipidomic signatures to distinguish effectively between benign and malignant tissue. As described in Chapter 4, the technology performed extremely well with a diagnostic accuracy of almost 90%. The sensitivity and specificity of the best performing models are sufficiently high to be translated into clinical practice, following prospective validation. The tissue diagnosis obtained from REIMS is virtually instantaneous and can therefore provide a POC diagnosis for patients attending the clinic. Given the high PPV (90-94%), women who test positive are very likely to have endometrial cancer and could go on to have blood tests and pre-operative imaging that day while awaiting final histopathological confirmation, minimising any treatment delays.

The learning model demonstrates that more endometrial tissue biopsy samples are needed to optimise performance of the iKnife/CO2 REIMS model. Future work would build on my work, by increasing the spectral library and prospectively validating the current pipelle model. Until the CO2 laser iKnife is validated, processing of the tissue using both the conventional diathermy iKnife and CO2 laser are required.

Variations in the lipidomic signature of benign and malignant endometrial tissue enable us to better characterise the metabolic variations between histological groups. Further cell line work will be needed to unravel the exact molecular pathways that underpin endometrial cancer progression based on the observed differences in phospholipid composition.

The other potential use for REIMS within endometrial cancer is in the intra-operative diagnosis of involved metastatic lymph nodes. Currently my ethics approval covers expansion of research into this area. However, due to limitations on my time and resources I was unable to pursue this avenue. Given the increased morbidity and

complexity of lymphadenectomy a method of diagnosing cancerous lymph nodes real-time will minimise the need for unnecessary surgery and its associated morbidity.

10.2.3 Development of 3D Ultrasound for pre-operative assessment

As described in Chapter 6, ideally a minimum of 56 endometrial cancer cases with concomitant 3D scans and MRIs would have been acquired. However, limitations on my time and resources meant that this was not possible; thus, a systematic review and meta-analysis of existing studies was performed. Cases will continue to be collected for this project. But, in addition to the current methodology using subjective assessment and the objective measurement of TDS, other methods of objective assessment will also be assessed including tumour/uterine antero-posterior diameter. Furthermore, assessment of cervical invasion will be analysed. Current methods to assess cervical invasion only have moderate diagnostic efficacy at best, and very few studies using 3D ultrasound have assessed this.

10.2.4 Development of radiomics model

The results of this radiomics pilot study are promising. However, as with all learning models, vast quantities of data are required. To this end, prospective validation using more cases are required. Given the need for 5-year outcome data, this process will be slow. Extension of my ethics to include other cancer centres and use their imaging dataset might provide a quicker way to expand the imaging repository and validate this work.

10.2.5 Future integrated pathway

All these novel technologies piloted in my PhD can now be integrated into a new diagnostic and treatment pathway. A large-scale clinical trial will be needed to validate the safety and effectiveness demonstrated in this PhD.

10.3 Final Conclusion

In summary, a shorter time from referral to treatment has psychological, financial and prognostic benefits. The iKnife and ultrasound guided biopsy enable a true point of care diagnosis. Three-dimensional ultrasound can facilitate immediate preoperative

imaging with minimal cost. Furthermore, radiomics can be used to predict adverse prognostic factors and survival, with promising results.

Whilst I suspect there will be no magic bullet for cancer during my lifetime, incremental improvements in the patient pathway and clinical care will undoubtedly improve patient outcomes. I sincerely hope that my research can act as a foundation for future work, streamlining patient management, thereby reducing patient anxiety, improving survival and minimising cost.

CHAPTER 11: REFERENCES

CHAPTER 11: REFERENCES

1. International Agency for Research on Cancer, G., *Corpus uteri factsheet, estimated cancer incidence, mortality and prevalence worldwide 2018*. 2018, World Health Organisation.
2. Lee, N.K., et al., *Prognostic factors for uterine cancer in reproductive-aged women.* Obstet Gynecol, 2007. **109**(3): p. 655-62.
3. Colombo, N., et al., *ESMO-ESGO-ESTRO Consensus Conference on Endometrial Cancer: diagnosis, treatment and follow-up.* Ann Oncol, 2016. **27**(1): p. 16-41.
4. Chen LM, B.J. *Endometrial cancer: epidemiology, risk factors, clinical features, diagnosis, and screening*. UpToDate, 2011.
5. Institute, N.C. *Endometrial cancer treatment* 2015; Available from: https://seer.cancer.gov/statfacts/html/corp.html.
6. Howlader N, N.A., Krapcho M, Miller D, Brest A, Yu M, Ruhl J, Tatalovich Z, Mariotto A, Lewis DR, Chen HS, Feuer EJ, Cronin KA (eds). . *SEER Cancer Statistics Review, 1975-2017*. Available from: https://seer.cancer.gov/csr/1975_2017/,.
7. Reeves, G.K., et al., *Cancer incidence and mortality in relation to body mass index in the Million Women Study: cohort study.* Bmj, 2007. **335**(7630): p. 1134.
8. Beral, V., D. Bull, and G. Reeves, *Endometrial cancer and hormone-replacement therapy in the Million Women Study.* Lancet, 2005. **365**(9470): p. 1543-51.
9. Smith, D.C., et al., *Association of exogenous estrogen and endometrial carcinoma.* N Engl J Med, 1975. **293**(23): p. 1164-7.
10. Mack, T.M., et al., *Estrogens and endometrial cancer in a retirement community.* N Engl J Med, 1976. **294**(23): p. 1262-7.
11. Ziel, H.K. and W.D. Finkle, *Increased risk of endometrial carcinoma among users of conjugated estrogens.* N Engl J Med, 1975. **293**(23): p. 1167-70.
12. Antunes, C.M., et al., *Endometrial cancer and estrogen use. Report of a large case-control study.* N Engl J Med, 1979. **300**(1): p. 9-13.
13. Aune, D., et al., *Anthropometric factors and endometrial cancer risk: a systematic review and dose-response meta-analysis of prospective studies.* Ann Oncol, 2015. **26**(8): p. 1635-48.
14. Dossus, L., et al., *Reproductive risk factors and endometrial cancer: the European Prospective Investigation into Cancer and Nutrition.* Int J Cancer, 2010. **127**(2): p. 442-51.
15. Linkov, F., et al., *Endometrial hyperplasia, endometrial cancer and prevention: gaps in existing research of modifiable risk factors.* Eur J Cancer, 2008. **44**(12): p. 1632-44.
16. Bergström A, P.P., Tenet V, Wolk A, Adami HO., *Overweight as an avoidable cause of cancer in Europe.* International journal of cancer, 2001. **91**(3): p. 421-30.
17. Kyrgiou, M., et al., *Adiposity and cancer at major anatomical sites: umbrella review of the literature.* BMJ, 2017. **356**: p. j477.
18. Esposito, K., et al., *Metabolic syndrome and endometrial cancer: a meta-analysis.* Endocrine, 2014. **45**(1): p. 28-36.
19. Tsilidis, K.K., et al., *Type 2 diabetes and cancer: umbrella review of meta-analyses of observational studies.* BMJ, 2015. **350**: p. g7607.

20. Murali, R., R.A. Soslow, and B. Weigelt, *Classification of endometrial carcinoma: more than two types.* Lancet Oncol, 2014. **15**(7): p. e268-78.
21. Kandoth, C., et al., *Integrated genomic characterization of endometrial carcinoma.* Nature, 2013. **497**(7447): p. 67-73.
22. Zighelboim, I., et al., *Microsatellite instability and epigenetic inactivation of MLH1 and outcome of patients with endometrial carcinomas of the endometrioid type.* J Clin Oncol, 2007. **25**(15): p. 2042-8.
23. Kuhn, E., et al., *Identification of molecular pathway aberrations in uterine serous carcinoma by genome-wide analyses.* J Natl Cancer Inst, 2012. **104**(19): p. 1503-13.
24. Moore, L., et al., *The mutational landscape of normal human endometrial epithelium.* Nature, 2020. **580**(7805): p. 640-646.
25. Talhouk, A., et al., *A clinically applicable molecular-based classification for endometrial cancers.* Br J Cancer, 2015. **113**(2): p. 299-310.
26. Mutter, G.L., *Endometrial intraepithelial neoplasia (EIN): will it bring order to chaos? The Endometrial Collaborative Group.* Gynecol Oncol, 2000. **76**(3): p. 287-90.
27. Allison, K.H., et al., *PAX2 loss by immunohistochemistry occurs early and often in endometrial hyperplasia.* Int J Gynecol Pathol, 2012. **31**(2): p. 151-159.
28. Sun, H., et al., *Mutational analysis of the PTEN gene in endometrial carcinoma and hyperplasia.* Am J Clin Pathol, 2001. **115**(1): p. 32-8.
29. Trimble, C.L., et al., *Concurrent endometrial carcinoma in women with a biopsy diagnosis of atypical endometrial hyperplasia: a Gynecologic Oncology Group study.* Cancer, 2006. **106**(4): p. 812-9.
30. Saso S, C.J., Georgiou E, Ditri AM, Smith JR, Ghaem-Maghami S., *Endometrial cancer.* BMJ, 2011. **343**(3954).
31. Münstedt, K., et al., *Cancer of the endometrium: current aspects of diagnostics and treatment.* World J Surg Oncol, 2004. **2**: p. 24.
32. Renaud, M.C. and T. Le, *No. 291-Epidemiology and Investigations forSuspected Endometrial Cancer.* J Obstet Gynaecol Can, 2018. **40**(9): p. e703-e711.
33. Win, A.K., J.C. Reece, and S. Ryan, *Family history and risk of endometrial cancer: a systematic review and meta-analysis.* Obstet Gynecol, 2015. **125**(1): p. 89-98.
34. Daniels, M.S., *Genetic testing by cancer site: uterus.* Cancer J, 2012. **18**(4): p. 338-42.
35. Lu, K.H., et al., *Prospective determination of prevalence of lynch syndrome in young women with endometrial cancer.* J Clin Oncol, 2007. **25**(33): p. 5158-64.
36. Broaddus, R.R., et al., *Pathologic features of endometrial carcinoma associated with HNPCC: a comparison with sporadic endometrial carcinoma.* Cancer, 2006. **106**(1): p. 87-94.
37. Lu, K.H., et al., *Gynecologic cancer as a "sentinel cancer" for women with hereditary nonpolyposis colorectal cancer syndrome.* Obstet Gynecol, 2005. **105**(3): p. 569-74.
38. Excellence, N.I.f.H.a.C. *Referral guidelines for suspected cancer* 2005.
39. Baekelandt, M.M. and M. Castiglione, *Endometrial carcinoma: ESMO clinical recommendations for diagnosis, treatment and follow-up.* Ann Oncol, 2009. **20 Suppl 4**: p. 29-31.

40. Emons, G. and R. Kimmig, *Interdisciplinary S2k guidelines on the diagnosis and treatment of endometrial carcinoma.* J Cancer Res Clin Oncol, 2009. **135**(10): p. 1387-91.
41. Gredmark, T., et al., *Histopathological findings in women with postmenopausal bleeding.* Br J Obstet Gynaecol, 1995. **102**(2): p. 133-6.
42. Clarke, M.A., et al., *Association of Endometrial Cancer Risk With Postmenopausal Bleeding in Women: A Systematic Review and Meta-analysis.* JAMA Intern Med, 2018. **178**(9): p. 1210-1222.
43. Goldstein, R.B., et al., *Evaluation of the woman with postmenopausal bleeding: Society of Radiologists in Ultrasound-Sponsored Consensus Conference statement.* J Ultrasound Med, 2001. **20**(10): p. 1025-36.
44. Amant F, M.P., Neven P, Timmerman D, Van Limbergen E, Vergote I., *Endometrial cancer.* Lancet, 2005. **366**(9484): p. 491-505.
45. Gupta, J.K., et al., *Ultrasonographic endometrial thickness for diagnosing endometrial pathology in women with postmenopausal bleeding: a meta-analysis.* Acta Obstet Gynecol Scand, 2002. **81**(9): p. 799-816.
46. Gull, B., et al., *Can ultrasound replace dilation and curettage? A longitudinal evaluation of postmenopausal bleeding and transvaginal sonographic measurement of the endometrium as predictors of endometrial cancer.* Am J Obstet Gynecol, 2003. **188**(2): p. 401-8.
47. Smith-Bindman, R., et al., *Endovaginal ultrasound to exclude endometrial cancer and other endometrial abnormalities.* JAMA, 1998. **280**(17): p. 1510-7.
48. Timmermans, A., et al., *Endometrial thickness measurement for detecting endometrial cancer in women with postmenopausal bleeding: a systematic review and meta-analysis.* Obstet Gynecol, 2010. **116**(1): p. 160-7.
49. Gerber, B., et al., *Effects of adjuvant tamoxifen on the endometrium in postmenopausal women with breast cancer: a prospective long-term study using transvaginal ultrasound.* J Clin Oncol, 2000. **18**(20): p. 3464-70.
50. Neven, P., et al., *Longitudinal hysteroscopic follow-up during tamoxifen treatment.* Lancet, 1998. **351**(9095): p. 36.
51. Fisher, B., et al., *Endometrial cancer in tamoxifen-treated breast cancer patients: findings from the National Surgical Adjuvant Breast and Bowel Project (NSABP) B-14.* J Natl Cancer Inst, 1994. **86**(7): p. 527-37.
52. DeMichele, A., et al., *Impact of raloxifene or tamoxifen use on endometrial cancer risk: a population-based case-control study.* J Clin Oncol, 2008. **26**(25): p. 4151-9.
53. van Leeuwen, F.E., et al., *Risk of endometrial cancer after tamoxifen treatment of breast cancer.* Lancet, 1994. **343**(8895): p. 448-52.
54. Bergman, L., et al., *Risk and prognosis of endometrial cancer after tamoxifen for breast cancer. Comprehensive Cancer Centres' ALERT Group. Assessment of Liver and Endometrial cancer Risk following Tamoxifen.* Lancet, 2000. **356**(9233): p. 881-7.
55. Lahti, E., et al., *Endometrial changes in postmenopausal breast cancer patients receiving tamoxifen.* Obstet Gynecol, 1993. **81**(5 (Pt 1)): p. 660-4.
56. Berridge, D.L. and T.C. Winter, *Saline infusion sonohysterography: technique, indications, and imaging findings.* J Ultrasound Med, 2004. **23**(1): p. 97-112; quiz 114-5.
57. de Kroon, C.D., et al., *Saline contrast hysterosonography in abnormal uterine bleeding: a systematic review and meta-analysis.* BJOG, 2003. **110**(10): p. 938-47.

58. Bingol, B., et al., *Comparison of diagnostic accuracy of saline infusion sonohysterography, transvaginal sonography and hysteroscopy in postmenopausal bleeding.* Arch Gynecol Obstet, 2011. **284**(1): p. 111-7.
59. Erdem, M., et al., *Comparison of transvaginal ultrasonography and saline infusion sonohysterography in evaluating the endometrial cavity in pre- and postmenopausal women with abnormal uterine bleeding.* Menopause, 2007. **14**(5): p. 846-52.
60. Nergiz, S., et al., *Comparison of diagnostic methods for evaluation of postmenopausal bleeding.* Eur J Gynaecol Oncol, 2014. **35**(3): p. 292-7.
61. Epstein, E., et al., *Transvaginal sonography, saline contrast sonohysterography and hysteroscopy for the investigation of women with postmenopausal bleeding and endometrium > 5 mm.* Ultrasound Obstet Gynecol, 2001. **18**(2): p. 157-62.
62. Laifer-Narin, S.L., et al., *Transvaginal saline hysterosonography: characteristics distinguishing malignant and various benign conditions.* AJR Am J Roentgenol, 1999. **172**(6): p. 1513-20.
63. Aleem, F., et al., *Transvaginal color and pulsed Doppler sonography of the endometrium: a possible role in reducing the number of dilatation and curettage procedures.* J Ultrasound Med, 1995. **14**(2): p. 139-45; quiz 147-8.
64. Alcazar, J.L. and R. Galvan, *Three-dimensional power Doppler ultrasound scanning for the prediction of endometrial cancer in women with postmenopausal bleeding and thickened endometrium.* Am J Obstet Gynecol, 2009. **200**(1): p. 44.e1-6.
65. Dragojević, S., et al., *The role of transvaginal colour Doppler sonography in evaluation of abnormal uterine bleeding.* Arch Gynecol Obstet, 2005. **271**(4): p. 332-5.
66. Samulak, D., et al., *The diagnostic value of evaluating the maximum velocity of blood flow in the uterine arteries of women with postmenopausal bleeding.* Arch Gynecol Obstet, 2011. **284**(5): p. 1175-8.
67. Weiner, Z., et al., *Uterine artery flow velocity waveforms and color flow imaging in women with perimenopausal and postmenopausal bleeding. Correlation to endometrial histopathology.* Acta Obstet Gynecol Scand, 1993. **72**(3): p. 162-6.
68. Wilczak, M., et al., *Clinical usefulness of evaluation of quality parameters of blood flow: pulsation index and resistance index in the uterine arteries in the initial differential diagnostics of pathology within the endometrium.* Eur J Gynaecol Oncol, 2010. **31**(4): p. 437-9.
69. Pandey, H., et al., *Utility of three dimensional (3-D) ultrasound and power Doppler in identification of high risk endometrial cancer at a tertiary care hospital in southern India: A preliminary study.* Taiwan J Obstet Gynecol, 2018. **57**(4): p. 522-527.
70. Emoto, M., et al., *Clinical usefulness of color Doppler ultrasound in patients with endometrial hyperplasia and carcinoma.* Cancer, 2002. **94**(3): p. 700-6.
71. Kurjak, A., et al., *Endometrial carcinoma in postmenopausal women: evaluation by transvaginal color Doppler ultrasonography.* Am J Obstet Gynecol, 1993. **169**(6): p. 1597-603.
72. Epstein, E., et al., *Ultrasound characteristics of endometrial cancer as defined by International Endometrial Tumor Analysis (IETA) consensus nomenclature: prospective multicenter study.* Ultrasound Obstet Gynecol, 2018. **51**(6): p. 818-828.

73. Leone, F.P., et al., *Terms, definitions and measurements to describe the sonographic features of the endometrium and intrauterine lesions: a consensus opinion from the International Endometrial Tumor Analysis (IETA) group.* Ultrasound Obstet Gynecol, 2010. **35**(1): p. 103-12.
74. Timmerman, D., et al., *The pedicle artery sign based on sonography with color Doppler imaging can replace second-stage tests in women with abnormal vaginal bleeding.* Ultrasound Obstet Gynecol, 2003. **22**(2): p. 166-71.
75. Perez-Medina, T., et al., *Predicting atypia inside endometrial polyps.* J Ultrasound Med, 2002. **21**(2): p. 125-8.
76. Gruboeck, K., et al., *The diagnostic value of endometrial thickness and volume measurements by three-dimensional ultrasound in patients with postmenopausal bleeding.* Ultrasound Obstet Gynecol, 1996. **8**(4): p. 272-6.
77. Opolskiene, G., et al., *Three-dimensional ultrasound imaging for discrimination between benign and malignant endometrium in women with postmenopausal bleeding and sonographic endometrial thickness of at least 4.5 mm.* Ultrasound Obstet Gynecol, 2010. **35**(1): p. 94-102.
78. Yaman, C., et al., *The role of three-dimensional volume measurement in diagnosing endometrial cancer in patients with postmenopausal bleeding.* Gynecol Oncol, 2008. **110**(3): p. 390-5.
79. Dueholm, M., et al., *Two- and three-dimensional transvaginal ultrasound with power Doppler angiography and gel infusion sonography for diagnosis of endometrial malignancy.* Ultrasound Obstet Gynecol, 2015. **45**(6): p. 734-43.
80. Kim, A., et al., *Diagnostic utility of three-dimensional power Doppler ultrasound for postmenopausal bleeding.* Taiwan J Obstet Gynecol, 2015. **54**(3): p. 221-6.
81. Jurkovic, D., *Three-dimensional ultrasound in gynecology: a critical evaluation.* Ultrasound Obstet Gynecol, 2002. **19**(2): p. 109-17.
82. Opolskiene, G., P. Sladkevicius, and L. Valentin, *Ultrasound assessment of endometrial morphology and vascularity to predict endometrial malignancy in women with postmenopausal bleeding and sonographic endometrial thickness >or= 4.5 mm.* Ultrasound Obstet Gynecol, 2007. **30**(3): p. 332-40.
83. Valentin, L., *Ultrasound deserves to play a prominent role in the diagnosis and management of endometrial cancer.* Ultrasound Obstet Gynecol, 2014. **43**(5): p. 483-7.
84. Dueholm, M., et al., *An ultrasound algorithm for identification of endometrial cancer.* Ultrasound Obstet Gynecol, 2014. **43**(5): p. 557-68.
85. Paschopoulos, M., et al., *Selecting distending medium for out-patient hysteroscopy. Does it really matter?* Hum Reprod, 2004. **19**(11): p. 2619-25.
86. RCOG, *RCOG / BSGE joint guideline. Best Practice in Outpatient Hysteroscopy. Green-top guideline no. 59.* . 2011.
87. Cooper, N.A., et al., *Vaginoscopic approach to outpatient hysteroscopy: a systematic review of the effect on pain.* BJOG, 2010. **117**(5): p. 532-9.
88. Clark, T.J., et al., *Accuracy of hysteroscopy in the diagnosis of endometrial cancer and hyperplasia: a systematic quantitative review.* JAMA, 2002. **288**(13): p. 1610-21.
89. van Dongen, H., et al., *Diagnostic hysteroscopy in abnormal uterine bleeding: a systematic review and meta-analysis.* Bjog, 2007. **114**(6): p. 664-75.
90. Garuti, G., et al., *Accuracy of hysteroscopic diagnosis of endometrial hyperplasia: a retrospective study of 323 patients.* J Minim Invasive Gynecol, 2005. **12**(3): p. 247-53.

91. Gkrozou, F., et al., *Hysteroscopy in women with abnormal uterine bleeding: a meta-analysis on four major endometrial pathologies.* Arch Gynecol Obstet, 2015. **291**(6): p. 1347-54.
92. Tahir, M.M., et al., *A randomised controlled trial comparing transvaginal ultrasound, outpatient hysteroscopy and endometrial biopsy with inpatient hysteroscopy and curettage.* Br J Obstet Gynaecol, 1999. **106**(12): p. 1259-64.
93. Jansen, F.W., et al., *Complications of hysteroscopy: a prospective, multicenter study.* Obstet Gynecol, 2000. **96**(2): p. 266-70.
94. Clark, T.J., et al., *Accuracy of outpatient endometrial biopsy in the diagnosis of endometrial cancer: a systematic quantitative review.* BJOG, 2002. **109**(3): p. 313-21.
95. Dijkhuizen, F.P., et al., *The accuracy of endometrial sampling in the diagnosis of patients with endometrial carcinoma and hyperplasia: a meta-analysis.* Cancer, 2000. **89**(8): p. 1765-72.
96. Guido, R.S., et al., *Pipelle endometrial sampling. Sensitivity in the detection of endometrial cancer.* J Reprod Med, 1995. **40**(8): p. 553-5.
97. Dimitraki, M., et al., *Clinical evaluation of women with PMB. Is it always necessary an endometrial biopsy to be performed? A review of the literature.* Arch Gynecol Obstet, 2011. **283**(2): p. 261-6.
98. Rodolakis, A., et al., *European Society of Gynecological Oncology Task Force for Fertility Preservation: Clinical Recommendations for Fertility-Sparing Management in Young Endometrial Cancer Patients.* Int J Gynecol Cancer, 2015. **25**(7): p. 1258-65.
99. Leitao, M.M., Jr., et al., *Comparison of D&C and office endometrial biopsy accuracy in patients with FIGO grade 1 endometrial adenocarcinoma.* Gynecol Oncol, 2009. **113**(1): p. 105-8.
100. Gimpelson, R.J. and H.O. Rappold, *A comparative study between panoramic hysteroscopy with directed biopsies and dilatation and curettage. A review of 276 cases.* Am J Obstet Gynecol, 1988. **158**(3 Pt 1): p. 489-92.
101. Ørtoft, G., et al., *Preoperative staging of endometrial cancer using TVS, MRI, and hysteroscopy.* Acta Obstet Gynecol Scand, 2013. **92**(5): p. 536-45.
102. Tinelli, R., et al., *The role of hysteroscopy with eye-directed biopsy in postmenopausal women with uterine bleeding and endometrial atrophy.* Menopause, 2008. **15**(4 Pt 1): p. 737-42.
103. Hammoud, A.O., et al., *Ultrasonography-guided transvaginal endometrial biopsy: a useful technique in patients with cervical stenosis.* Obstet Gynecol, 2006. **107**(2 Pt 2): p. 518-20.
104. Dua, A., S. Egan, and A. Balica, *Sonographically Guided Office Endometrial Sampling: Indications and Results.* J Ultrasound Med, 2019. **38**(5): p. 1223-1227.
105. Lotfallah, H., et al., *One-stop hysteroscopy clinic for postmenopausal bleeding.* J Reprod Med, 2005. **50**(2): p. 101-7.
106. Panda, J.K., *One-stop clinic for postmenopausal bleeding.* J Reprod Med, 2002. **47**(9): p. 761-6.
107. Geomini, P., et al., *Diagnostic accuracy of frozen section diagnosis of the adnexal mass: a metaanalysis.* Gynecol Oncol, 2005. **96**(1): p. 1-9.
108. Al-Ramahi, M., et al., *The value of frozen section Pipelle endometrial biopsy as an outpatient procedure in the diagnosis of ectopic pregnancy.* J Obstet Gynaecol, 2006. **26**(1): p. 63-5.

109. Timmermans, A., et al., *Follow-up of women after a first episode of postmenopausal bleeding and endometrial thickness greater than 4 millimeters.* Obstet Gynecol, 2008. **111**(1): p. 137-43.
110. Van Doorn, H.C., et al., *What is the recurrence rate of postmenopausal bleeding in women who have a thin endometrium during a first episode of postmenopausal bleeding?* Acta Obstet Gynecol Scand, 2008. **87**(1): p. 89-93.
111. Smith, P.P., et al., *Recurrent postmenopausal bleeding: a prospective cohort study.* J Minim Invasive Gynecol, 2014. **21**(5): p. 799-803.
112. Nagele, F., et al., *Endometrial cell dissemination at diagnostic hysteroscopy: a prospective randomized cross-over comparison of normal saline and carbon dioxide uterine distension.* Hum Reprod, 1999. **14**(11): p. 2739-42.
113. Tempfer, C., et al., *Does duration of hysteroscopy increase the risk of disease recurrence in patients with endometrial cancer? A multi-centre trial.* Exp Ther Med, 2011. **2**(5): p. 991-995.
114. Chang, Y.N., et al., *Effect of hysteroscopy on the peritoneal dissemination of endometrial cancer cells: a meta-analysis.* Fertil Steril, 2011. **96**(4): p. 957-61.
115. Polyzos, N.P., et al., *Intraperitoneal dissemination of endometrial cancer cells after hysteroscopy: a systematic review and meta-analysis.* Int J Gynecol Cancer, 2010. **20**(2): p. 261-7.
116. Takac, I. and B. Zegura, *Office hysteroscopy and the risk of microscopic extrauterine spread in endometrial cancer.* Gynecol Oncol, 2007. **107**(1): p. 94-8.
117. Goetz, J.G., *Metastases go with the flow.* Science, 2018. **362**(6418): p. 999-1000.
118. Massagué, J. and A.C. Obenauf, *Metastatic colonization by circulating tumour cells.* Nature, 2016. **529**(7586): p. 298-306.
119. Quail, D.F. and J.A. Joyce, *Microenvironmental regulation of tumor progression and metastasis.* Nat Med, 2013. **19**(11): p. 1423-37.
120. Steeg, P.S., *Tumor metastasis: mechanistic insights and clinical challenges.* Nat Med, 2006. **12**(8): p. 895-904.
121. Klein, C.A., *Cancer progression and the invisible phase of metastatic colonization.* Nat Rev Cancer, 2020. **20**(11): p. 681-694.
122. Eyles, J., et al., *Tumor cells disseminate early, but immunosurveillance limits metastatic outgrowth, in a mouse model of melanoma.* J Clin Invest, 2010. **120**(6): p. 2030-9.
123. Hosseini, H., et al., *Early dissemination seeds metastasis in breast cancer.* Nature, 2016. **540**(7634): p. 552-558.
124. Klein, C.A., *Selection and adaptation during metastatic cancer progression.* Nature, 2013. **501**(7467): p. 365-72.
125. Takahashi, A., et al., *Clinicopathological Features of Early and Late Recurrence of Endometrial Carcinoma After Surgical Resection.* Int J Gynecol Cancer, 2017. **27**(5): p. 967-972.
126. Shepherd, J.H., *Revised FIGO staging for gynaecological cancer.* BJOG, 1989. **96**(8): p. 889-92.
127. Odicino, F., et al., *History of the FIGO cancer staging system.* Int J Gynaecol Obstet, 2008. **101**(2): p. 205-10.
128. Pecorelli, S., *Revised FIGO staging for carcinoma of the vulva, cervix, and endometrium.* Int J Gynaecol Obstet, 2009. **105**(2): p. 103-4.

129. Creasman, W.T., et al., *Surgical pathologic spread patterns of endometrial cancer. A Gynecologic Oncology Group Study.* Cancer, 1987. **60**(8 Suppl): p. 2035-41.
130. Abu-Rustum, N.R., et al., *The revised 2009 FIGO staging system for endometrial cancer: should the 1988 FIGO stages IA and IB be altered?* Int J Gynecol Cancer, 2011. **21**(3): p. 511-6.
131. Horowitz, N.S., et al., *Prospective evaluation of FDG-PET for detecting pelvic and para-aortic lymph node metastasis in uterine corpus cancer.* Gynecol Oncol, 2004. **95**(3): p. 546-51.
132. Kakhki, V.R., et al., *Diagnostic performance of fluorine 18 fluorodeoxyglucose positron emission tomography imaging for detection of primary lesion and staging of endometrial cancer patients: systematic review and meta-analysis of the literature.* Int J Gynecol Cancer, 2013. **23**(9): p. 1536-43.
133. Renaud, M.C. and T. Le, *Epidemiology and investigations for suspected endometrial cancer.* J Obstet Gynaecol Can, 2013. **35**(4): p. 380-381.
134. Kinkel, K., et al., *Radiologic staging in patients with endometrial cancer: a meta-analysis.* Radiology, 1999. **212**(3): p. 711-8.
135. Alcázar, J.L., et al., *Transvaginal ultrasound versus magnetic resonance imaging for preoperative assessment of myometrial infiltration in patients with endometrial cancer: a systematic review and meta-analysis.* J Gynecol Oncol, 2017. **28**(6): p. e86.
136. Alcazar, J.L., et al., *Assessing myometrial infiltration by endometrial cancer: uterine virtual navigation with three-dimensional US.* Radiology, 2009. **250**(3): p. 776-83.
137. Alcazar, J.L., et al., *Transvaginal/transrectal ultrasound for assessing myometrial invasion in endometrial cancer: a comparison of six different approaches.* J Gynecol Oncol, 2015. **26**(3): p. 201-7.
138. Christensen, J.W., et al., *Assessment of myometrial invasion in endometrial cancer using three-dimensional ultrasound and magnetic resonance imaging.* Acta Obstet Gynecol Scand, 2016. **95**(1): p. 55-64.
139. Jantarasaengaram, S., et al., *Three-dimensional ultrasound with volume contrast imaging for preoperative assessment of myometrial invasion and cervical involvement in women with endometrial cancer.* Ultrasound Obstet Gynecol, 2014. **43**(5): p. 569-74.
140. Saarelainen, S.K., et al., *The preoperative assessment of deep myometrial invasion by three-dimensional ultrasound versus MRI in endometrial carcinoma.* Acta Obstet Gynecol Scand, 2012. **91**(8): p. 983-90.
141. Mascilini, F., et al., *Evaluating myometrial and cervical invasion in women with endometrial cancer: comparing subjective assessment with objective measurement techniques.* Ultrasound Obstet Gynecol, 2013. **42**(3): p. 353-8.
142. Yang, T., et al., *Magnetic Resonance Imaging (MRI) and Three-Dimensional Transvaginal Ultrasonography Scanning for Preoperative Assessment of High Risk in Women with Endometrial Cancer.* Med Sci Monit, 2019. **25**: p. 2024-2031.
143. Franchi, M., et al., *Clinical value of intraoperative gross examination in endometrial cancer.* Gynecol Oncol, 2000. **76**(3): p. 357-61.
144. Mavromatis, I.D., et al., *Validity of intraoperative gross examination of myometrial invasion in patients with endometrial cancer: a meta-analysis.* Acta Obstet Gynecol Scand, 2012. **91**(7): p. 779-93.

145. Kucera, E., et al., *Accuracy of intraoperative frozen-section diagnosis in stage I endometrial adenocarcinoma.* Gynecol Obstet Invest, 2000. **49**(1): p. 62-6.
146. Ozdemir, S., et al., *Assessment of myometrial invasion in endometrial cancer by transvaginal sonography, Doppler ultrasonography, magnetic resonance imaging and frozen section.* Int J Gynecol Cancer, 2009. **19**(6): p. 1085-90.
147. Kayikçioğlu, F., et al., *Is frozen-section diagnosis a reliable guide in surgical treatment of stage I endometrial carcinoma?* Acta Oncol, 2002. **41**(5): p. 444-6.
148. Ozturk, E., et al., *Intraoperative frozen section is essential for assessment of myometrial invasion but not for histologic grade confirmation in endometrial cancer: a ten-year experience.* Arch Gynecol Obstet, 2012. **285**(5): p. 1415-9.
149. Kumar, S., et al., *A prospective assessment of the reliability of frozen section to direct intraoperative decision making in endometrial cancer.* Gynecol Oncol, 2012. **127**(3): p. 525-31.
150. Celik, C., et al., *The clinical value of preoperative and intraoperative assessments in the management of endometrial cancer.* Int J Gynecol Cancer, 2010. **20**(3): p. 358-62.
151. Alcazar, J.L., et al., *Intraoperative Gross Examination and Intraoperative Frozen Section in Patients With Endometrial Cancer for Detecting Deep Myometrial Invasion: A Systematic Review and Meta-analysis.* Int J Gynecol Cancer, 2016. **26**(2): p. 407-15.
152. Dotters, D.J., *Preoperative CA 125 in endometrial cancer: is it useful?* Am J Obstet Gynecol, 2000. **182**(6): p. 1328-34.
153. Chung, H.H., et al., *Use of preoperative serum CA-125 levels for prediction of lymph node metastasis and prognosis in endometrial cancer.* Acta Obstet Gynecol Scand, 2006. **85**(12): p. 1501-5.
154. Hsieh, C.H., et al., *Can a preoperative CA 125 level be a criterion for full pelvic lymphadenectomy in surgical staging of endometrial cancer?* Gynecol Oncol, 2002. **86**(1): p. 28-33.
155. Yildiz, A., et al., *Preoperative serum CA 125 level in the prediction of the stage of disease in endometrial carcinoma.* Eur J Obstet Gynecol Reprod Biol, 2012. **164**(2): p. 191-5.
156. Ünsal, M., et al., *The preoperative serum CA125 can predict the lymph node metastasis in endometrioid-type endometrial cancer.* Ginekol Pol, 2018. **89**(11): p. 599-606.
157. de la Orden, S.G., et al., *Laparoscopic hysterectomy in the treatment of endometrial cancer: a systematic review.* J Minim Invasive Gynecol, 2008. **15**(4): p. 395-401.
158. Galaal, K., et al., *Laparoscopy versus laparotomy for the management of early stage endometrial cancer.* Cochrane Database Syst Rev, 2018. **10**(10): p. Cd006655.
159. Ju, W., et al., *Comparison of laparoscopy and laparotomy for management of endometrial carcinoma: a meta-analysis.* Int J Gynecol Cancer, 2009. **19**(3): p. 400-6.
160. Lin, F., et al., *Laparoscopically assisted versus open surgery for endometrial cancer--a meta-analysis of randomized controlled trials.* Int J Gynecol Cancer, 2008. **18**(6): p. 1315-25.
161. Kitchener, H., et al., *Efficacy of systematic pelvic lymphadenectomy in endometrial cancer (MRC ASTEC trial): a randomised study.* Lancet, 2009. **373**(9658): p. 125-36.

162. Frost, J.A., et al., *Lymphadenectomy for the management of endometrial cancer.* Cochrane Database Syst Rev, 2017. **10**(10): p. Cd007585.
163. Chan, J.K., et al., *The outcomes of 27,063 women with unstaged endometrioid uterine cancer.* Gynecol Oncol, 2007. **106**(2): p. 282-8.
164. Amant, F., et al., *Cancer of the corpus uteri.* Int J Gynaecol Obstet, 2018. **143 Suppl 2**: p. 37-50.
165. Antonsen, S.L., et al., *MRI, PET/CT and ultrasound in the preoperative staging of endometrial cancer - a multicenter prospective comparative study.* Gynecol Oncol, 2013. **128**(2): p. 300-8.
166. Arango, H.A., et al., *Accuracy of lymph node palpation to determine need for lymphadenectomy in gynecologic malignancies.* Obstet Gynecol, 2000. **95**(4): p. 553-6.
167. Bogani, G., et al., *Sentinel node mapping vs. lymphadenectomy in endometrial cancer: A systematic review and meta-analysis.* Gynecol Oncol, 2019. **153**(3): p. 676-683.
168. Bergstrom, J., et al., *Minimally invasive hysterectomy surgery rates for endometrial cancer performed at National Comprehensive Cancer Network (NCCN) Centers.* Gynecol Oncol, 2018. **148**(3): p. 480-484.
169. Holloway, R.W., et al., *Sentinel lymph node mapping and staging in endometrial cancer: A Society of Gynecologic Oncology literature review with consensus recommendations.* Gynecol Oncol, 2017. **146**(2): p. 405-415.
170. Favero, G., et al., *Laparoscopic sentinel lymph node detection after hysteroscopic injection of technetium-99 in patients with endometrial cancer.* Int J Gynecol Cancer, 2015. **25**(3): p. 423-30.
171. Rossi, E.C., et al., *A comparison of sentinel lymph node biopsy to lymphadenectomy for endometrial cancer staging (FIRES trial): a multicentre, prospective, cohort study.* Lancet Oncol, 2017. **18**(3): p. 384-392.
172. Bodurtha Smith, A.J., A.N. Fader, and E.J. Tanner, *Sentinel lymph node assessment in endometrial cancer: a systematic review and meta-analysis.* Am J Obstet Gynecol, 2017. **216**(5): p. 459-476.e10.
173. How, J.A., et al., *Sentinel lymph node mapping in endometrial cancer: a systematic review and meta-analysis.* Minerva Ginecol, 2018. **70**(2): p. 194-214.
174. Anastasiadis, P., et al., *The contribution of rapid intraoperative cytology in the evaluation of endometrial cancer spread.* Ann Acad Med Singapore, 2011. **40**(2): p. 80-3.
175. Lambrou, N.C., et al., *Optimal surgical cytoreduction in patients with Stage III and Stage IV endometrial carcinoma: a study of morbidity and survival.* Gynecol Oncol, 2004. **93**(3): p. 653-8.
176. Sonoda, Y., et al., *High incidence of positive peritoneal cytology in low-risk endometrial cancer treated by laparoscopically assisted vaginal hysterectomy.* Gynecol Oncol, 2001. **80**(3): p. 378-82.
177. Talhouk, A., et al., *Confirmation of ProMisE: A simple, genomics-based clinical classifier for endometrial cancer.* Cancer, 2017. **123**(5): p. 802-813.
178. Edmondson, R.J., et al., *Markers of the p53 pathway further refine molecular profiling in high-risk endometrial cancer: A TransPORTEC initiative.* Gynecol Oncol, 2017. **146**(2): p. 327-333.
179. Zeimet, A.G., et al., *L1CAM in early-stage type I endometrial cancer: results of a large multicenter evaluation.* J Natl Cancer Inst, 2013. **105**(15): p. 1142-50.

180. van der Putten, L.J., et al., *L1CAM expression in endometrial carcinomas: an ENITEC collaboration study.* Br J Cancer, 2016. **115**(6): p. 716-24.
181. Bosse, T., et al., *L1 cell adhesion molecule is a strong predictor for distant recurrence and overall survival in early stage endometrial cancer: pooled PORTEC trial results.* Eur J Cancer, 2014. **50**(15): p. 2602-10.
182. Trovik, J., et al., *Hormone receptor loss in endometrial carcinoma curettage predicts lymph node metastasis and poor outcome in prospective multicentre trial.* Eur J Cancer, 2013. **49**(16): p. 3431-41.
183. Visser, N.C., et al., *PIpelle Prospective ENDOmetrial carcinoma (PIPENDO) study, pre-operative recognition of high risk endometrial carcinoma: a multicentre prospective cohort study.* BMC Cancer, 2015. **15**: p. 487.
184. El-Aneed, A., A. Cohen, and J. Banoub, *Mass Spectrometry, Review of the Basics: Electrospray, MALDI, and Commonly Used Mass Analyzers.* Applied Spectroscopy Reviews, 2009. **44**(3): p. 210-230.
185. Takáts, Z., J.M. Wiseman, and R.G. Cooks, *Ambient mass spectrometry using desorption electrospray ionization (DESI): instrumentation, mechanisms and applications in forensics, chemistry, and biology.* J Mass Spectrom, 2005. **40**(10): p. 1261-75.
186. Veselkov, K.A., et al., *Chemo-informatic strategy for imaging mass spectrometry-based hyperspectral profiling of lipid signatures in colorectal cancer.* Proc Natl Acad Sci U S A, 2014. **111**(3): p. 1216-21.
187. Balog, J., et al., *Intraoperative tissue identification using rapid evaporative ionization mass spectrometry.* Sci Transl Med, 2013. **5**(194): p. 194ra93.
188. Schäfer, K.C., et al., *In vivo, in situ tissue analysis using rapid evaporative ionization mass spectrometry.* Angew Chem Int Ed Engl, 2009. **48**(44): p. 8240-2.
189. Balog, J., et al., *Identification of biological tissues by rapid evaporative ionization mass spectrometry.* Anal Chem, 2010. **82**(17): p. 7343-50.
190. Corporation, W. *Image of iKnife*. 2020; Available from: https://www.waters.com/waters/en_US/REIMS-Research-System-with-iKnife-Sampling-Device/nav.htm?locale=en_US&cid=134846529.
191. Cameron, S.J., et al., *Rapid Evaporative Ionisation Mass Spectrometry (REIMS) Provides Accurate Direct from Culture Species Identification within the Genus Candida.* Sci Rep, 2016. **6**: p. 36788.
192. Black, C., et al., *A real time metabolomic profiling approach to detecting fish fraud using rapid evaporative ionisation mass spectrometry.* Metabolomics, 2017. **13**(12): p. 153.
193. Guitton, Y., et al., *Rapid evaporative ionisation mass spectrometry and chemometrics for high-throughput screening of growth promoters in meat producing animals.* Food Addit Contam Part A Chem Anal Control Expo Risk Assess, 2018. **35**(5): p. 900-910.
194. Balog, J., et al., *In vivo endoscopic tissue identification by rapid evaporative ionization mass spectrometry (REIMS).* Angew Chem Int Ed Engl, 2015. **54**(38): p. 11059-62.
195. Alexander, J., et al., *A novel methodology for in vivo endoscopic phenotyping of colorectal cancer based on real-time analysis of the mucosal lipidome: a prospective observational study of the iKnife.* Surg Endosc, 2017. **31**(3): p. 1361-1370.
196. St John, E.R., et al., *Rapid evaporative ionisation mass spectrometry of electrosurgical vapours for the identification of breast pathology: towards an*

intelligent knife for breast cancer surgery. Breast Cancer Res, 2017. **19**(1): p. 59.
197. Vaqas, B., *The real-time molecular characterisation of human brain tumours during surgery using Rapid Evaporative Ionization Mass Spectrometry [REIMS] and Raman spectroscopy: a platform for precision medicine in neurosurgery*, in *Department of Medicine*. 2018, Imperial College London.
198. Tzafetas, M., et al., *The intelligent knife (iKnife) and its intraoperative diagnostic advantage for the treatment of cervical disease.* Proc Natl Acad Sci U S A, 2020. **117**(13): p. 7338-7346.
199. Phelps, D.L., et al., *The surgical intelligent knife distinguishes normal, borderline and malignant gynaecological tissues using rapid evaporative ionisation mass spectrometry (REIMS).* Br J Cancer, 2018. **118**(10): p. 1349-1358.
200. Lambin, P., et al., *Radiomics: extracting more information from medical images using advanced feature analysis.* Eur J Cancer, 2012. **48**(4): p. 441-6.
201. Lambin, P., et al., *Predicting outcomes in radiation oncology--multifactorial decision support systems.* Nat Rev Clin Oncol, 2013. **10**(1): p. 27-40.
202. Kumar, V., et al., *Radiomics: the process and the challenges.* Magn Reson Imaging, 2012. **30**(9): p. 1234-48.
203. Aerts, H.J., et al., *Decoding tumour phenotype by noninvasive imaging using a quantitative radiomics approach.* Nat Commun, 2014. **5**: p. 4006.
204. Anderson, R.E., R.B. Hill, and C.R. Key, *The sensitivity and specificity of clinical diagnostics during five decades. Toward an understanding of necessary fallibility.* JAMA, 1989. **261**(11): p. 1610-7.
205. Kassner, A. and R.E. Thornhill, *Texture analysis: a review of neurologic MR imaging applications.* AJNR Am J Neuroradiol, 2010. **31**(5): p. 809-16.
206. Lakhman, Y., et al., *Second-Opinion Interpretations of Gynecologic Oncologic MRI Examinations by Sub-Specialized Radiologists Influence Patient Care.* Eur Radiol, 2016. **26**(7): p. 2089-98.
207. Gillies, R.J., P.E. Kinahan, and H. Hricak, *Radiomics: Images Are More than Pictures, They Are Data.* Radiology, 2016. **278**(2): p. 563-77.
208. De Bernardi, E., et al., *Radiomics of the primary tumour as a tool to improve (18)F-FDG-PET sensitivity in detecting nodal metastases in endometrial cancer.* EJNMMI Res, 2018. **8**(1): p. 86.
209. Crivellaro, C., et al., *Combining positron emission tomography/computed tomography, radiomics, and sentinel lymph node mapping for nodal staging of endometrial cancer patients.* Int J Gynecol Cancer, 2020. **30**(3): p. 378-382.
210. Xu, X., et al., *Multiplanar MRI-Based Predictive Model for Preoperative Assessment of Lymph Node Metastasis in Endometrial Cancer.* Front Oncol, 2019. **9**: p. 1007.
211. Stanzione, A., et al., *Deep Myometrial Infiltration of Endometrial Cancer on MRI: A Radiomics-Powered Machine Learning Pilot Study.* Acad Radiol, 2020.
212. Ueno, Y., et al., *Endometrial Carcinoma: MR Imaging-based Texture Model for Preoperative Risk Stratification-A Preliminary Analysis.* Radiology, 2017. **284**(3): p. 748-757.
213. Ytre-Hauge, S., et al., *Preoperative tumor texture analysis on MRI predicts high-risk disease and reduced survival in endometrial cancer.* J Magn Reson Imaging, 2018. **48**(6): p. 1637-1647.

214. Luo, Y., et al., *Multiparametric MRI-Based Radiomics Nomogram for Predicting Lymphovascular Space Invasion in Endometrial Carcinoma.* J Magn Reson Imaging, 2020.
215. Bereby-Kahane, M., et al., *Prediction of tumor grade and lymphovascular space invasion in endometrial adenocarcinoma with MR imaging-based radiomic analysis.* Diagn Interv Imaging, 2020.
216. Yun, Y.H., et al., *The influence of hospital volume and surgical treatment delay on long-term survival after cancer surgery.* Ann Oncol, 2012. **23**(10): p. 2731-7.
217. Richards, M.A., et al., *Influence of delay on survival in patients with breast cancer: a systematic review.* Lancet, 1999. **353**(9159): p. 1119-26.
218. Robinson, K.M., et al., *Diagnostic delay, quality of life and patient satisfaction among women diagnosed with endometrial or ovarian cancer: a nationwide Danish study.* Qual Life Res, 2012. **21**(9): p. 1519-25.
219. Levy, T., A. Golan, and J. Menczer, *Endometrial endometrioid carcinoma: a glimpse at the natural course.* Am J Obstet Gynecol, 2006. **195**(2): p. 454-7.
220. Pirog, E.C., D.S. Heller, and C. Westhoff, *Endometrial adenocarcinoma--lack of correlation between treatment delay and tumor stage.* Gynecol Oncol, 1997. **67**(3): p. 303-8.
221. Menczer, J., et al., *The effect of diagnosis and treatment delay on prognostic factors and survival in endometrial carcinoma.* Am J Obstet Gynecol, 1995. **173**(3 Pt 1): p. 774-8.
222. Elit, L.M., et al., *Impact of wait times on survival for women with uterine cancer.* J Clin Oncol, 2014. **32**(1): p. 27-33.
223. Shalowitz, D.I., et al., *Survival implications of time to surgical treatment of endometrial cancers.* Am J Obstet Gynecol, 2017. **216**(3): p. 268.e1-268.e18.
224. Strohl, A.E., et al., *Surgical wait time: A new health indicator in women with endometrial cancer.* Gynecol Oncol, 2016. **141**(3): p. 511-515.
225. Elit, L.M., G. Pond, and H.Y. Seow, *Treatment delay in endometrial cancer. Reply to J. Menczer.* J Clin Oncol, 2014. **32**(19): p. 2114.
226. AlHilli, M.M., et al., *Time to surgery and its impact on survival in patients with endometrial cancer: A National cancer database study.* Gynecol Oncol, 2019. **153**(3): p. 511-516.
227. Matsuo, K., et al., *Time interval between endometrial biopsy and surgical staging for type I endometrial cancer: association between tumor characteristics and survival outcome.* Obstet Gynecol, 2015. **125**(2): p. 424-33.
228. England, N., *Delivering cancer waiting times*. 2014.
229. Johnson, N., et al., *Delays in treating endometrial cancer in the South West of England.* Br J Cancer, 2011. **104**(12): p. 1836-9.
230. Crawford, S.C., et al., *The waiting time paradox: population based retrospective study of treatment delay and survival of women with endometrial cancer in Scotland.* BMJ, 2002. **325**(7357): p. 196.
231. Dolly, D., et al., *A Delay from Diagnosis to Treatment Is Associated with a Decreased Overall Survival for Patients with Endometrial Cancer.* Front Oncol, 2016. **6**: p. 31.
232. Woo, Y.L., et al., *Centralisation of services for gynaecological cancer.* Cochrane Database Syst Rev, 2012. **2012**(3): p. Cd007945.
233. Macdonald, O.K., et al., *Does oncologic specialization influence outcomes following surgery in early stage adenocarcinoma of the endometrium?* Gynecol Oncol, 2005. **99**(3): p. 730-5.

234. Roland, P.Y., et al., *The benefits of a gynecologic oncologist: a pattern of care study for endometrial cancer treatment.* Gynecol Oncol, 2004. **93**(1): p. 125-30.
235. Chan, J.K., et al., *Influence of gynecologic oncologists on the survival of patients with endometrial cancer.* J Clin Oncol, 2011. **29**(7): p. 832-8.
236. Stitzenberg, K.B., et al., *Centralization of cancer surgery: implications for patient access to optimal care.* J Clin Oncol, 2009. **27**(28): p. 4671-8.
237. Birkmeyer, J.D., et al., *Regionalization of high-risk surgery and implications for patient travel times.* JAMA, 2003. **290**(20): p. 2703-8.
238. Adambekov, S., et al., *Patient and provider factors associated with endometrial Pipelle sampling failure.* Gynecol Oncol, 2017. **144**(2): p. 324-328.
239. Sartori, E., et al., *Surveillance procedures for patients treated for endometrial cancer: a review of the literature.* Int J Gynecol Cancer, 2010. **20**(6): p. 985-92.
240. Fung-Kee-Fung, M., et al., *Follow-up after primary therapy for endometrial cancer: a systematic review.* Gynecol Oncol, 2006. **101**(3): p. 520-9.
241. Sartori, E., et al., *Factors influencing survival in endometrial cancer relapsing patients: a Cooperation Task Force (CTF) study.* Int J Gynecol Cancer, 2003. **13**(4): p. 458-65.
242. Agboola, O.O., et al., *Costs and benefits of routine follow-up after curative treatment for endometrial cancer.* Cmaj, 1997. **157**(7): p. 879-86.
243. Menczer, J., *Endometrial carcinoma. Is routine intensive periodic follow-up of value?* Eur J Gynaecol Oncol, 2000. **21**(5): p. 461-5.
244. Boronow, R.C., et al., *Surgical staging in endometrial cancer: clinical-pathologic findings of a prospective study.* Obstet Gynecol, 1984. **63**(6): p. 825-32.
245. Wylie, J., et al., *Results of radical radiotherapy for recurrent endometrial cancer.* Gynecol Oncol, 2000. **77**(1): p. 66-72.
246. Simsek, S.Y., et al., *Clinicopathologic characteristics of recurrent endometrioid endometrial cancer patients and analysis of methods used during surveillance.* J Gynecol Obstet Hum Reprod, 2019. **48**(7): p. 473-477.
247. Jeppesen, M.M., et al., *Patient-initiated follow up affects fear of recurrence and healthcare use: a randomised trial in early-stage endometrial cancer.* BJOG, 2018. **125**(13): p. 1705-1714.
248. Wright, J.D., et al., *Trends in Periodic Surveillance Testing for Early-Stage Uterine Cancer Survivors.* Obstet Gynecol, 2016. **127**(3): p. 449-58.
249. Menczer, J., *Treatment delay in endometrial cancer.* J Clin Oncol, 2014. **32**(19): p. 2113-4.
250. Clegg, L.X., et al., *Impact of socioeconomic status on cancer incidence and stage at diagnosis: selected findings from the surveillance, epidemiology, and end results: National Longitudinal Mortality Study.* Cancer Causes Control, 2009. **20**(4): p. 417-35.
251. DeSantis, C., A. Jemal, and E. Ward, *Disparities in breast cancer prognostic factors by race, insurance status, and education.* Cancer Causes Control, 2010. **21**(9): p. 1445-50.
252. Collins, Y., et al., *Gynecologic cancer disparities: a report from the Health Disparities Taskforce of the Society of Gynecologic Oncology.* Gynecol Oncol, 2014. **133**(2): p. 353-61.
253. Mitchell, A.J., et al., *Prevalence of depression, anxiety, and adjustment disorder in oncological, haematological, and palliative-care settings: a meta-analysis of 94 interview-based studies.* Lancet Oncol, 2011. **12**(2): p. 160-74.

254. Horsboel, T.A., et al., *Increased risk for depression persists for years among women treated for gynecological cancers - a register-based cohort study with up to 19years of follow-up.* Gynecol Oncol, 2019.
255. Klaassen, Z., et al., *Cancer diagnosis and risk of suicide after accounting for prediagnosis psychiatric care: A matched-cohort study of patients with incident solid-organ malignancies.* Cancer, 2019.
256. Mitchell, A.J., et al., *Depression and anxiety in long-term cancer survivors compared with spouses and healthy controls: a systematic review and meta-analysis.* Lancet Oncol, 2013. **14**(8): p. 721-32.
257. Linden, W., et al., *Anxiety and depression after cancer diagnosis: prevalence rates by cancer type, gender, and age.* J Affect Disord, 2012. **141**(2-3): p. 343-51.
258. Boinon, D., et al., *Patient satisfaction with a rapid diagnosis of suspicious breast lesions: Association with distress and anxiety.* Breast J, 2018. **24**(2): p. 154-160.
259. Hislop, T.G., et al., *Satisfaction and anxiety for women during investigation of an abnormal screening mammogram.* Breast Cancer Res Treat, 2002. **76**(3): p. 245-54.
260. Brocken, P., et al., *The faster the better?-A systematic review on distress in the diagnostic phase of suspected cancer, and the influence of rapid diagnostic pathways.* Psychooncology, 2012. **21**(1): p. 1-10.
261. Liao, M.N., et al., *Uncertainty and anxiety during the diagnostic period for women with suspected breast cancer.* Cancer Nurs, 2008. **31**(4): p. 274-83.
262. Woodward, V. and C. Webb, *Women's anxieties surrounding breast disorders: a systematic review of the literature.* J Adv Nurs, 2001. **33**(1): p. 29-41.
263. MacFarlane, M.E. and S.D. Sony, *Women, breast lump discovery, and associated stress.* Health Care Women Int, 1992. **13**(1): p. 23-32.
264. Grupe, D.W. and J.B. Nitschke, *Uncertainty and anticipation in anxiety: an integrated neurobiological and psychological perspective.* Nat Rev Neurosci, 2013. **14**(7): p. 488-501.
265. Reuman, L., et al., *Uncertainty as an anxiety cue at high and low levels of threat.* J Behav Ther Exp Psychiatry, 2015. **47**: p. 111-9.
266. Deane, K.A. and L.F. Degner, *Information needs, uncertainty, and anxiety in women who had a breast biopsy with benign outcome.* Cancer Nurs, 1998. **21**(2): p. 117-26.
267. Mishel, M.H., *Uncertainty in illness.* Image J Nurs Sch, 1988. **20**(4): p. 225-32.
268. Bolwell, B.J. and A.A. Khorana, *Enhancing Value for Patients With Cancer: Time to Treatment as a Surrogate for Integrated Cancer Care.* J Natl Compr Canc Netw, 2016. **14**(1): p. 115-6.
269. Johannessen-Henry CT, D.I., Bidstrup PE, Dalton SO, Johansen C., *Associations between faith, distress and mental adjustment--a Danish survivorship study.* Acta Oncol., 2013. **52**(2): p. 364-71.
270. Dunn, J., et al., *Trajectories of psychological distress after colorectal cancer.* Psychooncology, 2013. **22**(8): p. 1759-65.
271. Jeong, H., et al., *Discordance between self-report and clinical diagnosis of Internet gaming disorder in adolescents.* Sci Rep, 2018. **8**(1): p. 10084.
272. Dolbeault, S., et al., *Screening for psychological distress in two French cancer centers: feasibility and performance of the adapted distress thermometer.* Palliat Support Care, 2008. **6**(2): p. 107-17.

273. Andersen, B.L., et al., *Screening, assessment, and care of anxiety and depressive symptoms in adults with cancer: an American Society of Clinical Oncology guideline adaptation.* J Clin Oncol, 2014. **32**(15): p. 1605-19.
274. Beekers, N., et al., *Symptoms of Anxiety and Depression Are Associated With Satisfaction With Information Provision and Internet Use Among 3080 Cancer Survivors: Results of the PROFILES Registry.* Cancer Nurs, 2015. **38**(5): p. 335-42.
275. Galloway, S.C. and J.E. Graydon, *Uncertainty, symptom distress, and information needs after surgery for cancer of the colon.* Cancer Nurs, 1996. **19**(2): p. 112-7.
276. Wieser, T., et al., *Factors influencing the level of patients using the internet to gather information before anaesthesia: a single-centre survey of 815 patients in Switzerland : The internet for patient information before anaesthesia.* BMC Anesthesiol, 2017. **17**(1): p. 39.
277. McLeod, J., I. Yu, and P.A. Ingledew, *Peering into the Deep: Characterizing the Internet Search Patterns of Patients with Gynecologic Cancers.* J Cancer Educ, 2017. **32**(1): p. 85-90.
278. Marcasciano, M., et al., *The New Trend of Pre-pectoral Breast Reconstruction: An Objective Evaluation of the Quality of Online Information for Patients Undergoing Breast Reconstruction.* Aesthetic Plast Surg, 2019. **43**(3): p. 593-599.
279. Zhang, D., C. Schumacher, and M.B. Harris, *The quality and readability of internet information regarding clavicle fractures.* J Orthop Sci, 2016. **21**(2): p. 143-6.
280. Lawrentschuk, N., et al., *Health information quality on the internet in gynecological oncology: a multilingual evaluation.* Eur J Gynaecol Oncol, 2016. **37**(4): p. 478-483.
281. Trevino, K.M., A.D. Naik, and J. Moye, *Perceived and Actual Change in Religion/Spirituality in Cancer Survivors: Longitudinal Relationships With Distress and Perceived Growth.* Psycholog Relig Spiritual, 2016. **8**(3): p. 195-205.
282. Kamen, C., et al., *The association between partner support and psychological distress among prostate cancer survivors in a nationwide study.* J Cancer Surviv, 2015. **9**(3): p. 492-9.
283. Borstelmann, N.A., et al., *Partner support and anxiety in young women with breast cancer.* Psychooncology, 2015. **24**(12): p. 1679-85.
284. Hill, J., et al., *Predictors of onset of depression and anxiety in the year after diagnosis of breast cancer.* Psychol Med, 2011. **41**(7): p. 1429-36.
285. Carlson, L.E., et al., *What goes up does not always come down: patterns of distress, physical and psychosocial morbidity in people with cancer over a one year period.* Psychooncology, 2013. **22**(1): p. 168-76.
286. Bradley, S., et al., *Quality of life and mental health in cervical and endometrial cancer survivors.* Gynecol Oncol, 2006. **100**(3): p. 479-86.
287. Dietsch, E. and C. Davies, *The nocebo effect for women in waiting.* Collegian, 2007. **14**(3): p. 9-14.
288. Sardo, A.D.S., G. Calagna, and C. Di Carlo, *Tips and tricks in office hysteroscopy.* Gynecology and Minimally Invasive Therapy, 2015. **4**(1): p. 3-7.
289. Young, A., et al., *Entonox® inhalation to reduce pain in common diagnostic and therapeutic outpatient urological procedures: a review of the evidence.* Ann R Coll Surg Engl, 2012. **94**(1): p. 8-11.

290. Dey, P., et al., *Costs and benefits of a one stop clinic compared with a dedicated breast clinic: randomised controlled trial.* BMJ, 2002. **324**(7336): p. 507.
291. Poole, K., et al., *Psychological distress associated with waiting for results of diagnostic investigations for breast disease.* Breast, 1999. **8**(6): p. 334-8.
292. Woo, A.K., *Depression and Anxiety in Pain.* Rev Pain, 2010. **4**(1): p. 8-12.
293. Biddiss, E., T.J. Knibbe, and A. McPherson, *The effectiveness of interventions aimed at reducing anxiety in health care waiting spaces: a systematic review of randomized and nonrandomized trials.* Anesth Analg, 2014. **119**(2): p. 433-48.
294. Stafford, L., et al., *Predictors of depression and anxiety symptom trajectories in the 24 months following diagnosis of breast or gynaecologic cancer.* Breast, 2016. **26**: p. 100-5.
295. Beck, A.T., et al., *An inventory for measuring clinical anxiety: psychometric properties.* J Consult Clin Psychol, 1988. **56**(6): p. 893-7.
296. Spitzer, R.L., et al., *A brief measure for assessing generalized anxiety disorder: the GAD-7.* Arch Intern Med, 2006. **166**(10): p. 1092-7.
297. Moore, M.T., et al., *Using the GAD-Q-IV to identify generalized anxiety disorder in psychiatric treatment seeking and primary care medical samples.* J Anxiety Disord, 2014. **28**(1): p. 25-30.
298. Zigmond, A.S. and R.P. Snaith, *The hospital anxiety and depression scale.* Acta Psychiatr Scand, 1983. **67**(6): p. 361-70.
299. Meyer, T.J., et al., *Development and validation of the Penn State Worry Questionnaire.* Behav Res Ther, 1990. **28**(6): p. 487-95.
300. Hopko, D.R., et al., *Assessing worry in older adults: confirmatory factor analysis of the Penn State Worry Questionnaire and psychometric properties of an abbreviated model.* Psychol Assess, 2003. **15**(2): p. 173-83.
301. Spielberger CD, G.R., Lushene R, *State Trait Anxiety Inventory for Adults Manual*. 1983, Palo Alto, CA,: Consulting Psychologists Press,.
302. Hall, A., R. A'Hern, and L. Fallowfield, *Are we using appropriate self-report questionnaires for detecting anxiety and depression in women with early breast cancer?* Eur J Cancer, 1999. **35**(1): p. 79-85.
303. Parkerson, H.A., et al., *Cultural-based biases of the GAD-7.* J Anxiety Disord, 2015. **31**: p. 38-42.
304. Plummer, F., et al., *Screening for anxiety disorders with the GAD-7 and GAD-2: a systematic review and diagnostic metaanalysis.* Gen Hosp Psychiatry, 2016. **39**: p. 24-31.
305. Herr, N.R., et al., *Does this patient have generalized anxiety or panic disorder?: The Rational Clinical Examination systematic review.* JAMA, 2014. **312**(1): p. 78-84.
306. Rolstad, S., J. Adler, and A. Ryden, *Response burden and questionnaire length: is shorter better? A review and meta-analysis.* Value Health, 2011. **14**(8): p. 1101-8.
307. Vohra, S., et al., *Measuring reliability and validity of "Stressometer((R))": A computer-based mass screening and assessment tool for evaluation of stress level and sources of stressors.* Indian J Psychiatry, 2019. **61**(3): p. 295-299.
308. Amirkhan, J.H., *Stress overload: a new approach to the assessment of stress.* Am J Community Psychol, 2012. **49**(1-2): p. 55-71.
309. Cohen, S., T. Kamarck, and R. Mermelstein, *A global measure of perceived stress.* J Health Soc Behav, 1983. **24**(4): p. 385-96.
310. Coleman, M.P., et al., *Cancer survival in Australia, Canada, Denmark, Norway, Sweden, and the UK, 1995-2007 (the International Cancer*

Benchmarking Partnership): an analysis of population-based cancer registry data. Lancet, 2011. **377**(9760): p. 127-38.
311. Huang, C. and C. Freter, *Lipid metabolism, apoptosis and cancer therapy.* Int J Mol Sci, 2015. **16**(1): p. 924-49.
312. Maxfield, F.R. and I. Tabas, *Role of cholesterol and lipid organization in disease.* Nature, 2005. **438**(7068): p. 612-21.
313. Wickner, W.T., *Eugene Patrick Kennedy, 1919-2011.* Proc Natl Acad Sci U S A, 2011. **108**(48): p. 19122-3.
314. Oude Weernink, P.A., et al., *Dynamic phospholipid signaling by G protein-coupled receptors.* Biochim Biophys Acta, 2007. **1768**(4): p. 888-900.
315. Zechner, R., et al., *FAT SIGNALS--lipases and lipolysis in lipid metabolism and signaling.* Cell Metab, 2012. **15**(3): p. 279-91.
316. Hannun, Y.A. and L.M. Obeid, *Principles of bioactive lipid signalling: lessons from sphingolipids.* Nat Rev Mol Cell Biol, 2008. **9**(2): p. 139-50.
317. Baenke, F., et al., *Hooked on fat: the role of lipid synthesis in cancer metabolism and tumour development.* Dis Model Mech, 2013. **6**(6): p. 1353-63.
318. institute, N.c. *Uterine cancer*. 2020; Available from: https://portal.gdc.cancer.gov/exploration?filters=%7B%22op%22%3A%22and%22%2C%22content%22%3A%5B%7B%22op%22%3A%22in%22%2C%22content%22%3A%7B%22field%22%3A%22cases.primary_site%22%2C%22value%22%3A%5B%22corpus%20uteri%22%5D%7D%7D%5D%7D&searchTableTab=genes.
319. Chen, C.Y., et al., *PTEN: Tumor Suppressor and Metabolic Regulator.* Front Endocrinol (Lausanne), 2018. **9**: p. 338.
320. Lau, C.E., et al., *Metabolomic characterisation of the effects of oncogenic PIK3CA transformation in a breast epithelial cell line.* Sci Rep, 2017. **7**: p. 46079.
321. Qu, Y.L., et al., *Arid1a regulates insulin sensitivity and lipid metabolism.* EBioMedicine, 2019. **42**: p. 481-493.
322. Parrales, A. and T. Iwakuma, *p53 as a Regulator of Lipid Metabolism in Cancer.* Int J Mol Sci, 2016. **17**(12).
323. Koundouros, N. and G. Poulogiannis, *Reprogramming of fatty acid metabolism in cancer.* British Journal of Cancer, 2020. **122**(1): p. 4-22.
324. Menendez, J.A. and R. Lupu, *Fatty acid synthase and the lipogenic phenotype in cancer pathogenesis.* Nat Rev Cancer, 2007. **7**(10): p. 763-77.
325. Lupu, R. and J.A. Menendez, *Pharmacological inhibitors of Fatty Acid Synthase (FASN)--catalyzed endogenous fatty acid biogenesis: a new family of anti-cancer agents?* Curr Pharm Biotechnol, 2006. **7**(6): p. 483-93.
326. Luu, W., et al., *The role of signalling in cellular cholesterol homeostasis.* IUBMB Life, 2013. **65**(8): p. 675-84.
327. Danilo, C. and P.G. Frank, *Cholesterol and breast cancer development.* Curr Opin Pharmacol, 2012. **12**(6): p. 677-82.
328. Santos, C.R. and A. Schulze, *Lipid metabolism in cancer.* Febs j, 2012. **279**(15): p. 2610-23.
329. Abramson, H.N., *The lipogenesis pathway as a cancer target.* J Med Chem, 2011. **54**(16): p. 5615-38.
330. Janardhan, S., P. Srivani, and G.N. Sastry, *Choline kinase: an important target for cancer.* Curr Med Chem, 2006. **13**(10): p. 1169-86.

331. Trousil, S., et al., *Alterations of choline phospholipid metabolism in endometrial cancer are caused by choline kinase alpha overexpression and a hyperactivated deacylation pathway.* Cancer Res, 2014. **74**(23): p. 6867-77.
332. Altadill, T., et al., *Metabolomic and Lipidomic Profiling Identifies The Role of the RNA Editing Pathway in Endometrial Carcinogenesis.* Sci Rep, 2017. **7**(1): p. 8803.
333. Knific, T., et al., *Models including plasma levels of sphingomyelins and phosphatidylcholines as diagnostic and prognostic biomarkers of endometrial cancer.* J Steroid Biochem Mol Biol, 2018. **178**: p. 312-321.
334. Henkels, K.M., et al., *Cell invasion of highly metastatic MTLn3 cancer cells is dependent on phospholipase D2 (PLD2) and Janus kinase 3 (JAK3).* J Mol Biol, 2011. **408**(5): p. 850-62.
335. Chen, Q., et al., *Key roles for the lipid signaling enzyme phospholipase d1 in the tumor microenvironment during tumor angiogenesis and metastasis.* Sci Signal, 2012. **5**(249): p. ra79.
336. Rysman, E., et al., *De novo lipogenesis protects cancer cells from free radicals and chemotherapeutics by promoting membrane lipid saturation.* Cancer Res, 2010. **70**(20): p. 8117-26.
337. Byrne, F.L., et al., *Metabolic vulnerabilities in endometrial cancer.* Cancer Res, 2014. **74**(20): p. 5832-45.
338. Li, W., et al., *Repression of endometrial tumor growth by targeting SREBP1 and lipogenesis.* Cell Cycle, 2012. **11**(12): p. 2348-58.
339. Knapp, P., et al., *Altered sphingolipid metabolism in human endometrial cancer.* Prostaglandins Other Lipid Mediat, 2010. **92**(1-4): p. 62-6.
340. institute, N.C. *Endometrial Cancer Treatment (PDQ®)–Health Professional Version*. 2020; Available from: https://www.cancer.gov/types/uterine/hp/endometrial-treatment-pdq#cit/section_3.4.
341. Sud, M., et al., *LMSD: LIPID MAPS structure database.* Nucleic Acids Res, 2007. **35**(Database issue): p. D527-32.
342. trust, W. *LipidMaps*. 2020 [cited 2020; Available from: https://www.lipidmaps.org/resources/databases/index.php.
343. Yoshida, G.J., *Metabolic reprogramming: the emerging concept and associated therapeutic strategies.* J Exp Clin Cancer Res, 2015. **34**: p. 111.
344. Espinosa, I., et al., *Stromal signatures in endometrioid endometrial carcinomas.* Mod Pathol, 2014. **27**(4): p. 631-9.
345. Sahoo, S.S., et al., *The Emerging Role of the Microenvironment in Endometrial Cancer.* Cancers (Basel), 2018. **10**(11).
346. McAllister, S.S. and R.A. Weinberg, *The tumour-induced systemic environment as a critical regulator of cancer progression and metastasis.* Nat Cell Biol, 2014. **16**(8): p. 717-27.
347. Omi, T. and K. Numano, *The Role of the CO2 Laser and Fractional CO2 Laser in Dermatology.* Laser Ther, 2014. **23**(1): p. 49-60.
348. Genangeli, M., R.M.A. Heeren, and T. Porta Siegel, *Tissue classification by rapid evaporative ionization mass spectrometry (REIMS): comparison between a diathermic knife and CO(2) laser sampling on classification performance.* Anal Bioanal Chem, 2019. **411**(30): p. 7943-7955.
349. Talbi, S., et al., *Molecular phenotyping of human endometrium distinguishes menstrual cycle phases and underlying biological processes in normo-ovulatory women.* Endocrinology, 2006. **147**(3): p. 1097-121.

350. Gatius, S., et al., *Tumor Heterogeneity in Endometrial Carcinoma: Practical Consequences.* Pathobiology, 2018. **85**(1-2): p. 35-40.
351. McCluggage, W.G., *My approach to the interpretation of endometrial biopsies and curettings.* J Clin Pathol, 2006. **59**(8): p. 801-12.
352. Melissa Gordon, K.I. *Pathology of Endometrial Carcinoma*. 2008; Available from: https://www.glowm.com/section_view/heading/Pathology%20of%20Endometrial%20Carcinoma/item/238.
353. Bodai, Z., St John, E., White, E., Temelkuran, B., Wang, H., Hui-Yu, H., McKenzie, J., Rosini F., Balog J., Leff D., Yang, G-Z., Takats, Z. *Comparison of Radiative and Conductive Rapid Evaporation Ionisation Mass Spectrometry on Healthy and Cancerous Breast Tissue for Real-Time Tissue Identification*. in *MSACL* 2017.
354. Glowka, T.R., et al., *Argon and helium plasma coagulation of porcine liver tissue.* J Int Med Res, 2017. **45**(5): p. 1505-1517.
355. Deb, S., et al., *Comparison of tissue effects quantified histologically between PlasmaJet coagulator and Helica thermal coagulator.* Arch Gynecol Obstet, 2012. **286**(2): p. 399-402.
356. Aue-Aungkul, A., P. Kleebkaow, and C. Kietpeerakool, *Incidence and risk factors for insufficient endometrial tissue from endometrial sampling.* Int J Womens Health, 2018. **10**: p. 453-457.
357. Altmäe, S., et al., *Guidelines for the design, analysis and interpretation of 'omics' data: focus on human endometrium.* Hum Reprod Update, 2014. **20**(1): p. 12-28.
358. Guenther, S., et al., *Spatially resolved metabolic phenotyping of breast cancer by desorption electrospray ionization mass spectrometry.* Cancer Res, 2015. **75**(9): p. 1828-37.
359. Hilvo, M., et al., *Novel theranostic opportunities offered by characterization of altered membrane lipid metabolism in breast cancer progression.* Cancer Res, 2011. **71**(9): p. 3236-45.
360. Wang, J., C. Wang, and X. Han, *Tutorial on lipidomics.* Anal Chim Acta, 2019. **1061**: p. 28-41.
361. Farrokhi Yekta, R., et al., *The metabolomics and lipidomics window into thyroid cancer research.* Biomarkers, 2017. **22**(7): p. 595-603.
362. Min, H.K., et al., *Shotgun lipidomics for candidate biomarkers of urinary phospholipids in prostate cancer.* Anal Bioanal Chem, 2011. **399**(2): p. 823-30.
363. Perez, O., et al., *Abstract 3496: Breast cancer and obesity impact the lipid composition of breast adipose tissue: a preliminary study using shotgun lipidomics.* Cancer Research, 2014. **74**(19 Supplement): p. 3496.
364. Hutt, S., et al., *The role of biomarkers in endometrial cancer and hyperplasia: a literature review.* Acta Oncol, 2019. **58**(3): p. 342-352.
365. Srinivas, P.R., B.S. Kramer, and S. Srivastava, *Trends in biomarker research for cancer detection.* Lancet Oncol, 2001. **2**(11): p. 698-704.
366. Hanash, S.M., C.S. Baik, and O. Kallioniemi, *Emerging molecular biomarkers--blood-based strategies to detect and monitor cancer.* Nat Rev Clin Oncol, 2011. **8**(3): p. 142-50.
367. Cohen, J.D., et al., *Detection and localization of surgically resectable cancers with a multi-analyte blood test.* Science, 2018. **359**(6378): p. 926-930.

368. Elshimali, Y.I., et al., *The clinical utilization of circulating cell free DNA (CCFDNA) in blood of cancer patients.* Int J Mol Sci, 2013. **14**(9): p. 18925-58.
369. Wang, L., et al., *Circulating microRNAs as a fingerprint for endometrial endometrioid adenocarcinoma.* PLoS One, 2014. **9**(10): p. e110767.
370. Jia, W., et al., *Identification of four serum microRNAs from a genome-wide serum microRNA expression profile as potential non-invasive biomarkers for endometrioid endometrial cancer.* Oncol Lett, 2013. **6**(1): p. 261-267.
371. Torres, A., et al., *Diagnostic and prognostic significance of miRNA signatures in tissues and plasma of endometrioid endometrial carcinoma patients.* Int J Cancer, 2013. **132**(7): p. 1633-45.
372. Li, L.M., et al., *Human epididymis protein 4 in endometrial cancer: A meta-analysis.* Clin Chim Acta, 2018. **482**: p. 215-223.
373. Bian, J., et al., *Clinical Significance of Serum HE4, CA125, CA724, and CA19-9 in Patients With Endometrial Cancer.* Technol Cancer Res Treat, 2017. **16**(4): p. 435-439.
374. Jiang, T., L. Huang, and S. Zhang, *Preoperative serum CA125: a useful marker for surgical management of endometrial cancer.* BMC Cancer, 2015. **15**: p. 396.
375. Jiang, T., et al., *Clinical significance of serum DKK-1 in patients with gynecological cancer.* Int J Gynecol Cancer, 2009. **19**(7): p. 1177-81.
376. Benati, M., et al., *The clinical significance of DJ-1 and HE4 in patients with endometrial cancer.* J Clin Lab Anal, 2018. **32**(1).
377. Di Cello, A., et al., *DJ-1 is a reliable serum biomarker for discriminating high-risk endometrial cancer.* Tumour Biol, 2017. **39**(6): p. 1010428317705746.
378. Njoku, K., et al., *Proteomic Biomarkers for the Detection of Endometrial Cancer.* Cancers (Basel), 2019. **11**(10).
379. Bahado-Singh, R.O., et al., *Metabolomic prediction of endometrial cancer.* Metabolomics, 2017. **14**(1): p. 6.
380. Troisi, J., et al., *Metabolomic Signature of Endometrial Cancer.* J Proteome Res, 2018. **17**(2): p. 804-812.
381. Farias-Eisner, G., et al., *Validation of serum biomarkers for detection of early- and late-stage endometrial cancer.* Am J Obstet Gynecol, 2010. **202**(1): p. 73.e1-5.
382. Paraskevaidi, M., et al., *Detecting Endometrial Cancer by Blood Spectroscopy: A Diagnostic Cross-Sectional Study.* Cancers (Basel), 2020. **12**(5).
383. Clark, T.J., et al., *Investigating postmenopausal bleeding for endometrial cancer: cost-effectiveness of initial diagnostic strategies.* BJOG, 2006. **113**(5): p. 502-10.
384. Visser, N.C.M., et al., *Accuracy of Endometrial Sampling in Endometrial Carcinoma: A Systematic Review and Meta-analysis.* Obstet Gynecol, 2017. **130**(4): p. 803-813.
385. van Hanegem, N., et al., *The accuracy of endometrial sampling in women with postmenopausal bleeding: a systematic review and meta-analysis.* Eur J Obstet Gynecol Reprod Biol, 2016. **197**: p. 147-55.
386. Ahmad, G., et al., *Pain relief in office gynaecology: a systematic review and meta-analysis.* Eur J Obstet Gynecol Reprod Biol, 2011. **155**(1): p. 3-13.
387. Abbas, A.M., et al., *Medications for pain relief in outpatient endometrial sampling or biopsy: a systematic review and network meta-analysis.* Fertil Steril, 2019. **112**(1): p. 140-148.e12.

388. Mattar, O.M., et al., *Efficacy and safety of tramadol in pain relief during diagnostic outpatient hysteroscopy: systematic review and meta-analysis of randomized controlled trials.* Fertil Steril, 2019. **111**(3): p. 547-552.
389. O'Flynn, H., et al., *Pain relief in outpatient hysteroscopy: a survey of current UK clinical practice.* Eur J Obstet Gynecol Reprod Biol, 2011. **154**(1): p. 9-15.
390. Paulo, A.A.S., et al., *What proportion of women refers moderate to severe pain during office hysteroscopy with a mini-hysteroscope? A systematic review and meta-analysis.* Arch Gynecol Obstet, 2016. **293**(1): p. 37-46.
391. Samy, A., et al., *Pain management during diagnostic office hysteroscopy in postmenopausal women: a randomized study.* Climacteric, 2020: p. 1-7.
392. Issat, T., et al., *A randomized, single blind, placebo-controlled trial for the pain reduction during the outpatient hysteroscopy after ketoprofen or intravaginal misoprostol.* J Minim Invasive Gynecol, 2014. **21**(5): p. 921-7.
393. Ahmad, G., et al., *Pain relief for outpatient hysteroscopy.* Cochrane Database Syst Rev, 2010(11): p. Cd007710.
394. Soriano, D., et al., *Lidocaine spray and outpatient hysteroscopy: randomized placebo-controlled trial.* Obstet Gynecol, 2000. **96**(5 Pt 1): p. 661-4.
395. Hassan, L. and M.J. Gannon, *Anaesthesia and analgesia for ambulatory hysteroscopic surgery.* Best Pract Res Clin Obstet Gynaecol, 2005. **19**(5): p. 681-91.
396. Siddle, N.C., et al., *A controlled trial of naproxen sodium for relief of pain associated with Vabra suction curettage.* BJOG, 1983. **90**(9): p. 864-9.
397. Acmaz, G., et al., *Effect of paracetamol, dexketoprofen trometamol, lidocaine spray, pethidine & diclofenac sodium application for pain relief during fractional curettage: A randomized controlled trial.* Indian J Med Res, 2015. **142**(4): p. 399-404.
398. Einarsson, J.I., G. Henao, and A.E. Young, *Topical analgesia for endometrial biopsy: a randomized controlled trial.* Obstet Gynecol, 2005. **106**(1): p. 128-30.
399. Yilmazer, M., et al., *Efficacy of transcutaneous electrical nerve stimulation for pain relief in women undergoing office endometrial biopsy.* Arch Gynecol Obstet, 2012. **285**(4): p. 1059-64.
400. Somchit, W., A.A. Lertkhachonsuk, and S.A. Vallipakorn, *Naproxen for Pain Relief during Endometrial Biopsy: A Randomized Controlled Trial.* J Med Assoc Thai, 2015. **98**(7): p. 631-5.
401. Telli, E., et al., *Vaginal misoprostol versus a rectal nonsteroidal anti-inflammatory drug to reduce pain during Pipelle endometrial biopsies: a prospective, randomized, placebo-controlled trial.* Gynecol Obstet Invest, 2014. **78**(4): p. 230-4.
402. Perrone, J.F., et al., *Oral misoprostol before office endometrial biopsy.* Obstet Gynecol, 2002. **99**(3): p. 439-44.
403. Sargin, M.A., et al., *Lidocaine and tenoxicam effectiveness for pain relief during Pipelle: Non-randomised double-blind placebo-controlled trial.* J Pak Med Assoc, 2017. **67**(4): p. 527-533.
404. Güney, M., B. Oral, and T. Mungan, *Intrauterine lidocaine plus buccal misoprostol in the endometrial biopsy.* Int J Gynaecol Obstet, 2007. **97**(2): p. 125-8.
405. Kosus, N., et al., *Transcervical intrauterine levobupivacaine or lidocaine infusion for pain control during endometrial biopsy.* Pain Res Manag, 2014. **19**(2): p. 82-6.

406. Trolice, M.P., C. Fishburne, Jr., and S. McGrady, *Anesthetic efficacy of intrauterine lidocaine for endometrial biopsy: a randomized double-masked trial.* Obstet Gynecol, 2000. **95**(3): p. 345-7.
407. Cengiz, H., et al., *Comparing the efficacy of intrauterine lidocaine and paracervical block in decreasing the pain associated with endometrial biopsy: a randomised trial.* Arch Gynecol Obstet, 2014. **289**(3): p. 609-14.
408. Dogan, E., et al., *Anesthetic effect of intrauterine lidocaine plus naproxen sodium in endometrial biopsy.* Obstet Gynecol, 2004. **103**(2): p. 347-51.
409. Kaya, C., et al., *Comparison of placebo and intrauterine lidocaine with/or without rectal diclofenac sodium suppositories used in office endometrial biopsy.* J Pak Med Assoc, 2015. **65**(1): p. 29-34.
410. Wood, M.A., et al., *Overcoming the Challenging Cervix: Identification and Techniques to Access the Uterine Cavity.* Obstet Gynecol Surv, 2018. **73**(11): p. 641-649.
411. Fatih Toy, M., et al., *Accelerated autofocusing of off-axis holograms using critical sampling.* Opt Lett, 2012. **37**(24): p. 5094-6.
412. Christianson, M.S., M.A. Barker, and S.R. Lindheim, *Overcoming the challenging cervix: techniques to access the uterine cavity.* J Low Genit Tract Dis, 2008. **12**(1): p. 24-31.
413. Bettocchi, S., et al., *Challenging the cervix: strategies to overcome the anatomic impediments to hysteroscopy: analysis of 31,052 office hysteroscopies.* Fertil Steril, 2016. **105**(5): p. e16-e17.
414. Scanlan, K.A., P.A. Propeck, and F.T. Lee, Jr., *Invasive procedures in the female pelvis: value of transabdominal, endovaginal, and endorectal US guidance.* Radiographics, 2001. **21**(2): p. 491-506.
415. Hunter, R.E., K. Reuter, and E. Kopin, *Use of ultrasonography in the difficult postmenopausal dilation and curettage.* Obstet Gynecol, 1989. **73**(5 Pt 1): p. 813-6.
416. Lieng, M., O. Istre, and E. Qvigstad, *Treatment of endometrial polyps: a systematic review.* Acta Obstet Gynecol Scand, 2010. **89**(8): p. 992-1002.
417. Anastasiadis, P.G., et al., *Endometrial polyps: prevalence, detection, and malignant potential in women with abnormal uterine bleeding.* Eur J Gynaecol Oncol, 2000. **21**(2): p. 180-3.
418. Clevenger-Hoeft, M., et al., *Sonohysterography in premenopausal women with and without abnormal bleeding.* Obstet Gynecol, 1999. **94**(4): p. 516-20.
419. Nagele, F., et al., *2500 Outpatient diagnostic hysteroscopies.* Obstet Gynecol, 1996. **88**(1): p. 87-92.
420. Van Bogaert, L.J., *Clinicopathologic findings in endometrial polyps.* Obstet Gynecol, 1988. **71**(5): p. 771-3.
421. Uglietti, A., et al., *The risk of malignancy in uterine polyps: A systematic review and meta-analysis.* Eur J Obstet Gynecol Reprod Biol, 2019. **237**: p. 48-56.
422. Lee, S.C., et al., *The oncogenic potential of endometrial polyps: a systematic review and meta-analysis.* Obstet Gynecol, 2010. **116**(5): p. 1197-205.
423. Clark, T.J. and H. Stevenson, *Endometrial Polyps and Abnormal Uterine Bleeding (AUB-P): What is the relationship, how are they diagnosed and how are they treated?* Best Pract Res Clin Obstet Gynaecol, 2017. **40**: p. 89-104.
424. Pasqualotto, E.B., et al., *Accuracy of preoperative diagnostic tools and outcome of hysteroscopic management of menstrual dysfunction.* J Am Assoc Gynecol Laparosc, 2000. **7**(2): p. 201-9.

425. Demirkiran, F., et al., *Which is the best technique for endometrial sampling? Aspiration (pipelle) versus dilatation and curettage (D&C).* Arch Gynecol Obstet, 2012. **286**(5): p. 1277-82.
426. Kazandi, M., et al., *Comparison of the success of histopathological diagnosis with dilatation-curettage and Pipelle endometrial sampling.* J Obstet Gynaecol, 2012. **32**(8): p. 790-4.
427. Garg, G., et al., *Positive peritoneal cytology is an independent risk-factor in early stage endometrial cancer.* Gynecol Oncol, 2013. **128**(1): p. 77-82.
428. Turner, D.A., et al., *The prognostic significance of peritoneal cytology for stage I endometrial cancer.* Obstet Gynecol, 1989. **74**(5): p. 775-80.
429. Zerbe, M.J., et al., *Retrograde seeding of malignant cells during hysteroscopy in presumed early endometrial cancer.* Gynecol Oncol, 2000. **79**(1): p. 55-8.
430. Obermair, A., et al., *Does hysteroscopy facilitate tumor cell dissemination? Incidence of peritoneal cytology from patients with early stage endometrial carcinoma following dilatation and curettage (D & C) versus hysteroscopy and D & C.* Cancer, 2000. **88**(1): p. 139-43.
431. Lo, K.W., et al., *Hysteroscopic dissemination of endometrial carcinoma using carbon dioxide and normal saline: a retrospective study.* Gynecol Oncol, 2002. **84**(3): p. 394-8.
432. Chen, J., et al., *Does hysteroscopy worsen prognosis in women with type II endometrial carcinoma?* PLoS One, 2017. **12**(3): p. e0174226.
433. Jensen, M.P., C. Chen, and A.M. Brugger, *Interpretation of visual analog scale ratings and change scores: a reanalysis of two clinical trials of postoperative pain.* J Pain, 2003. **4**(7): p. 407-14.
434. Heller, G.Z., M. Manuguerra, and R. Chow, *How to analyze the Visual Analogue Scale: Myths, truths and clinical relevance.* Scand J Pain, 2016. **13**: p. 67-75.
435. De Iaco, P., et al., *Acceptability and pain of outpatient hysteroscopy.* J Am Assoc Gynecol Laparosc, 2000. **7**(1): p. 71-5.
436. Morgan, M., et al., *Women's views and experiences of outpatient hysteroscopy: implications for a patient-centered service.* Nurs Health Sci, 2004. **6**(4): p. 315-20.
437. Downes, E. and F. al-Azzawi, *How well do perimenopausal patients accept outpatient hysteroscopy? Visual analogue scoring of acceptability and pain in 100 women.* Eur J Obstet Gynecol Reprod Biol, 1993. **48**(1): p. 37-41.
438. Larson, D.M., et al., *Prognostic significance of gross myometrial invasion with endometrial cancer.* Obstet Gynecol, 1996. **88**(3): p. 394-8.
439. AlHilli, M.M., et al., *Risk-scoring system for the individualized prediction of lymphatic dissemination in patients with endometrioid endometrial cancer.* Gynecol Oncol, 2013. **131**(1): p. 103-8.
440. Luomaranta, A., A. Leminen, and M. Loukovaara, *Magnetic resonance imaging in the assessment of high-risk features of endometrial carcinoma: a meta-analysis.* Int J Gynecol Cancer, 2015. **25**(5): p. 837-42.
441. Chiappa, V., et al., *Agreement of two-dimensional and three-dimensional transvaginal ultrasound with magnetic resonance imaging in assessment of parametrial infiltration in cervical cancer.* Ultrasound Obstet Gynecol, 2015. **45**(4): p. 459-69.
442. Daskalakis, G., et al., *3D vocal power Doppler sonography for the estimation of tumor volume and vascularization in stage IB1 cervical cancer.* Arch Gynecol Obstet, 2018. **298**(3): p. 617-622.

443. Palsdottir, K., et al., *Preoperative prediction of lymph node metastasis and deep stromal invasion in women with invasive cervical cancer: prospective multicenter study using 2D and 3D ultrasound.* Ultrasound Obstet Gynecol, 2015. **45**(4): p. 470-5.
444. Xu, Y., et al., *Three-dimensional power Doppler ultrasound in the early assessment of response to concurrent chemo-radiotherapy for advanced cervical cancer.* Acta Radiol, 2017. **58**(9): p. 1147-1154.
445. St-Amant, P., et al., *Use of 3D transabdominal ultrasound imaging for treatment planning in cervical cancer brachytherapy: Comparison to magnetic resonance and computed tomography.* Brachytherapy, 2017. **16**(4): p. 847-854.
446. Alcázar, J.L., et al., *Assessing myometrial infiltration by endometrial cancer: uterine virtual navigation with three-dimensional US.* Radiology, 2009. **250**(3): p. 776-83.
447. Mercé, L.T., et al., *Clinical usefulness of 3-dimensional sonography and power Doppler angiography for diagnosis of endometrial carcinoma.* J Ultrasound Med, 2007. **26**(10): p. 1279-87.
448. Yildirim, N., et al., *Predictability of myometrial, lower uterine segment and cervical invasion with 3D transvaginal ultrasonography and magnetic resonance imaging in endometrial cancer patients: a prospective cohort study.* Med Ultrason, 2018. **20**(3): p. 348-354.
449. Ergenoglu, M., et al., *The prediction of myometrial infiltration by three-dimensional ultrasonography in patients with endometrial carcinoma: a validation study from Ege University Hospital.* Med Ultrason, 2016. **18**(2): p. 201-6.
450. Alcázar, J.L., et al., *Endometrial volume and vascularity measurements by transvaginal 3-dimensional ultrasonography and power Doppler angiography in stimulated and tumoral endometria: an interobserver reproducibility study.* J Ultrasound Med, 2005. **24**(8): p. 1091-8.
451. Cohen, J.F., et al., *STARD 2015 guidelines for reporting diagnostic accuracy studies: explanation and elaboration.* BMJ Open, 2016. **6**(11): p. e012799.
452. Bi, Q., et al., *The Diagnostic Value of MRI for Preoperative Staging in Patients with Endometrial Cancer: A Meta-Analysis.* Acad Radiol, 2019.
453. Torricelli, P., et al., *3-T MRI in the preoperative evaluation of depth of myometrial infiltration in endometrial cancer.* AJR Am J Roentgenol, 2008. **190**(2): p. 489-95.
454. Sanjuán, A., et al., *Role of magnetic resonance imaging and cause of pitfalls in detecting myometrial invasion and cervical involvement in endometrial cancer.* Arch Gynecol Obstet, 2008. **278**(6): p. 535-9.
455. Alcazar, J.L., et al., *Transvaginal ultrasound for preoperative assessment of myometrial invasion in patients with endometrial cancer: a systematic review and meta-analysis.* Ultrasound Obstet Gynecol, 2015. **46**(4): p. 405-13.
456. Lindauer, J., et al., *Is there a prognostic difference between depth of myometrial invasion and the tumor-free distance from the uterine serosa in endometrial cancer?* Gynecol Oncol, 2003. **91**(3): p. 547-51.
457. Ortoft, G., et al., *Lymph-vascular space invasion (LVSI) as a strong and independent predictor for non-locoregional recurrences in endometrial cancer: a Danish Gynecological Cancer Group Study.* J Gynecol Oncol, 2019. **30**(5): p. e84.
458. Stalberg, K., et al., *Lymphovascular space invasion as a predictive factor for lymph node metastases and survival in endometrioid endometrial cancer - a*

Swedish Gynecologic Cancer Group (SweGCG) study. Acta Oncol, 2019. **58**(11): p. 1628-1633.
459. Bogani, G., et al., *Role of pelvic and para-aortic lymphadenectomy in endometrial cancer: current evidence.* J Obstet Gynaecol Res, 2014. **40**(2): p. 301-11.
460. Marcickiewicz, J. and K. Sundfeldt, *Accuracy of intraoperative gross visual assessment of myometrial invasion in endometrial cancer.* Acta Obstet Gynecol Scand, 2011. **90**(8): p. 846-51.
461. Sethasathien, P., K. Charoenkwan, and S. Siriaunkgul, *Accuracy of intraoperative gross examination of myometrial invasion in stage I-II endometrial cancer.* Asian Pac J Cancer Prev, 2014. **15**(17): p. 7061-4.
462. Traen, K., B. Hølund, and O. Mogensen, *Accuracy of preoperative tumor grade and intraoperative gross examination of myometrial invasion in patients with endometrial cancer.* Acta Obstet Gynecol Scand, 2007. **86**(6): p. 739-41.
463. Pineda, L., et al., *Agreement between preoperative transvaginal ultrasound and intraoperative macroscopic examination for assessing myometrial infiltration in low-risk endometrioid carcinoma.* Ultrasound Obstet Gynecol, 2016. **47**(3): p. 369-73.
464. Berretta, R., et al., *Preoperative transvaginal ultrasonography and intraoperative gross examination for assessing myometrial invasion by endometrial cancer.* J Ultrasound Med, 2008. **27**(3): p. 349-55.
465. Tanaka, T., et al., *Preoperative MRI and intraoperative frozen section diagnosis of myometrial invasion in patients with endometrial cancer.* Int J Gynecol Cancer, 2015. **25**(5): p. 879-83.
466. Hahn, H.S., et al., *Magnetic resonance imaging and intraoperative frozen sectioning for the evaluation of risk factors associated with lymph node metastasis in endometrial cancer.* Int J Gynecol Cancer, 2013. **23**(8): p. 1411-6.
467. Gallego, J.C., et al., *Evaluation of myometrial invasion in endometrial cancer: comparison of diffusion-weighted magnetic resonance and intraoperative frozen sections.* Abdom Imaging, 2014. **39**(5): p. 1021-6.
468. Andreano, A., et al., *MR diffusion imaging for preoperative staging of myometrial invasion in patients with endometrial cancer: a systematic review and meta-analysis.* Eur Radiol, 2014. **24**(6): p. 1327-38.
469. Kim, S.H., et al., *Detection of deep myometrial invasion in endometrial carcinoma: comparison of transvaginal ultrasound, CT, and MRI.* J Comput Assist Tomogr, 1995. **19**(5): p. 766-72.
470. Antonsen, S.L., et al., *MRI, PET/CT and ultrasound in the preoperative staging of endometrial cancer - a multicenter prospective comparative study.* Gynecol Oncol, 2013. **128**(2): p. 300-8.
471. Cacciatore, B., et al., *Contribution of vaginal scanning to sonographic evaluation of endometrial cancer invasion.* Acta Oncol, 1989. **28**(4): p. 585-8.
472. Gordon, A.N., A.C. Fleischer, and G.W. Reed, *Depth of myometrial invasion in endometrial cancer: preoperative assessment by transvaginal ultrasonography.* Gynecol Oncol, 1990. **39**(3): p. 321-7.
473. Karlsson, B., et al., *The use of endovaginal ultrasound to diagnose invasion of endometrial carcinoma.* Ultrasound Obstet Gynecol, 1992. **2**(1): p. 35-9.
474. Raine-Fenning, N.J., et al., *The reliability of virtual organ computer-aided analysis (VOCAL) for the semiquantification of ovarian, endometrial and subendometrial perfusion.* Ultrasound Obstet Gynecol, 2003. **22**(6): p. 633-9.

475. Galván, R., et al., *Three-dimensional power Doppler angiography in endometrial cancer: correlation with tumor characteristics.* Ultrasound Obstet Gynecol, 2010. **35**(6): p. 723-9.
476. Epstein, E., et al., *Gray-scale and color Doppler ultrasound characteristics of endometrial cancer in relation to stage, grade and tumor size.* Ultrasound Obstet Gynecol, 2011. **38**(5): p. 586-93.
477. Galvan, R., et al., *Three-dimensional power Doppler angiography in endometrial cancer: correlation with tumor characteristics.* Ultrasound Obstet Gynecol, 2010. **35**(6): p. 723-9.
478. Kinkel, K., et al., *Staging of endometrial cancer with MRI: guidelines of the European Society of Urogenital Imaging.* Eur Radiol, 2009. **19**(7): p. 1565-74.
479. Nougaret, S., et al., *Endometrial Cancer MRI staging: Updated Guidelines of the European Society of Urogenital Radiology.* Eur Radiol, 2019. **29**(2): p. 792-805.
480. Horváth, K., et al., *Evaluation of the accuracy of preoperative MRI in measuring myometrial infiltration in endometrial carcinoma.* Pathol Oncol Res, 2014. **20**(2): p. 327-33.
481. Thieme, S.F., et al., *Preoperative Evaluation of Myometrial Invasion in Endometrial Carcinoma: Prospective Intra-individual Comparison of Magnetic Resonance Volumetry, Diffusion-weighted and Dynamic Contrast-enhanced Magnetic Resonance Imaging.* Anticancer Res, 2018. **38**(8): p. 4813-4817.
482. Sala, E., et al., *Added value of dynamic contrast-enhanced magnetic resonance imaging in predicting advanced stage disease in patients with endometrial carcinoma.* Int J Gynecol Cancer, 2009. **19**(1): p. 141-6.
483. Nagar, H., et al., *The diagnostic accuracy of magnetic resonance imaging in detecting cervical involvement in endometrial cancer.* Gynecol Oncol, 2006. **103**(2): p. 431-4.
484. Duncan, K.A., et al., *Staging cancer of the uterus: a national audit of MRI accuracy.* Clin Radiol, 2012. **67**(6): p. 523-30.
485. Whiting, P.F., et al., *QUADAS-2: a revised tool for the quality assessment of diagnostic accuracy studies.* Ann Intern Med, 2011. **155**(8): p. 529-36.
486. (EUnetHTA)., E.N.f.H.T.A. *EUnetHTA guideline: meta-analysis of diagnostic test accuracy studies*. 2014; Available from: http://www.eunethta.eu/eunethta-guidelines.
487. Higgins, J.P., et al., *Measuring inconsistency in meta-analyses.* BMJ, 2003. **327**(7414): p. 557-60.
488. Epstein, E., et al., *Gray-scale and color Doppler ultrasound characteristics of endometrial cancer in relation to stage, grade and tumor size.* Ultrasound Obstet Gynecol, 2011. **38**(5): p. 586-93.
489. Green, R.W., et al., *Endometrial cancer off-line staging using two-dimensional transvaginal ultrasound and three-dimensional volume contrast imaging: Intermethod agreement, interrater reliability and diagnostic accuracy.* Gynecol Oncol, 2018. **150**(3): p. 438-445.
490. Saarelainen, S.K., et al., *The preoperative assessment of deep myometrial invasion by three-dimensional ultrasound versus MRI in endometrial carcinoma.* Acta Obstet Gynecol Scand, 2012. **91**(8): p. 983-90.
491. Rodríguez-Trujillo, A., et al., *Preoperative Assessment of Myometrial Invasion in Endometrial Cancer by 3D Ultrasound and Diffusion-Weighted Magnetic Resonance Imaging: A Comparative Study.* Int J Gynecol Cancer, 2016. **26**(6): p. 1105-10.

492. Konno, Y., et al., *A retrospective analysis of postoperative complications with or without para-aortic lymphadenectomy in endometrial cancer.* Int J Gynecol Cancer, 2011. **21**(2): p. 385-90.
493. Volpi, L., et al., *Long term complications following pelvic and para-aortic lymphadenectomy for endometrial cancer, incidence and potential risk factors: a single institution experience.* Int J Gynecol Cancer, 2019. **29**(2): p. 312-319.
494. Todo, Y., et al., *Risk factors for postoperative lower-extremity lymphedema in endometrial cancer survivors who had treatment including lymphadenectomy.* Gynecol Oncol, 2010. **119**(1): p. 60-4.
495. Das, S.K., et al., *Usefulness of DWI in preoperative assessment of deep myometrial invasion in patients with endometrial carcinoma: a systematic review and meta-analysis.* Cancer Imaging, 2014. **14**(1): p. 32.
496. Manfredi, R., et al., *Local-regional staging of endometrial carcinoma: role of MR imaging in surgical planning.* Radiology, 2004. **231**(2): p. 372-8.
497. Network., N.C.I., *Stage Breakdown by CCG 2014.* . 2014.
498. Saarelainen, S.K., et al., *Preoperative assessment of endometrial carcinoma by three-dimensional power Doppler angiography.* Ultrasound Obstet Gynecol, 2012. **39**(4): p. 466-72.
499. Leminen, A., M. Forss, and P. Lehtovirta, *Endometrial adenocarcinoma with clinical evidence of cervical involvement: accuracy of diagnostic procedures, clinical course, and prognostic factors.* Acta Obstet Gynecol Scand, 1995. **74**(1): p. 61-6.
500. Haldorsen, I.S. and H.B. Salvesen, *What Is the Best Preoperative Imaging for Endometrial Cancer?* Curr Oncol Rep, 2016. **18**(4): p. 25.
501. Haldorsen, I.S., et al., *Magnetic resonance imaging performs better than endocervical curettage for preoperative prediction of cervical stromal invasion in endometrial carcinomas.* Gynecol Oncol, 2012. **126**(3): p. 413-8.
502. Rockall, A.G., et al., *Evaluation of endometrial carcinoma on magnetic resonance imaging.* Int J Gynecol Cancer, 2007. **17**(1): p. 188-96.
503. Christensen, J.W., et al., *Assessment of myometrial invasion in endometrial cancer using three-dimensional ultrasound and magnetic resonance imaging.* Acta Obstet Gynecol Scand, 2016. **95**(1): p. 55-64.
504. Marusyk, A. and K. Polyak, *Tumor heterogeneity: causes and consequences.* Biochim Biophys Acta, 2010. **1805**(1): p. 105-17.
505. Hanahan, D. and R.A. Weinberg, *Hallmarks of cancer: the next generation.* Cell, 2011. **144**(5): p. 646-74.
506. Simpson-Herren, L., P.E. Noker, and S.D. Wagoner, *Variability of tumor response to chemotherapy. II. Contribution of tumor heterogeneity.* Cancer Chemother Pharmacol, 1988. **22**(2): p. 131-6.
507. Zahra, M.A., et al., *Dynamic contrast-enhanced MRI as a predictor of tumour response to radiotherapy.* Lancet Oncol, 2007. **8**(1): p. 63-74.
508. Andor, N., et al., *Pan-cancer analysis of the extent and consequences of intratumor heterogeneity.* Nat Med, 2016. **22**(1): p. 105-13.
509. Morris, L.G., et al., *Pan-cancer analysis of intratumor heterogeneity as a prognostic determinant of survival.* Oncotarget, 2016. **7**(9): p. 10051-63.
510. Gerlinger, M., et al., *Intratumor heterogeneity and branched evolution revealed by multiregion sequencing.* N Engl J Med, 2012. **366**(10): p. 883-892.
511. Diehn, M., et al., *Identification of noninvasive imaging surrogates for brain tumor gene-expression modules.* Proc Natl Acad Sci U S A, 2008. **105**(13): p. 5213-8.

512. Segal, E., et al., *Decoding global gene expression programs in liver cancer by noninvasive imaging.* Nat Biotechnol, 2007. **25**(6): p. 675-80.
513. Reuzé, S., et al., *Prediction of cervical cancer recurrence using textural features extracted from 18F-FDG PET images acquired with different scanners.* Oncotarget, 2017. **8**(26): p. 43169-43179.
514. El Naqa, I., et al., *Exploring feature-based approaches in PET images for predicting cancer treatment outcomes.* Pattern Recognit, 2009. **42**(6): p. 1162-1171.
515. Bowen, S.R., et al., *Tumor radiomic heterogeneity: Multiparametric functional imaging to characterize variability and predict response following cervical cancer radiation therapy.* J Magn Reson Imaging, 2018. **47**(5): p. 1388-1396.
516. Torheim, T., et al., *Classification of dynamic contrast enhanced MR images of cervical cancers using texture analysis and support vector machines.* IEEE Trans Med Imaging, 2014. **33**(8): p. 1648-56.
517. Limkin, E.J., et al., *Promises and challenges for the implementation of computational medical imaging (radiomics) in oncology.* Ann Oncol, 2017. **28**(6): p. 1191-1206.
518. Wu, W., et al., *Exploratory Study to Identify Radiomics Classifiers for Lung Cancer Histology.* Front Oncol, 2016. **6**: p. 71.
519. Mu, W., et al., *Staging of cervical cancer based on tumor heterogeneity characterized by texture features on (18)F-FDG PET images.* Phys Med Biol, 2015. **60**(13): p. 5123-39.
520. Liang, C., et al., *The development and validation of a CT-based radiomics signature for the preoperative discrimination of stage I-II and stage III-IV colorectal cancer.* Oncotarget, 2016. **7**(21): p. 31401-12.
521. Davnall, F., et al., *Assessment of tumor heterogeneity: an emerging imaging tool for clinical practice?* Insights Imaging, 2012. **3**(6): p. 573-89.
522. Chaddad, A., et al., *Radiomics in Glioblastoma: Current Status and Challenges Facing Clinical Implementation.* Front Oncol, 2019. **9**: p. 374.
523. Ganeshan, B., et al., *Non-small cell lung cancer: histopathologic correlates for texture parameters at CT.* Radiology, 2013. **266**(1): p. 326-36.
524. Ahmed, A., et al., *Texture analysis in assessment and prediction of chemotherapy response in breast cancer.* J Magn Reson Imaging, 2013. **38**(1): p. 89-101.
525. Fan, M., et al., *Radiomic analysis of DCE-MRI for prediction of response to neoadjuvant chemotherapy in breast cancer patients.* Eur J Radiol, 2017. **94**: p. 140-147.
526. Yang, F., et al., *Magnetic resonance imaging (MRI)-based radiomics for prostate cancer radiotherapy.* Transl Androl Urol, 2018. **7**(3): p. 445-458.
527. Yan, B.C., et al., *Radiologists with MRI-based radiomics aids to predict the pelvic lymph node metastasis in endometrial cancer: a multicenter study.* Eur Radiol, 2020.
528. Thomas, J.V., et al., *MR Imaging Texture Analysis in the Abdomen and Pelvis.* Magn Reson Imaging Clin N Am, 2020. **28**(3): p. 447-456.
529. Ghosh, A., et al., *DTI histogram parameters correlate with the extent of myoinvasion and tumor type in endometrial carcinoma: a preliminary analysis.* Acta Radiol, 2020. **61**(5): p. 675-684.
530. Colombo, N., et al., *ESMO-ESGO-ESTRO Consensus Conference on Endometrial Cancer: Diagnosis, Treatment and Follow-up.* Int J Gynecol Cancer, 2016. **26**(1): p. 2-30.

531. Lambin, P., et al., *Radiomics: the bridge between medical imaging and personalized medicine.* Nat Rev Clin Oncol, 2017. **14**(12): p. 749-762.
532. Park, J.E., et al., *Quality of science and reporting of radiomics in oncologic studies: room for improvement according to radiomics quality score and TRIPOD statement.* Eur Radiol, 2020. **30**(1): p. 523-536.
533. Rizzo, S., et al., *CT Radiogenomic Characterization of EGFR, K-RAS, and ALK Mutations in Non-Small Cell Lung Cancer.* Eur Radiol, 2016. **26**(1): p. 32-42.
534. Larue, R., et al., *Influence of gray level discretization on radiomic feature stability for different CT scanners, tube currents and slice thicknesses: a comprehensive phantom study.* Acta Oncol, 2017. **56**(11): p. 1544-1553.
535. Rizzo, S., et al., *Radiomics: the facts and the challenges of image analysis.* Eur Radiol Exp, 2018. **2**(1): p. 36.
536. Lee, G., et al., *Radiomics and its emerging role in lung cancer research, imaging biomarkers and clinical management: State of the art.* Eur J Radiol, 2017. **86**: p. 297-307.
537. Thawani, R., et al., *Radiomics and radiogenomics in lung cancer: A review for the clinician.* Lung Cancer, 2018. **115**: p. 34-41.
538. Ergen, B. and M. Baykara, *Texture based feature extraction methods for content based medical image retrieval systems.* Biomed Mater Eng, 2014. **24**(6): p. 3055-62.
539. Thibault, G., et al., *Texture Indexes and Gray Level Size Zone Matrix Application to Cell Nuclei Classification*. 2009.
540. Yip, S.S. and H.J. Aerts, *Applications and limitations of radiomics.* Phys Med Biol, 2016. **61**(13): p. R150-66.
541. van Griethuysen, J.J.M., et al., *Computational Radiomics System to Decode the Radiographic Phenotype.* Cancer Res, 2017. **77**(21): p. e104-e107.
542. van der Walt, S., et al., *scikit-image: image processing in Python.* PeerJ, 2014. **2**: p. e453.
543. van Rossum, G., *Python reference manual*. 1995, CWI.
544. Tustison, N.J., et al., *N4ITK: improved N3 bias correction.* IEEE Trans Med Imaging, 2010. **29**(6): p. 1310-20.
545. Yang, X. and M.V. Knopp, *Quantifying tumor vascular heterogeneity with dynamic contrast-enhanced magnetic resonance imaging: a review.* J Biomed Biotechnol, 2011. **2011**: p. 732848.
546. Fisher, R., L. Pusztai, and C. Swanton, *Cancer heterogeneity: implications for targeted therapeutics.* Br J Cancer, 2013. **108**(3): p. 479-85.
547. Maley, C.C., et al., *Genetic clonal diversity predicts progression to esophageal adenocarcinoma.* Nat Genet, 2006. **38**(4): p. 468-73.
548. Chicklore, S., et al., *Quantifying tumour heterogeneity in 18F-FDG PET/CT imaging by texture analysis.* Eur J Nucl Med Mol Imaging, 2013. **40**(1): p. 133-40.
549. Marusyk, A., V. Almendro, and K. Polyak, *Intra-tumour heterogeneity: a looking glass for cancer?* Nat Rev Cancer, 2012. **12**(5): p. 323-34.
550. Yan, B.C., et al., *Preoperative Assessment for High-Risk Endometrial Cancer by Developing an MRI- and Clinical-Based Radiomics Nomogram: A Multicenter Study.* J Magn Reson Imaging, 2020: p. e27289.
551. Parmar, C., et al., *Robust Radiomics feature quantification using semiautomatic volumetric segmentation.* PLoS One, 2014. **9**(7): p. e102107.

552. Evans, T., et al., *Differential trends in the rising incidence of endometrial cancer by type: data from a UK population-based registry from 1994 to 2006.* Br J Cancer, 2011. **104**(9): p. 1505-10.
553. Pennington, M., et al., *Long-Term Secondary Care Costs of Endometrial Cancer: A Prospective Cohort Study Nested within the United Kingdom Collaborative Trial of Ovarian Cancer Screening (UKCTOCS).* PLoS One, 2016. **11**(11): p. e0165539.
554. Cohn, D.E., et al., *Cost-effectiveness analysis of strategies for the surgical management of grade 1 endometrial adenocarcinoma.* Obstet Gynecol, 2007. **109**(6): p. 1388-95.
555. Gemignani, M.L., et al., *Laparoscopic-assisted vaginal hysterectomy for endometrial cancer: clinical outcomes and hospital charges.* Gynecol Oncol, 1999. **73**(1): p. 5-11.
556. Ghosh, K., et al., *The implementation of critical pathways in gynecologic oncology in a managed care setting: a cost analysis.* Gynecol Oncol, 2001. **83**(2): p. 378-82.
557. Brooks, S.E., et al., *Health care cost and utilization project analysis of comorbid illness and complications for patients undergoing hysterectomy for endometrial carcinoma.* Cancer, 2001. **92**(4): p. 950-8.
558. Spirtos, N.M., et al., *Cost and quality-of-life analyses of surgery for early endometrial cancer: laparotomy versus laparoscopy.* Am J Obstet Gynecol, 1996. **174**(6): p. 1795-9; discussion 1799-800.
559. Graves, N., et al., *The cost-effectiveness of total laparoscopic hysterectomy compared to total abdominal hysterectomy for the treatment of early stage endometrial cancer.* BMJ Open, 2013. **3**(4).
560. Bijen, C.B., et al., *Laparoscopic hysterectomy is preferred over laparotomy in early endometrial cancer patients, however not cost effective in the very obese.* Eur J Cancer, 2011. **47**(14): p. 2158-65.
561. Ashih, H., et al., *Cost-effectiveness of treatment of early stage endometrial cancer.* Gynecol Oncol, 1999. **74**(2): p. 208-16.
562. Park, D.A., et al., *Comparative safety and effectiveness of robot-assisted laparoscopic hysterectomy versus conventional laparoscopy and laparotomy for endometrial cancer: A systematic review and meta-analysis.* Eur J Surg Oncol, 2016. **42**(9): p. 1303-14.
563. Clements, A.E., et al., *Is selective lymphadenectomy more cost-effective than routine lymphadenectomy in patients with endometrial cancer?* Gynecol Oncol, 2013. **128**(2): p. 166-70.
564. Brooks, S.E., et al., *Resource utilization for patients undergoing hysterectomy with or without lymph node dissection for endometrial cancer.* Gynecol Oncol, 2002. **85**(2): p. 242-9.
565. Kwon, J.S., et al., *Cost-effectiveness analysis of treatment strategies for Stage I and II endometrial cancer.* J Obstet Gynaecol Can, 2007. **29**(2): p. 131-139.
566. Havrilesky, L.J., J.P. Chino, and E.R. Myers, *How much is another randomized trial of lymph node dissection in endometrial cancer worth? A value of information analysis.* Gynecol Oncol, 2013. **131**(1): p. 140-6.
567. Havrilesky, L.J., et al., *Cost effectiveness of a test to detect metastases for endometrial cancer.* Gynecol Oncol, 2009. **112**(3): p. 526-30.
568. Lau, S., et al., *Outcomes and cost comparisons after introducing a robotics program for endometrial cancer surgery.* Obstet Gynecol, 2012. **119**(4): p. 717-24.

569. Yu X, B.R., Lum D, Kiet T, Fuh K, Orr J,, *Trends in utilization and cost of minimally invasive robotic surgery for endometrial cancer: A statewide analysis of 2296 patients.* Gynecol Oncol., 2011. **120**.
570. Martino, M.A., et al., *A cost analysis of postoperative management in endometrial cancer patients treated by robotics versus laparoscopic approach.* Gynecol Oncol, 2011. **123**(3): p. 528-31.
571. Coronado, P.J., et al., *Comparison of perioperative outcomes and cost of robotic-assisted laparoscopy, laparoscopy and laparotomy for endometrial cancer.* Eur J Obstet Gynecol Reprod Biol, 2012. **165**(2): p. 289-94.
572. Bell, M.C., et al., *Comparison of outcomes and cost for endometrial cancer staging via traditional laparotomy, standard laparoscopy and robotic techniques.* Gynecol Oncol, 2008. **111**(3): p. 407-11.
573. Wright, J.D., et al., *Comparative effectiveness of robotic versus laparoscopic hysterectomy for endometrial cancer.* J Clin Oncol, 2012. **30**(8): p. 783-91.
574. Herling, S.F., et al., *Cost-analysis of robotic-assisted laparoscopic hysterectomy versus total abdominal hysterectomy for women with endometrial cancer and atypical complex hyperplasia.* Acta Obstet Gynecol Scand, 2016. **95**(3): p. 299-308.
575. Iavazzo, C., E.K. Papadopoulou, and I.D. Gkegkes, *Cost assessment of robotics in gynecologic surgery: a systematic review.* J Obstet Gynaecol Res, 2014. **40**(11): p. 2125-34.
576. Delaloge, S., et al., *The challenge of rapid diagnosis in oncology: Diagnostic accuracy and cost analysis of a large-scale one-stop breast clinic.* Eur J Cancer, 2016. **66**: p. 131-7.
577. Husereau, D., et al., *Consolidated Health Economic Evaluation Reporting Standards (CHEERS) statement.* BMJ, 2013. **346**: p. f1049.
578. Ward, Z., *Amua: An open source modeling framework.* 2019.
579. Breijer, M.C., et al., *Diagnostic strategies for endometrial cancer in women with postmenopausal bleeding: cost-effectiveness of individualized strategies.* Eur J Obstet Gynecol Reprod Biol, 2012. **163**(1): p. 91-6.
580. Bachmann, L.M., et al., *Probability analysis for diagnosis of endometrial hyperplasia and cancer in postmenopausal bleeding: an approach for a rational diagnostic workup.* Acta Obstet Gynecol Scand, 2003. **82**(6): p. 564-9.
581. Opmeer, B.C., et al., *Improving the existing diagnostic strategy by accounting for characteristics of the women in the diagnostic work up for postmenopausal bleeding.* BJOG, 2007. **114**(1): p. 51-8.
582. Curtis, L.A.a.B., Amanda., *Unit Costs of Health and Social Care 2018*. 2018, University of Kent
583. *Reference Cost Collection: National Schedule of Reference Costs - Year 2017-18 - NHS trust and NHS foundation trusts*, N.I. https://improvement.nhs.uk/resources/reference-costs/#rc1718, Editor. 2017-2018.
584. Drummond, M.F. and T.O. Jefferson, *Guidelines for authors and peer reviewers of economic submissions to the BMJ. The BMJ Economic Evaluation Working Party.* BMJ, 1996. **313**(7052): p. 275-83.
585. Briggs, A. and A. Gray, *Using cost effectiveness information.* BMJ, 2000. **320**(7229): p. 246.
586. Raftery, J., *NICE: faster access to modern treatments? Analysis of guidance on health technologies.* BMJ, 2001. **323**(7324): p. 1300-3.

587. Ciatto, S., et al., *Association of endometrial thickness assessed at trans-vaginal ultrasonography to endometrial cancer in postmenopausal women asymptomatic or with abnormal uterine bleeding.* Radiol Med, 2002. **104**(5-6): p. 437-42.
588. Gupta, J.K., et al., *How should we investigate women with postmenopausal bleeding?* Acta Obstet Gynecol Scand, 1996. **75**(5): p. 475-9.
589. Elwyn, G., et al., *Decision analysis in patient care.* Lancet, 2001. **358**(9281): p. 571-4.
590. Drummond, M.F., et al., *Users' guides to the medical literature. XIII. How to use an article on economic analysis of clinical practice. A. Are the results of the study valid? Evidence-Based Medicine Working Group.* JAMA, 1997. **277**(19): p. 1552-7.
591. Clark, T.J., et al., *Evaluation of outpatient hysteroscopy and ultrasonography in the diagnosis of endometrial disease.* Obstet Gynecol, 2002. **99**(6): p. 1001-7.
592. Briggs, A.H. and A.M. Gray, *Handling uncertainty when performing economic evaluation of healthcare interventions.* Health Technol Assess, 1999. **3**(2): p. 1-134.
593. Feldman, S., R.S. Berkowitz, and A.N. Tosteson, *Cost-effectiveness of strategies to evaluate postmenopausal bleeding.* Obstet Gynecol, 1993. **81**(6): p. 968-75.
594. Broeze, K.A., et al., *Individual patient data meta-analysis of diagnostic and prognostic studies in obstetrics, gynaecology and reproductive medicine.* BMC Med Res Methodol, 2009. **9**: p. 22.

CHAPTER 12: APPENDIX

CHAPTER 12: APPENDIX

12.1 Publications, presentations, prizes and grants

12.1.1. Publications

The psychological study has been accepted in the journal of psycho-oncology. My work on the iKnife, survival analysis, radiomics and 3D ultrasound are in the process of submission to number of journals.

12.1.2 Conference presentations

Marcus D et al, Do delays to surgery influence survival in endometrial cancer? (oral) *Royal College of Obstetricians and Gynaecologists, World Congress.* Virtual 2021

Marcus D et al, Can Rapid Evaporative Ionization Mass Spectrometry (REIMS), the intelligent surgical knife (iKnife) provide a Point-Of-Care diagnosis for women with suspected endometrial (womb) cancer? (oral) *MSACL* Salzburg 2019

Marcus D et al, Endometrial Cancer: Is iKnife the future for Point-Of-Care diagnosis? *Royal College of Obstetricians and Gynaecologists, World Congress.* London 2019

Marcus D et al, How anxious are patients attending the Rapid Access Clinic for suspected cancer? *Royal College of Obstetricians and Gynaecologists, World Congress* London 2019

Marcus D et al, Can the rapid evaporative ionization mass spectrometry (REIMS) intelligent surgical knife (iKnife) differentiate between normal and malignant endometrial tissue? *ASMS*, Indianapolis 2017

Marcus D et al, Can the intelligent surgical knife (iKnife) differentiate between benign and malignant endometrial tissue? Proof of concept' (oral) *Victor Bonney,* RCOG 2017

12.1.3 Prizes and grants

Eve Grant: Rapid tissue diagnosis of endometrial cancer in patients with abnormal uterine bleeding. Awarded £75'000 project grant for my iKnife work on endometrial cancer

Young Investigator Educational grant MSACL. Award grant to cover costs of travel and conference to give an oral presentation in Salzburg.

Oral prize (3rd) RCOG international congress 2021. Do delays to surgery influence survival in endometrial cancer?

12.2 Summary Clinical Trial Protocol

Study design: Prospective cohort study

Setting: Imperial College NHS Trust Hospitals/ Imperial College, London

Participants: 500 women referred to rapid access clinic with postmenopausal bleeding or intermenstrual bleeding. An additional 100 women will be recruited who were referred to Imperial college following a diagnosis of cancer in other hospitals.

- INCLUSION CRITERIA
  All women presenting to rapid access gynaecology clinic with postmenopausal bleeding or intermenstrual bleeding.

- EXCLUSION CRITERIA
  Anyone lacking capacity. <18years old. Pregnant. Any contra-indications to carrying out a biopsy.

Duration: 8 years (includes 5 year follow up data)

Primary outcome measures:
(1) Histological diagnosis of ultrasound guided biopsy compared to routine care (hysteroscopy guided biopsy). Diagnostic ability (sensitivity, specificity, NPV, PPV) will be compared to gold standard.
(2) Accuracy of diagnosing myometrial invasion in 3D USS compared to MRI
(3) Comparison of radiomics model against standard histological diagnosis in the determination of grade and type of tumour.

Secondary outcome measures:
(1) Patient satisfaction (visual analogue score) of USS guided biopsy
(2) Comparison of accuracy of diagnosis of grade and type of tumour using MR spectrometry compared to gold standard histopathology
(3) Diagnosis of endometrial cancer and hyperplasia (pre-cancer) in endometrial biopsy samples, and diagnose lymph node metastasis (spread of cancer to lymph

glands), compared with standard histology. Comparison of mass spectrometry findings of lymph nodes with the primary tumour (the womb cancer)

Statistical analysis: Sample size was calculated on the basis of recently published work and anticipated ease of recruitment. It is estimated that approximately 10% of women attending rapid access clinic will have endometrial cancer. In previous studies assessing new endometrial sampling devices a population of 50 women was used. In this population it is expected that 80 women will require a hysteroscopy and could be offered an ultrasound guided biopsy.

PART 1: PRE-DIAGNOSIS OF CANCER

All women presenting to the rapid access clinic with post menopausal bleeding (PMB) and intermenstrual bleeding will be approached for consent for inclusion into this study (group A). When women normally attend this clinic the doctor will discuss what will happen - this includes an internal (pelvic scan) and an examination. If the womb lining is thickened on the scan the patient will need a tissue biopsy (this is not that common, most women only need a scan), this will be taken at the same time as the examination in clinic. The device used to take the tissue biopsy is called a pipelle. Only if the patient still needs a biopsy but the patient can't tolerate the examination, or the sample is insufficient or focal (in a small area of the womb as opposed to generalised) then the patient will need to have a hysteroscopy. The hysteroscopy is a small camera inserted into the womb under local or general anaesthetic, this will happen at a different appointment.

In this study, all women in group A will be approached for enrollement into the study. Prior to any imaging or examination women will be told what the research involves and if they are happy to proceed. They can consent to all or part of the study. The extra elements of the study include: a 3D ultrasound (not just standard 2D), a second pipelle biopsy sample (only if patients actually would have needed a pipelle anyway) and ultrasound guided biopsy (again only if patients actually would have needed a hysteroscopy guided biopsy). Each will now be discussed in more detail.

All women (group A) will receive a pelvic (internal) ultrasound as per routine care. In addition to the normal 2D ultrasound, women will receive a 3D ultasound and images

will be saved. This adds an additional 1-2 minutes scan time. Depending on the clinician it is sometimes performed as part of routine care.

If the endometrium (womb lining) is thickened >4mm on ultrasound they will require an endometrial biopsy. Usually this will be a pipelle. If the patient is agreeable a second endometrial sample will be taken specifically for research. The histology of first sample will be analysed by conventional pathology and the second sample will be analysed by the new technology REIMS/DESI. REIMS is Rapid Evaporative Ionization Mass Spectrometry and DESI is Desorption Electrospray Ionization. Both are new technologies that use mass spectrometry to analyse chemical composition, and in this case tissue composition. REIMS has been dubbed the 'iKnife' or 'intelligent knife' colloquially as when coupled with surgical diathermy the gas pattern produced is unique to the tissue and helps surgeons know where to cut. The diagnostic ability of this new technology will be compared against the gold standard, which is histological examination.

In cases where the pipelle biopsy cannot be performed in clinic due to poor tolerance, insufficient material or focal lesions a hysteroscopy guided biopsy will be required (local or GA). In this case, the patients will be offered an ultrasound (USS) guided biopsy in the first instance, this will be performed at the same time in clinic. The biopsy will be taken under scan guidance using a very fine forceps such as Bettochi forceps. These forceps are used routinely during hysteroscopy so whilst the instruments are common the application is novel. The biopsy results of this will be sent for standard histology. If the results are inadequate patients will be sent for standard hysteroscopy and biopsy. Patients will also be asked to assess tolerability of the procedure using a visual analogue score.

PART 2: AFTER DIAGNOSIS OF CANCER

In those women with confirmed cancer on histology (subgroup B) - an MRI is performed to assess stage of cancer (current routine standard of care). This will include T1, T2, DWI and contrast enhanced sequences. Patients referred to Hammersmith Hospital from other trusts who are diagnosed with endometrial cancer will be approached for consent and enrolment into latter part of study. These patients will have had an MRI but may not have had all the sequences needed and may therefore require a further

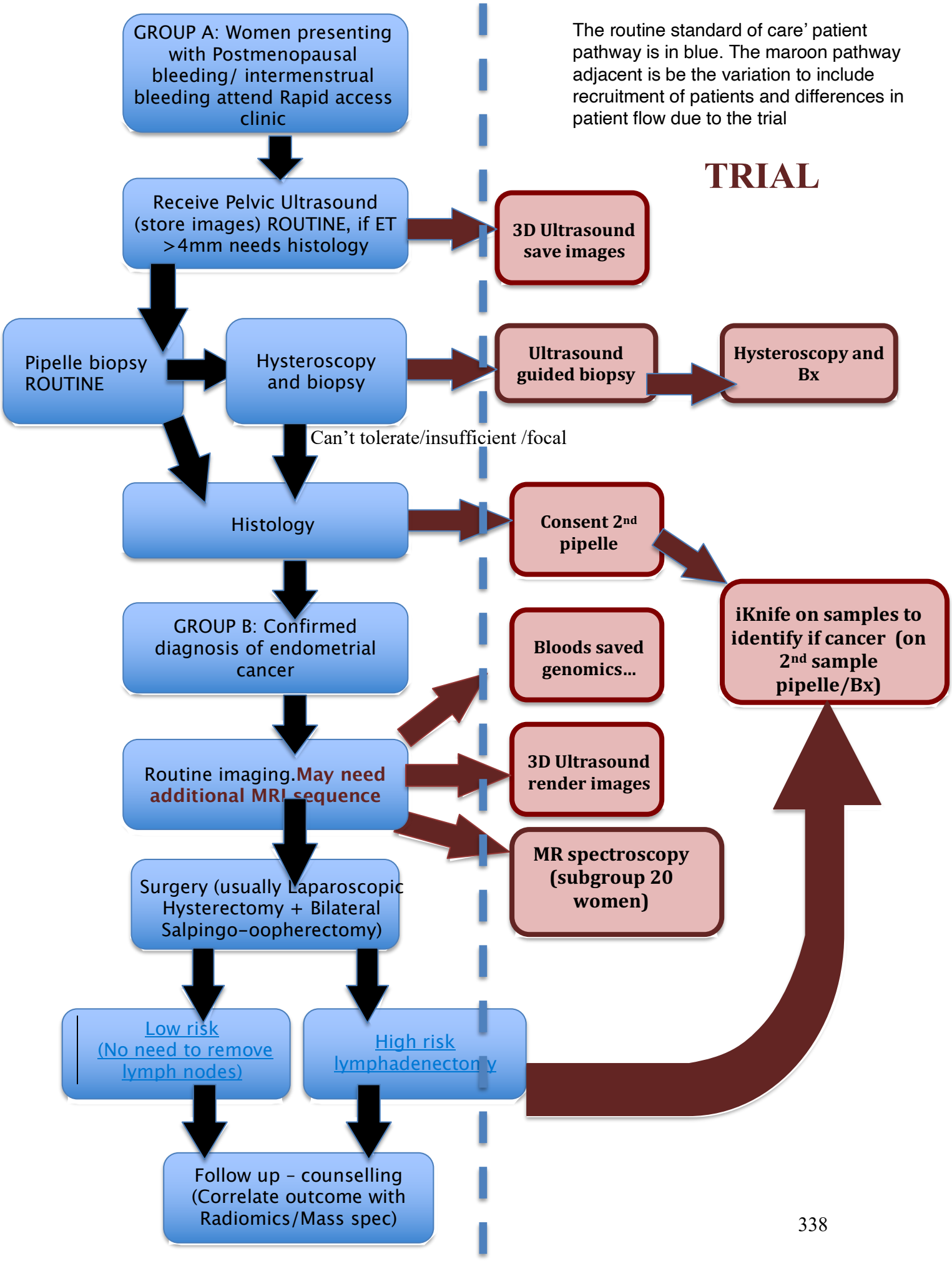
MRI scan with additional sequences. MR spectroscopy will be performed on a subset of patients with confirmed cancer (20 patients).

Definitive management of endometrial cancer includes a hysterectomy and the surgical specimen will be examined for depth of myometrial invasion. In the meantime, the saved 3D images from the rapid access clinic will be analysed and rendered to predict the stage of the endometrial cancer. The results of 3D ultrasound, and MRI will be compared against the stage found on the gold standard test (on histological examination).

In women with confirmed endometrial cancer who later go on to require lymphadenectomy as part of standard care (e.g. advanced stage, type 2 tumours or high grade) following MDT discussion will have their lymph nodes examined ex-vivo using REIMS/iKnife/DESI in addition to the gold standard histopathological examination. The diagnostic capabilities of this new technology to identify cancerous lymph nodes will be compared to standard histopathological diagnosis. If this technology is accurate at diagnosing involved lymph nodes it could be used in vivo to enhance intra- operative decision-making. In addition to build the data for endometrial tissue, women receiving surgery will also be consented for an additional endometrial biopsy (under GA or as an ex-vivo sample).

FOLLOW UP:

Following surgery patients will continue with routine standard of care and follow up. Patients will be followed up for 5 years to provide 5-year survival data. Images from ultrasound, MRI pelvis and MR spectrometry will be analysed to see if they can predict the 5-year survival.


The routine standard of care' patient pathway is in blue. The maroon pathway adjacent is be the variation to include recruitment of patients and differences in patient flow due to the trial
TRIAL
GROUP A: Women presenting with Postmenopausal bleeding/ intermenstrual bleeding attend Rapid access clinic
Receive Pelvic Ultrasound (store images) ROUTINE, if ET >4mm needs histology
3D Ultrasound save images
Pipelle biopsy ROUTINE
Hysteroscopy and biopsy
Ultrasound guided biopsy
Hysteroscopy and Bx
Can't tolerate/insufficient /focal
Histology
Consent 2nd pipelle
GROUP B: Confirmed diagnosis of endometrial cancer
Bloods saved genomics...
iKnife on samples to identify if cancer (on 2nd sample pipelle/Bx)
Routine imaging.May need additional MRI sequence
3D Ultrasound render images
MR spectroscopy (subgroup 20 women)
Surgery (usually Laparoscopic Hysterectomy + Bilateral Salpingo-oopherectomy)
Low risk (No need to remove lymph nodes)
High risk lymphadenectomy
Follow up - counselling (Correlate outcome with Radiomics/Mass spec)

12.3 Patient Information Sheet and questionnaire

IRAS Project ID: 210195

Principal Investigator details: Miss Sadaf Ghaem-Maghami consultant gynaecological oncologist

Study title: Clinical application and evaluation of advanced diagnostic tools in women with suspected endometrial cancer.

Date: October 2018. **Version**: 2.3

Introduction

We would like to invite you to take part in this short research survey. The study is looking at ways to speed up the diagnosis of gynaecological cancer. We observe that a lot of women coming to our clinic are very worried. In this part of the study, we want to get a clearer picture about this. We are asking all women coming to this clinic to fill out a brief anonymous questionnaire, looking at anxiety levels. We also want to see if things like age, and education can influence anxiety levels. This evidence may help us make changes to how we support women in this clinic.

The study is sponsored by Imperial College London and has been reviewed and approved by the Research Ethics Committee.

By filling in this survey, you consent to the study. The study is voluntary, meaning that you may or may not choose to take part. You are also free to omit any questions. A decision to withdraw at any time, or a decision not to take part, will not affect your future medical care.

There is also no follow up needed for this research – just simply fill in the short questionnaire. It should take less than 5minutes. All data is anonymised and will be stored in a password protected electronic format. The results of the survey will be used for academic research purposes only.

If you have any questions about the research study please feel free to ask the clinical research doctor in clinic Dr Diana Marcus, she will be present in the rapid access clinic. You can also email her on dianamarcus@nhs.net You can also ask the clinical doctors looking after you in clinic. If you have questions in general about your care please ask the doctor or nurse in clinic looking after you, or your GP. You may also contact PALS (Patient Advice and Liaison Services) for further information on participating on clinical trials.

Thank you for taking the time to read this information

The Questionnaire:

About you… (please circle)

1. Age?

<30	30-39	40-49	50-59	60-69	70-79	80+

2. Ethnicity?

White e.g. British, Irish	Mixed e.g. White & Asian	Asian e.g. Indian, Chinese	Black / African /Caribbean	Other e.g. Arab

3. Religion?

No religion	Christian	Buddhist	Hindu	Jewish	Muslim	Sikh	Other

4. Education?

Primary school	Secondary school (GCSEs)	Sixth form (A-levels)	University degree	Further degree (PhD, Masters)	Other

5. Is English your First language, 'mothers tongue'?

Yes	No

6. Do you consider yourself to have a long-term disability?

Yes	No

About the appointment today: … (please circle)

7. Did you receive any prior information about today's clinic appointment?

Yes	No

8. If so, what were your sources of information? Circle all that apply

GP	Oher healthcare professional	information leaflet	Internet and google	Family or friend	Been to clinic before so know what to expect

9. Do you feel you received enough information to know what to expect today? Please Mark on scale

Too little information	Sufficient information	Too much information

10. How beneficial do you feel a quick diagnosis or result today is? Choose a point on the scale between 0 (not important at all) – 5 (very important)

0 NOT important at all to have quick diagnosis	**1**	**2**	**3**	**4**	**5** Very Important to have quick diagnosis

11. How stressed have you felt about this appointment?

Choose a point on the scale between 0 (not stressed at all) – 5 (very stressed)

0 Not stressed at all	**1**	**2**	**3**	**4**	**5** Very stressed

12. In your own mind, do you believe that the test will show cancer?

Just put down your first automatic reaction or thought. Choose a point on the scale between: 0 (very sure it will not show cancer) – 5 (very sure it will show cancer)

0 Very sure NOT cancer	**1**	**2**	**3**	**4**	**5** Very sure it IS cancer

Over the last 2 weeks, how often have you been bothered by any of the following problems?

13. Feeling nervous, anxious or on edge?

- Not at all
- Several days
- More than half the days
- Nearly every day

14. Not being able to stop or control worrying?

- Not at all
- Several days
- More than half the days
- Nearly every day

15. Worrying too much about different things?

- Not at all
- Several days
- More than half the days
- Nearly every day

16. Trouble relaxing?

- Not at all
- Several days
- More than half the days
- Nearly every day

17. Being so restless that it is hard to sit still?

- Not at all
- Several days
- More than half the days
- Nearly every day

18. Becoming easily annoyed or irritable?

- Not at all
- Several days
- More than half the days
- Nearly every day

19. Feeling afraid as if something awful might happen?

- Not at all
- Several days
- More than half the days
- Nearly every day

Many thanks for filling this in. Please hand to the doctor in clinic.

12.4 Tissue bank classification of uterine samples

Batch	Sample label	Tissue Bank classification	Tissue type on review	Burns seens	Tumour percentage
BATCH 1	DM_01_CG	Benign	Endometrium (only stroma) and Myometrium	4	no tumour
BATCH 1	DM_01_CT	Benign	Myometrium	2	no tumour
BATCH 1	DM_02_CG	Hyperplasia	Endometrium (stroma and glands) and myometrium (no tumour)	2	no tumour
BATCH 1	DM_02_CT	Hyperplasia	Endometrium (stroma and glands) and myometrium (no tumour)	2	no tumour
BATCH 1	DM_03_CG	Benign	Endometrium (stroma and glands) and myometrium	2	no tumour
BATCH 1	DM_03_CT	Benign	Endometrium (glands and stroma)	2	no tumour
BATCH 1	DM_04_CG	Endometroid Ca	Several glands + muscle	1	?
BATCH 1	DM_04_CT	Endometroid Ca	Several glands + muscle	3	?
BATCH 1	DM_05_CG	Benign	Endometrium (stroma and glands) and myometrium (no tumour)	2	no tumour
BATCH 1	DM_05_CT	Benign	Endometrium (stroma and glands) and myometrium (no tumour)	3	no tumour
BATCH 1	DM_06_CG	Carciniosarcoma	Stroma + inflammatory cells (no glands)	2	no tumour
BATCH 1	DM_06_CT	Carciniosarcoma	Stroma + inflammatory cells (no glands)	2	no tumour
BATCH 1	DM_07_CG	Benign	Endometrium (stroma and glands) and myometrium (no tumour)	2	no tumour
BATCH 1	DM_07_CT	Benign	Myometrium	2	no tumour
BATCH 1	DM_08_CG	Serous papillary carcinoma	Tumour	2	90%
BATCH 1	DM_08_CT	serous papillary carcinoma	Tumour	4	80%
BATCH 1	DM_09_CG	MMT	Necrotic tissue (100%)	2	just necrosis
BATCH 1	DM_09_CT	MMT	Necrotic tissue (100%)	3	just necrosis
BATCH 1	DM_10_CG	endometroid Ca	Myometrium	2	no tumour
BATCH 1	DM_10_CT	endometroid Ca	Myometrium	2	no tumour
BATCH 1	DM_11_CG	benign	Endometrium (glands and stroma)	3	no tumour
BATCH 1	DM_11_CT	benign	Endometrium (glands and stroma) and myometrium	3	no tumour
BATCH 1	DM_12_CG	benign	Myometrium	2	no tumour
BATCH 1	DM_12_CT	benign	Myometrium	2	no tumour
BATCH 1	DM_13_CG	benign	Endometrium (only stroma) and Myometrium	2	no tumour
BATCH 1	DM_13_CT	benign	Endometrium (stroma and glands) and myometrium (no tumour)	2	no tumour
BATCH 2	DM_14_CG	benign	Myometrium	2	no tumour
BATCH 2	DM_14_CT	benign	Myometrium	1	no tumour
BATCH 2	DM_15_CT	endometroid Ca	Endometrium (glands and stroma)	1	no tumour
BATCH 2	DM_16_CG	endometroid Ca	Tumour +muscle	2	90%
BATCH 2	DM_16_CT	endometroid Ca	Tumour +muscle	1	80%
BATCH 2	DM_17_CG	endometroid Ca	Tumour	2	90%
BATCH 2	DM_17_CT	endometroid Ca	Tumour and necrosis	1	50%
BATCH 2	DM_18_CG	endometroid Ca	Myometrium	2	no tumour
BATCH 2	DM_18_CT	endometroid Ca	Endometrium (glands and stroma) and myometrium	2	no tumour
BATCH 2	DM_19_CG	endometroid Ca	Tumour	1	95%
BATCH 2	DM_19_CT	endometroid Ca	Tumour	2	95%
BATCH 2	DM_20_CG	endometroid Ca	70% necrtotic tissue 30% inflammation and tumour(solid)	5	20%
BATCH 2	DM_20_CT	endometroid Ca	50% necrtotic tissue 50% inflammation and tumour(solid)	4	30%
BATCH 2	DM_21_CG	Hyperplasia	Endometrium (stroma and glands) and myometrium (no tumour)	2	no tumour
BATCH 2	DM_21_CT	Hyperplasia	Endometrium (stroma and glands) and myometrium (no tumour)	2	no tumour
BATCH 2	DM_22_CG	carciniosarcoma	Necrotic tissue (100%)	2	just necrosis
BATCH 2	DM_22_CT	Carciniosarcoma	Necrotic tissue (100%)	3	just necrosis
BATCH 2	DM_23_CG	benign	Endometrium (glands and stroma)	3	no tumour
BATCH 2	DM_23_CT	benign	Endometrium (glands and stroma)	2	no tumour
BATCH 2	DM_24_CG	endometroid Ca	Myometrium	2	no tumour
BATCH 2	DM_24_CT	endometroid Ca	Endometrium (stroma and glands) and myometrium (no tumour)	4	no tumour
BATCH 2	DM_25_CG	clear cell	Tumour + necrotic tissue	2	90%
BATCH 2	DM_25_CT	clear cell	Tumour + necrotic tissue	4	80%
BATCH 2	DM_26_CG	carciniosarcoma	Endometrial Stroma+Mucus+Necrotic Tissue	3	no tumour
BATCH 2	DM_26_CT	carciniosarcoma	Endometrial Stroma+Mucus+Necrotic Tissue	1	no tumour
BATCH 2	DM_27_CG	benign	Endometrium (glands and stroma)	3	no tumour
BATCH 2	DM_27_CT	benign	Endometrium (glands and stroma)	1	no tumour
BATCH 2	DM_28_CG	clear cell	Tumour and myometrium	3	40%
BATCH 2	DM_28_CT	clear cell	Tumour and myometrium	4	50%
BATCH 3	DM_29_CG	Neuroendocrine tumour	Tumour (solid), Fibrosis and Necrosis	2	10%
BATCH 3	DM_29_CT	Neuroendocrine tumour	Tumour (solid), Fibrosis and Necrosis	3	25%
BATCH 3	DM_30_CG	endometroid Ca	Tumour	2	85%
BATCH 3	DM_30_CT	endometroid Ca	Tumour	1	80%
BATCH 3	DM_31_CG	endometroid Ca	Tumour + necrosis	1	50%
BATCH 3	DM_31_CT	endometroid Ca	Tumour + necrosis	3	90%
BATCH 3	DM_32_CG	benign	Myometrium	2	no tumour
BATCH 3	DM_32_CT	benign	Myometrium and Endometrium (stroma and glands)	2	no tumour
BATCH 3	DM_33_CG	endometroid Ca	Tumour + muscle	3	60%
BATCH 3	DM_33_CT	endometroid Ca	Tumour + muscle	3	40%
BATCH 3	DM_34_CG	endometroid Ca	Tumour + myometrium	1	40%
BATCH 3	DM_34_CT	endometroid Ca	Tumour + necrosis+ myometrium	3	25%
BATCH 3	DM_35_CG	endometroid Ca	Tumour? + muscle	4	50%
BATCH 3	DM_35_CT	endometroid Ca	Tumour? + muscle	3	60%
BATCH 3	DM_36_CG	clear cell	Tumour + necrosis	2	5%
BATCH 3	DM_36_CT	clear cell	Tumour + necrosis	3	30%
BATCH 3	DM_37_CG	Endometroid Ca	Tumour	2	25%
BATCH 3	DM_37_CT	endometroid Ca	Tumour	1	50%
BATCH 3	DM_38_CG	cervical cancer	Endometrium (glands and stroma)	1	no tumour
BATCH 3	DM_38_CT	cervical cancer	Endometrium (glands and stroma) + myometrium	2	no tumour

Batch	Sample label	Tissue Bank classification	Tissue type on review	Burns seens	Tumour percentage
BATCH 3	DM_39_CG	endometroid Ca	Tumour	3	100%
BATCH 3	DM_39_CT	endometroid Ca	Tumour	2	100%
BATCH 3	DM_40_CG	endometroid Ca	Tumour	2	80%
BATCH 3	DM_40_CT	endometroid Ca	Tumour + myometrium	4	70%
BATCH 3	DM_41_CG	clear cell	Tumour (solid) + necrosis+inflammation	2	95%
BATCH 3	DM_41_CT	clear cell	Tumour (solid) + necrosis+inflammation	2	90%
BATCH 3	DM_42_CG	endometroid Ca	Tumour	2	100%
BATCH 3	DM_42_CT	endometroid Ca	Tumour	2	100%
BATCH 3	DM_43_CG	endometroid Ca	Tumour	3	40%
BATCH 3	DM_43_CT	endometroid Ca	Tumour	2	60%
BATCH 3	DM_44_CG	clear cell	Tumour + myometrium	2	40%
BATCH 3	DM_44_CT	clear cell	Tumour + myometrium	3	25%
BATCH 3	DM_45_CG	endometroid Ca	Endometrium (glands and stroma) + myometrium	3	no tumour
BATCH 3	DM_45_CT	endometroid Ca	Myometrium	2	no tumour
BATCH 3	DM_46_CG	benign	Myometrium	2	no tumour
BATCH 3	DM_46_CT	benign	Endometrium (glands and stroma) + myometrium	3	no tumour
BATCH 3	DM_47_CG	clear cell	Tumour + necrosis	2	90%
BATCH 3	DM_47_CT	clear cell	Tumour + necrosis	2	50%
BATCH 3	DM_48_CG	endometroid Ca	Tumour?	2	30%
BATCH 3	DM_48_CT	endometroid Ca	Tumour? + myometrium	1	40%
BATCH 3	**DM_49_CG**	endometroid Ca	??? Tumour??		100%
BATCH 3	DM_49_CT	endometroid Ca	Tumour?	2	100%
BATCH 3	DM_50_CG	endometroid Ca	Mucinous glands and mucus	2	100%
BATCH 3	DM_50_CT	endometroid Ca	Mucinous glands and mucus	2	100%
BATCH 3	DM_51_CG	endometroid Ca	Tumour + Myometrium	2	2%
BATCH 3	DM_51_CT	endometroid Ca	Tumour + Myometrium+ Adenomyosis	4	25%
BATCH 3	DM_52_CG	clear cell	Tumour	3	100%
BATCH 3	DM_52_CT	clear cell	Tumour + necrosis	4	90%
BATCH 3	DM_53_CG A	endometroid Ca	Tumour+myometrium	2	50%
BATCH 3	DM_53_CT A	endometroid Ca	Tumour+myometrium	3	40%
BATCH 3	DM_53_CG B	endometroid Ca	Tumour+myometrium	1	10%
BATCH 3	DM_53_CT B	endometroid Ca	Tumour+myometrium	1	20%
BATCH 3	DM_53_CG C	endometroid Ca	Fibrous tissue and muscle	2	no tumour
BATCH 3	DM_53_CT C	endometroid Ca	Fibrous tissue and muscle	3	no tumour
BATCH 3	DM_53_CG D	endometroid Ca	Ovary	2	no tumour
BATCH 3	DM_53_CT D	endometroid Ca	Ovary	3	no tumour
BATCH 3	DM_54_CG A	endometroid Ca	Tumour + necrosis+blood	3	90%
BATCH 3	DM_54_CT A	endometroid Ca	Tumour + necrosis+blood	3	90%
BATCH 3	DM_54_CG B	endometroid Ca	Myometrium	3	no tumour
BATCH 3	DM_54_CT B	endometroid Ca	Myometrium	2	no tumour
BATCH 3	DM_54_CG C	endometroid Ca	Ovary	1	no tumour
BATCH 3	DM_54_CT C	endometroid Ca	Ovary	1	no tumour
BATCH 4	DM_55_CG	benign	Endometrium (glands and stroma) + myometrium	4	no tumour
BATCH 4	DM_55_CT	benign	Endometrium (glands and stroma) + myometrium	2	no tumour
BATCH 4	DM_56_CG	endometroid Ca	Tumour + blood	2	10%
BATCH 4	DM_56_CT	endometroid Ca	Tumour + blood	3	70%
BATCH 4	DM_57_CG	endometroid Ca	Myometirum + only 2 endometrial glands	2	?
BATCH 4	DM_57_CT	endometroid Ca	Myometrium	3	no tumour
BATCH 4	DM_58_CG	MMT	Fibrous Tissue + necrosis (80%)	2	no tumour
BATCH 4	DM_58_CT	MMT	Fibrous Tissue + necrosis (80%)	4	no tumour
BATCH 4	DM_59_CG	serous papillary carcinoma	Tumour	1	80%
BATCH 4	DM_59_CT	serous papillary carcinoma	Tumour	2	90%
BATCH 4	DM_60_CG	endometroid Ca	Tumour + Mucus	2	90%
BATCH 4	DM_60_CT	endometroid Ca	Tumour + Mucus	2	100%
BATCH 4	DM_61_CG	mMT	Tumour?+fibrose tissue+adipose tissue(steatonecrosis)	2	5%
BATCH 4	DM_61_CT	mMT	Tumour?+fibrose tissue+adipose tissue(steatonecrosis) +necrosis	2	5%
BATCH 4	DM_62_CG	clear cell	Tumour?+Necrotic Tissue	3	50%
BATCH 4	DM_62_CT	clear cell	Tumour?+Necrotic Tissue	2	60%
BATCH 4	DM_63_CG	endometroid Ca	Tumour	2	90%
BATCH 4	DM_63_CT	endometroid Ca	Tumour	2	90%
BATCH 4	DM_64_CG	serous papillary carcinoma	Tumour	3	95%
BATCH 4	DM_64_CT	serous papillary carcinoma	Tumour	3	90%
BATCH 4	DM_65_CG	endometroid Ca	Tumour+Myometrium+Adenomyosis	2	50%
BATCH 4	DM_65_CT	endometroid Ca	Tumour+Myometrium+Adenomyosis	1	70%
BATCH 4	DM_66_CG	benign	Endometrium (glands and stroma) + myometrium	3	no tumour
BATCH 4	DM_66_CT	benign	Endometrium (glands and stroma) + myometrium	3	no tumour
BATCH 4	DM_67_CG	benign	Myometrium	2	no tumour
BATCH 4	DM_67_CT	benign	Myometrium	2	no tumour
BATCH 4	DM_68_CG	benign	Tumour	4	80%
BATCH 4	DM_68_CT	benign	Tumour	3	100%
BATCH 4	DM_69_CG	endometroid Ca	Tumour	2	100%
BATCH 4	DM_69_CT	endometroid Ca	Tumour	3	100%
BATCH 4	DM_70_CG	serous papillary carcinoma	Endocervix	2	no tumour
BATCH 4	DM_70_CT	serous papillary carcinoma	Endocervix + isthmus	3	no tumour
BATCH 4	DM_71_CG	endometroid Ca	Tumour+fibrose tissue+adipose tissue(steatonecrosis)	2	10%
BATCH 4	DM_71_CT	endometroid Ca	Tumour+fibrose tissue+adipose tissue(steatonecrosis)	2	10%
BATCH 4	DM_72_CG	endometroid Ca	Mucus+Histiocytes+mucinous glands	1	
BATCH 4	DM_72_CT	endometroid Ca	Mucus+Histiocytes+mucinous glands	2	
BATCH 4	DM_73_CG	endometroid Ca	Tumour?	4	90%
BATCH 4	DM_73_CT	endometroid Ca	Tumour?	4	90%
BATCH 4	DM_74_CG	ovarian cancer	Myometrium	2	no tumour
BATCH 4	DM_74_CT	ovarian cancer	Myometrium	1	no tumour
BATCH 5	DM_75_CG	cervical cancer	Muscle	2	no tumour
BATCH 5	DM_75_CT	cervical cancer	Muscle + a tiny cluster of burnt epithelial cells	2	
BATCH 5	DM_76_CG	endometroid Ca	Tumour	3	100%
BATCH 5	DM_76_CT	endometroid Ca	Tumour	2	100%
BATCH 5	DM_77_CG	benign	Myometrium	1	no tumour
BATCH 5	DM_77_CT	benign	Myometrium	2	no tumour
BATCH 5	DM_78_CG	endometroid Ca	Tumour	1	100%
BATCH 5	DM_78_CT	endometroid Ca	Tumour	2	100%
BATCH 5	DM_79_A_C	endometroid Ca	Tumour	1	100%
BATCH 5	DM_79_A_C	endometroid Ca	Tumour	2	100%
BATCH 5	DM_79_B_C	endometroid Ca	Myometrium	2	no tumour
BATCH 5	DM_79_B_C	endometroid Ca	Myometrium	2	no tumour

Batch	Sample label	Tissue Bank classification	Tissue type on review	Burns seens	Tumour percentage
BATCH 5	DM_80_CG	serous papillary carcinoma	Myometrium + tiny cluster of glands (endometrial glands?)	2	no tumour
BATCH 5	DM_80_CT	serous papillary carcinoma	Endometrium (glands and stroma) + myometrium	3	no tumour
BATCH 5	DM_81_CG	benign	Muscle	2	no tumour
BATCH 5	DM_81_CT	benign	Muscle	2	no tumour
BATCH 5	DM_82_CG	benign	Myometrium + a small piece of detached endometroid tumour	2	5%
BATCH 5	DM_82_CT	benign	Myometrium + a small piece of detached epithelial glands	2	5%
BATCH 5	DM_83_CG	endometroid Ca	Myometrium	2	no tumour
BATCH 5	DM_83_CT	endometroid Ca	Myometrium	1	no tumour
BATCH 5	DM_84_CG	endometroid Ca	Tumour	1	100%
BATCH 5	DM_84_CT	endometroid Ca	Tumour	2	100%
BATCH 5	DM_85_CG	endometroid Ca	Myometrium	1	no tumour
BATCH 5	DM_85_CT	endometroid Ca	Myometrium	1	no tumour
BATCH 5	DM_86_CG	benign	Myometrium	1	no tumour
BATCH 5	DM_86_CT	benign	Myometrium	2	no tumour
BATCH 5	DM_87_CT	endometroid Ca	Muscle and blood	3	no tumour
BATCH 5	DM_88_CG	clear cell	Muscle	1	no tumour
BATCH 5	DM_88_CT	clear cell	Muscle	1	no tumour
BATCH 5	DM_89_CT	high grade endometrial cancer	Myometrium + Endometrial Stroma	2	no tumour
BATCH 5	DM_90_CT	benign	Myometrium + Endometrial Stroma	2	no tumour
BATCH 5	DM_91_CG	endometroid Ca	Tumour	1	100%
BATCH 5	DM_91_CT	endometroid Ca	Tumour	2	100%
BATCH 5	DM_92_CG	endometroid Ca	Myometrium + Endometrial Stroma	2	no tumour
BATCH 5	DM_92_CT	endometroid Ca	Myometrium	2	no tumour
BATCH 5	DM_93_CG	benign	Myometrium	1	no tumour
BATCH 5	DM_93_CT	benign	Myometrium	2	no tumour
BATCH 6	DM_94_CG	mmT	Muscle + Lymphocytes	2	no tumour
BATCH 6	DM_94_CT	mmT	Muscle	3	no tumour
BATCH 6	DM_95_CG	endometroid Ca	Tumour	1	100%
BATCH 6	DM_95_CT	endometroid Ca	Tumour	2	100%
BATCH 6	DM_96_CG	benign	Myometrium	1	no tumour
BATCH 6	DM_96_CT	benign	Myometrium	1	no tumour
BATCH 6	DM_97_CG	mmT	Carcinosarcoma	2	100%
BATCH 6	DM_97_CT	mmT	Carcinosarcoma	2	100%
BATCH 6	DM_98_CG	cervical cancer	Endometrium (glands and stroma) + myometrium	1	no tumour
BATCH 6	DM_98_CT	cervical cancer	Endometrium (glands and stroma) + myometrium	2	no tumour
BATCH 6	DM_99_CG	carciniosarcoma	Tumour (sarcoma?) + necrosis (50%)	1	50%
BATCH 6	DM_99_CT	carciniosarcoma	Tumour (sarcoma?) + necrosis (40%)	1	60%
BATCH 6	DM_100_CG	endometroid Ca	Muscle	1	no tumour
BATCH 6	DM_100_CT	endometroid Ca	Muscle	1	no tumour
BATCH 6	DM_101_CG	benign	Myometrium	1	no tumour
BATCH 6	DM_101_CT	benign	Myometrium	2	no tumour
BATCH 6	DM_102_CG	endometial cancer	Tumour (undifferentiated?)	2	100%
BATCH 6	DM_102_CT	endometial cancer	Tumour (undifferentiated?)	2	100%
BATCH 6	DM_103_CG	endometroid Ca	Tumour	2	100%
BATCH 6	DM_103_CT	endometroid Ca	Tumour	2	100%
BATCH 5	DM_104_CG	endometroid Ca	Myometrium + a small piece of detached endometroid tumour	2	2%
BATCH 5	DM_104_CT	endometroid Ca	Myometrium + Endometrial tumour	3	10%
BATCH 6	DM_105_CG	benign	Tumour (most likely Endometroid)	1	90%
BATCH 6	DM_105_CT	benign	Tumour (most likely Endometroid)	1	100%
BATCH 6	DM_106_CG	mixed endometroid clear cell	Muscle (Leyomioma?)	1	no tumour
BATCH 6	DM_106_CT	mixed endometroid clear cell	Muscle (Leyomioma?)	1	no tumour
BATCH 6	DM_107_CG	cancer	Muscle	2	no tumour
BATCH 6	DM_107_CT	cancer	Muscle	2	no tumour
BATCH 6	DM_108_CG	endometroid Ca	Endometrium + tumour + necrosis	1	10%
BATCH 6	DM_108_CT	endometroid Ca	Endometrium + tumour + necrosis	1	50%
BATCH 6	DM_109_CG	benign	Muscle	1	no tumour
BATCH 6	DM_109_CT	benign	Muscle	1	no tumour
BATCH 6	DM_110_CG	endometrial cancer	Muscle	1	no tumour
BATCH 6	DM_110_CT	endometrial cancer	Muscle	2	no tumour
BATCH 6	DM_111_CG	endometrial cancer	Tumour + necrosis(90%) + calcium deposits	1	10%
BATCH 6	DM_111_CT	endometrial cancer	Tumour + necrosis(70%) + calcium deposits	2	30%
BATCH 6	DM_112_CG	serous papillary carcinoma	Tumour	2	100%
BATCH 6	DM_112_CT	serous papillary carcinoma	Tumour + muscle	2	50%
BATCH 6	DM_113_CG	endometroid Ca	Tumour	1	100%
BATCH 6	DM_113_CT	endometroid Ca	Tumour	2	100%
BATCH 6	DM_114_CG	endometroid Ca	Tumour	1	90%
BATCH 6	DM_114_CT	endometroid Ca	Tumour	1	100%
BATCH 6	DM_115_CG	carciniosarcoma	Solid tumour	1	80%
BATCH 6	DM_115_CT	carciniosarcoma	Solid tumour	1	90%
BATCH 7	DM_116_CT	ovarian cancer	Endometrium stroma + myometrium	1	no tumour
BATCH 7	DM_117_CT	benign	Endometrium (glands and stroma) + myometrium	2	no tumour
BATCH 7	DM_118_CT	benign	Endometrium (glands and stroma) + myometrium	2	no tumour
BATCH 7	DM_119_CT	benign	Endometrium (glands and stroma) + myometrium	2	no tumour
BATCH 7	DM_120_CT	benign	Muscle	4	no tumour
BATCH 7	DM_121_CT	benign	Muscle	2	no tumour
BATCH 7	DM_122_CT	benign	Muscle	3	no tumour
BATCH 7	DM_123_CT	benign	Muscle	1	no tumour
BATCH 7	DM_124_CT	benign	Muscle	3	no tumour
BATCH 7	DM_125_CT	benign	Muscle	3	no tumour
BATCH 7	DM_126_CT	benign	Muscle	3	no tumour
BATCH 7	DM_127_CT	benign	Myometrium	3	no tumour
BATCH 7	DM_128_CT	benign	Muscle	4	no tumour
BATCH 7	DM_129_CT	benign	Muscle	3	no tumour
BATCH 7	DM_130_CT	benign	Endometrium (glands and stroma) + myometrium	2	no tumour
BATCH 7	DM_131_CT	Benign	Endometrium (glands and stroma) + myometrium	1	no tumour

Batch	Sample labe	Tissue Bank classification	Tissue type on review	Burns seens	Tumour percentage
BATCH 7	DM_132_CT	benign	Solid tissue composed of large and atypical cells but no mitosis + Necrosi	2	
BATCH 7	DM_133_CT	benign	Muscle	2	no tumour
BATCH 7	DM_134_CT	mixed endometroid clear cell	Myometrium (no glands)	3	no tumour
BATCH 7	DM_135_CT	clear cell	tumour glands, Mucus and stroma	2	20%
BATCH 8	DM_136_CT	endometrial cancer	Endometrial stroma + 2 normal endometrial glands	1	no tumour
BATCH 8	DM_137_CT	endometrial ca	Tumour (Mucinous)	1	90%
BATCH 8	DM_138_CT	Endometroid cancer	Tumour	1	80%
BATCH 8	DM_139_CT	stromal ca	Muscle/Fibrose tissue	2	
BATCH 8	DM_140_CT	endometrial ca	Poorly differentiated tumour	2	100%
BATCH 8	DM_141_CT	serous endo ca	Myometrium + Endometrial Stroma	3	no tumour
BATCH 8	DM_142_CT	Endometroid Ca	Tumour(Squamous differentiation?) + Myometrium+Adenomyosis	2	10%
BATCH 8	DM_143_CT	Endometroid Ca	Tumour (Tiny sample)	1	40%
BATCH 8	DM_144_CT	Benign	Endometrium (Cystic changes + hyperplastic glands)	2	no tumour
BATCH 8	DM_145_CT	Benign	Myometrium + Adenomyosis	1	no tumour
BATCH 8	DM_146_CT	Neuroendocrine and Endometroi	Solid tumour	1	90%
BATCH 8	DM_147_CT	Endometroid Ca	Myometrium	2	no tumour
BATCH 8	DM_148_CT	endometroid cancer	Tumour	2	100%
BATCH 8	DM_149_CT	benign myometrium	Endometrium (Hyperplasia) + Myometrium	1	no tumour
BATCH 8	DM_150_CT	endometroid ca	Muscle	3	no tumour
BATCH 8	DM_151_CT	endometrial cancer	Tumour	2	90%
BATCH 8	DM_152_CT	normal	Muscle	1	no tumour
BATCH 8	DM_153_CT	serous ca	Muscle + a couple of burnt glands	1	
BATCH 8	DM_154_CT	serous ca	Tumour + Necrosis(10%)	2	90%

12.5 Other tissue bank models evaluated

Statistical modelling using tissue bank samples: normal vs cancer. Post-Histopathological quality control. Outlier assessment

As can be seen from the PC plots several outliers exist (points distinctly further away from neighbouring points or mixing of normal data point within cancer area). These are illustrated in PCA plot below with yellow arrows (Fig 100).

The samples from which these data points were generated were analysed. All, bar two came from different processing batches.

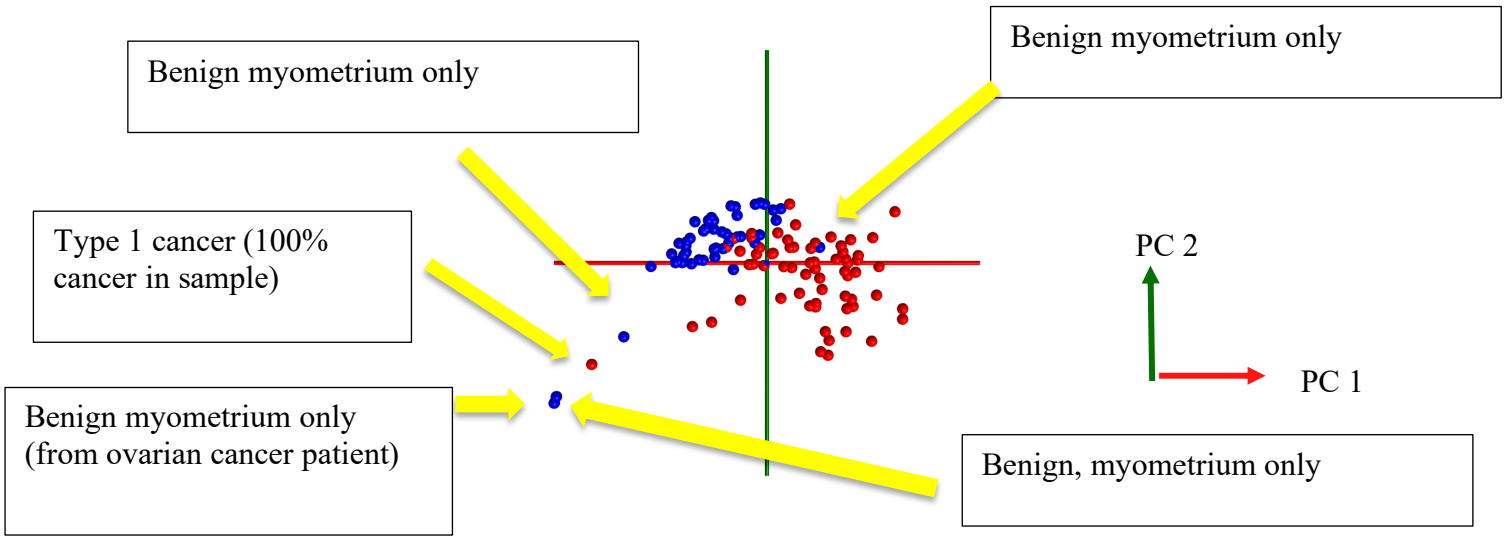


Figure 100. Investigation of outliers from the normal vs cancer tissue bank PCA.
Each outlier is highlighted by a yellow arrow, and possible reasons for it, outlined.

Tissue bank model: Can the iKnife distinguish between Type 1 vs Type 2 vs normal? Outlier assessment

As can be seen from the PC/LDA plots several outliers exist (points distinctly further away from neighbouring points and outside the appropriate cluster). These are illustrated in LDA plot below with yellow arrows (Figure 101). Analysis of these

processing points revealed that most (7 of 9) came from a single batch processing, which suggests there might be an element of batch effect. Most of the outliers are the same as the model above. Two of the samples which had cancer only had minimal amount of cancer (5-10%) within the specimen.

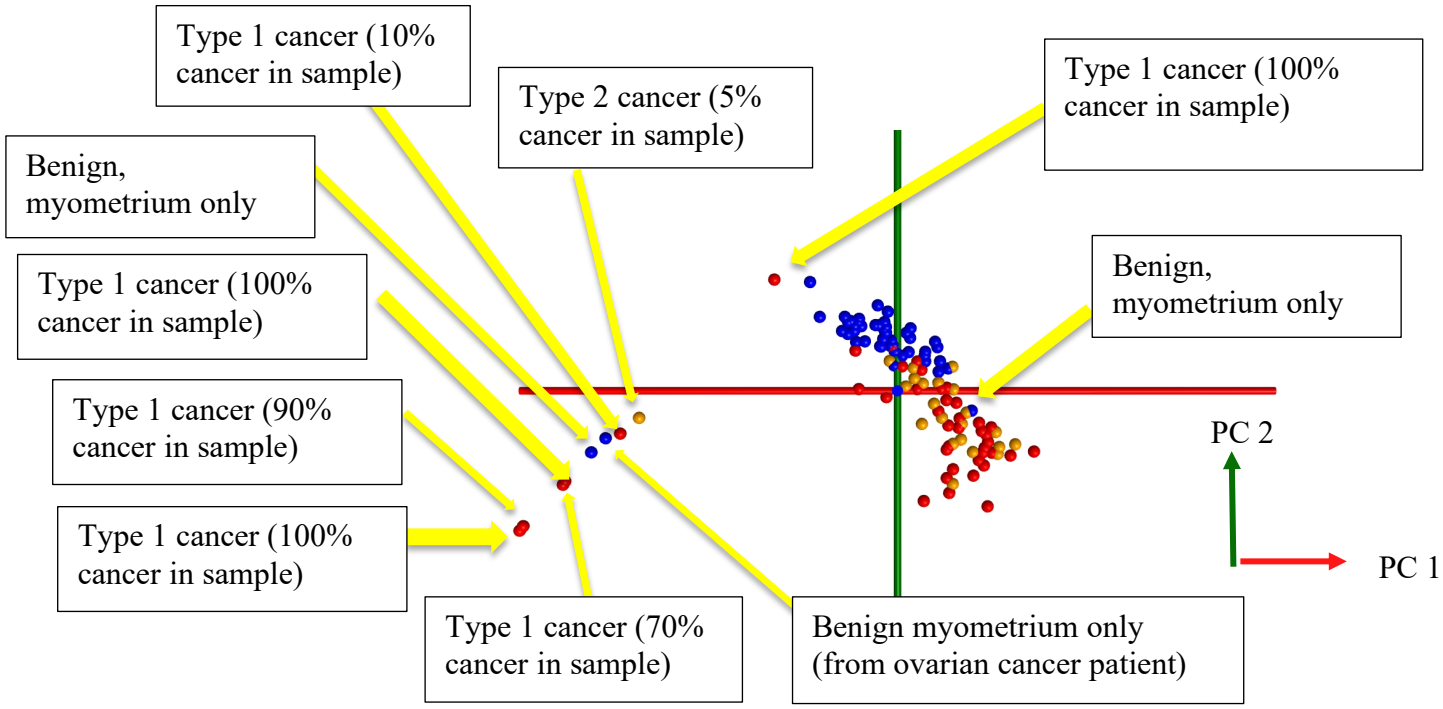


Figure 101. Investigation of outliers from the normal vs type 1 vs type 2 cancer tissue bank model.
Each outlier is highlighted by a yellow arrow, and possible reasons for it, outlined.

Tissue bank model sensitivity analysis: does removal of the outliers improve the model?

As seen on the previous few PC/LDA models, several outlier samples were persistent in most models. In an effort to optimise the model these 9 outliers were removed from the Type 1 vs normal model and analysis was performed again. Each dot on the PCA plots represents the average spectra for a single sample. Red dots represented cancer samples and blue normal (Figure 102). The confusion table is shown beneath the PCA plots. Principal component one accounted 36.3% of the model and principal component two 17.8%. Good separation of cancer and normal is seen again on the PCA. The overall sensitivity and specificity were good: 81% and 95% respectively.

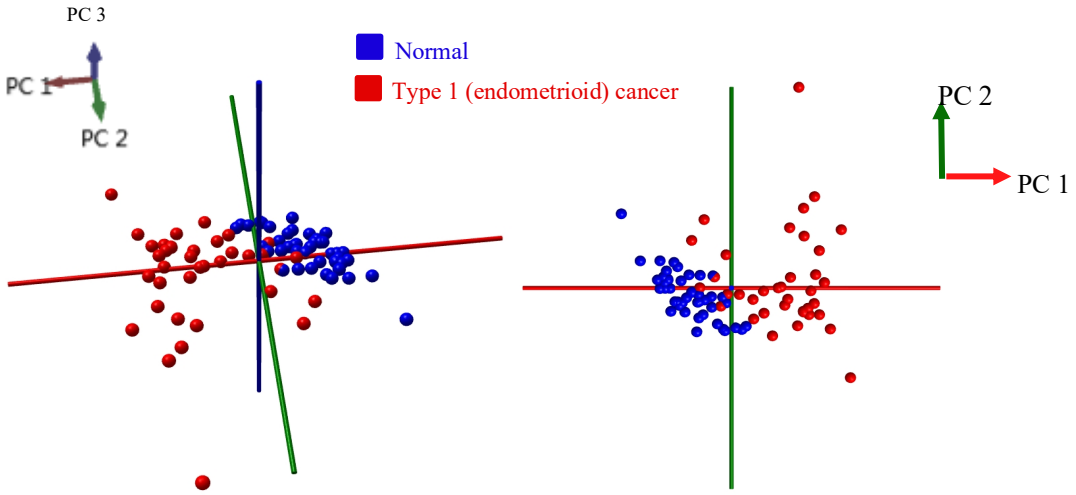


Figure 102. Multivariate analysis of normal vs type 1 cancer (endometrioid) tissue bank samples, after exclusion outliers.

Red dots represent endometrioid cancer and blue normal. Each dot represents the average spectra of a single sample. The diagram on the left is the 3D PCA, right 2D. The confusion table is outlined below.

		MODEL CLASSIFICATION, n (%)		TOTAL
		TYPE 1	NORMAL	
ACTUAL HISTOLOGY	TYPE 1 CA	30 (81%)	7 (19%)	37
	NORMAL	2 (5%)	42 (95%)	44

Confusion table for Figure 102

12.6 Other pipelle models evaluated

12.6.1 Does CO2 laser vs diathermy iKnife make a difference?

Learning models fair better with larger reference datasets. In an effort to increase the spectral library and also to see how similar, or indeed dissimilar CO2 laser and iKnife spectra are, the two datasets were amalgamated and a combined model of 155 samples post histopathological validation was created. All samples were reclassified according to their energy modality (CO2 laser vs iKnife) as well as tissue class.

The PCA and LDA plots are depicted below, with each dot representing the average spectra of a single sample (Figure 103). A very clear separation of laser and iKnife is seen along PC 1, which is even more obvious on the LDA. Tissue classes are separated along the y axis (LD component 2). The iKnife samples are more densely clustered than the CO2 laser samples. The confusion table shows the results of the cross validation. In keeping with the PCA and LDA plots, the model had a tendency to classify samples according to energy modality not tissue class. For example, of the 35 CO2 cancer laser samples, 30 were classified correctly, but the remaining 5 were classified as CO2 laser normal samples. This suggests that the two spectral libraries are too different to combine.

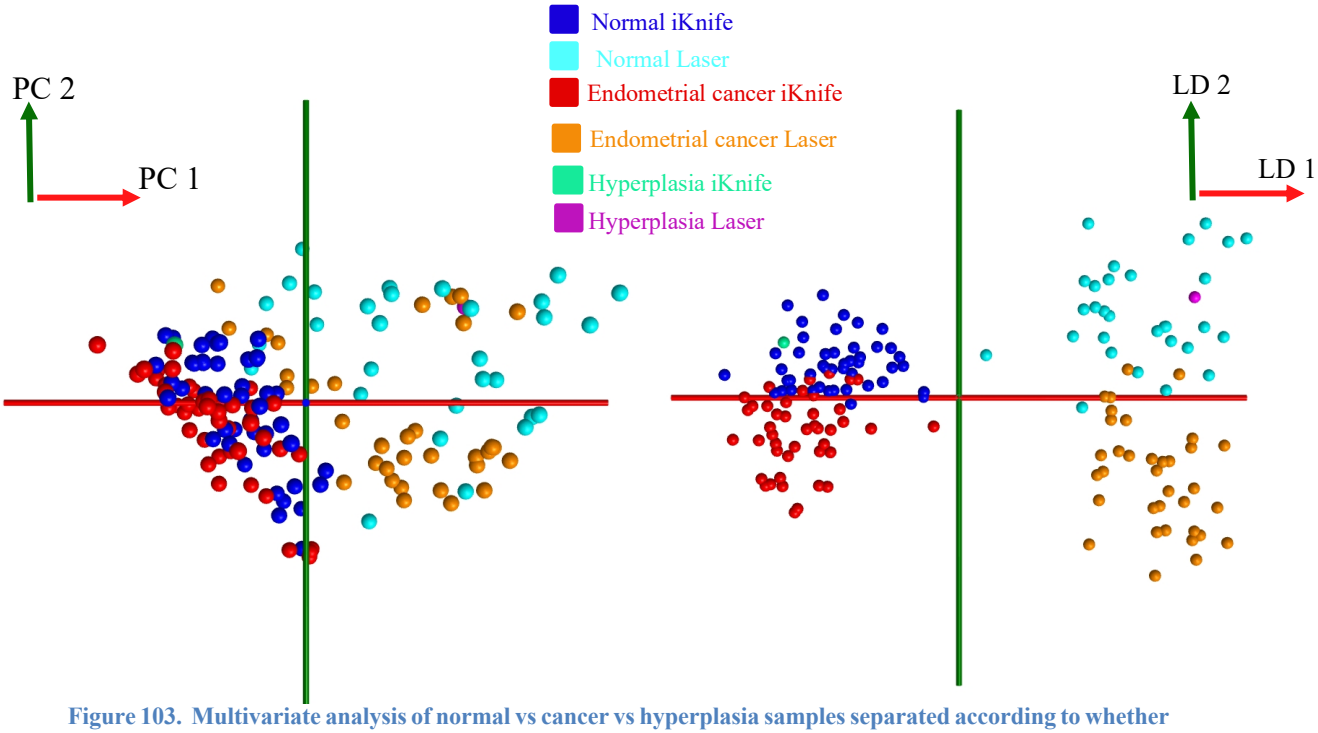


Figure 103. Multivariate analysis of normal vs cancer vs hyperplasia samples separated according to whether processed with the diathermy iKnife or CO2 laser.
Red and orange dots represent endometrial cancer samples and blue samples normal and green/purple hyperplasia. Each dot represents the average spectra of a single sample. The diagram on the left is a 2D PCA and right 2D LDA. Principal component one accounted for 44.2% of the variance in the model and principal component two 15.4%. The confusion table is shown below.

			MODEL CLASSIFICATION							TOTAL
			CANCER		HYPERPLASIA		NORMAL		OUTLIER	
			iKnife	Laser	iKnife	Laser	iKnife	Laser		
ACTUAL HISTOL-OGY	CANCER	iKnife	32	0	0	0	9	0	2	43
		Laser	0	30	0	0	0	5	0	35
	HYPER-PLASIA	iKnife	0	0	0	0	1	0	0	1
		Laser	0	0	0	0	0	1	0	1
	NORMAL	iKnife	5	0	0	0	29	0	11	45
		Laser	0	2	0	0	1	18	9	30

Confusion table for Figure 103

In addition, reclassifying all spectra from the CO2 laser and diathermy iKnife pipelle samples into cancer and normal (and removing the energy modality characteristic), and then creating a new model with this; had 79% sensitivity and 89% specificity (Table 33). This is worse than the separate diathermy iKnife and CO2 laser models, providing

further evidence that the spectra from the diathermy iKnife and CO2 laser cannot be combined.

Table 33. Confusion table of a model combining samples processed with the CO2 laser and standard diathermy iKnife reclassified according to whether samples were normal or cancer, not energy modality.

		MODEL CLASSIFICATION, n (%)		TOTAL
		CANCER	NORMAL	
ACTUAL HISTOLOGY	CANCER	62 (79%)	16 (21%)	78
	NORMAL	8 (11%)	67 (89%)	75

12.6.2 Results of the Liquid probe

A total of 17 samples were processed with the liquid probe, 5 exclusively with the liquid probe and 12 samples were processed with at least one other modality (diathermy iKnife or CO2 laser iKnife) too. The consistency of all these samples were very watery and the diathermy iKnife and/or CO2 laser often did not detect any signal when burnt. Most of these poor-quality samples were normal endometrium (12/17).

The liquid probe generated 177 spectra (50 cancer, 127 normal); no spectra were excluded by the AMX spectral quality control feature. Whilst no spectra were removed due to poor quality, histopathological validation of the processed samples was not possible for any of the samples; as the histologist felt all the samples were inadequate. Instead the reference standard was the final histology of the patient. Very little separation of normal and cancer samples is seen on the PCA (Figure 104). The overall sensitivity and specificity were: 50% and 92% respectively.

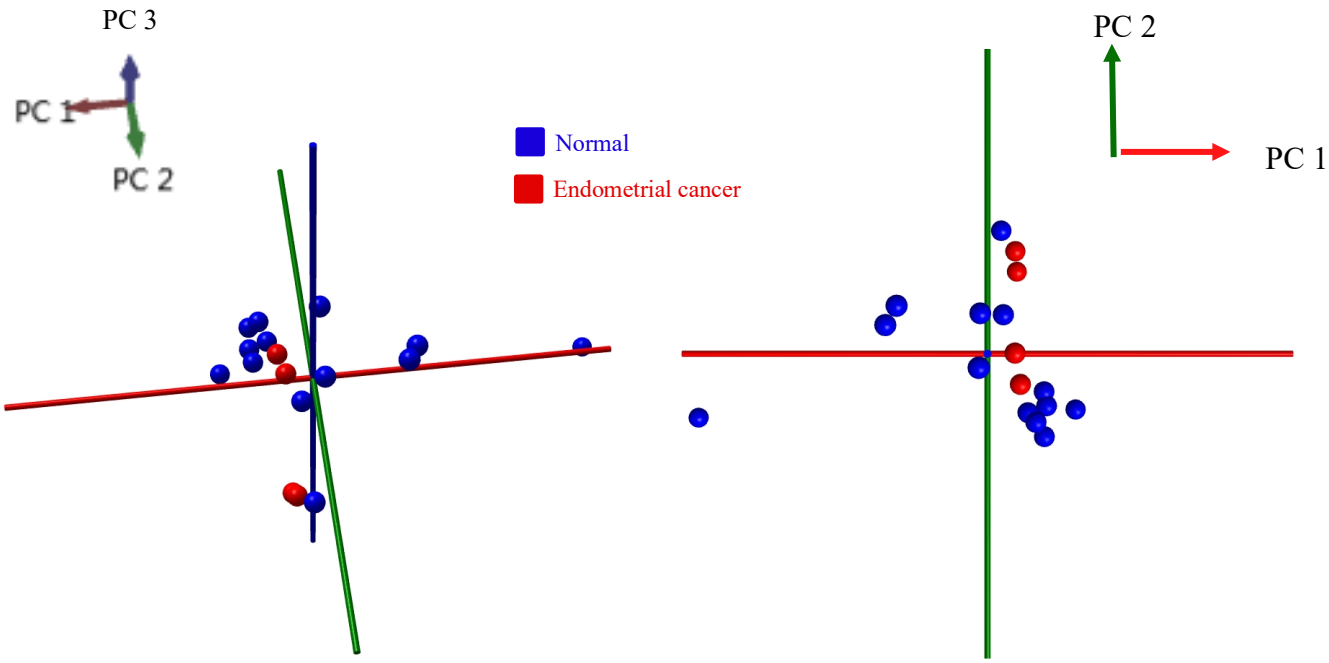


Figure 104. Multivariate analysis of normal vs cancer pipelle samples, processed with the liquid probe.
Red dots represent endometrial cancer samples and blue normal. Each dot represents the average spectra of a single sample. The diagram on the left is a 3D PCA, and right 2D PCA. The confusion table is shown below.

		MODEL CLASSIFICATION, n (%)		TOTAL
		CANCER	NORMAL	
ACTUAL HISTOLOGY	CANCER	2 (50%)	2 (50%)	4
	NORMAL	1 (7%)	12 (92%)	13

Confusion table for Figure 104

Combining the standard diathermy iKnife, CO2 laser and liquid probe samples into a single model reveals that the liquid probe samples cluster much more with the iKnife samples as oppose to the CO2 laser, with respect to phospholipid profiles (Figure 105). The same finding is seen on the confusion table.

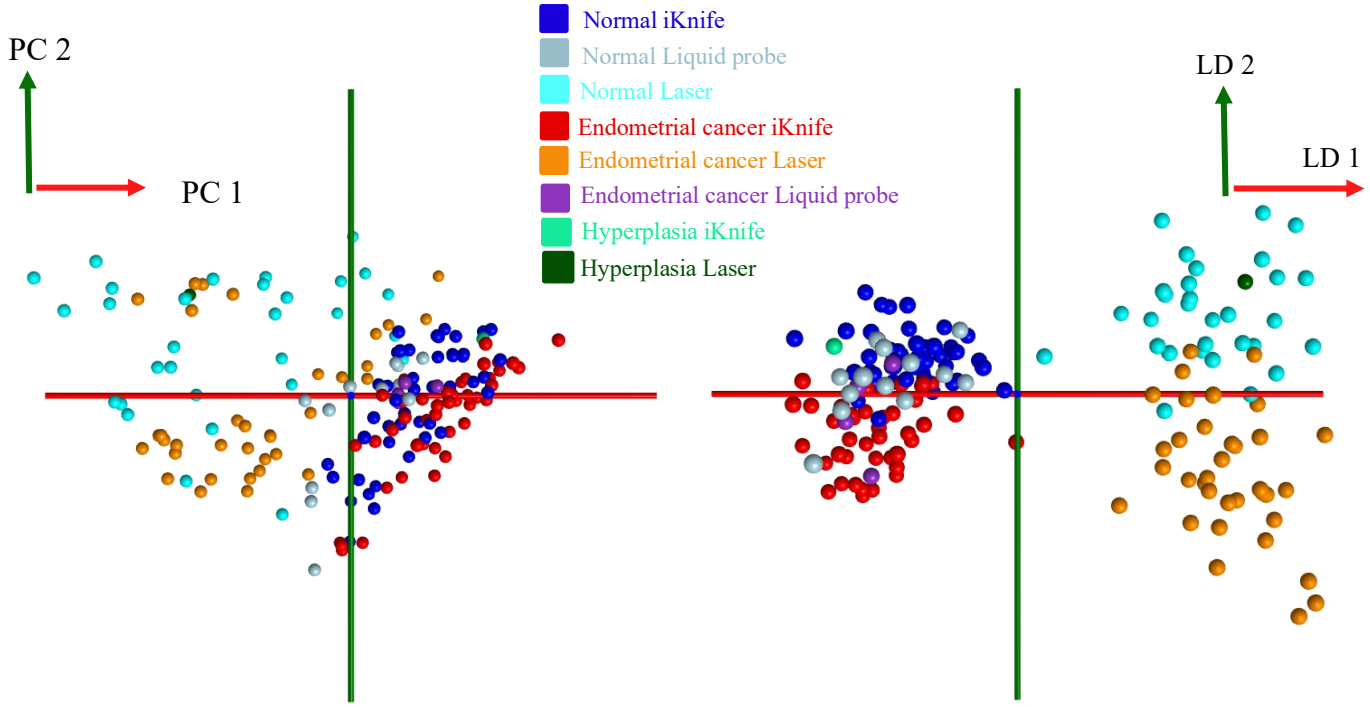


Figure 105. Multivariate analysis of normal vs cancer vs hyperplasia samples separated according to whether processed with the diathermy iKnife, CO2 laser or liquid probe.
Each dot represents the average spectra of a single sample. The diagram on the left is a 2D PCA and right 2D LDA. The confusion table is shown below. Annotation in table: K = processed iKnife, LA = processed laser, L = processed liquid line probe.

			MODEL CLASSIFICATION									TOTAL
			CANCER			HYPERPLASIA		NORMAL			OUTLIER	
			K	LA	L	K	LA	K	LA	L		
ACTUAL HISTOLOGY	CANCER	K	27	0	3	0	0	9	0	0	4	43
		LA	0	0	29	0	0	0	6	0	0	35
		L	1	0	1	0	0	0	0	1	1	4
	HYPER-PLASIA	K	0	0	1	0	0	0	0	0	0	1
		LA	0	0	0	0	0	0	1	0	0	1
	NORMAL	K	4	0	2	0	0	30	0	3	6	45
		LA	0	2	0	0	0	1	19	0	8	30
		L	0	0	2	0	0	3	0	8	0	13

Confusion table for Figure 105. Annotation in table: K = processed iKnife, LA = processed with the CO2 laser, L = processed liquid line probe.

12.7 Combining pipelle and tissue bank model

Can pipelle and tissue bank samples processed with the standard diathermy iKnife be combined?

In general, models looking for differences in phospholipid profiles amongst different classes requires large spectral libraries. Histopathological validation reduced the number of samples within each class significantly. As seen earlier, CO2 laser and diathermy iKnife samples are too different to be combined. However, is it possible to combine either the CO2 laser pipelle spectra or the diathermy iKnife pipelle spectra with spectra derived from the tissue bank model?

The PCA shows that tissue sampling method is distributed along PC1, with tissue bank samples predominately left and pipelle samples right (Figure 106). The same is seen on the confusion table, where samples have a tendency to classify according to their sampling method not just malignancy status, suggesting these two datasets should not be combined. On the supervised analysis all the samples separate clearly into their own specific clouds of data.

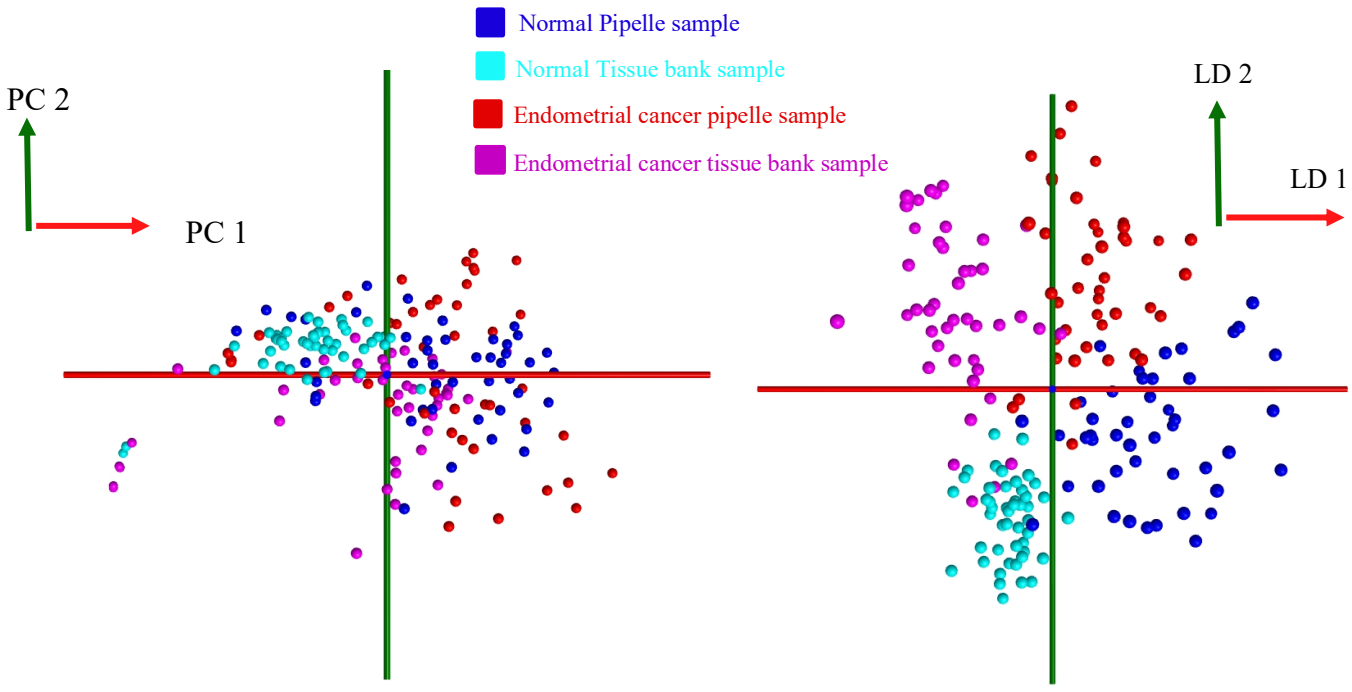


Figure 106. Multivariate analysis of normal vs cancer samples processed with the iKnife, separated according to whether samples were obtained from pipelle biopsies or tissue bank.
Red and pink dots represent endometrial cancer samples and blue samples normal. Each dot represents the average spectra of a single sample. The confusion table is shown below. Annotation in confusion table, TB = tissue bank sample.

			MODEL CLASSIFICATION				TOTAL
			CANCER		NORMAL		
			TB	Pipelle	TB	Pipelle	
ACTUAL HISTOLOGY	CANCER	Tissue bank	34	3	5	1	43
		pipelle	1	32	4	6	43
	NORMAL	Tissue bank	2	1	44	0	47
		Pipelle	2	4	2	37	45

Confusion table for Figure 106

Annotation in table: K = processed iKnife, LA = processed laser, L = processed liquid line probe.

The Table 34 below depicts accuracy of combined spectral dataset of both pipelle and tissue bank iKnife samples. The overall sensitivity and specificity were: 83% and 97% respectively.

		MODEL CLASSIFICATION, n (%)		TOTAL
		CANCER	NORMAL	
ACTUAL HISTOLOGY	CANCER	71 (83%)	15 (17%)	86
	NORMAL	3 (3%)	89 (97%)	92

Table 34. Confusion table of tissue bank (TB) and pipelle samples processed with the iKnife, classified according to tissue class status (normal vs cancer) and not the sampling modality.

12.8 Combining pipelle CO2 laser samples and iKnife diathermy tissue bank

Can the pipelle samples processed with the CO2 laser be combined with tissue bank samples processed with the diathermy iKnife?

Similarly, all tissue bank samples and pipelle samples processed with the laser were combined into a single model. As seen on the PCA, tissue bank samples clustered on the left and pipelle samples along the right, of PC1 (Figure 107). LDA separated all the tissue classes in separate clouds of data. The confusion table shows that samples tend to cluster in preference with their sampling method (pipelle vs tissue bank) as oppose to malignancy status. This suggests that CO2 laser pipelle samples should not be combined with the tissue bank samples.

Despite this, the overall accuracy of the model actually improved with the inclusion of spectra from both tissue bank and pipelle samples (Table below 35). The overall sensitivity and specificity of this model were: 84% and 96% respectively.

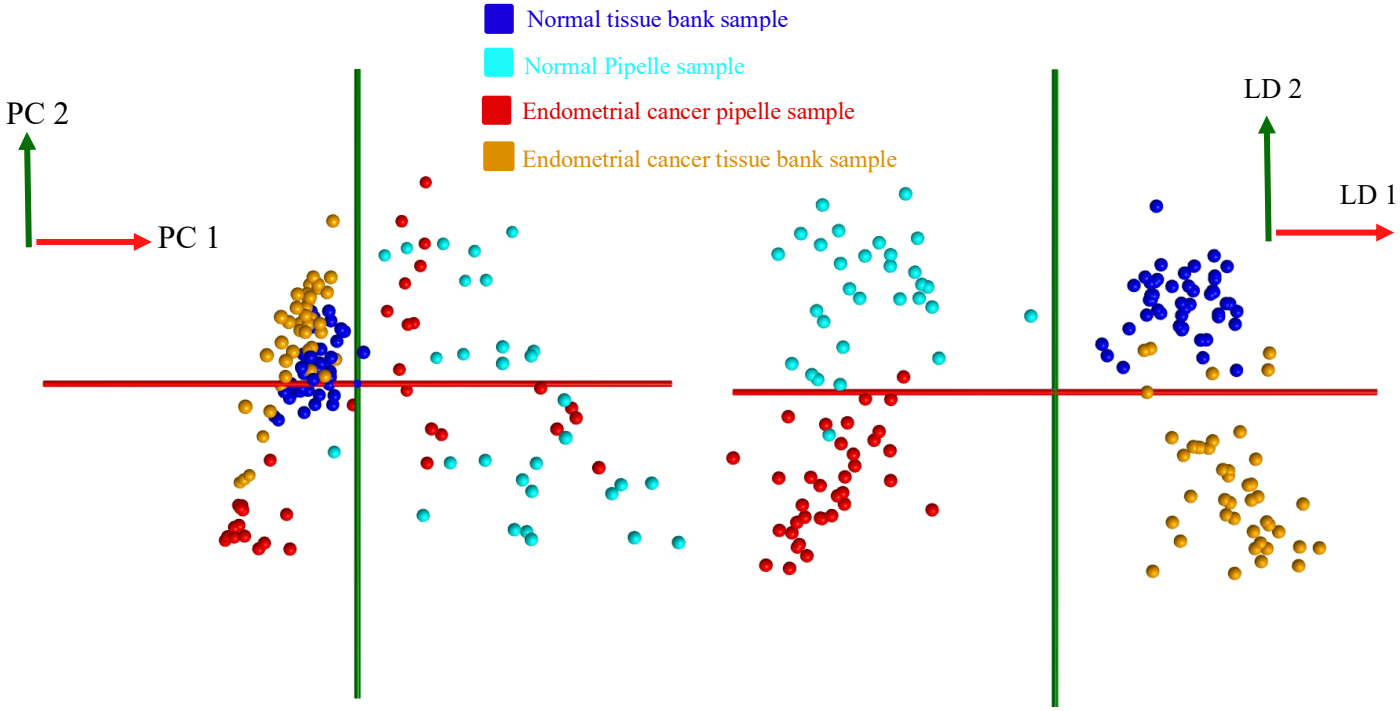


Figure 107. Multivariate analysis of pipelle samples processed with the CO2 laser and tissue bank samples processed with the iKnife, separated according to whether samples were obtained from pipelle biopsies or tissue bank.
Red and orange dots represent endometrial cancer samples and blue samples normal. Each dot represents the average spectra of a single sample. The confusion table is shown below. Annotation TB = tissue bank sample.

Confusion table for Figure 107

			MODEL CLASSIFICATION				TOTAL
			CANCER		NORMAL		
			TB	Pipelle	TB	Pipelle	
ACTUAL HISTOLOGY	CANCER	Tissue bank	36	0	7	0	43
		pipelle	1	29	0	5	35
	NORMAL	Tissue bank	0	0	47	0	47
		Pipelle	0	4	1	25	30

		MODEL CLASSIFICATION, n (%)		TOTAL
		CANCER	NORMAL	
ACTUAL HISTOLOGY	CANCER	66 (85%)	12 (15%)	78
	NORMAL	3 (4%)	74 (96%)	77

Table 35. Confusion table of tissue bank processed with the diathermy iKnife and pipelle samples processed with the CO2 laser, classified according to tissue class status (normal vs cancer) and not the sampling modality.